Energy Saving and Reliability of Wireless Body Area Networks for Health Applications

HISHAM ALSHAHEEN

School of Computing, Science, and Engineering, University of Salford, Manchester, United Kingdom

Submitted in Partial Fulfilment of the

Requirements of the Degree of

Doctor of Philosophy

2018

Table of Contents

Lists of Figures

Lists of Tables

Acknowledgment

I am thankful and grateful to Almighty Allah for giving me power to complete this work. I offer sincere thanks to my supervisor Professor Haifa Takruri for the encouragement, advice provided, and guidance in the preparation of this thesis. Professor Haifa played a major role in this thesis; I will always be grateful to her for her help. Also, I would like to thank Professor David Percy and Dr John Bacon for their assistance. I would like to record my gratitude for the library staff at Clifford Whitworth library, especially Anne Sherwin and the CSE staff, especially Catriona Nardone.

Beside my supervisor, I would like to acknowledge the Ministry of Higher Education and Scientific Research (MOHESR)/ Iraq which has sponsored me and my family during my PhD journey. Special thanks to Iraqi Cultural Attaché in London for the guidance, encouragement and continuous support.

Finally, I owe my deep and loving thanks to my mother, my brothers, my sisters, my wife, and my children, for their endless support. Thank you to my mother who asks and requests help for me from Allah. Thank you to my wife who helped me, supported me, and cared for our children when I was busy with the research. Also, I would like to thank my friends, Dr Kim Wasey, Mr Stephen Horrocks, and Mr Phil Jayes for their encouragement and support.

Dedication

"In the name of God, most Gracious, most compassionate"

I dedicate this thesis to my father, you are always in my thoughts.

I dedicate to my uncle who had a heart of gold; I miss you every day; I will remember you all my life.

I dedicate to my mother, my brothers, my sisters, my wife, and my children for their unconditional love and encouragement.

Publications

Publications Outcome from this Research:

Refereed Journals and Conferences Papers

1. **Full journal paper,** H. Alshaheen and H. Takruri-Rizk, Energy Saving and Reliability for Wireless Body Area Networks (WBSN), *IEEE Access (Open Access Journal),* vol. 6, no.1, pp. 16678-16695, March 2018.

2. **Full journal paper,** H. Alshaheen and H. Takruri-Rizk , Improving the energy efficiency for the WBSN bottleneck zone based on random linear network coding, published in IET Wireless Sensor Systems, vol. 8, no. 1, pp. 17-25, February 2018.

3. **Full conference paper,** H. Alshaheen and H. Takruri-Rizk ,Improving the Energy Efficiency for a WBSN based on a Coordinate Duty Cycle and Network Coding, published in the 13th International Wireless Communication and Mobile Computer Conference (IWCMC 2017), IEEE, Valencia, Spain; 26-30 June 2017.

4. **Short conference paper,** H. Alshaheen and H. Takruri-Rizk, Energy Saving for Biosensor Nodes in the Wireless Body Sensor Network, published in *Proceedings of the CSE 2017 Annual PGR Symposium 2017 (CSE-PGSym17)*, University of Salford, Salford, UK, 17th March 2017. (short paper 4 pages)

5. **Full conference paper,** H. Alshaheen and H. Takruri-Rizk, Improving the Energy Efficiency for Biosensor Nodes in the WBSN Bottleneck Zone Based on a Random Linear Network Coding, published in 11th International Symposium on Medical Information and Communication Technology (ISMICT 2017), IEEE, Lisbon, Portugal, 6-8 February 2017.

Abstracts in Published Conference Proceedings

1. H. Alshaheen and H. Takruri-Rizk, Improving Energy Efficiency for a WBSN based on Coordinate Duty Cycle and Network Coding, in *Proceedings of the CSE 2016 Annual PGR Symposium 2016 (CSE-PGSym16)*, University of Salford, Salford, UK , 27th April 2016, pp. 24.

2. H. Alshaheen and H. Takruri-Rizk , Improving Energy Efficiency for a WBSN based on Coordinate Duty Cycle and Network Coding, *Salford Postgraduate Annual Research Conference 2016 (SPARC 2016)*, University of Salford, Salford, UK, 14 – 15 June 2016, pp. 95

3. H. Alshaheen and H. Takruri-Rizk, Energy Saving for Biosensor Nodes in the Wireless Body Sensor Network, in *Proceedings of the CSE 2017 Annual PGR Symposium 2017 (CSE-PGSym17)*, University of Salford, Salford, UK,17th March 2017, pp. 24.

Posters Published In Conference Proceedings

1- H. Alshaheen and H. Takruri-Rizk, Improving Energy Efficiency for a WBSN based on Coordinate Duty Cycle and Network Coding [Poster presentation], *Salford Postgraduate Annual Research Conference 2016 (SPARC 2016)*, University of Salford, Salford, UK, 14 – 15 June 2016.

2- H. Alshaheen and H. Takruri-Rizk, Improving Energy Efficiency for a WBSN based on Coordinate Duty Cycle and Network Coding, [Poster film which lasted 60 second], *http://www.pg.salford.ac.uk/page/sparc2016*, *Salford Postgraduate Annual Research Conference 2016 (SPARC 2016)*, University of Salford, Salford, UK, June 2016.

List of Abbreviations

AP	Access Point
BAN	Body Area Network
BCU	Body Control Unit
BI	Beacon Interval
BO	Beacon Order
BPSK	Binary Phase Shift Keying
CAP	Contention Access Period
CDC	Coordinate Duty Cycle
CFP	Contention-Free Period
CSMA	Carrier Sense Multiple Access
CSMA/ CA	Carrier Sense Multiple Access/Collision avoidance
DC	Duty Cycle
DSSS	Direct Sequence Spread Spectrum
ECG	Electrocardiography
EEG	Electroencephalography
GTS	Guaranteed Time Slots
IEEE	Institute of Electrical and Electronics Engineers
kbps	Kilobits per Second
LNC	Linear Network Coding
MAC	Media Access Control
Mbps	Megabits per Second
MS	Medical Server
NC	Network Coding

NEC	Network-Enabled Capability
OQPSK	Orthogonal Quadrature Phase Shift Keying
PDA	Personal Digital Assistance
PDR	Packet Delivery Ratio
PhY	Physical Layer
PL	Packet Latency
PS	Personal Server
RLC	Random Linear Coding
RLNC	Random Linear Network Coding
SD	Superframe Duration
SMS	Short Message Service
SO	Superframe Order
SpO2	Pulse Oximetry
TDMA	Time Division Multiple Access
WBAN	Wireless Body Sensor Network
WBSN	Wireless Body Sensor Network
WSN	Wireless Sensor Network
XOR NC	Exclusive OR Network Coding

Abstract

A Wireless Body Sensor Network (WBSN) consists of several biological sensors. WBSN can be employed to monitor patients' medical conditions. Energy consumption and reliability are critical issues in WBSNs, as the nodes that are placed near the sink node consume more energy. All biomedical packets are aggregated through these nodes, forming a bottleneck zone. The nodes usually use small batteries and in the case of implantable devices; it is important to prolong battery life. The main consideration of this thesis is the reduction of energy consumption of WBSN devices (sensor nodes) and the successful delivery of biomedical data at sink nodes based on medium access control (MAC) protocol IEEE 802.15.4 standard.

A novel mathematical model for WBSN topology is proposed in this thesis to explain the deployment of and connection between biosensor nodes, simple relay nodes, network coding relay nodes, and the sink node. Also, the Coordinated Duty Cycle Algorithm (CDCA) is the proposed novel approach which is adopted for the body area network. CDCA achieves energy savings for nodes through the implementation of mechanisms such as the selection of superframe order based on real traffic and the priority of the nodes in the WBSN, and the calculation of the Coordinated Duty Cycle (CDC). In addition, RLNC is employed to achieve the required level of reliability in WBSNs and delivery of packets through the calculation of the probability of successful reception at the sink node.

This research identified that energy consumption in WBSNs is affected by the following parameters: the distances and locations of the nodes on the human body, WBSN topology, employing relay nodes, the propagation model such as the line of sight (LOS) and the non-line of sight (NLOS).

Simulation results are presented to show that CDCA improves the energy consumption of biosensor nodes. Also, the results from a comparative analysis of RLNC and XOR NC show that RLNC provides a higher probability of successful reception of data packets at the sink node than the XOR NC technique. Overall, this work demonstrates a new scheme for achieving energy reductions for the biosensor nodes in WBSNs which operate at low data rate; also, it achieves the required level of reliability in WBSNs.

Chapter 1:
Introduction

1.1 Introduction

The wireless body area network has the potential to dramatically change the lifestyle and wellbeing of individuals, especially in the area of health monitoring. In emergency situations or the normal situations, the monitored patient needs to use the biomedical sensor nodes which are attached to the patient or implanted inside the body of the patient; the medical data should be correctly received at the sink node. The medical staff are interested in observing the patient through the received medical data. With respect to health monitoring, the energy usage of sensor nodes has represented one of the 'hottest' topics in the wireless body sensor networks for a long time, to achieve the functions of monitoring in the long term. A large amount of biomedical data flow occurs near the sink node; so the nodes closer to the sink node consume more energy than other nodes, leading to reduction in reliability and wastage of energy. Therefore, the reduction of the energy consumption for the sensor nodes and guaranteeing delivery of biomedical data to the sink node are most important for body area networks in the healthcare system.

A Wireless Body Sensor Network (WBSN) consists of several biological sensors. WBANs are used in both medical and non-medical applications[1]. In medical applications, such sensor devices fall into two types: wearable medical devices and implantable medical devices, according to the type of signal acquired (blood pressure, Electroencephalography (EEG), Electrocardiography (ECG), heart rate, blood glucose level, body temperature, body posture, blood oxygen saturation, etc.). As Figure 1.1 shows, WBSNs are used to show and measure different vital signs. Implantable medical devices are implanted inside the human body while wearable medical devices are worn or placed on the skin or very near to the patient. The biomedical sensor nodes sense or otherwise measure the different health signs of the body, and the medical data is then transmitted to the sink node. The sink node is situated on the human body or at a nearby location[2].

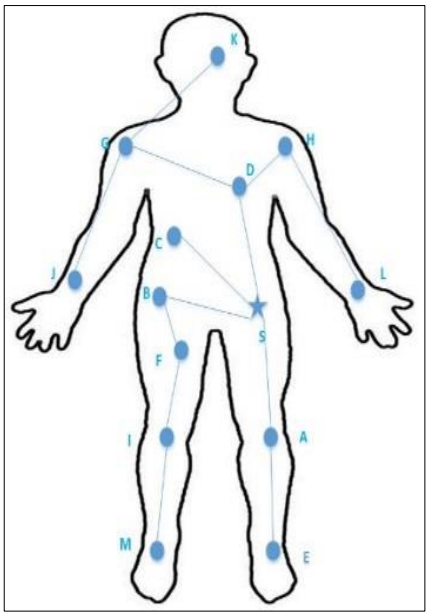

Figure 1.1: WBSN topology with 13 biosensors

The major existing approaches proposed are reviewed to address the problem of energy consumption in wireless sensor networks. The classification of energy-efficient mechanisms is shown in Figure 1.2, which represents a summary of the energy-efficient methods[3]. There, it can be seen that one of the most popular techniques is to reduce the energy consumption provided to sensor nodes by using a duty cycle. Also, network coding is used to improve the reliability. The main goal of using the coordinate duty cycle and random linear network coding in WBSNs is to reduce the energy consumption and improve the reliability. Moreover, it aims to achieve better energy usage and increase the probability of successful reception at the sink node. Both mechanisms are applied in the model which is considered in this thesis.

The rest of this chapter is organised as follows. Section 1.2 describes the motivation of this research. Section 1.3 presents definitions of the problems. Section 1.4 explains the research aim and objectives. Section 1.5 provides the research methodology to address the identified problems. Section 1.6 explains the research contributions. Finally, section 1.7 describes the thesis structure.

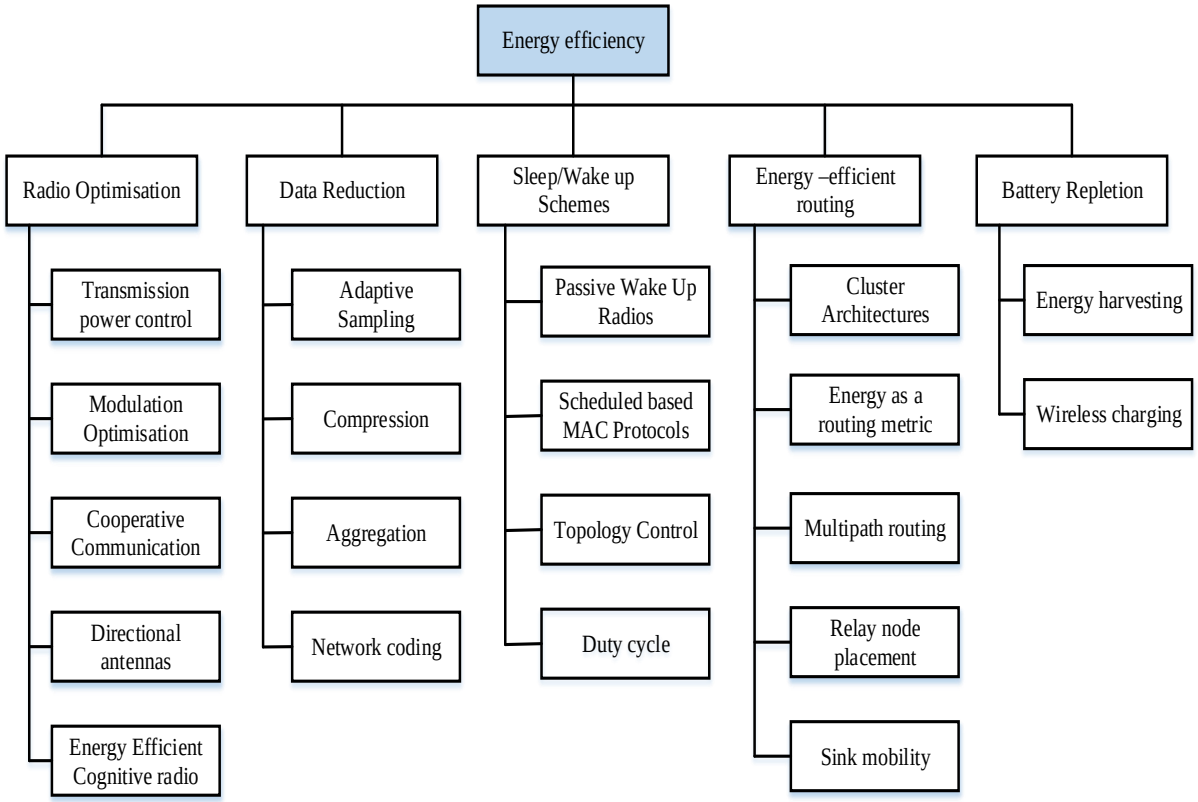

Figure 1.2: The classification of energy-efficient mechanisms

1.2 Research Motivation

Lower energy consumption of each biosensor node and reliable transmission of biomedical data are of immense significance in wireless body area networks (WBANs). The monitored patient in the hospital requires the measurement of multiple medical parameters by using biomedical sensor nodes, which are attached to the patient or implanted inside the body of the patient, such as EMG, ECG, temperature, oxygen saturation, heart rate, and blood pressure. The medical staff will be interested in monitoring the patient. In some situations, the patient needs a large number of biomedical sensor nodes to collect the medical data; the monitored patient requires more attention because sensed and measured information represent emergency situation or normal medical data which needs more reliability for transmission of biomedical data from biosensor node to sink node and increased lifetime for biosensor nodes.

Low energy consumption for biosensor nodes and high reliability are necessary to support this motivation. The motivation for the former is the energy consumption of biomedical sensor nodes which are placed near the sink node: they consume more energy and deplete

energy quickly. Therefore, one of the most popular techniques is to reduce the energy provided to sensor nodes by using a duty cycle. In addition, the distances and locations of the biomedical sensor nodes on the human body have an effect on energy consumption for WBSNs and also the topology impacts on the energy usage, especially when employing relay nodes to WBANs. As far as the propagation model in the WBSN is concerned, two types may apply to WBSNs: line of sight (LOS) and non-line of sight (NLOS) propagation. The former applies along the front of the torso and the latter is around the torso.

The motivation for the latter is the reliable transmission of medical data. When the patient is at risk, WBANs carry life-critical biomedical packets, such as heart rate or electrocardiograms, which have to be delivered reliably. Therefore, a lost biomedical packet may cause the life of the patient to be at risk or may be the cause of misinterpretation as the total set of packets would be incomplete. Although there are previous studies into the reliability procedures to address this issue, reliable data transmission is still a challenge for WBSNs, and medical monitoring systems, such as in the event of an emergency. Hence, there is further need for this research to be considered and developed[4,5].

Moreover, WBSNs are not designed for the reliable transmission of medical data. Therefore, the Network Coding (NC) technique is used to achieve reliability in the transmission of data in healthcare. Motivated by network coding characteristics, the performance of reliability of data transmission is improved in WBSNs.

Reliable transmission in WBSN and better energy consumption for biosensor nodes are most important for body area networks, which represent a key requirement in WBSN application, especially in healthcare systems. The main motivation of the problem addressed in this thesis is to reduce the energy consumption of biomedical sensor nodes and ensure reliable transmission of biomedical data in order to achieve the successful delivery of the medical data transmission.

1.3 Definition of Research Problems

The research in this thesis reduces the energy consumption of the biosensor nodes which are placed in the bottleneck zone of a WBSN; also, this work improves the reliability of transmission of physiological data in the WBSN. The research problems are defined as follows:

Problem 1:

The significant body of research into MAC (Media Access Control) protocol designs which employ duty cycle discussed in Chapter 3 has been investigated for minimising energy consumption, which mostly use random duty cycle. However, the energy consumption of nodes is still a problem and a challenge in WBSNs, especially the biosensor nodes placed near the sink node. These nodes consume more energy because all biomedical packets are aggregated through these nodes forming a bottleneck zone. Furthermore, the energy wastage in the bottleneck zone which deploys nodes near the sink node, which then consume more energy and deplete energy quickly. Consequently, this area has heavy traffic which limits the network lifetime[6].

The duty cycle is a "green" technique which is utilised to reduce the energy usage through increasing the inactive period for the biosensor node in a WBSN with guaranteed delivery of data. Although previous work considered adjusting duty cycle for sensor nodes which implement the IEEE 802.15.4 MAC standard, the majority of the previous studies did not review the energy consumption of biosensor nodes in the bottleneck for WBSNs based on priority and traffic changes. The main issue to be investigated is how to reduce the energy consumption of biosensor nodes in WBSNs.

Problem 2:

The reliable transmission of physiological data is still a challenge for WBSN and medical monitoring systems, and this needs to be considered and developed[4,5]. In addition, previous work did not consider the reliability in the bottleneck zone of WBSNs, although there are previous studies on the reliability procedures to address lost biomedical packets in a WBSN. Moreover, these works have been investigated in Chapter 3. Reliability is most important for body area networks, and represents a key requirement in WBSN application, especially in healthcare. The issue to investigate and determine is how to improve reliable transmission for the medical data in the bottleneck zone of WBSNs in order to achieve a high probability of successful reception at the sink node. The random linear network coding (RLNC) technique is resilient for biomedical data to improve network reliability in WBSNs[4]. Therefore, the investigation of Network Coding (NC) has shown that RLNC improves the reliability of data delivery in a WBSN when compared with another technique such as XOR NC.

Recently, there have been studies published on the combination of duty cycle (DC) and network coding (NC). In [7], Rout and Ghosh combined the random duty cycle with NC to

enhance the network lifetime in WSN; they applied XOR NC only on the NC node in the bottleneck zone. However, simple nodes do not benefit from NC in terms of reducing energy usage and the reliability of data delivery is reduced by XOR NC. Lee et al [8] proposed a technique using a random duty cycle with RLNC in the bottleneck area to improve energy efficiency and reliability. The sensor nodes near the sink deplete their energy quickly due to heavy traffic, which limits the network lifetime[8]. The main problems in the bottleneck zone are the energy wastage and lost biomedical packets in this area; to address the problems a combination between the coordinated duty cycle (CDC) and the random linear network coding (RLNC) is proposed.

1.4 Research Aim and Objectives

1.4.1 The Research Aim

The aim of the research reported in this thesis is to develop a novel approach for reducing energy consumption of biosensor nodes and improving reliability in Wireless Body Sensor Networks, along with increasing the level of successful delivery at the sink node.

1.4.2 The Research Objectives

The research objectives have been identified as follows:

1- To design and define a novel mathematical model for a body area network (BAN) topology which considers the connection and relationships of the biomedical sensor nodes, the simple relay nodes, the network coding relay nodes, and the sink node.

2- To design and apply the Coordinated Duty Cycle Algorithm (CDCA) technique and to use Random Linear Network Coding (RLNC) inside the bottleneck zone; and CDCA to all nodes in the WBSN.

3- To implement and derive the expression (statistical model) for the three techniques (forwarding, encoding, and combination) concerning the probability of successful reception at the sink node. Also, to obtain the accuracy in terms of the improvement percentage for the three techniques based on testing and measurement.

4- To test and analyse the results evaluating the performance of the proposed WBSN and compare with another solution.

5- To validate the results for the mathematical models with the simulation results; and compare the results to evaluate it.

1.5 Research Methodology

A scientific quantitative research methodology has been adopted for this research as it employs mathematical models based on the hypotheses, experiments, and theories which use the data generated from them[9,10]. The main phases of the research methodology are defined in Figure 1.3 ; it is more appropriate to the research. It includes the following stages: studying the literature review and the mathematical respects, identifying the problems, studying and analysing these problems, designing a mathematical model and algorithms, and implementing, processing, and evaluating the results. Also, the modification allows to enhance and improve the performance of the design model. This methodology technique will help to achieve the aim and the objectives of this research. The main steps of the methodology are as shown in Figure 1.3.

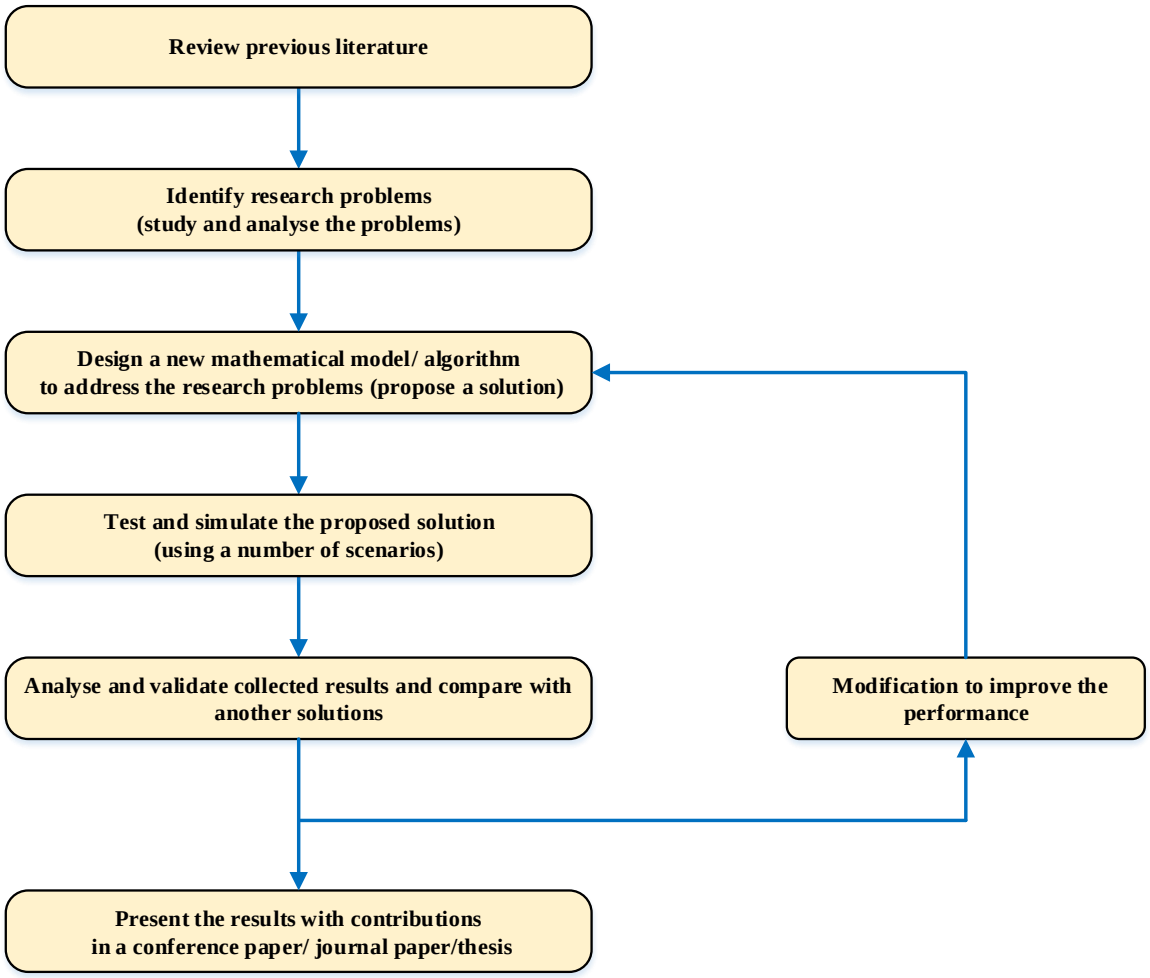

Figure 1.3: The main steps of research methodology

1.6 Research Contribution

The main contributions are directed toward addressing the challenges which are mentioned in this thesis, that is, reduction of the energy consumption for the biosensor nodes in WBSNs and improvement of the reliability of WBSNs. The specific contributions are further described in the following paragraphs as they relate to each chapter.

Chapter 4's main contribution can be summarised as follows:

- A novel mathematical model for body area network (BAN) topology, which comprises sequences of equations to develop the calculation of energy consumption of biosensor nodes in WBSNs, to explain the deployment and connection between biosensor nodes, simple relay nodes, network coding relay nodes, and the sink node based on a proposed novel model for a BAN. Moreover, two algorithms for encoding and decoding biomedical packets which employ the RLNC in WBSN. Also, the model may be generalised to other types of sensor networks.

Chapter 5's main contribution can be summarised as follows:

- A novel Coordinated Duty Cycle Algorithm (CDCA) describing the mechanisms of implementing it, for instance calculation of the slots algorithm; identification of the priority with the equations used to determine the queue state value; selection of the type of slots such as CAP slots and GTS slots; effects of the remaining pending packets in the queue and the received packets at the sink node (the real traffic); calculation of CDC. The CDCA is implemented in the proposed WBSN model which uses RLNC. The algorithm could be generalised to other types of sensor networks. An analysis of the results which report on the reduction of energy consumption for the nodes in WBSNs especially the CDCA was used in the model.

Chapter 6's main contribution can be summarised as follows:

- A novel mathematical model for reliability in WBSNs, which is based on the forwarding technique, encoding technique, and a combination of both for the biosensor nodes in the bottleneck zone of a WBSN and the sample WBSN and calculating the probability of successful reception (PSR) at the sink node. This model was designed to guarantee that the biomedical data would be delivered correctly to the sink node. Also, to calculate the accuracy of the improvement between the three techniques.

1.7 Thesis Structure

This section presents an overview of the organisation of the thesis, which includes eight chapters.

Chapter 1 presents an introduction to the thesis, which includes the research motivation, definition of research problems, research aim and objectives of the thesis, research methodology, and the main contributions that have been made.

Chapter 2 introduces the definition of Wireless Body Area Network (WBAN) and gives a general background about WBANs which includes WBAN applications, types of nodes in a WBAN, and WBAN architecture.

Chapter 3 performs a comprehensive survey of literature on the development of MAC protocols in BAN and Duty Cycle (DC) in WBSN MAC protocols. In addition, it provides the literature review covering Network Coding which is performed in the area of BANs. Also, the chapter discusses how to address the identified problems.

Chapter 4 contributes a novel mathematical model design for a body area network (BAN) topology; Chapter 4 proposes the model which explains the deployment and connection between biosensor nodes, simple relay nodes, network coding relay nodes and the sink node. Therefore, this chapter is dedicated to researching both the energy saving and delivery of data if there is a failure in one of the links of the transmission, which relates to the proposed Random Linear Network Coding (RLNC) model in the WBSN. In addition, the encoding and decoding algorithms are proposed in this chapter.

Chapter 5 proposes Coordinated Duty Cycle Algorithm (CDCA) in WBSN and describes the mechanisms of implementing it. Also, it is used to select the superframe order (SO) based on the real traffic and the priority of the nodes in the WBSN; the calculation of Coordinated Duty Cycle (CDC) is used in the model, which utilises RLNC. Moreover, in Chapter 5, the results are presented for the energy consumption of nodes in WBSNs based on CDCA and those without CDCA.

Chapter 6 proposes a novel mathematical model for the reliability of WBSNs. In this chapter, RLNC is highlighted and employed to achieve the required level of reliability in a WBSN and the delivery of packets through the calculation of the probability of successful reception at the sink node. In addition, the simulation is discussed for the RLNC and XOR NC technique.

Chapter 7 presents the validation of the results which are collected from scenarios based on the proposed model and CDCA. The Chapter provides the performance of WBSN and analysis of this.

Chapter 8 provides major conclusions of this thesis and recommendations for future work from this research.

Chapter 2:

WBAN Background

2.1 Introduction

This chapter provides a brief definition of WBAN (Wireless Body Area Network). The goal of this chapter is to explain WBAN application and details of the sensor nodes which are used in WBANs. In the hospital, medical staff monitor patients through the measurement of emergency or normal vital signs by using biomedical sensor nodes; each biosensor node has a specific data rate; the data rates in the health application are heterogeneous. In addition, the WBAN architecture with different types of node are explained, such as ECG (Electrocardiogram), blood pressure sensor, EEG (Electroencephalogram), EMG (Electromyography), and motion sensors, which are distributed in/on/around the human body.

The chapter is organised as follows. Section 2.2 describes the Wireless Body Area Network (WBAN). Section 2.3 presents the application of WBAN. Section 2.4 discusses the types of nodes in a WBAN. Section 2.5 presents the data rate in a WBAN. Section 2.6 discusses WBAN architecture. Finally, a summary of the chapter is drawn in section 2.7.

2.2 Wireless Body Area Network

The definition of Wireless Body Area Network (WBAN) is given as a wireless network on the human body, which includes multiple nodes each equipped with a sensor. With respect to the Institute of Electrical and Electronics Engineers (IEEE), a WBAN refers to a network on the human body; however, certain researchers use the term Wireless Body Sensor Network. The naming of WBAN by the IEEE is based on the area, for instance local Area Network (LAN), Wide Area Network (WAN), etc. Furthermore, the Wireless Body Sensor Network (WBSN) represents a special case of a Wireless Sensor Network (WSN) [1].

As shown in Figure 2.1, a Wireless Body Area Network (WBAN) consists of multiple nodes which are located in different positions on the human body depending on the function of the sensor node. Moreover, the sensor nodes collect information through monitoring [1].

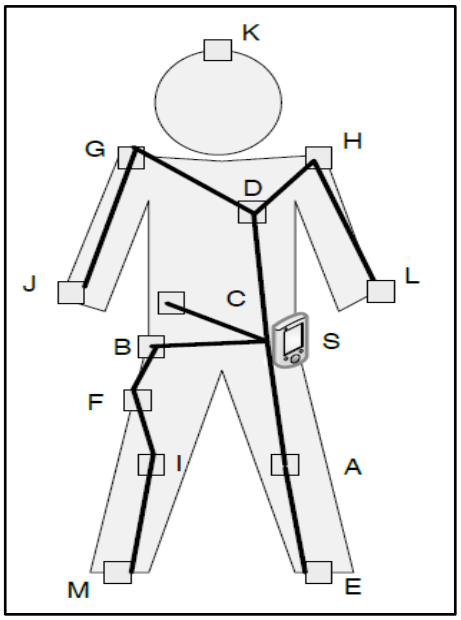

Figure 2.1: WBSN topology

In addition, the WBAN is a special kind of wireless sensor network; the services vary widely. Typical application scenarios could be monitoring of body temperature, heartbeat, body position, location of the subject, or overall monitoring of ill patients both at home and in the hospital. A simple WBAN application scenario is shown in Figure 2.2 [12].

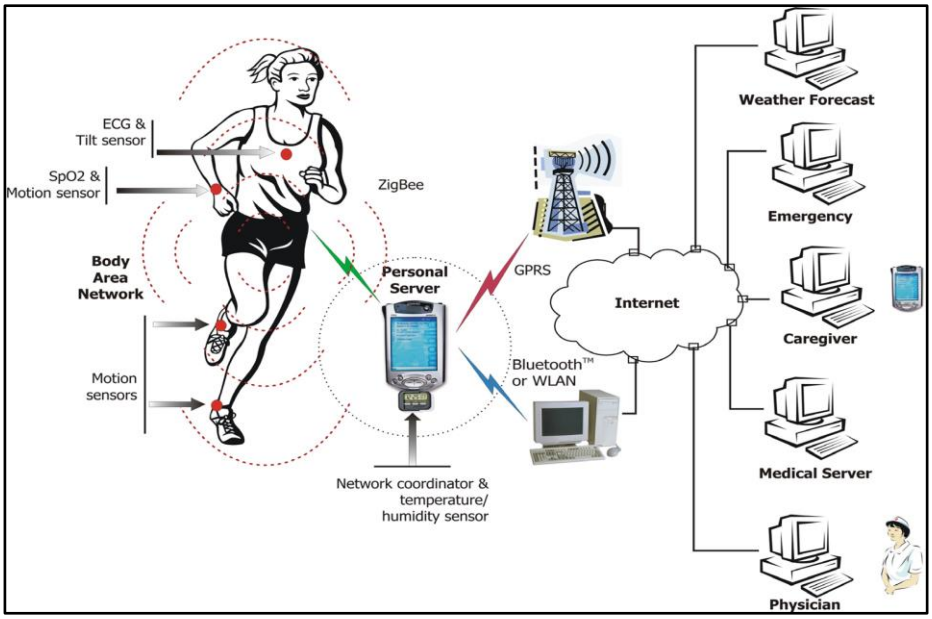

Figure 2.2: A typical WBAN application

2.3 Applications of WBAN

In this section, the applications of WBANs are explained, which can be categorised into two: medical and non-medical, according to the function of the application [3].

2.3.1 Medical Applications

In medical applications, WBAN allows for the continual monitoring of physiological parameters such as body temperature, blood pressure, and heartbeat. Moreover, the various biomedical sensor nodes are deployed to monitor various vital signs of a patient for detecting abnormality in the vital signs, and then transmit the data to a gateway such as a cell phone [4].

2.3.1.1 Wearable Applications

In healthcare, the wearable medical devices are worn or placed on the skin or very near to the patient; these nodes sense or measure the different health signs of the body and then send the medical data to the sink node [5]. Temperature monitoring, glucose level monitoring, Electrocardiogram(ECG), SpO_2, blood pressure monitoring, Electroencephalogram(EEG), and Electromyography(EMG) are examples of wearable medical applications[14].

2.3.1.2 Implant Applications

Implantable medical devices are implanted inside the human body[2], being implanted in the stream of the blood, such as cancer detection and diabetes control systems, and cardiovascular diseases[13].

2.3.2 Non- Medical Applications of WBANs

The non-medical applications of WBANs can be used in different fields such as entertainment, sport, and the military[14]. In the field of entertainment, the monitoring of speed and differences in direction of a human body by accelerometers and gyroscope which are worn by the user on the body can be seen[15]. For example, in a simple exercise sensing experiment, the placement of accelerometer nodes on the right and left legs and ankles of human body can measure different activities such as sitting, standing, running, and walking [16].

2.4 Types of Nodes in WBAN

(Wireless) sensor node measures specific parameters that respond to and collect data on physical stimuli, process the data if necessary, then wirelessly reports this information[17]. Moreover, *(wireless) actuator node* represents a device which interacts with the user upon receiving data from the sensors. Also, the components of the sensor are similar to the actuator [9]. With respect to WBANs, the kinds of sensor nodes available for human body are as follows with briefly explanations:

(1) Electrocardiogram (ECG) sensor:

The ECG nodes are used for electrocardiograph signal monitoring; they are used to diagnose heart disease in the healthcare system. In addition, ECG nodes are used to monitor how different heart medications are working; the electrodes are attached at specific positions on the skin such as the chest or limbs of the body [19].

(2) Blood pressure:

The blood pressure sensor uses the oscillometric technique, which is designed to measure systolic and diastolic human blood pressure[20].

(3) Electroencephalogram(EEG):

The EEG sensor detects the brain's electrical activity through the attaching of electrodes to the human's scalp at multiple locations. The electrodes sense the electrical activity of the brain and transmit to an amplifier produce a pattern of tracings [20].

(4) Electromyography (EMG) sensor:

This measures electrical signals which are generated by muscles through contractions or at rest. In the human body, the impulses represent electrical signals which make the muscles react in different ways; both nerve and muscle cause this response [11].

(5) Blood glucose:

Diabetes is a long-term medical problem [14], which requires regular monitoring of the patient's blood sugar level [12]. Blood glucose is measured as the amount of the sugar (glucose) circulating in the blood. Also, it is called blood sugar or glucose monitoring. Glucose measurements are done by tradition methods such as the glucose meter (optical meter) and recent methods of monitoring such as optical sensing and infrared technology [11]. In addition, another example for the monitoring of glucose levels is Glucowatch, which represents one of a set of wearable systems [13].

(6) Pulse Oximetry(SpO_2):

Oxygen saturation is measured using a non-invasive probe. Pulse Oximetry represents a sensor with a small clip which attaches to the human's earlobe, finger, or toe, but it usually attaches to the finger to obtain a blood oxygen reading. The sensor throws out a light signal which passes through the skin in order to detect how much oxygen is in the blood. Moreover, the ratio of oxygenated hemoglobin to the total amount of hemoglobin represented the ratio of measurement for oxygen level. Also in [20].

(7) Temperature sensors:

In health monitoring, temperature sensors measure the temperature through the collected vital sign information from the human body. Furthermore, if there is a certain amount of change in what is measured, an alarm signal could be issued. Also, the humidity sensor measures the humidity of the environment around a human [11].

(8) Pacemaker:

This is a small device which helps the heart beat more regularly. It is implanted under the skin on the human's chest. In addition, it sends electrical pulses to the heart in order to keep heart beating regularly and not slowly[22]. Moreover, a pacemaker is an implanted device, which should operate for the months or years depending on the lifetime of the battery, because it is difficult to achieve replacement or recharging[18].

In addition, there are other devices which are to be found in the health application area such as *(wireless) personal device (PD), coordinator node, and relay node.* As for the (wireless) personal device, this device is responsible for the collection of all the information received from actuators and sensors and addresses interaction with other users such as a patient, a nurse, or a GP through an external gateway or a display on the device. This device may also be called sink node, Body Control Unit (BCU), body gateway, or Personal Digital Assistant (PDA) in some applications [14]. *The coordinator node* is analogous to a gateway to the outside world, another WBAN, an access coordinator, or a trust centre. All nodes in a WBAN communicate through the coordinator node of the WBAN, which is a PDA [4]. *The relay node* in a WBAN represents an intermediate node; it has a parent node, a child node, and a relayed message. The main function of the relay node is forwarding data which is received to other nodes until they reach the PDA[14].

2.5 Data Rate in WBAN

The data rates vary strongly because of strong heterogeneity among health applications; the range of data rate stretches from a few kbit/s (1 kbit/s) to several Mbit/s (10 Mbit/s). The

biomedical data can be sent in bursts(a packet burst contains of a certain number of packets, which arrive at or leave a system in a relatively short period) which are sent at higher rate during these times [24]. For example, the data rate of a pacemaker is a few kbps but the data rate of an EEG is a several kbps. Table 2.1 shows the data rates for the different medical applications [4] [18] [25]; it also describes the function of each sensor node.

Table 2.1: Examples of medical WBAN applications

Biosensor node	Monitoring	Data rate
ECG	Heart activity	192Kbps
EEG	Brain electrical activity	86.4 Kbps
EMG	Muscle activity	1536 Kbps
Blood pressure	Blood pressure	1.92 Kbps
Body temperature	Temperature	1 Kbps
Pulse rate	Number of beats per minute for heart	2.4 Kbps
Motion sensor	Speed and direction	35 Kbps
Blood saturation	Oxygen-saturated blood	16 Kbps
Blood glucose	Blood Glucose	1 Kbps
Pacemaker	Regular heart beat	Few Kbps

2.6 WBANs Architecture

Figure 2.3 shows WBAN network architecture with different types of nodes that are distributed in/on/around the human body and its multiple tiers [20]. The sensor nodes such as EEG, ECG, EMG, blood pressure sensors, and motion sensors transmit biomedical data toward personal server (PS) devices. After this, through WLAN (Wireless Local Area Network) connection or Bluetooth, these biomedical data are remotely transmitted to a medical doctor's site for diagnosis, or to request assistance on an emergency issue, or for record keeping in a medical database. The communication architecture of WBANs can be separated into three different tiers: intra-WBAN communication (Tier-1-Comm design), inter-WBAN communication (Tier-2-Comm design), and beyond-WBAN Communication (Tier-3-Comm design) as shown in Figure 2.3 [11].

2.6.1 Tier-1: Intra-WBAN Communication

Tier 1 communication (intra-BAN communications) is between the WBAN nodes and coordinator node (master node) as shown in Figure 2.3. Furthermore, it is between the WBAN nodes themselves. This communication tier is directly related to the human body; it requires high or low data rate depending on the type of sensor; it is supplied with small

batteries and has a short range of between 1 and 5 metres, therefore it has limited energy [17]. In Tier-1, the different sensor nodes are forwarding body signals to a personal server (PS) that is located in Tier-1. The physiological data is processed after that transmitted to an access point in inter-WBAN communication, which represents Tier-2 [4].

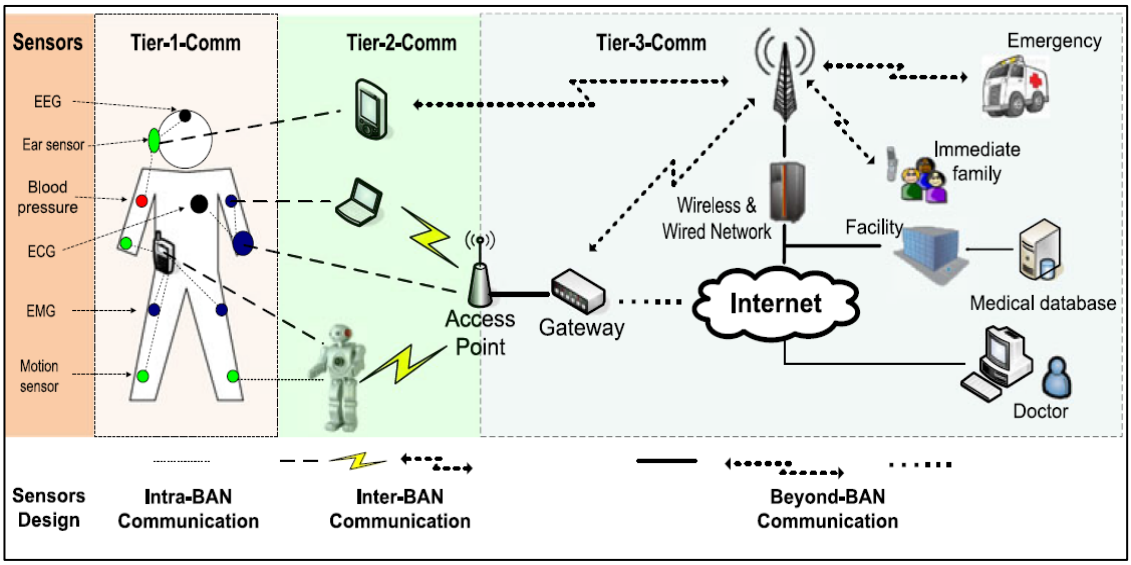

Figure 2.3: Three-tier architecture based on a BAN communications system

2.6.2 Tier-2: Inter-WBAN Communication

In this, Tier 2, the communication is between the PS (personal server) and the gateway or one (or more) access points (APs). One of the parts of the infrastructure is the access points, which may be strategically placed in a dynamic environment to handle emergency situations. Moreover, it aims to interconnect WBANs with different networks, which can be simply accessed in daily life by further cellular networks and the Internet [20].

2.6.3 Tier-3: Beyond-WBAN Communication

Beyond-WBAN Communication is designed for use in metropolitan areas. A gateway such as a PDA, is used to bridge the connection between this tier and inter-WBAN communication (Tier-2), then from Internet to a specific application such as the Medical Server(MS) [9]. However, the design of Tier-3 beyond-WBAN communication represents the specific application. One of the most important components of Tier-3 is a database of the medical environment. In addition, the medical database includes the profile of the user and medical history. Thus, patients or doctors can be warned of an emergency status through either a Short Message Service (SMS) or the Internet [11].

2.7 Chapter Summary

This chapter provided a brief overview of WBANs (Wireless Body Area Networks). Firstly, WBAN is defined; two figures have provided the simple WBAN application scenario. Secondly, two main types of WBAN application, namely medical application and non-medical application, have been illustrated. In addition, the data rates for the wireless biomedical sensor node and types thereof in WBANs have been explained. This gives the values of data rates for nodes used in this thesis. Finally, the WBAN architecture has been discussed. The material in this Chapter presents background knowledge on WBANs but does not provide any new results. However, it is intended to provide understanding of WBANs. The next chapter will study a literature review regarding WBSN MAC protocol, duty cycle, and network coding in WBSNs.

Chapter 3:

Literature Review

3.1 Introduction

In recent years, there has been an increasing interest in the requirements of WBSNs, such as the reduction of energy consumption and the successful delivery of data. This chapter deals with terms comprising the following: firstly, it describes *MAC protocol* in section 3.2 which employed in WBSNs; secondly, it presents an overview of the developments in *Duty Cycle (DC)* in section 3.3. In addition, there are other subjects referred to so as to cover the area of research, such as the energy consumption formulas, path loss model for the body, and the deployment relay node, in sections 3.4, 3.5, and 3.6, respectively. Section 3.7 explains the *Network Coding (NC) technique*. Finally, section 3.8 concludes this chapter.

In this chapter, an overview of the developments in *MAC WBSN protocol* is provided, *duty cycle (DC),* and *network coding (NC)* to explain the research problem. Furthermore, the main properties of duty cycle and network coding are utilised to reduce energy consumption and improve the transmissions reliability, respectively, which are presented to achieve the research aim.

3.2 Energy Efficient MAC Protocols for WBAN

A comprehensive explanation and discussion for most existing MAC protocols proposed for the energy efficiency for WBANs is presented in this section, and the protocols to address the sources of energy inefficiency are discussed.

The main properties of WBANs are support for low data rate application and low power communication, therefore the IEEE 802.15.4 standard is suitable for WBANs. In[27], IEEE 802.15.4 MAC protocol is a low power standard, the protocol being designed for low data rate applications. It operates with three frequency bands, such as 868 MHz, 915 MHz, and 2.4 GHz bands. In addition, there are twenty seven sub channels which are allocated in IEEE 802.15.4 standard, for instance sixteen sub channels in 2.4 GHz bands, ten sub channels in

the 915 MHz band, and one sub channel in the 868 MHz band. IEEE 802.15.4 MAC protocol has two communication methods: beacon mode and non-beacon mode. Furthermore, there is the beacon enabled mode with superframe, which uses slotted CSMA/CA methods in the contention access period (CAP), and utilises guaranteed time slots (GTS) in the contention free period (CFP). Non-beacon enabled mode without the superframe uses unslotted CSMA/CA[27].

In beacon-enabled mode[27], the superframe structure is bound by the transmission beacon frame by the coordinator. The beacon interval (BI) is the time period between two beacon frames. In addition, the superframe has an active/inactive portion which saves power through the inactive portion. The superframe duration (SD) represents the length of the active portion of the superframe, which contains sixteen slots comprising three portions: beacon period, contention access period (CAP), and contention-free period (CFP) respectively, as shown in Figure 3.1. The superframe is periodically sent by the coordinator and the beacons used to describe the superframe. At the beginning of the active period, the first slot is a beacon for each superframe. These slots are termed Guaranteed Time Slots (GTS), which are allocated in the Contention Free Period (CFP), and the Contention Access Period (CAP). Although the coordinator node can communicate with the nodes at will, the nodes need to wake up to receive the beacon[27].

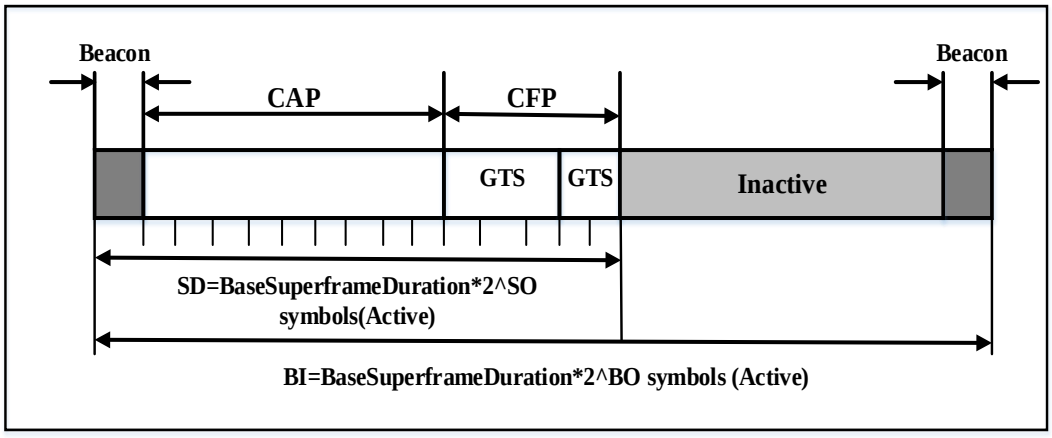

Figure 3.1: The structure of superframe in the IEEE 802.15.4

In beacon-enabled networks, the coordinator node (sink node) is specified as the superframe duration (SD) and beacon interval (BI) by determining values of both superframe order (SO) and beacon order (BO) in the beacon frame, which govern the structure of the superframe. The beacon order (BO) and superframe order (SO) are defined by the numerical parameters for BO and SO and define the value of BI and SD as follows[27]:

$$BI = BaseSuperframeDuration.2^{BO} \quad \text{for } 0 \le \text{BO} \le 14 \tag{3-1}$$

$$SD = BaseSuperframeDuration.2^{SO} \quad \text{with } 0 \le SO \le BO \le 14$$
$$where \quad BO \text{ is Beacon Oder and } SO \text{ is Superframe Order} \tag{3-2}$$

$$BaseSuperframeDuration = 960 \text{ symbols}(1\text{symbol} = 16\mu s)$$
$$BaseSuperframeDuration = 960 \text{ symbols} * 16\ \mu s \tag{3-3}$$
$$BaseSuperframeDuration = 15.36 \text{ ms}$$

The BaseSuperframeDuration is equal to the base slot duration multiplied by the number of superframe slots, for instance, the BaseSuperframeDuration is 15.36 ms based on a bit rate of 250 kbps. The range limitation of values for BO and SO is between 0 and 14 intervals. The duty cycle is a ratio between SO and BO given in equation (3-4)[27]. The duty cycle is lower when the inactive period is larger. The Duty Cycle (DC) is equal to one when the values of SO and BO are equal, which means no inactive period exists.

$$dutycycle = \frac{SO}{BO} \tag{3-4}$$

In [28], the authors proposed a MAC protocol based on a TDMA mechanism for WBSN to minimise idle listening and the probability of collision. Each node represents a slave node which is assigned a time slot by the master node (central node), with an extra time slot for the node if there is alarm which occurred at the node. Although it is designed for WBSNs, it only considers the implantable medical device. The devices are used to monitor medical conditions, for instance diabetes, muscle stimulants etc.

Lamprinos et al. proposed an energy efficient MAC protocol which supports medical applications. It is used to improve energy efficiency through the reduction of energy wastage sources, for instance, idle listening, extra power, and collision[29]. Moreover, the authors used the master-slave topology. Although improvement in energy efficiency is achieved in this protocol, some slaves will have a low DC whereas the nodes which are served later have a higher DC[29].

PB-TDMA protocol (Preamble-Based TDMA) is designed based on the TDMA protocol, the slots are allocated to the biosensor node which is used for the data transmission, avoiding the collision, and reducing energy consumption[30]. In PB-TDMA protocol, each TDMA

frame contains two sub slots: a preamble transmission slot and a data transmission slot, the preamble slots are utilised to activate the destination node then the node identifies the biosensor node which is a source node. Moreover, if a biosensor node has no data for transmission, the node turns off in order to save energy usage; the authors used NS-2 for the simulation. However, the PB-TDMA protocol supports the single hop TDMA protocol for WBSN, it does not consider on-demand traffic and critical data rate to handle life-threatening events in WBSN[30].

Omeni et al proposed a novel energy-efficient MAC protocol for WBAN based on TDMA MAC protocol in order to reduce the energy usage by controlled wakeup/sleep time[31]. Omeni's MAC protocol is designed for a star-networked WBAN which includes the master node (coordinator node) and slave nodes (on-body/implanted biosensor nodes). In addition, the main operation of the protocol involves three communication processes: the establishment of the link process, wakeup service, and alarm process. Furthermore, in Omeni's MAC protocol, all slave nodes are kept in the sleep mode until allocated a time slot form the master node, the protocol uses the wakeup back time (WFT) to address the time slot overlaps and the authors introduced the concept of WFT technique to minimise collision. If a slave node has a failure in its communication with master node, then the node goes back to the sleep mode depending on the WFT. However, the data of the slave node is buffered through the sleep time. The proposed protocol could reduce the problems such as idle listening and overhearing because the master node manages the traffic in the WBSN. For example, the performance of the simulation results shows reduction in the extra energy consumption which is generated from the overhearing and idle listening in the different application such as ECG, glucose monitoring, EEG, and human body temperature. Although Omeni's MAC protocol minimises the energy consumption and collision, only slave node (one node) can establish the link with the master node at a time. In addition, the implementation of the protocol is more complex, it does not consider the on-demand traffic, and it is designed for single hop topology WBANs[31].

In [32], a DTDMA protocol (reservation-based dynamic TDMA) is designed for the normal WBSN traffic; the allocated slots for the biosensor nodes are buffered biomedical packets, after that they are released to other biosensor nodes when the transmission of the biomedical data is completed. The DTDMA protocol provides more dependability in terms of low energy usage and low packet dropping rate when compared with IEEE 802.15.4. Moreover, the channel in the DTDMA protocol is bounded by the superframe which

contains three parts: beacon, Contention-Free Period(CFP) duration, and Contention Access Period (CAP) duration[32]. The structure of the superframe in DTDMA is different when compared with the superframe structure of IEEE 802.15.4, the CFP period being followed by the CAP period, which enables the biosensor node to send CFP traffic before CAP traffic. The configuration of an inactive duration is used to save energy usage at the biosensor node depending on the CFP. The inactive duration will be increased if there is no CFP traffic. Although the DTDMA protocol has dedicated slots for the biosensor nodes depending on the traffic information, it has several limitations such as that it does not consider sub-channels of the Medical Implant Communications Service band (MICS). Furthermore, in WBSN, the DTDMA protocol does not consider on-demand and emergency traffic[32].

The Distributed Queuing Body Area Network (DQBAN protocol) is alternatively enhanced 802.15.4 MAC in the Body Sensor Network (BSN). It uses a novel cross-layer fuzzy logic dependent on the scheduling algorithm[33]. In the experimental results of DQBAN MAC protocol, it is proven that there is no delay increase seen in the measurement of end to end delay, better transmission mechanisms which use less energy consumption, and less collisions in healthcare application. In addition, the DQBAN protocol is adopted with heterogeneous traffic, the number of the biosensor nodes in a hospital BSN, and interferences. Although the performance of the DQBAN protocol is the best when compared with other protocols, it has a complex algorithm and it does not adopt channel condition[33].

In [34], BodyMAC protocol is proposed, the energy efficiency based on TDMA protocol for WBSNs, the protocol uses three bandwidth allocations: periodic, adjust, and burst bandwidth to enhance the energy efficiency and the flexible bandwidth used to reduce the packet collision, idle listening, and control packet overhead. In addition, if the sensor nodes have no data to transmit, they remain in the sleep mode which is implemented for the low duty cycle of the sensor nodes. The superframe structure of BodyMAC protocol is divided into three parts: beacon, downlink, and uplink frame. The beacon period represents the synchronisation, the data transmission from coordinate node to sensor utilises the downlink which accommodates on-demand traffic. However, the uplink frame is divided into two types: firstly, CAP, which is used to send small sized MAC packets and secondly, CFP, which is used to avoid collision through the coordinator node allocating the GTS to the sensor nodes. The CFP is used to reduce the energy usage through the communication. Although the simulation results of the performance for BodyMAC protocol is better than

IEEE 802.15.4 MAC standard performance as regards saving energy and end-to-end delay packets, BodyMAC protocol could not handle emergency traffic[34].

In [35], Medical Medium Access Control (MedMAC protocol) is proposed for WBSN to reduce energy dissipation and enhance the channel access mechanism based upon adaptive TDMA MAC protocol. MedMAC protocol assigns the time slots for the biosensor nodes which are required to transmit the data by using the TDMA approach. However, the slots are of variable length and vary depending on the requirements of the biosensor nodes. Moreover, the protocol uses the multi-superframe structure. Although the performance of MedMAC protocol is better than IEEE 802.15.4 standard in the energy usage because it uses GTS, MedMAC protocol is not suited for biosensor nodes in WBSN because it relies on the low data traffic. In addition, the authors implement the MedMAC protocol by using OPNET simulator[35].

The power-efficient MAC protocol is proposed as a novel mechanism of MAC protocol for WBSNs, it considers traffic such as on demand, normal, and emergency traffic[36]. The protocol is defined with two wakeup approaches: firstly, a wakeup radio technique for the normal traffic transmission which is generated periodically by the biosensor node in normal situations, and secondly, a wakeup radio technique for the emergency traffic transmission (or on–demand traffic) which is generated unpredictably in emergency situations. Furthermore, the proposed protocol improves both the network lifetime for WBSNs and reliability. The performance of the results for the proposed protocol is better than WiseMAC protocol in terms of energy consumption and delay[36].

Stevan Jovica Marinkovic et al. proposed a low duty cycle MAC protocol based on TDMA, which is designed for the single hop topology; the protocol implements a TDMA mechanism, which is not suitable for the dynamic networks[37]. The authors used a guard time between every sequential slot to prevent overlaps and minimise bandwidth waste. Also, the protocol uses the TDMA strategy to avoid collision and reduce the energy in the WBSN. Although the communication idle listening and overhead are reduced by using the protocol and by improvement of energy efficiency, the protocol considers the static BAN and it could not achieve a wake up mechanism for low duty cycle nodes[37].

A battery dynamics-driven MAC protocol is proposed based on TDMA MAC protocol with cross-layer design to prolong the network lifetime[38]. This protocol considers the properties such as time-varying wireless channels, battery, and packet queuing; it has the

same divide for the slots as in IEEE 802.15.4, which includes the beacon slot, active slots, and inactive slots. The biosensor node transmits the data through the active period and then it returns to the sleep mode to decrease the energy usage. In addition, the protocol uses Guaranteed Time Slots (GTS) to achieve timely and reliable delivery of packets. Although the performance of the results of the analytical analysis and simulation show significant improvement of battery life of the biosensor nodes in a WBSN, the protocol cannot handle emergency data[38].

In medical applications, an Urgency-based MAC (U-MAC) protocol is proposed depend on IEEE 802.15.4a standard for WBSN; it allows an increase in the probability of access for the critical nodes which have urgent health data through the cutting–off of the packet retransmissions for the non-critical nodes[39]. In U-MAC, the protocol classifies the biosensor nodes into two kinds: the critical nodes and non-critical nodes. The critical biosensor nodes have a priority for packet transmission over non-critical biosensor nodes. Furthermore, the mathematical results for the star topology of WBSN is shown to be affected by the number of packet retransmissions for both critical and non-critical nodes[39].

In [40], Heartbeat Driven MAC (H-MAC) employs human heartbeat rhythm information for synchronisation of the biosensor nodes to reduce the energy consumption through avoiding the external clock. In the H-MAC protocol, from the sensory data of biosensor nodes a BSN could extract the heartbeat rhythm by detecting waveform peaks. Also, it improves the energy efficiency for the star topology WBAN, which avoids collision through allocated Guaranteed Time Slots (GTS) for each node in the network. In addition, the coordinator node sends the control packets to the biosensor nodes when necessary, then the transmission exists only between the biosensor nodes and coordinator node. Although the extra energy of synchronisation is reduced by the H-MAC protocol, it could not support emergency events. In addition, the allocated slots for each node are not suitable for variable traffic. H- MAC is designed for a star topology WBAN only; the energy gain is not shown in the simulations. The patient's heartbeat rhythm information may vary based on their condition[40].

In[41], the authors proposed a priority guaranteed MAC protocol (PG-MAC) which supports medical applications and non-medical applications (consumer electronic). The contention access period (CAP) and contention-free period (CFP) are combined, which represent the superframe structure in the PG-MAC protocol. The CAP period is divided into two periods: C1 is utilised for the medical applications of a life-critical nature and C2 is used

for the consumer electronic applications. On the other hand, CFP period is divided into two time slots: TSRP (Time Slot Reserved for Periodic Traffic) periods used for the periodic traffic and TSRB (Time Slot Reserved for Bursty Traffic) periods used for the bursty traffic. Moreover, the aim of the GP-MAC protocol is to provide high reliability and low latency for medical applications via an energy efficiency technique, while it also provides a high data service for consumer electronic applications. Although the performance of the simulation is significantly improved in terms of energy consumption and throughput when compared to IEEE 802.15.4 MAC protocol, PG-MAC has a complicated superframe structure and is not a suitable the emergency traffic and on-demand in WBSNs[41].

In [42], the researchers proposed a novel MAC protocol which integrates the relay node and power control mechanism to decrease the energy usage in the WBSN; the protocol is termed Enhanced MAC (EMAC). On the one hand, when the EMAC protocol selects the relay node to network to save energy, this switches the topology from single hop to multi hop. Also, the structure of the superframe is modified. On the other hand, the EMAC protocol performs the dynamic power algorithm in the sensor nodes which have packets to transmit in order to increase the network lifetime. With respect to the simulation results, the performance of the EMAC protocol significantly prolongs the network lifetime compared to standard IEEE 802.15.4[42].

In [43], the authors proposed a new MAC protocol which is named Adaptive MAC (Ada-MAC), which depends on IEEE 802.15.4 standard for medical health care solutions (MHCS). It is used to minimise packet collision ratio and packet loss ratio according to the adjustment of dynamic traffic loads. Also, Ada-MAC protocol achieves reliability and transmission in real time, it represents the hybrid protocol which combines contention-based CSMA/CA and schedule-based time triggered protocol (TTP). In addition, the authors used the priority queue mechanism in order to reduce the delay for the high priority data in the queue. The superframe structure for Ada-MAC is divided into three parts: CFP, CAP, and inactive period. In proposed protocol, the CFP period is followed by CAP duration in order to transmit data packets earlier than in the CAP. With respect to simulation, the authors used OMNET++ simulator to examine the proposed protocol; the performance results for the proposed protocol outperform IEEE 802.15.4 MAC protocol in terms of real time response and reliability for critical data transmission. However, the proposed protocol is not a practical scheme for WBSNs as it uses multiple priorities queues for the traffic[43].

The Decrease of Transmission Delay (DTD MAC protocol) is proposed in [44] and is used to reduce the transmission delay and packet loss depending on the data process in the WBSN. In addition, the proposed protocol has a new pattern bit map (PBM) configuration in the Pre-Slot Assignment Period (PSAP) slot according to pattern exchange time slot (PET) in the Bio-MAC. In the simulation, the DTD-MAC protocol significantly minimises the average transmission delay compared to the Bio-MAC protocol. However, the proposed protocol considers only the environments which have no urgent data, therefore the response to processing data (mixed urgent data and general data) is not flexible[44].

In [45], the authors proposed a Medical Emergency Monitoring MAC protocol (MEM-MAC) which represents an energy-efficient WBAN MAC protocol, used to monitor BSNs in medical emergencies. The main concept of the protocol is that it uses short active time slots which are embedded in long inactive durations, then uses these slots to transfer the emergency data and commands. Moreover, the protocol classifies the data into two types: small and big data. The performance of the MEM-MAC protocol depends on the medical emergency traffic. At the same time, both the energy consumption is effectively decreased and the delivery delay is satisfied when traffic is a low. However, MEM-MAC performance deteriorates quickly when the traffic of a medical emergency is high. Although the MEM-MAC protocol has a greater energy efficiency than IEEE 802.15.4 standard, the superframe structure is a fixed one which operates with low data rate biosensor nodes without consideration of the high data rate for the medical monitoring nodes[45].

In [46], a Low Duty-Cycling MAC (LDC-MAC protocol) is designed for low data-rate medical WBANs, it is specially designed to enhance the energy efficiency and increase the network lifetime. Moreover, LDC-MAC uses a longer superframe which is exploited to decrease the energy usage through reducing the redundant frames of each transmission and reception. The authors have integrated the CSMA and TDMA mechanisms. The LDC-MAC protocol could support complex traffic modes; it operates with low/high data rate medical monitoring nodes, and it represents adaptive MAC protocol. The biosensor node transmits the data toward the coordinator node, which is called an upload data subsection, whereas the data transmission from the coordinator node to the biosensor node is called a download data subsection. In addition, the insertion time slot in the two subsections are termed an upload and download insertion time slot[46]. Although the results of LDC-MAC performance are better in the low data rate for the medical monitoring traffic and highly improved energy efficiency than IEEE 802.15.4 standard, the LDC-MAC protocol cannot solve the problem

of overhearing and idle listening when they happen in the broadcast time, ACK subsection, and download data subsection. Furthermore, if the coordinator has urgent data for transmission, it should wait until the current superframe for the biosensor node is completed then use a new superframe to transmit the data[46]. Table 3.1 summarises the reviewed MAC WBSN protocols.

Table 3.1: Comparison of MAC WBSN protocols

The proposed MAC protocols	**IEEE 802.15.4 based**	**TDMA based**	**CSMA based**	**Star topology**	**Key Features**	**Medical application**	**Free collision**	**Energy efficiency**	**Publication**
[28]	√	√		√	Data transmission on the periodic intervals DC: Beacon + CAP+CFP	√	√		2004
Lamprinos [29]		√		√	DC: Beacon +CAP+GTS			√	2005
PB TDMA [30]	√	√		√	Employs traditional TDMA principle DC: Preamble + time slots allocated	√	√	√	2008
Omeni MAC [31]	√	√		√	Three communication processes: The establishment of the link process, wakeup service, and alarm process. It uses wakeup back time (WFT). Fixed traffic in multi-channel and centrally controlled synchronisation.	√	√	√	2008
DTDMA [32]	√	√		√	DC: Beacon + CFP+ CAP+ inactive period	√		√	2009
DQBAN [33]	√	√		√	Fuzzy rule-based scheduling algorithm DC: Body to coordinator: m (access min-slots) + n (scheduling min-slots) + data slot. DC: Coordinator to body: Ack+ Syh. preamable + Fix slots	√	√	√	2009
BodyMAC [34]	√	√	√	√	Scheduled contention-based, Flexible bandwidth allocation DC: Beacon+ downlink+ uplink	√		√	2009
MedMAC [35]	√	√		√	It is suited to periodic data. DC: Beacon + optional contention period + CFP. Dynamic adjustments for QoS requirements are obtained to maximise energy efficiency.	√		√	2009

Table 3.1: Continued

The power efficient MAC [36]	√	√			Traffic-based wakeup / wakeup radio mechanism DC: Beacon + configurable contention access period (CCAP) + CFP.	√		√	2009
LDC MAC [37]	√	√		√	A low duty cycle MAC protocol. DC: Timeslot(Sn) + Guard interval + RSn (reserved for retransmission)	√	√	√	2009
[38]	√	√			It considers the properties such as time varying wireless channels, battery, and packet queuing DC: Beacon active slots + inactive period	√		√	2009
U-MAC[39]	√		√	√	It allows increase in the probability of access for the critical nodes Allocate to critical nodes	√		√	2010
H-MAC[40]		√		√	Exploit heartbeat rhythm for synchronisation fixed slot allocation (GTS) for each node	√	√	√	2010
PG-MAC [41]	√	√		√	Periodic + bursty DC:Beacon+TSRP+C1+C2+TSRB+inactive	√ + non	√	√	2011
[42]	√	√		√	EMAC integrates the relay and power control mechanism DC: Received Beacon + Incoming (received) superframe + inactive + transmitted beacon + outgoing (transmitted) superframe + inactive + received beacon	√		√	2013
[43]	√	√		√	It is a hybrid protocol: contention-based CSMA/CA and schedule based TTP DC: Beacon + CFP + CAP	√	√		2015
[44]	√	√	√		DTD MAC is Pre-Slot Assignment Period slot DC: Beacon + GTS periods + inactive + PSAP (PreSlot Assignment Period)	√	√		2015
MEM-MAC [45]		√		√	Short active time slots DC: Beacon + CAP1 (optional) + interposition slot (data/ACK selection) + inactive + CAP2 (optional)	√		√	2016
LDC-MAC [46]		√	√		Low data rate medical WBSN DC: Beacon + optional CFP + loop period + CAP optional	√		√	2017

3.3 The Duty Cycle Mechanism

The details of the Duty Cycle (DC) are demonstrated, which is used in the IEEE 802.15.4 MAC standard in this section. Subsections provide the information about DC as per the following: the first subsection defines the term of Duty Cycle (DC) technique, the second subsection classifies the types of duty cycle, the final subsection explains, and discusses some of the existing duty cycles mechanisms proposed for the IEEE 802.15.4 MAC standard.

3.3.1 A Brief Definition of Duty Cycle

The concept of switching the node to active or sleep mode can be achieved with a duty cycle. The nodes can be activated whenever they need to transmit the data to the sink node; otherwise they will be in sleep mode to reduce the energy consumption [47]. In addition, in fact, duty cycling may be the most important of all the "green" techniques [48], a primary mechanism in general wireless networks, and a necessity if there is a requirement for nodes to operate for more than a few days before recharging the battery. This is a typical condition of Wireless Sensor Networks (WSNs). The proportion of the time during which the node stays in the active state to the whole time of active and sleep states is called the duty cycle. The sensor nodes in duty cycle turn their status between active and sleep mode[49].

3.3.2 Taxonomy of Duty Cycle Mechanism

In this subsection is the classification of the duty cycling mechanism into two types: synchronous mechanism and asynchronous mechanism [50].

3.3.2.1 Synchronous Duty Cycle MAC Protocol

In coordinated (synchronous) duty-cycle WSNs, the sensor nodes swap the synchronisation information of neighbouring nodes periodically with each other to consult their sleep/wake schedules, so that data transmission can transmit during the awake time slots. Moreover, in a Coordinated Duty Cycle (CDC), sensor nodes are required to broadcast extra information about their active-sleep schedule [51]. In addition, synchronous mechanisms tend to be more complex in the computation, transmission/reception overhead, or hardware. It is also more expensive in the above terms[52]. For example, S-MAC protocol [53], T-MAC protocol [54], and B-MAC [55] represent synchronous duty-cycled MAC protocol.

In [53], a Sensor MAC (S-MAC) protocol is designed based on the scheduled contention mechanism to avoid the idle listening problem. It uses the low duty cycle as a default for the nodes. The coordinator node is allocated a wakeup time for all the nodes in the network; the node wakes up in its own specific time which is scheduled from the coordinator node. In addition, if a node has data for transmission, it uses the wakeup duration for the transmission, then it switches to the sleep mode, the sleeping period of each node is the same in the S-MAC protocol, in order to avoid packet collision and idle listening, and reduce overhearing. Moreover, the energy consumption is minimised in the S-MAC protocol. Although the S-MAC protocol is designed for multi-hop WSNs and it reduces the energy wastage, it could not support priority given to emergency traffic, and it does not support the fluctuation of traffic. Furthermore, the S-MAC protocol cannot achieve reliability for WBSNs[53].

In [54], Time-out MAC (T-MAC) protocol uses the flexible duty cycle; it achieves an increase in the energy efficiency in WBSNs. Each node in the T-MAC protocol is waked after it has been allocated a time slot, then the node starts to transmit the pending packets. In addition, if the node has no activation event for the time interval, the node switches to the sleep mode. In addition, if the node has not received the Clear To Send (CTS) after it has sent the RTS Request To Send (RTS), then it sends RTS more times, after that it is gone to the sleeping. Although T-MAC protocol reduces the energy consumption for the nodes and achieves minimised delay, it suffers from the sleeping problems[54].

In [55], the authors proposed the B-MAC protocol based on CSMA mechanism; this uses a long preamble for the transmission and reception. In addition, B-MAC employs the long preamble which causes a longer delay. The energy consumption is low for the low traffic in B-MAC which does not include synchronisation overhead. However, the transmission of data from the source node toward the destination requires extra time[55].

3.3.2.2 Asynchronous Duty Cycle MAC Protocol

This refers to where sensor nodes are turned on and off in a random fashion separate from each other. As to the random duty cycling, it has advantages such as that it has good scalability and simplicity, without including any further communication overhead for coordination among neighbours. However, if the wireless radio is randomly turned off, it will not achieve certain connectivity of the network[56].

Furthermore, asynchronous mechanisms are less than synchronous mechanisms in expense, however the end-to-end latency is higher because of the sleep waiting. Sleep

waiting happens when a node is required to wait for another node to wake up, before the transmission of the frame [52]. For instance, X-MAC [57] and WiseMAC protocols [58] are representative examples of asynchronous duty cycle MAC protocols. In the X-MAC protocol is employed a short preamble to minimise energy consumption and to minimise latency through the selection of the sleeping time in a wireless sensor network[57].

In [58], the WiseMAC protocol is designed based on the CSMA, which uses Low Power Listening (LPL) to reduce the power consumed. Preamble sampling mechanisms are used in WiseMAC protocol to active the receiving node of a packet arrival. Moreover, WiseMAC protocol is performed under variable traffic; however, in the star topology of WBSN, LPL technique is not given as the optimal solution to support both wearable and implantable medical sensor node communication simultaneously. In addition, WiseMAC cannot support the energy efficient WBSN[58].

3.3.3 Overview of Duty Cycle Mechanism

In the IEEE 802.15.4 standard, there are several approaches which have been developed toward the adaptive or adjusting duty cycle control.

Ramachandran et al. [59] have presented a non-persistent CSMA algorithm with backoff period in order to improve the energy consumption and throughput. The authors use the Markov models which separately develop the node states and channels. In addition, the main objective of the proposed scheme is presented as the effect of the shutdown for nodes with no packets for transmission. The ns-2 is used for the simulation with the depending on IEEE 802.15.4[59].

In [60], the authors introduced a new Beacon Order Adaptation Algorithm (BOAA) for the standard IEEE 802.1.5.4 based on beacon-enabled mode. The new algorithm is determined by the adaptation of the beacon interval (BI) and required duty cycle (DC); it considers the star topology. The dynamic beacon order has an impact on the duration of the duty cycle in wireless personal area network (WPAN), and the value of SO is fixed. If the value of the beacon order (BO) is greater than that of SO, then the length of the inactive period will be more than the length of the active period within the beacon interval (BI). Moreover, the coordinator node adjusts the beacon order depending on the amount of traffic through the beacon interval. Although the algorithm reduces the energy consumption, throughput is decreased and the number of nodes is static, which works with low data rates[60].

Barbieri et al. proposed an Adaptive MAC Protocol for Efficient (AMPE) which can dynamically vary the duty cycle scheme at each node depending on the estimation of the traffic load[61]. AMPE considers a beacon-enabled personal area network, the superframe structure being split into two parts: active period and inactive period. In addition, the coordinator node calculates the superframe occupation ratio, then it compares with the lower and upper threshold. If the value of the SO occupation is higher than the upper threshold, the coordinator node increases the superframe order (SO); if the value of SO is less than the lower threshold, the coordinator node decreases the superframe order (SO). In another case, if the value of superframe occupation is not in range of the threshold, the coordinator node adapts the duty cycle. Moreover, the performance of simulation results is enhanced in the link throughput and node lifetime[61].

In [62], Jeon et al. proposed a novel DCA (DC adaptation) algorithm for the beacon-enabled approach based on IEEE 802.15.4. The DCA algorithm uses information about queueing delay and buffer occupancy at the MAC, which is termed a MAC layer status index (MSID), to adjust the length of the active period. The proposed algorithm achieves increased energy efficiency and serves to minimise the packet drop when it employs the duty cycle[62]. However, DCA uses a fixed beacon interval (BI) which could increase energy consumption if the value of the beacon order (BO) is smaller. Also, the DCA algorithm could not consider traffic deadlines for the adjustment of the duty cycle. Although the DCA algorithm increases the energy efficiency and reduces the packet drop in a one hop beacon-enabled network, it is not considered a multi hop beacon-enabled network[62].

In [63], the researchers proposed Extended Contention Access Period algorithm (ECAP), a bursty traffic adaptation algorithm based on beacon-enabled networks for IEEE 802.14.5. In addition, the proposed algorithm is designed to dynamically extend the active duration depending on the requests from the nodes; it exploits the busy tone transmitted, which is transmitted from some nodes to the coordinator node after the contention access period (CAP) to indicate that some nodes were not able to transmit all data because of heavy traffic. Although the transmission of the busy tone consumes energy, the energy usage and end-to-end delay are reduced per packet transmission by using the algorithm in simulation[63].

In an IEEE 802.15.4-based WSN, the researchers propose a Dynamic Duty Cycle Adaptation to Real time data (DDCAR); the proposed algorithm adapts the duty cycle in order to minimise the packet delay and support time of delivery in the real time data. Moreover, the superframe structure has active and inactive duration, the adjustment of the

active period for real time is performed by the coordinator node which employs the proposed algorithm based on beacon-enabled mode. The coordinator node immediately extends the active period to adjust the period of real time traffic through the switching time between a node and a coordinator node[64].

An Individual Beacon Order Adaptation (IBOA) Algorithm is proposed for IEEE 802.15.4. The IBOA algorithm considers reducing of the energy consumption; it uses individual beacon order adaption and DC at the same time[65]. Moreover, if the value of BO is high and the value of SO is low, the inactive period of the SO should be greater than the active period. Then, the packets will be held in the queue of nodes and the value of the end-to-end delay will rise. Moreover, the coordinator node adjusts the value of BO for the next period depending on the status of the queue for the transmission of nodes. With respect to simulation of the IBOA algorithm, it operates with variable traffic: the energy consumption is minimised under light traffic, whereas it improves the performance of end-to-end delay under heavy traffic[65]. Although it reduces the energy consumption and it considers BO for improvement of the network performance, SO defines the active period and duty cycle of the nodes. In addition, the number of nodes is static; the authors used six nodes only[65].

In [66], the authors proposed a novel mechanism which reduces energy consumption and enhances throughput in the standard IEEE 802.15.4 by using information on data traffic. The nodes cannot transmit their packets during the active time but they can transmit packets in the inactive period (the time intervals allocated to inactive period), which is called sentinel duration. Moreover, the proposed model utilises ATS (Arbitrary Traffic Signal) and TTO (Traffic Time-Out) to improve IEEE 802.15.4 with an adaptive active period[66].

Kouba et al. [67] presented a scheduling scheme which is named Time Division/Beacon Scheduling (TDBS), TDBS employs the Superframe Duration Scheduling algorithm (SDS). The SDS is used to avoid beacon collision. Moreover, the SDS and efficient duty cycle scheme distribute the bandwidth in an equal manner based on traffic needs by using a set of linear equations. The TDBS technique is implemented in the test bed[67].

In [68], the authors have designed a learning algorithm based on the reinforcement learning (RL) theory. The proposed algorithm uses the optimal strategy for adjusting the superframe order. The performance of the results could reduce the energy consumption and delay of the packet, then it makes a good tradeoff between the energy consumption and delay

packets. However, the proposed algorithm is more complicated when calculating for the practical network[68].

In [69], the authors proposed Dynamic Superframe Adjustment Algorithm (DSAA) which can dynamically adjust the superframe structure of DC according to the certain features for IEEE 802.15.4 such as collision ratio and channel opportunity; the coordinator node observes the collision ratio and channel opportunity. Moreover, the DSAA changes the value of superframe order which will change the SD whereas the value of BO is constant. The aim of this protocol is to reduce the energy usage and enhance channel utilisation. The coordinator node computes the next superframe order depending on the calculation of the collision rate and the occupation rate. The performance of the simulation results improves the energy efficiency[69].

Valero et al. In [70] presented a Deployable Energy Efficient 802.15.4 MAC Protocol (DEEP) which optimises the distribution of GTS in order to effectively reduce energy usage through reducing the size of the communication beacons. Furthermore, upon the implementation of the DEEP protocol in the simulation, the GTS optimisation was increased, saving energy from 15% to around 50% when compared with IEEE 802.15.4 standard at the same level of function[70].

Gadallah and Jaafari in [71] have introduced a reliable energy-efficient WSNs MAC scheme which is dependent on IEEE 802.15.4 non-beacon enabled mode. Furthermore, the duty cycle is basically divided into two types: active periods and inactive periods. The nodes contend to access the medium during the active duration based on the unslotted CSMA technique; the nodes remain in the active mode until the delivery of critical data traffic, which achieves higher reliability. On the other hand, the nodes are asleep during the inactive periods, which conserves more energy than the standard non-beacon-enabled IEEE 802.15.4 protocol. In addition, the nodes are always awake and contend to the access medium. The experimental results of the proposed mechanism performed generally better than the standard protocol (IEEE 802.15.4) in terms such as energy conservation and all traffic types[71].

In [72], the authors proposed a Duty Cycle Learning Algorithm (DCLA) which adapts the duty cycle in order to decrease the energy usage. In this algorithm, the optimal value of SO and BO is achieved based on a complex calculation, which balances the delay and probability of successful data delivery with reduced energy consumption. Although the

energy consumption is reduced and DCLA uses reinforcement learning (RL), which represents the scheme for the selection of a best DC based on the learning, DCLA could not be implemented by the testbed or simulations because it is more complicated calculation. The DCLA is considered only for fixed traffic[72].

In [73], the authors presented an extension to the IEEE 802.15.4 standard in order to achieve saving energy for the nodes, improve the reliability, and achieve better channel utilisation; they used adaptive sleeping periods, which makes it possible to save energy consumption and reduce packet collisions. Although the theoretical analysis is dependent on Markov chain, and the results of the proposal achieve more saving of energy, improve reliability, and achieve better channel utilisation by using Matlab software, the proposed model considers the fixed traffic network and the performance is not validated by using test beds or the simulations[73].

In [74], the researchers examined the impact of changing values of BO and SO on medium access delay, energy consumption, and packet loss ratio. In the simulation scenario, the authors utilised two biosensor nodes (ECG and blood analysis module) in order to study the MAC protocol parameter for the network behaviour and also for reducing energy consumption. In addition, the values for BO and SO are equal from zero (0) to fourteen (14); if the BO value is lower than three (3), the energy consumption is more than at the high values of BO according to the simulation results[74].

In [75], the authors proposed an Enhanced Beacon Enabled Mode for the application of the low rate based on IEEE 802.15.4 standard; the proposed mode uses two mechanisms: Synchronised Low Power Listening (S-LPL mechanism) and Periodic Wakeup (PW mechanism). In addition, the overhead of synchronisation is reduced by S-LPL for low data rate; S-LPL improves the ability of nodes to save energy consumption: it allows the nodes to sleep for multiple beacon intervals, while PW, is implemented through inactive periods of superframe and reduces the packet loss rate and transmission delay; PW allows the nodes to transmit at scheduled times through the inactive period. The performance of the simulation results for the proposed enhanced mode is better than IEEE 802.15.4, the standard, in terms of reducing power consumption, reducing packet loss rate, and duty cycle. The authors use OPNET as the simulation software[75].

In [76], the researchers presented Adaptive Algorithm to Optimise the Dynamics (AAOD) for IEEE 802.15.4 networks to reduce energy consumption. Moreover, the

adaptation and optimisation for the activity periods and time of transmission are employed in the proposed algorithms, which consider IEEE 802.15.4. In the AAOD algorithm, the coordinator device calculates the received packets number in each superframe order and it compares them with the received packets number in the previous superframe. Then, the coordinator can adjust the active period depending on the comparison. If the number of received packets is increased above the threshold, the SO length is increased by the coordinator node and vice versa depending on the traffic in the network. Although the AAOD algorithm can reduce the number of the collisions and it is compliant with IEEE 802.15.4, the consumed energy is high than other algorithms and AAOD does not consider traffic deadlines and congestion level[76].

In [77], the researchers proposed a dynamic and self-adaptive algorithm, used to adjust a DC based on the adjustment of beacon order (BO) and superframe order (SO), which is termed Dynamic Beacon Interval and Superframe Adaptation Algorithm(DBSAA). Moreover, the coordinator node dynamically adjusts the BO and SO depending on the four parameters such as the number of nodes in the network, the received packets number at the coordinator node, the collision ratio, and the superframe occupation. DBSAA is more flexible to adapt the duty cycle, which achieves energy saving, growth in throughput, and reduced end-to-end delay. However, DBSAA supposes that all nodes in the networks use the same data rate[77].

Gilani et al. [78] proposed an adaptive hybrid MAC protocol to decrease energy consumption and enhance throughput based on some modifications to the original IEEE 802.15.4 standard. Moreover, in this proposed approach, the coordinator node is adaptively divided Contention Access Period(CAP) between slotted CSMA/CA and TDMA depending on the data queue of nodes and the collisions level in the network. When the amount of data traffic is light, the setting of the contention access period (CAP) should be lengthened in order to achieve fast channel access[78]. By contrast, if the data traffic is heavy, the setting of the contention free period should be lengthened to relieve collision of the channel access. In the simulation results, the CSMA/TDMA hybrid protocol performs more efficiently than IEEE 802.15.4 standard by both metrics: energy consumption and throughput. However, the end-to-end delay is increased as a consequence of the hybrid protocol. The proposed protocol is implemented by using OMNET++ simulator [78].

In [79], the authors proposed a hybrid context-aware MAC (CAMAC) protocol which is a context-aware and varying traffic MAC protocol. It is used to enhance energy efficiency

and to minimise delay under real-time varying traffic management. In the CAMAC protocol, the duty cycle is dynamically adjusted for each sensor node under adaptive traffic in order to decrease the delay to the packet delivery in CAMAC protocol. Also, the data rate for each sensor node is dynamically adjusted in order to make the CAMAC protocol adapt with traffic.

In addition, the researchers introduced a new hybrid superframe structure which includes three parts: beacon, contention, and TDMA. Although the length of the superframe and beacon is a constant period, the period can be adaptively adjusted, which allocates time to the contention or TDMA part[79]. With respect to the contention part, the slots are adapted for the CSMA/CA mechanism. The contention free TDMA part has two subparts: scheduling-based slots and polling-based slots. The schedule-based slots are allocated to the biosensor nodes based on the traffic nature by the coordinator during the CAP. However, the polling-based slots are assigned to the biosensor nodes in emergency cases by the coordinator node. Although the proposed protocol improves energy efficiency and reliability, the adjustment of the dynamic traffic is not based on traffic load estimation[79].

In [80], the researchers is proposed a new Adaptive Duty Cycle Algorithm (ADCA) to improve energy efficiency based on beacon-enabled WSN. The coordinator node collects network information, such as the queue state of the nodes and the idle time; it enhances the capability for estimation of the network traffic, and it adjusts the DC of the network. Furthermore, the coordinator node selects the next superframe order (SO). The ADCA increases the accuracy and the speed of adjustment for the duty cycle[80].

Shu et al. [81] used an interrupt mechanism (I-MAC) to propose a hybrid MAC protocol which improves the energy efficiency, time slots, and the delivery of needed data. The I-MAC protocol uses a long superframe structure for the emergency data transmission [81].

In [82], the authors studied two main parts; the first part represents the survey which deals with IEEE 802.15.4 MAC protocol and parameters, the second part is that which studies the impacts of MAC parameters on WBSN performance gains in the presence of interference though simulation. Furthermore, it is observed that both beacon order (BO) and superframe order (SO) have an impact on WBSN.

In [83], the authors proposed a novel mathematical model for body area network (BAN) topology to explain the deployment of and connection between biosensor nodes, simple relay nodes, network coding relay nodes, and the sink node. This model uses the coordinated

duty cycle (CDC) technique and Random Linear Network Coding (RLNC) to improve the energy efficiency in the bottleneck zone. It was apparent that energy consumption is reduced with the proposed mechanism but the proposed approach is not implemented with a real BAN. Table 3.2 summarises duty cycle protocols.

Table 3.2: Comparison for duty cycle protocols in WBSN

The proposed scheme	IEEE 802.15.4 based	Beacon enabled	Non- Beacon enabled	Star topology	Key features	BO	SO	Energy efficiency	Publication
[59]	√	√		√	Non- persistent CSMA with backoff.	Fixed (=6)		√	2005
BOAA[60]	√	√		√	Dynamic BO adjustment scheme. Adjustment of DC	Dynamic	Fixed	√	2005
AMPE[61]	√	√		√	The estimation of the traffic load. Vary the duty cycle	Fixed (BO=6)	Dynamic		2006
DCA[62]	√	√			MAC layer status index (MSID) Adaptive duty cycle	Fixed (BO=7)	Dynamic	√	2007
ECAP[63]	√	√			Bursty traffic adaptation algorithm. Adjustment DC (Extend CAP).	Fixed	Dynamic	√	2007
DDCAR[64]	√	√		√	Adaptive DC with real time data	Fixed	Dynamic	√	2008
IBOAA[65]	√	√		√	Dynamic BO adjustment scheme. Adjustment of DC	Dynamic	Dynamic	√	2008
[66]	√	√		√	Adaptive active period Adjustment of DC	Fixed	Dynamic	√	2008
TDBS[67]	√	√			Time Division Beacon Scheduling (TDBS) mechanism Efficient DC	Variable	Variable	√	2008
[68]	√	√		√	Utilises Reinforcement Learning (RL). Optimal strategy for the DC	Optimal	Dynamic (Optimal)	√	2009
DSAA[69]	√	√		√	Dynamic superframe adjustment. Dynamic DC	Fixed	Dynamic	√	2010
DEEP[70]	√	√		√	Distribution of the guaranteed time slots			√	2010
[71]	√		√	√	Unslotted CSMA technique with critical data traffics			√	2010
DCLA[72]	√	√		√	Used reinforcement learning (RL). Learning the best DC.	Fixed	Dynamic	√	2011

Table 3.2: Continued

DCLA[72]	√	√		√	Used reinforcement learning (RL). Learning the best DC.	Fixed	Dynamic	√	2011
[73]	√	√		√	Adaptive sleeping period. Adjustment of DC.	Fixed	Dynamic	√	2011
[74]	√				BO and SO have impact on the network behaviour. The network load does not allow low duty cycles.	Variable (1-14)	Variable (1-14)	√	2011
DBSAA[75]	√	√		√	S-LPL and PW mechanism are used. Adaptive DC is used.	Fixed (0-14)	Variable	√	2012
AAOD[76]	√	√		√	Adaptation and optimisation for activity periods and time of transmission. Dynamic optimisation SO.	Fixed	Dynamic		2013
DBSAA[77]	√	√		√	Dynamic Beacon interval and Superframe Adaptation Algorithm. Adaptive DC.	Variable (Dynamic)	Variable (Dynamic)	√	2013
[78]	√	√		√	CSMA/TDMA hybrid protocol	Variable (3,7)	Variable (2, 6)	√	2013
[79]	√			√	Hybrid superframe structure of CA-MAC. Beacon + contention + TDMA			√	2013
ADCA[80]	√	√		√	The coordinator node has information such as Queue status and idle time. Adaptive DC.	Fixed	Dynamic	√	2014
[81]	√	√		√	CAP periods with the interrupt slots.			√	2015
[82]	√	√		√	Superframe order less than Beacon order.	Variable 1) BO=4 2) BO=4 3) BO=7 4) BO=7	Variable 1) SO=1 2) SO=3 3) SO=1 4) SO=3	√	2015
[83]	√	√			Coordinated Duty cycle	Fixed	Dynamic	√	2017

3.4 The Energy Consumption Model

There are four different states for the energy consumption of a sensor node: sensing and processing data, receiving, transmitting, and sleeping state[7]. Here, the energy consumption for communication in the body sensor network is considered. There are two formulas for transmission energy and reception energy[84].

$$E_{tx}(k_{bio}, d) = E_{TXelect}.k_{bio} + E_{amp}(n).k_{bio}.d^{n} \quad (3\text{-}5)$$

$$E_{rx}(k_{bio}) = E_{RXelect}.k_{bio} \quad (3\text{-}6)$$

In the former formula, the E_{tx} represents the transmission energy, $E_{TXelect}$ represents the dissipated radio energy to run the circuit for transmission, k_{bio} represents the number of transmitted biomedical bits, E_{amp} represents the energy consumption for the transmitter amplifier, and finally n is the path loss coefficient (there are two values: 3.38 and 5.9 for line of sight (LOS) and non-line of sight propagation (NLOS) respectively). In the latter formula for receiver energy, E_{rx} represents the receiver energy and $E_{RXelect}$ represents the dissipated radio energy. Total energy consumption for transmitting and receiving for the node is given as:

$$E_{txr}(k_{bio}, d) = E_{tx}(k_{bio}, d) + E_{rx}(k_{bio}) \quad (3\text{-}7)$$

$$E_{txr}(k_{bio}, d) = \left(E_{TXelect}.k_{bio} + E_{amp}(n).k_{bio}.d^{n}\right) + E_{RXelect}.k_{bio} \quad (3\text{-}8)$$

The duty cycle achieves energy saving through switching between active and sleep states in the WSN. The energy usage in equation (3-9) can be calculated for a duty cycle (β) based on a WSN. In addition, the total energy usage in time t (period is [0, t]) is given as:

$$E_T = t\left\lfloor \beta.E_{txr} + (1-\beta)E_{sleep} \right\rfloor \quad (3\text{-}9)$$

Where β is the duty cycle and E_{sleep} is the sleep state energy consumption for a sensor node per second. The sensor nodes remain in active and sleep states with probability β, (1-β) until time t, respectively. All nodes are active when the duty cycle (β=1), meaning there is no any energy for sleep [7].

Nordic nRF2401 has low power consumption, it operates in 2.4-2.45 GHz, and commonly used in WSNs. Table 3.3 shows the values of the specific parameters for Nordic nRF2401[84].

Table 3.3: Shows the values of the specific parameters for Nordic nRF2401

Parameter	nRF2401	Parameter	nRF2401
E_{TXelec}	16.7 nJ/bit	$E_{amp}(3.38)$	1.97e-9 J/bit
E_{RXelec}	36.1 nJ/bit	$E_{amp}(5.9)$	7.99e-6 J/bit

3.5 Path Loss Model for the Body

This model is a function of the distance between the transmitting and the receiving antenna[85]. It is measured by (3-10). There are two types of propagation model in the WBSN: the line of sight (LOS) and the non-line of sight (NLOS) propagation. The former applies to propagation along the front of the torso. It was investigated in [86], but it did not consider the communication between the front of the torso and the back. The latter propagation is a higher path loss around the torso[87]. The semi-empirical formula is used for both models as follows:

$$P_{dB} = P_{0,dB} + 10.n.\log\left(\frac{d}{d_0}\right) \tag{3-10}$$

In the above formula, $p_{0,dB}$ represents the path loss at a reference distance d_0 and n represents the path loss exponent, which is equal to 2 in free space [87]. Table 3.4 demonstrates the two different propagation models of path loss according to (3-10). The path loss coefficient (n) for line of sight and non-line of sight are taken as 3.38, and 5.9 respectively[84].

Table 3.4: The path loss model: values of parameters

Parameter	Value LOS	Value NLOS
d0	10 cm	10 cm
P0,dB	35.7 dB	48.8 dB
σ	6.2 dB	5.0 dB
n	3.38	5.9

3.6 Deployment of Relay Nodes

In this section, the deployment of the relay nodes in the topology with specific reference to WBANs is explained. The following subsection provides detail of the existing approaches such as single hop, multi-hop, relay network, relaying, and cooperation approaches. How to calculate energy consumption for these approaches is also discussed.

Relay nodes or relays are special devices which are added to a WBSN to aggregate the biomedical data from the biosensor nodes and transmit it to the sink node; this improves the network lifetime and enhances reliability. Moreover, it reduces the communication power for biosensor nodes [84],[88],[89].

In [88], the authors had proposed the relaying approach to improve the network lifetime in the WBSN. This technique is similar to a multi-hop approach because each relay at each level forwards the biomedical packet to the node at the next level; the researchers calculated the number of relays depending on two factors: firstly, the distance between the biosensor nodes and sink node, and secondly, the path loss coefficient of the human body. Aehyaie et al. assumed the addition of relay nodes to the network was continued until at least one relay node was in line of sight for the biosensor nodes and relay nodes. However, the increased number of relay nodes has an impact on the mobility of the patient[88].

In [89], the authors proposed two approaches to improving energy efficiency and network lifetime: the relaying and cooperation approaches. In the former approach they used the relay node to forward the packets from the biosensor nodes, which were placed far away from the sink node, to the sink node. In the latter, the authors assume the wireless devices are cooperation devices to forward the packets toward the sink node. However, the positions of relay nodes are fixed. In [90], the researchers solved the problem of the number and position of relay nodes: the authors calculated the optimal number of relay nodes and then determined the positions of relay nodes to increase the network lifetime by using a mixed integer linear programming model. In [91], D'Andreagiovanni and Nardin proposed a mathematical optimisation model for BANs to solve the uncertainty of traffic in the BAN by using relay nodes. The previous works have improved the energy efficiency in WBSNs by adding relay nodes. However, most of the previous works did not consider the relay nodes in the bottleneck zone.

3.6.1 Existing Approaches

In this subsection, the characteristics of the different approaches such as the single hop approach, multi-hop approach, the relay network approach, the relaying approach, and the cooperation approach are explained. The authors of [88] propose the relay network. All the remainder are proposed by[89].

3.6.1.1 Single Hop Approach

All single-hop transmissions use a high path loss (non-line of sight) and the coefficient is equal to 5.9 in this state. However, the nodes close to the sink node use line of sight (LOS), which uses the coefficient equal to 3.38 [84]. To calculate the energy usage for the single hop in the tree topology, the tree topology composed of the L levels; the equation (3-11) used to compute the energy consumption (J/bit) per bit for the node at level y.

$$E_{sh}(y,d) = E_{TXelect} + E_{amp}(n).[(L-y+1).d]^n \qquad (3\text{-}11)$$

In this approach the nodes which are situated furthest from the sink node consume more energy when to compare with other nodes. Therefore, they will expire first.

3.6.1.2 Multi-Hop Approach

This type of network is uses the line of sight (LOS) of the nodes for transmissions to neighbouring nodes, which uses the coefficient equal to 3.38[84]. The energy consumption of the node at level y (J/bit) is calculated by using the equation given in (3-12).

$$E_{mh}(y,d) = (2^y - 2).E_{RXelect} + (2^y - 1).[E_{TXelect} + E_{amp}(n).d^n] \qquad (3\text{-}12)$$

The nodes situated far away from the sink forward the packets via intermediate nodes towards the sink node. The nodes closest to the sink node consume more energy in the multi-hop: they become hotspots because these nodes are relaying a great many packets from the nodes at the other level. The depletion rate of energy is decreased by adding relay nodes to the body area network.

3.6.1.3 Relay Network Approach

In WBAN, Ehyaie et al. have proposed the relay network to improve energy efficiency and network lifetime [88]. The relay nodes have received the packet from biosensor nodes or other relay nodes and forward the packet to the sink node. They decrease the energy usage of biosensor nodes because they use short hops for the transmission to the nearest relay node. There are differences between the nodes in line of sight and the nodes in non-line of sight.

The latter consume much more energy in the communication compared with the former. With respect to the relay network, there is at least possible one relay node in line of sight using the equation (3-13) to compute the relay node number to be used in the body area network. There are three important factors: firstly number of biosensor nodes in the network, secondly the distance between biosensor and sink node, and finally the path loss coefficient.

$$R_{\max} = \sum_{i=1}^{m} \left\{ \left\lceil \frac{D_i}{d_{LOS}} \right\rceil - 1 \right\} \tag{3-13}$$

where $R_{\max}$ represents a number of relay nodes in the network, m is a number of biosensor nodes in the BAN, D_i is the distance between the ith biosensor nodes and a sink node, and d_{LOS} represents the near field distance. The results are used from the above equation (3-13) to compute the energy usage of the relay network. The total energy consumption can be calculated as:

$$E_r(k,d) = R_{\max}.[E_{RXelect} + (E_{TXelect} + E_{amp}(n).d^n)] \tag{3-14}$$

In this scheme, the energy usage of the biosensors for communication is dramatically reduced and the network lifetime is increased when compared to the transmission of the single hop and multi-hop network[88].

3.6.1.4 Relaying Approach

The aim of the approach is to reduce the consumption energy in the single and multi-hop network. In the former, the nodes are further away from the sink node and which much more energy usage, they will die first. However in the latter it is the nodes which are closest to the sink which consume more energy: the hotspots forward the packets received from the nodes far away. Reusens et al. proposed a relaying approach to improving the energy efficiency and enhance the lifetime of the BAN[89]. The relay nodes represent the bridges between the nodes situated far away from the sink node and the sink node in the single hop state. Moreover, in the state of multi-hop traffic, they are used to distribute the traffic from the nodes nearer to the sink. The following equation is used to compute the energy consumption (J/bit).

$$E_r(z,d) = z.[E_{RXelect} + (E_{TXelect} + E_{amp}(n).d^n)] \quad (3\text{-}15)$$

With respect to the above formula, the z represents the number of relay nodes and d is a distance. The relaying mechanism improves the network lifetime but adding more relay nodes to WBANs is not comfortable for human body.

3.6.1.5 Cooperation Approach

An additional solution to improve the lifetime of the network is called the cooperation method. In this technique, the nodes cooperate in forwarding the packets from one node to the sink node[89]. Reusens et al. have compared the energy usage in a single hop topology to the energy usage in a multi-hop topology. It is apparent that residual energy is available in the network, and they use this energy to improve the energy usage. The packets coming from the nodes further away to sink node; they are forwarded to a sink node by the nodes closer to the sink. The number of nodes is computed that are used to relay at level k when the limitation is the energy usage by the nodes in level l. The following equation is given[89]:

$$\text{no. relay node} = \left\lfloor \frac{E_{sh}(l,d_{in}) - E_{sh}(k,d_{in})}{E_r\left(l,(L-k+1)d_{in}\right)} \right\rfloor \quad (3\text{-}16)$$

It is clear that combination between single hop and multi-hop networks could improve the network lifetime and the energy efficiency. The summary of all approaches is shown in Table 3.5.

Table 3.5: Summary for all approaches including main characteristic for the WBAN design

Technique	Characteristic	Relay node
Single Hop[84]	The biomedical packets are directly transmitted to sink node, which uses higher path loss.	This is formula used to compute the energy consumption (J/bit) per bit for the node at level y_{node}. $E_{sh}(y,d) = E_{TXelect} + E_{amp}(n).[(L-y+1).d]^n$
Multi-Hop[84]	The nodes far away from the sink relay the packets by intermediate nodes towards the sink node.	The energy consumption of the node at level y_{node} (J/bit) is calculated by using the given equation: $E_{mh}(y,d) = (2^y - 2).E_{RXelect} + (2^y - 1).[E_{TXelect} + E_{amp}(n).d^n]$
Relay network[88]	The relay nodes have received the packet from biosensor nodes or relay nodes which forward the packet to the sink node.	The total energy usage can be calculated as: $E_r(k,d) = R_{\max}.[E_{RXelect} + (E_{TXelect} + E_{amp}(n).d^n)]$ [88].
Relaying [89]	The relay nodes represent the bridges between the biosensor nodes situated far away from the sink node and the sink node.	The following equation is used to compute the energy consumption (J/bit). $E_r(z,d) = z.[E_{RXelect} + (E_{TXelect} + E_{amp}(n).d^n)]$
Cooperation [89]	The nodes cooperated in forwarding packets from one node to the sink node[89].	The number of nodes that are used to relay by nodes at level k when the limitation is energy usage by the nodes in level l is computed. The following equation is given[89]: $\text{no. relay node} = \left\lfloor \frac{E_{sh}(l,d_{in}) - E_{sh}(k,d_{in})}{E_r(l,(L-k+1)d_{in})} \right\rfloor$

3.7 Network Coding Technique

An overview of Network Coding (NC) is provided in this section, which includes the following subsections such as the definition of Network Coding, Galois Field (GF), types of Network Coding technique, and Network Coding in WBSN.

3.7.1 A Brief Definition of Network Coding

The term 'network coding' (NC) was used for the first time by Ahlswede in 2000 in an article entitled Network Information Flow [92]. NC has become one of the most popular research areas in practical networking systems[92]. It is a technique that integrates different sets of data at relay nodes in such a way that they can be decoded at the destination. This technique can lead to better throughput of the network [93] [94]. Based on the NC concept, instead of simply forwarding the received packets, the intermediate node will combine them and create one or several output packets [94]. NC has enhanced the efficiency and the reliability of transmission in WSN by decreasing the number of packet losses [95] and has been used for various applications [96].

3.7.2 Galois Field

A Galois Field is usually indicated to be a finite field; it includes the set of numbers $GF(n)$, where n is a prime number and the elements represent the range $\{0,1,.....,n-1\}$ [97]. In addition, in [98], the authors proposed efficient methods to perform Galois Field (GF) represented as GF(2) and the Galois field is {0, 1}. They designed and analysed the architectures for practical network coding that perform Galois field (GF) dot product network coding and inverse matrix for GF. With respect to [99], $GF(2^n)$ generates a coding vector from the set GF(2) and each element is multiplied with the incoming packet, and all multiplied packets are summed to become the outgoing packets. For instance, the node generates the $GF(2^4)=\{1,0,1,1\}$; the output packet is $(1A_1+1A_2+0A_3+1A_4)$ at the node. Galois Field (GF) is employed in most network coding techniques such as network coding. The basic concepts and operations in GF are briefly explained in the following [100]. The addition and multiplication operations are defined in GF(2) which perform modulo 2; $GF(2)$ (with elements {0, 1}) can be extended as $GF(2^m)$. The vector field of dimension m over $GF(2)$ is a result and the elements of $GF(2^m)$ can be represented as m bits. The irreducible polynomial $f(x)$ characterises the field where

$$f(x)=x^m+f_{m-1}x^{m-1}+.....+f_1x+f_0 \qquad \text{with } f_i \text{ in } GF(2) \qquad (3\text{-}17)$$

All elements (2^m) in a Galois Field can be represented as vector$\{\alpha^{m-1},\ldots\ldots.\alpha^1,\alpha^0\}$, where α is a primitive element of the field and it represents the root of the irreducible polynomial $f(x)$. The expression of the element A in $GF(2^m)$ is given as

$$A = a_{m-1}\alpha^{m-1} + ... + a_1\alpha^1 + a_0\alpha^0 \quad \text{with } a_i \text{ in } GF(2) \qquad (3\text{-}18)$$

With respect to elements of $GF(2^m)$, the polynomial has a coefficients in $GF(2)$ and the coefficient of (α^i) represents the position the (i^{th}) bit. For instance, $GF(2^4)$ the element (1101) corresponds to $1\alpha^3 + 1\alpha^2 + 0\alpha^1 + 1\alpha^0$. The operations on the polynomial's coefficients belonging to $GF(2)$ have modulo-2. The addition operation in $GF(2^m)$ is implemented by bitwise XORing for the m coefficients of the two polynomials. Similarly, multiplication operation on $GF(2^m)$ is calculated as the modulo-2 sum of shifted partial products. Moreover, the sum is calculated by using bitwise XOR operations [100].

3.7.3 Types of Network coding Technique

In this subsection, the types of Network Coding are reviewed. Such network coding schemes fall into three types: Simple Network Coding (XOR NC), Linear Network Coding (LNC), and Random Linear Network Coding (RLNC).

3.7.3.1 Simple Network Coding Technique

In the simple network coding technique the XOR operation is used between packet data; it represents one of the most easily understood network coding techniques. When the node receives the data, packets from two different source nodes then apply simple XOR on them, and send them to destination nodes[101]. The destination node applies simple XORs on the data received, with the packet kept in memory to get the full packet[99]. In all network coding approaches, the receiving nodes must have some data to use to decode packet information received[101]. The simple network coding scheme is used for broadcasting, multicasting, or two way communication; it is used for wireless communication.

3.7.3.1.1 Example of Simple Network Coding

The basic concept of network coding (NC) is usually represented using a simple example such as the famous butterfly[93], which employed a simple XOR operation in a certain node (relay node). In Figure 3.2, source sender S1 and source sender S2 wanted to send the stream of messages a_i and b_i to both R1 and R2, as shown in Figure 3.2, with the capacity of all links in the network assumed to be one message per unit of time. When NC is not used, the relay node only forwards the one received message to the destination; the middle link will became a bottleneck zone because the relay node is receiving two messages from, S1 and S2. However the XOR process will be done by node r1, which employs XOR NC on the a_i

and b_i $(a_i - XOR - b_i)$ to mix bits in order to create an encoded message, then the encoded packet will pass through the same way to the destination node using normal transmission. The receivers obtain two messages in every time unit. At the receiving side, receiver R1 and receiver R2 must have the a_i and b_i from S1 and S2, respectively. Otherwise, they will be unable to decode anything from the coded packet received.

The NC has the ability to decrease the number of transmissions and avoid the packet loss of data transmission, thereby reducing the number of packet losses in the network when the number of transmissions is fixed. The operation of a simple XOR is executed at a certain node (relay node) to process two input packets which creates data encoding [102].

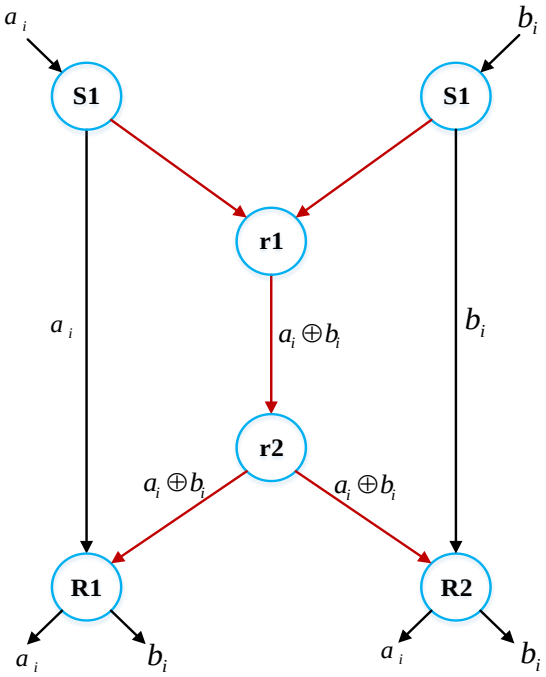

Figure 3.2: Example for XOR Network Coding

3.7.3.2 Linear Network Coding Technique

In this scheme, the node can multiply the coefficient from the Galois Field with the fixed size of data in the native packet, and combine its own data with a coefficient. The linear network coding technique is a more complex encoding and decoding scheme than the simple network coding. With regard to technique, the Galois Field is used to create the coefficient matrix which used at encoding and decoding nodes [99]. Furthermore, in both techniques, any node may encode two or more packets together in the network except the destination node [99],[103].

One of simplest decoding procedures is implemented by Gaussian elimination: the total rank of the coefficient matrix must be greater than or equal to the number of encoding packets. One disadvantage of linear network coding (LNC) is an increase in the overhead of data - encoding and decoding[99].

3.7.3.2.1 Example of Linear Network Coding

A useful example of linear network coding (LNC) is shown in Figure 3.3[104], each node in the network generating linear combinations of incoming packets, then the new coded packets are transmitted. In linear network coding, a linear combination is performed over a fixed set of original data chunks, which is named a generation of the original message; a node divides an original message X of length l into m chunks in order to create a generation of the original data message such as $\{x_1, x_2, x_3, ..., x_m\}$ where the length l is equal to m. Moreover, each chunk of data in linear network coding consists of k elements of Galois Field (2^w) .The calculation of length for the data message can be represented as $l = k * m * w$ where the value m is represented as a generation size. Alnuweiri et al. used twelve bytes (12 bytes) as an original data X which was spilt into three chunks such as X1, X2, and X3, each chunk having four bytes (4 bytes), where each element of the split chunk represents Galois Field (2^w) as shown in Figure 3.3[99]. The generation size (m) and each element size are three and one byte respectively, and $\alpha 1, \alpha 2, and \quad \alpha 3$ are represent as three coefficients of length w bits[105]. The new encoded chunk is computed by implementing the operation of linear combination as given:

$$y = \alpha_1 x_1 + \alpha_2 x_2 + \alpha_3 x_3 \tag{3-19}$$

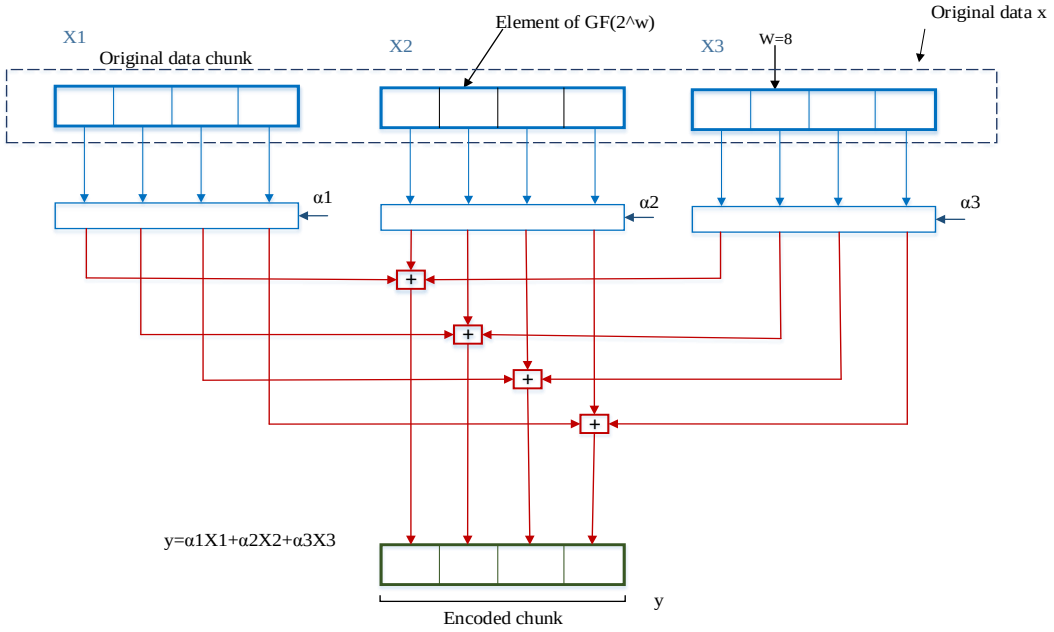

Figure 3.3: The operation of linear network coding

3.7.3.3 Random Linear Network Coding Technique

The Random Linear Network Coding (RLNC) approach is defined by [106] and [107]. In the RLNC approach, the nodes transmit linear combinations of the incoming packets to the outgoing edges, utilising randomly and independently chosen coefficients of code from some finite fields. However, on the receiver side, a decoder is needed to compute the overall linear combination of source processes. The authors computed a lower bound on coding success probability in networks with unreliable links, amount of redundancy, and in terms of link failure probability[107].

Furthermore, when the selection of linear coding coefficients is random, the NC scheme is called Random Linear Network Coding (RLNC), which does not require knowledge of the topology information for whole network, while the coding node encodes the incoming packets with the global coefficients(encoding vectors) embedded in the header [99]. Therefore, the destination node is not expected to know all information such as network topology and global encoding information, which are used to recover the original packets (native packets)[95]. If the rank of the matrix composing the global coefficient vectors (encoding vectors) is equal to the original number of packets in each round, the original packets could be released last. Moreover, the intermediate nodes are assigned local encoding vectors (coefficient vectors) to edges and the nodes randomly select the number in a finite field of the Galois Field(2^m) without checking the correlation [99].

The main characteristics of RLNC are the randomly chosen linear combinations, which are suitable for the dynamic environments. However, one drawback here is the probability of error decoding, which is based on the size of the Galois Field selected (finite field) for the code [108]. Furthermore, the solution of network coding is termed non-linear (random) when all intermediate nodes have a non-linear function of the incoming symbol; otherwise, it is linear [97].

3.7.3.3.1 Example of Random Linear Network Coding

The example of RLNC is shown in Figure 3.4. Here, node B has received two packets B_1 and B_2, and node D has received B_2, although nodes B and D send packets toward node E. In addition, node A has received B_1.When node B uses the network coding to create encoded packets, that is $c_1^E B_1 + c_2^E B_2$, it then transmits toward node E, with the coefficients c_1^E and c_2^E,which are randomly chosen. Node E has a block encoding $c_1^E B_1 + c_2^E B_2$ from node B and block B_2 from node D, which can solve block B_1 [109].

Similarly, node B transmits the encoded block $c_1^F B_1 + c_2^F B_2$ to the node F, with another coefficient c_1^F and c_2^F, which are randomly chosen as shown in Figure 3.4. In addition, node F has received B_1, so node F can retrieve block B_2 depending on the received encoded block $c_1^F B_1 + c_2^F B_2$ and received B_2.Moreover, the transmission for diversity of blocks is increased through using RLNC. However, computation of RLNC is complex with increasing number of blocks [109].

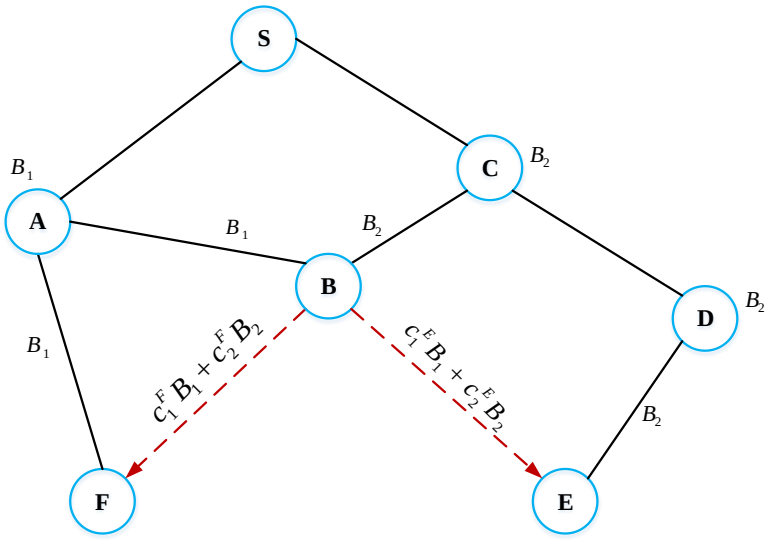

Figure 3.4: Example for Random Linear Network Coding (RLNC)

In general, supposing the number of packets (n) from one or several source nodes is $p_1, p_2, p_3,....., p_n$, all packets have the same size as assumed with the same number of bits. Intermediate nodes receive these packets and encode at w packets. The rate of encoding is n/w and represents the generation of the number of packets at the encoder node, which then forwards these to the destination node. There are two techniques of linear network coding: the encoding and decoding techniques. Both techniques are explained below [94],[110].

The procedure of Encoding: to compute the encoding of the packets, the node chooses as a sequence coefficient $q = (q_1, q_2, q_3,....., q_n)$ from Galois Field $GF(2^s)$, which called an encoding vector. The single output encoded packet is calculated as the sum of the products of each of the n native packets that are received at a node $G_i (i = 1,2,3,....., n)$ with a random coefficient q_i.The output encoded packet is described below.

$$Y = \sum_{i=1}^{n} q_i G_i \qquad q_i \in GF(2^s) \tag{3-20}$$

where Y and G_i are the coded and original packets, respectively; the encoded packets with the coefficients are transmitted to the destination node. The receiver side uses the encoding vector to decode the encoded packets.

Decoding procedure: The network coded data with the encoding vector q are received at the destination. Supposing the node has received a set of packets $(q^1, Y^1),.....(q^m, Y^m)$, the symbols Y^j and q_i^j represent the jth received packet for the encoded packet and coding vector respectively.

$$Y^j = \sum_{i=1}^{n} q_i^j G_i \qquad j = 1,...., m \tag{3-21}$$

Where Y^j and q_i^j represent the network coded data and encoding vector respectively; the recipients must receive at least n linearly independent packets to decode the original packets. In the above equation (3-21) the term G_i is unknown, which comprises the native packets transmitted in the network. By using the linear system in equation (3-21), the receiver side can retrieve the number of native packets. All source packets are recovered by Gaussian elimination, if the global encoding vector is full rank [111].

3.7.4 Review of Network Coding Literature in WBSN

Some authors have only used the relay node in a WBSN without employing the Network Coding (NC) technique in the relay nodes. In[88], the authors have proposed the relaying approach to improve the network lifetime in the WBSN. This technique is similar to a multi-hop approach because each relay at each level forwards the biomedical packet to the node at the next level. Moreover, relay network provides more reliability because there is more than one path which could be set from biosensor node to sink node. However, the increased number of relay nodes has an impact on the mobility of the patient[88]. Similarly, a number of studies have presented analytical expressions for the energy efficiency of an increased relay node dependent on the cooperative transmission mechanism in WBANs. The results of the proposed scheme have shown improvement of the communication reliability with multiple relay nodes. However, increasing the number of relay nodes is not useful in terms of energy efficiency[112]. Furthermore, in [90], the researchers solved the problem of the number and position of relay nodes, as they calculated the optimal number of relay nodes and then determined their positions in order to increase the network lifetime and to improve energy efficiency and data reliability by using a mixed integer linear programming model.

On the other hand, other researchers are exploiting the Network Coding (NC) technique in the relay node. Also, a large and growing body of literature has investigated the reliability in WBSNs based on the NC scheme which is employed in the relay node. In [113], the authors exploited the benefits of RLNC to enhance the energy efficiency and throughput; the researchers proposed a cloud-assisted RLNC-based MAC protocol which was named CLNC-MAC protocol. In addition, the CLNC-MAC protocol quickly allows the information flow between the sensor nodes which are worn on the body and the medical data centre. Although energy efficiency and average throughput are significantly enhanced, the performance delay is slight increased. Also, in [114], the researcher proposed a NC scheme to improve the energy efficiency of WBAN. Moreover, in [115], the researchers proposed an encoding approach which is low power and achieves less error in the communication in WBSNs; they utilised XOR network coding operations in the proposed scheme. In addition, the proposed scheme achieves lower power consumptions for XOR encodings when compared with another scheme [115].

Regarding the multi-relay concept, a number of authors proposed an Adaptive Reliable Cooperative Data Transmission technique (ARCDT) to avoid the data transmission loss in WBSNs based on the multi-relay concept. The biosensor nodes transmit biomedical packets

to relay nodes, which collect data from biosensor nodes then forward to the sink node. The proposal significantly improves the Quality of Service (QoS) of wireless body sensor networks[116]. As far as NC in relay nodes is concerned, in [117] the proposed scheme is an adaptive network coding (NC)-based error recovery mechanism; NC makes the encoding technique at relay nodes adaptive. This study explores the Quality of Service (QoS) requirements of WBSNs. A number of studies provide improvement of QoS in terms of energy efficiency, real time delivery, and reliability[117].

Researchers used the cooperative coding mechanism which integrates cooperative communication and network coding. The network coding could improve the communication reliability and reduce the number of packet transmissions. Furthermore, the proposed scheme achieves a significant improvement in the reliability and throughput with analysis of the probability of successful reception at the destination node[118]. Another study proposed Network Coding-based Cooperative Communications scheme (NCCC) at the source cluster where the NCCC encodes original packets with random network coding. In this study, the authors consider the packet delivery in multi-hop relay WSNs [118].

In [119], the authors used cooperation network coding (CNC) to improve the reliability of WBSN in the node failure or link failure. However, the proposal is not adaptive to dynamic network conditions because the nodes were fixed[119]. Moreover, a number of researchers have presented and contrasted novel approaches of Cooperative Network Coding (CNC) and Cooperative Diversity Coding (CDC) to increase the reliability and enhance throughput for wireless body area networks. With respect to proposed approaches, CDC reveals higher throughput than CNC because the biomedical packet and coded packets are transmitted to the destination node while in CNC only the coded packets are transmitted to the destination node. Then, to decode the original packets, the destination node should receive a number of the coded biomedical packets that are at least equal to the number of the original packets [120]. The Cooperative Diversity Coding (CDC) is used to code the biomedical packets. In addition, the proposed scheme achieves the performance of CNC and CDC in terms of the probability of successful reception at destination node as well as the required level of reliability in WBSNs[120].

With regard to RLNC, Movassaghi et al. proposed a novel cooperative transmission scheme based on demodulate-and-forward and network coding for WBSNs [121]. The study proposed Random XOR Network Coding (RXNC) to improve the reliability for WBSN, the source node is transmitted to the relay node, which demodulates the received packet. After

that, each relay selects the different coded symbols from demodulated symbols and XORs them to create the network coded symbol. Moreover, authors calculate an error probability of the created network coded symbols and computed the optimum value to minimising the error probability[121].

Movassaghi et al. presented an energy efficient NC scheme for WBANs which is termed decode and forward network coding (DF-NC) relays; the proposed scheme utilises the decode and forward mechanisms, it integrates the messages which are received from different sensor nodes to create only one message. Thus, only one transmission slot is required for transmission and close optimal outage probability is achieved while reducing the number of time slots for transmissions, improving the energy efficiency, and minimising the delay [122]. However, the researchers in [123] exploited a decode and forward mechanism based on cooperation strategy.

Furthermore, the assistance of relays combined with an NC scheme can increase reliability of a WBAN with lower computation and hardware costs. In this study, the authors used a UEP Unequally Error Protection (UEP) concept which cooperates with NC at the relay node. The biomedical packets are directly transmitted to relay nodes then data are forwarded to the sink node. However, a drawback of the proposed approach is that the sensor nodes are not using the advantages of the network coding mechanism, and the author utilises six sensor nodes and two relay nodes only in the proposed system[124]. In addition, Alshaheen and Takruri have designed a novel mathematical model which is proposed for body area network topology based on graph theory. The results show that the proposed RLNC model improves the energy efficiency for biosensor nodes in the bottleneck zone and guarantees data delivery in the case of link failure[125].Also, this can be seen in [126].

A few studies have considered the use of network coding for WBSN, and in [5], a simple XOR network coding technique is proposed and simulated, which can be used in a WBSNs to improve reliable biomedical packet transfer.

The biomedical data is transmitted from each biosensor node toward the sink node through the two relay nodes. Moreover, this study has shown an improvement in the packets transmission rate by the simulation according to measuring the physiological signals such as electrocardiograms (ECG) and electroencephalography (EEG). In addition, the proposed employment of relays combined with network coding scheme can improve network reliability of a WBAN with lower computation hardware cost [5]. Although Marinkovic and

Popovici showed improvement in the packet rate by the simulating, improving the proposed scheme remain as future work. In addition, the numbers of sensors and relay nodes are fixed, and relay nodes alone use the advantages of network coding in the proposed system[5].

However, most of the previous works did not consider reliability in the bottleneck zone in WBSN. In this thesis, Random Linear Network coding (RLNC) is employed in the relay node to create an NC relay node which can improve the probability of successful reception at the sink node. Table 3.6 summarises network coding (NC) techniques in WBSNs.

Table 3.6: Comparison for NC technique in WBSN

The proposed scheme	Type of NC	Key features	Medical application	Reliability	Energy efficiency	Publication
[88]	NC Not used	Main concept is adding a relay network to the WBSN	√		√	2009
[112]	NC Not used	Incremental relay-based cooperative communications in WBAN	√		√	2013
[90]	NC Not used	Energy-Aware WBAN Design (EAWD)	√		√	2014
[113]	RLNC	The proposed scheme exploits the benefits of RLNC	√		√	2014
[114]	NC	The proposed scheme uses NC, it can reduce the wake up time number for sensor nodes in order to receive control signals.	√		√	2011
[115]	XOR	Encoding methods are low power.	√		√	2013
[127]	XOR NC	Applying NC scheme on the multi-relays. The proposed scheme considers multi relay concept.	√		√	2013
[116]	XOR coding	QoS aware error recovery mechanism.	√	√	√	2015
[128]	RLNC	Cooperative communication with NC. The encoded packets is transmitted which is generated from native packets product with coefficients randomly based on Galois field.	√	√		2010

Table 3.6: Continued

[118]	NC	Encoding native packets with Random Network Coding	√	√		2014
[119]	CNC	The proposed scheme utilises CNC for a multiple source – multiple destination network.	√			2011
[120]	CNC and CDC	Coded and uncoded packets transmission.	√	√		2011
[129]	CNC and CDC	The linear independence of the combination packets for multi- hop was studied in the proposed scheme.	√	√	√	2014
[123]	XOR NC	Transmission of the physiological data from biosensor nodes to base station based on cooperation mechanisms which used NC	√			2014
[121]	Random XOR NC (RXNC)	The complexity of the proposed scheme is lower than the existing proposals such as Decode and Forward cooperative mechanisms.	√	√		2013
[122]	XOR operation for NC	The proposed scheme for WBAN with decode and forward relays which is called decode and forward network coding (DF-NC)	√		√	2013
[5]	simple XOR NC	Using the code and decode the packets, which is generated by simple XOR network coding scheme, can achieve reliable medical data transfer.	√	√		2009
[124]	The bitwise XOR NC operation	Combining the relay nodes with network coding technique in WBSN	√	√	√	2010
[125],[126]	RLNC	Applying RLNC scheme on the relay node. Implementation of two algorithms: Encoding and decoding algorithms	√		√	2017

3.8 Chapter Summary

This chapter was divided into three parts. In the first part, the most important MAC WBSN protocols were explained and discussed based on the energy efficiency; also, these protocols are summarised. After that, most of the previous work relates to MAC WBSN protocols, which are considered in the main research problem. In addition, the protocols are

operated with IEEE 802.15.4 MAC standard and support low data rate application; the term which is called Duty Cycle (CD), which represents the main parameter which has an impact on the energy consumption is found.

The second part covers a Duty Cycle (DC) which is implemented in the IEEE 802.15.4 MAC standard; duty cycle is a "green" technique which is used to reduce the energy usage through increasing the inactive period for the biosensor node in a WBSN. After an extensive search about duty cycle (DC), it was found that the previous works exist on adjusting DC for sensor node through the adjustment in Beacon Order (BO) and Superframe Order (SO) which are affected on the value of duty cycle. The value of DC is identified the active period (wake up duration) and inactive period (sleep duration) for sensor node. Moreover, the adjustment BO and SO of the studies done to mitigate the research problems were studied. Then, the DC protocols are summarised based on the energy efficiency and the value of SO and BO.

The third part was about Network Coding (NC), it can improve the transmission reliability of WBSN. The explanation and discussion for most existing Network Coding (NC) technique in WBSN, the types of NC with examples are classified such as XOR NC, LNC, and RLNC. Then the most previous studies are discussed, which used NC to address lost biomedical packets. After an extensive search about NC, it was found that one of the benefits of RLNC is used to improve the reliability of data delivery and energy efficiency in the medical application. Also, this point addresses the research problem and achieves the research aim. Then, the NC family of approaches are summarised based on the reliability and energy efficiency in WBSN applications, especially in healthcare.

Although previous works exist on the adjustment of duty cycle for sensor nodes in the IEEE 802.15.4 MAC standard, the majority of the previous studies did not review the energy consumption of the biosensor nodes in the bottleneck for WBSNs based on priority and traffic changes. In addition, the nodes placed next to the sink node consumes more energy because all biomedical packets are aggregated through these nodes, forming a bottleneck zone. Also, although there are previous studies into the reliability of procedures to address lost biomedical packets, reliable data transmission is still a challenge for WBSNs and medical monitoring systems and this needs to be considered and developed [5] [4]. In addition, the previous works did not consider the reliability in the bottleneck zone of WBSN; reliability is most important for body area networks.

Finally, after all these studies, the challenges in WBSNs can be addressed through applying the duty cycle technique and RLNC to a novel mathematical model in order to achieve the reduction of energy consumption for biosensor nodes and the improvement of reliability, respectively. Therefore, the next chapter presents with a novel mathematical model for WBSN implementing RLNC.

Chapter 4:

The Energy Consumption for the WBSN

4.1 Introduction

The reduction of energy consumption and the successful delivery of data are important for the WBSN. There is some energy wastage in the bottleneck zone by the nodes that are placed near the sink node, which consume more energy as they are required to forward data from nodes outside the bottleneck zone. For this reason, the proposed design of a mathematical model for the body area network attempts to explain the deployment and connection of nodes. Furthermore, in this chapter, a technique is considered to reduce energy usage for the biosensor nodes in the WBSN bottleneck zone.

This chapter proposes a novel mathematical model for body area network (BAN) topology to explain the deployment and connection between biosensor nodes, simple relay nodes, network coding relay nodes and the sink node. Therefore, this chapter is dedicated to researching both the energy saving and delivery of data if there is a failure in one of the links of the transmission, which relates to the proposed Random Linear Network Coding (RLNC) model in the WBSN. Using a novel mathematical model for a WBSN, it is apparent that energy consumption is reduced and data delivery achieved with the proposed mechanism. The content of this chapter has appeared in IET Wireless Sensor Systems journal[125] and at international conference (ISMICT)[126].

The chapter is organised as follows. Section 4.2 describes the body area network model design. Section 4.3 presents the proposed design for RLNC. Section 4.4 discusses wireless body sensor network performance. Finally, chapter summary is drawn in section 4.5.

4.2 The Body Area Network (BAN) Model Design

This section contributes a novel mathematical model design for a body area network (BAN) topology which considers the connection and relationship for the biomedical sensor nodes, the simple relay nodes, the network coding relay nodes and the sink node. In this

model, network coding technique is installed in a sample of the relay nodes to create the network coding relay node inside the bottleneck zone. Moreover, applying the new algorithm to the nodes in the bottleneck zone of the WBSNs will improve energy consumption of biosensor nodes and guarantees better data delivery.

In the field of Graph Theory, A graph G is formally defined as a pair G = (V, A), where V is a finite set of the graph vertices (or nodes) and A is a finite set of the graph arcs (edges or links) connecting the graph vertices [130]. Figure 4.1 shows a diagram of a simple graph, where vertices are represented by the points u, v, w, x, and y and the arcs (links) are represented by lines connecting the vertices a, b, c, d, e, f, g, and h in this example.

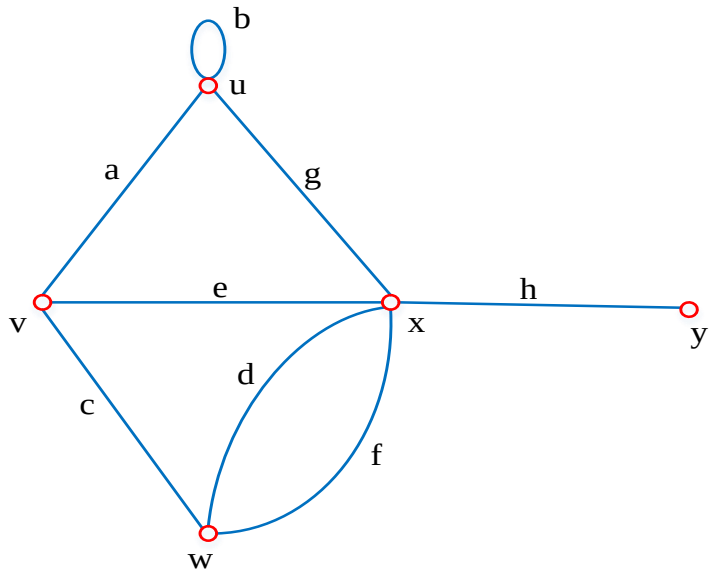

Figure 4.1: The diagram of a simple graph

Each vertex is indicated by a point which represents the node in the BAN topology for instance biosensor node, simple relay node, network coding relay node, and sink node. Furthermore, each arc is indicated by a line joining two points which represent the link between nodes such as the connection between a biosensor node and a simple relay node, or the connection between a biosensor node and sink node. It is worth noting that, a tree topology represents the simplest class of graphs.

A model of a BAN is usually represented by a directed graph G (V, A) based on graph theory[130].There is a set of vertices V that include one element for each wireless device (biosensor node, simple relay node, network coding relay node or sink node) of the network. The A represents a number of links (arcs). However, in[91], the authors explained the relationship between biosensor nodes, relay nodes and sink node only without network

coding relay nodes. With respect to the set of vertices, the set V is the union of four disjointed sets of vertices as follows: the set B of vertices refers to biosensor nodes, the set R_r of vertices refers to the deployment of relay nodes, the set R_{nc} of vertices refers to network coding relay node, and the set S of vertices refers to sink nodes (assume that the number of sink nodes in this model is one).

$$V = B_b \cup R_r \cup R_{nc} \cup S \tag{4-1}$$

Each node is a device situated within a range depending on the power of the transmitting device. However, the network coding relay node transmits only to the sink node within its transmission range. The subsets of devices that can transmit within the range of transmission are noted below.

- For each biosensor node $b \in B$, the subsets $R_b \subseteq R_r, R_{ncb} \subseteq R_{nc}, and\ S_b \subseteq S$ represent the simple relay nodes, network coding relay nodes, and sink nodes within the range of the transmission for biosensor b, respectively.
- For each simple relay node $r \in R_r$, the subsets $R_r \subseteq R_{rr}, R_{ncr} \subseteq R_{nc}, and\ S_r \subseteq S$ represent the simple relay nodes, network coding relay nodes, and sink nodes within the range of transmission of the simple relay nodes r, respectively.
- For each network coding relay node $rnc \in R_{nc}$, the subsets $R_{rnc} \subseteq R_r, R_{rnc} \subseteq R_{nc}, and\ S_{nc} \subseteq S$ represent the simple relay nodes, network coding relay nodes, and sink nodes within the range of the transmission for the network coding relay nodes, respectively.
- More generally, the representation of body area network devices for any type assumes a vertex $i \in V$; this is symbolised this by $V_i \subseteq V$ the subset of vertices representing devices within the range of the transmission for i.

Each biosensor generates the data which is routed from a source node b to a destination node s (sink node) in the network is represented by the graph G (V, A). Moreover, the capacity of relay node in a WBSN is $(0 < cap_r \leq 250\ \text{kbps})$ for each relay $r \in R$. Arcs A, each arc $(a = (i, j) \in A)$ represents the directional wireless link from the transmitting device $(i \in V)$ to the receiving device $(j \in V_i)$ within the transmission range of the transmitting

device (i). The transmission link from the bio-medical sensor node to the sink node through a simple relay node and a network code relay node can be expressed as

$$A = A_{B\to S} \cup A_{B\to Rr} \cup A_{B\to Rnc} \cup A_{Rr\leftrightarrow Rr} \cup A_{Rr\to S} \cup A_{Rr\to Rnc} \cup A_{Rnc\to S} \quad (4\text{-}2)$$

4.2.1 Energy Consumption Assumptions of the Designed Model

The connectivity parameters for WBAN of the designed model represent the relationship between biosensor nodes, simple relay nodes, network coding relay nodes and the sink node as follows [125]:

If the biosensor node b can establish a link with the simple relay node r, it can be expressed as

$$a_{ij}^{br} = \begin{cases} 1 \text{ a link on } arc(i,j) \in A_{B\to Rr} \\ 0 \qquad\qquad Otherwise \end{cases} \quad (4\text{-}3)$$

Sometimes, in WBSN topology, the biosensor node is connected to more than the simple relay node. In this case $a_{ij}^{br} = hr$ where hr is the number of relay nodes that receive the packets from biosensor b.

If the biosensor node b can establish a link with the NC node, it is represented as

$$a_{ij}^{bnc} = \begin{cases} 1 \text{ a link on } arc(i,j) \in A_{B\to Rnc} \\ 0 \qquad\qquad Otherwise \end{cases} \quad (4\text{-}4)$$

If the biosensor node b can establish a link with the sink node, it follows as

$$a_{ij}^{bs} = \begin{cases} 1 \text{ link on } arc(i,j) \in A_{B\to S} \\ 0 \qquad\qquad Otherwise \end{cases} \quad (4\text{-}5)$$

If the simple relay node r can establish a link with the sink node s, it can be expressed as

$$e_{ij}^{rs} = \begin{cases} 1 \text{ link on } arc(i,j) \in A_{Rr\to S} \\ 0 \qquad\qquad Otherwise \end{cases} \quad (4\text{-}6)$$

If the simple relay node r can establish a link with the NC node, it is represented as

$$e_{ij}^{rnc} = \begin{cases} 1 & \text{link on } arc(i,j) \in A_{Rr \to Rnc} \\ 0 & Otherwise \end{cases} \quad (4\text{-}7)$$

If the simple relay node r can establish a link with another simple relay node l, it can be represented as

$$e_{ij}^{rl} = \begin{cases} 1 & \text{link on } arc(i,j) \in A_{Rr \to Rr} \\ 0 & Otherwise \end{cases} \quad (4\text{-}8)$$

If the NC relay node can establish a link with the sink node s, it is expressed as

$$e_{ij}^{ncs} = \begin{cases} 1 & \text{link on } arc(i,j) \in A_{Rnc \to S} \\ 0 & Otherwise \end{cases} \quad (4\text{-}9)$$

There are two binary decision variables:

Binary generated data variable is $x_{ij}^{bs} \in \{0,1\} \forall b \in B, s \in S, (i,j) \in A$, and the biosensor node generated data transmitted to the sink node can be expressed as

$$x_{ij}^{bs} = \begin{cases} 1 & \text{link on } arc(i,j) \in A \\ 0 & Otherwise \end{cases} \quad (4\text{-}10)$$

The binary NC relay node deployment variable $z_{nc} \in \{0,1\} \forall nc \in Rnc$ is represented as

$$z_{nc} = \begin{cases} 1 & \text{if install NC in relay node} \\ 0 & Otherwise \end{cases} \quad (4\text{-}11)$$

Eequation (4-10) relates to the data generated from the biosensor node while equation(4-11) is a decision variable of the installation of the network coding technique in the simple relay node which creates the NC relay node in the network [83].

With respect to Section 3.4, the Section 3.4 describes the energy consumption formulas for the transmission and reception. The total transmission and reception energy for all wireless nodes in the WBSNs represents the total energy consumption. The explanation of all terms used in WBSN model are shown in Table 4.1.

Table 4.1: Explanation of all terms used in the WBSN model

Term	Description
f_{bs}	The traffic generated by the biosensor nodes b towards the sink node S
$D_{br}^{n_{br}}$	The distance between the biosensor nodes and the simple relay nodes
f_{rl}^{s}	The total traffic transmitted by the simple relay node to neighbouring node (another relay node).
$D_{rl}^{n_{rl}}$	The distance between the simple relay nodes and the neighbouring node (another relay node).
f_{rs}^{s}	Traffic from the simple relay node to the sink node
$D_{rs}^{n_{rs}}$	The distance between the simple relay nodes and the sink node.
$D_{bnc}^{n_{bnc}}$	The distance between the biosensor nodes and the NC relay nodes
f_{rnc}^{s}	The total traffic transmitted by the simple relay node to the NC relay node toward the sink node
$D_{rnc}^{n_{rnc}}$	The distance between the simple relay nodes and the NC relay node.
f_{ncr}^{s}	The total traffic received from the NC relay node to the simple relay node toward the sink node.
$D_{ncs}^{n_{ncs}}$	The distance between the NC relay nodes and the sink node.

The calculation of the total energy consumption to transmit medical data from all biosensor nodes to the relay nodes is given as

$$E_{TXbr}^{t} = \sum_{b\in B, r\in R, s\in S} k_{bio}^{bs} x_{ij}^{bs} a_{ij}^{br} \left((E_{TXelec} + E_{amp}(n_{br})) D_{br}^{n_{br}} \right) \qquad (4\text{-}12)$$

The simple relay nodes receive the medical data from the biosensor nodes. The total energy consumption for reception is computed by (4-13).

$$E_{RXbr}^{t} = \sum_{b\in B, r\in R, s\in S} k_{bio}^{bs} x_{ij}^{bs} a_{ij}^{br} E_{RXelec} \qquad (4\text{-}13)$$

Table 4.1 details all terms used in this model. The simple relay nodes consume energy to forward the medical packets to another relay node l as follows

$$E_{TXrl}^{t} = \sum_{r,l \in R, s \in S} f_{rl}^{s}\left((E_{TXelec} + E_{amp}(n_{rl}))\right) D_{rl}^{n_{rl}} + E_{RXelec} \quad (4\text{-}14)$$

The total energy consumption to relay medical data from simple relay nodes to the sink node is given as

$$E_{TXrs}^{t} = \sum_{r \in R, s \in S} f_{rs}^{s}\left((E_{TXelec} + E_{amp}(n_{rs}))\right) D_{rs}^{n_{rs}} + E_{RXelec} \quad (4\text{-}15)$$

4.2.2 Energy Consumption with Network Coding

The calculation of the total energy consumption to transmit medical data from all biosensor nodes to the network coding relay nodes is given as

$$E_{TXbnc}^{t} = \sum_{b \in B, nc \in NC, s \in S} k_{bio}^{bs} x_{ij}^{bs} a_{ij}^{bnc}\left((E_{TXelec} + E_{amp}(n_{bnc}))\right) D_{bnc}^{n_{bnc}} \quad (4\text{-}16)$$

The NC relay nodes receive the medical data from the biosensor nodes. The total energy consumption for reception is computed by (4-17)

$$E_{RXbnc}^{t} = \sum_{b \in B, nc \in NC, s \in S} k_{bio}^{bs} x_{ij}^{bs} a_{ij}^{bnc} E_{RXelec} \quad (4\text{-}17)$$

The simple relay nodes consume energy to forward the medical packets to the network coding relay nodes which can be expressed as

$$E_{TXrnc}^{t} = \sum_{r \in R, nc \in NC, s \in S} f_{rnc}^{s}\left(E_{TXelec} + E_{amp}(n_{rnc})\right) D_{rnc}^{n_{rnc}} + E_{RXelec} \quad (4\text{-}18)$$

The total energy consumption to relay medical data from the NC relay nodes to the sink node is given by (4-19).

$$E_{TXncs}^{t} = \sum_{nc \in NC, s \in S} f_{ncs}^{s}\left(E_{TXelec} + E_{amp}(n_{ncs})\right) D_{ncs}^{n_{ncs}} + E_{RXelec} \quad (4\text{-}19)$$

The calculation of the traffic flow in WBSNs is as follows: Let k_{bio}^{bs} represent the number of transmitted biomedical bits through WBSN and received by the simple relay node, NC

relay node and sink node. The total traffic generated by the biosensor node toward the sink node is given below (4-20).

$$\sum_{b\in B} k_{bio}^{bs} x_{ij}^{bs} a_{ij}^{br} \qquad \forall r,l \in R, s \in S \tag{4-20}$$

Therefore, all traffic is destined towards the sink node S as given by (4-21)

$$\sum_{b\in B} k_{bio}^{bs} x_{ij}^{bs} a_{ij}^{br} + \sum_{l\in R} (f_{lr}^{s} - f_{rl}^{s}) - f_{rs}^{t} = 0 \qquad \forall r \in R, s \in S \tag{4-21}$$

Where the term $\sum_{b\in B} k_{bio}^{bs} x_{ij}^{bs} a_{ij}^{br}$ represent the total generated traffic by the biosensor nodes towards the sink node S. The term $\sum_{l\in R} f_{lr}^{s}$ represents the total traffic received by the simple relay node from neighbouring nodes, $\sum_{l\in R} f_{rl}^{s}$ is the total traffic transmitted by the simple relay node to neighbouring nodes and $\sum_{l\in R} f_{rs}^{t}$ is the transmission of traffic towards the sink node, those are expressed as

$$f_{rl}^{s} \le \sum_{b\in B} k_{bio}^{bs} e_{ij}^{rl} \approx f_{lr}^{s} \qquad \forall\, r,l \in R, s \in S \tag{4-22}$$

$$f_{rl}^{s} - f_{lr}^{s} = 0 \qquad \forall r,l \in R, s \in S \tag{4-23}$$

$$\sum_{b\in B} k_{bio}^{bs} e_{ij}^{rl} - \sum_{b\in B} k_{bio}^{bs} e_{ij}^{lr} = 0 \qquad \forall r,l \in R, s \in S \tag{4-24}$$

$$\sum_{b\in B, s\in S} k_{bio}^{bs} x_{ij}^{bs} a_{ij}^{br} + \sum_{l\in R, s\in S} f_{lr}^{s} \le cap_{r} \qquad \forall r \in R \tag{4-25}$$

Where cap_r represents the capacity of the relay node in WBSN. The traffic must not exceed the capacity of the node. The total traffic transmitted towards the sink node s as shown in (4-26) which represents the original flow (native data) in BAN.

$$f_{rs}^{t} \le \sum_{b\in S} k_{bio}^{bs} e_{ij}^{rs} = f_{native\_rs}^{s} \qquad \forall r \in R, s \in S \tag{4-26}$$

Where the value

$$e_{ij}^{rs} = 1 \qquad \forall r \in R, s \in S \tag{4-27}$$

Meaning that, there is a connection between the simple relay node and the sink node. The traffic is expressed as

$$f_{rs}^{t} = k_{bio}^{bs} \qquad \forall r \in R, s \in S \tag{4-28}$$

On the other hand, the total traffic flow received in the NC nodes is transmitted from the biosensor nodes and the simple relay nodes. After that, NC relay node encodes the received biomedical data and forwards to the sink node S. The total traffic in the NC relay node is given as

$$\sum_{b \in B} k_{bio}^{bs} x_{ij}^{bs} a_{ij}^{bnc} z_{nc} + \sum_{l \in R} f_{rnc}^{s} \qquad \forall r \in R, nc \in NC, s \in S \tag{4-29}$$

$$where\ f_{ncr}^{s} \le \sum_{b \in B} k_{bio}^{bs} e_{ij}^{rnc} z_{nc} \qquad \forall r \in R, nc \in NC, s \in S \tag{4-30}$$

Where the terms $a_{ij}^{bnc}, x_{ij}^{bs}, z_{nc}$ and e_{ij}^{rnc} are equal to 1, NC relay node receives k_{bio}^{bs} from a bio-sensor node and receives k_{bio}^{bs} from a simple relay node, the total traffic can be expressed as

$$G_i \le \sum_{b \in B} k_{bio}^{bs} \text{ from biosensor node} + \sum_{b \in B} k_{bio}^{bs} \text{ from relay node} \tag{4-31}$$

Subsection 3.7.3.3 describes the encoding and decoding techniques for the RLNC. To encode biomedical packets, the NC relay node is chosen as a sequence coefficient $q = (q_1, q_2, ..., q_n)$ from Galois Field $GF(2^s)$, this is called an encoding vector. The single output encoded packet is calculated as the sum of products of each of the n native packets that are received at a node $G_i (where\ i = 1,2,3,...n)$ with a random coefficient q_i. The output encoded packet is described as

$$Y = \sum_{i=1}^{n} q_i G_i \qquad q_i \in GF(2^s) \tag{4-32}$$

The ingress flow to the sink node S from NC relay node is expressed as

$$D_{sending\_from\_NC} = [q_i + Y] \quad q_i \in GF(2^s) \tag{4-33}$$

Where $D_{sending\_from\_NC}$ represents the traffic in the sink node which is received from NC relay node and q_i represents the random coefficient based on Galois Field.

Decoding in the sink node: The sink node receives data from both the simple relay node and the NC relay node which represents the native data and encoding data respectively. With respect to Gaussian elimination, the sink node decodes the received packets to recover the native packets [111] as follows.

$$D_{native\_PKT} = \sum_{i=1}^{n} q_i D_{encoding\_nc\_i} \qquad q_i \in GF(2^s) \tag{4-34}$$

The total energy consumption in the time t (for instance the duration is [0,t]) for the network is defined as:

$$E_{whole\_network}^{total} = \left\{ t \left[\begin{array}{l} (E_{TXbr}^{t} + E_{RXbr}^{t} + E_{TXrl}^{t} + E_{TXrs}^{t} + E_{TXbnc}^{t} + E_{RXbnc}^{t} \\ + E_{TXrnc}^{t} + E_{TXncs}^{t}) \end{array} \right] \right\} \tag{4-35}$$

4.3 The Proposed Design for RLNC

The system model is composed of the biosensor nodes, simple relay nodes, network coding relay nodes and the sink node as in Figure 4.2[125]. The biosensor nodes set is positioned at specific points on the human body. Each biosensor generates biomedical data which is transmitted to the sink node through the set of relay nodes and NC relay nodes in the network. These nodes represent the bridges between the biosensor nodes and the sink node which improve energy efficiency. The set of simple relay nodes (R) transport the packets collected by the biosensor nodes to the sink node. Moreover they forward the data aggregated from the biosensor nodes to another relay node or to the NC relay node towards the sink node. The nodes are around the sink node, and this area is called the bottleneck zone. The definition of the bottleneck zone is an area within a certain radius from the sink node, where the radius is represented by the transmission range of the sensor nodes [125,126].

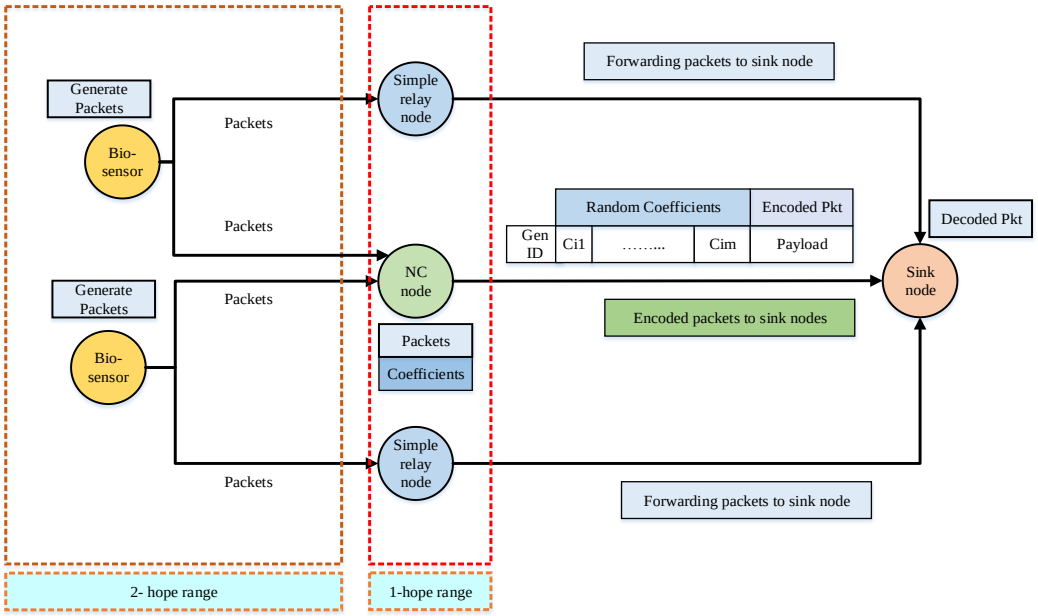

Figure 4.2: The proposed design model in the WBSN

Each biosensor node transmits duplicate biomedical packets, one to the simple relay node and the other to the NC relay node. The processing of packets at the node site (simple relay node and NC relay node) has been given in Figure 4.3, showing the algorithm which implements the forwarding of the medical packets and the encoding algorithm at the simple relay node and the NC relay node respectively[125,126]. Each node in the bottleneck zone receives a queue (RQueue) into which received packets are placed, and the node checks the packet to see whether or not the packet is a native.

4.3.1 Algorithm for Packets Processing

As far as the algorithm for the processing of packets is concerned, as shown in Figure 4.3, each node has a receive queue (RQueue), which includes biomedical packets, and the node deposits biomedical packets in the queue (RQueue). In the first section of the algorithm, if the node acts as a simple relay node, it checks the packet which is received. If it is already forwarded toward the sink node then it should be removed from the queue and inserted into the forward packet set; otherwise, the simple relay node transmits the packet toward the sink node[125].

In the second section of the algorithm, as shown in Figure 4.3, if the node represents NC relay node and the biomedical packet is a native packet, the NC relay node is chosen as a sequence coefficient based on the Galois Field GF (2^8). The NC node encodes the medical packets by applying a random coefficients to the packets. After successfully creating the

encoded packets, the NC node transmits the encoded packets and coefficients to the sink node[125].

4.3.2 Algorithm for Packets Decoding

The decoding procedure for biomedical packets at the sink node is as follows: the sink node receives the native packets and encoded packets from the simple relay node and the NC relay node, respectively. The decoding procedure is shown in Figure 4.4 where the sink node receives the native packets from the simple relay node[125]. Additionally, it receives the encoded packets with random coefficient from the NC relay node and performs the decoding procedure for the encoded packets. The sink node applies Gaussian elimination on the encoded packets and coefficient in order to retrieve all source packets.

ALGORITHM 1: Packet process (Pi),

```
1.  Pick the packet Pi from RQueue                    % Receive Queue for node n
2.    If Packet Pi is forward packet set exit;
3.      If Node N acts as R Then                      % R=Simple Relay Node
4.        R transmit packet Pi to Sink
5.        Insert packet Pi to forward packet set
6.        Else
7.         Node N acts as Rc                          % Rc= Network Coding Relay Node
8.           If Pi is a native packet Then
9.             Generate Ci random coefficient
10.            Pencoding= product Ci.Pi               % Pencoding = Encoding the medical packets
11.            Rc transmit both Pencoding,Ci to Sink node
12.            Insert Pi to forward packet set
13.          Else
14.            Discards Pi
15.          Endif
16.     Endif
17.   Endif
18.  If RQueue is not empty
19.     Go to 1:
20.   Else exist
21.   Endif
```

Figure 4.3: The algorithm for the processing of packets

Algorithm 2: Decoding produce in the sink node

```
1.  If Sink node receive packet from Rc  Then          % Rc= Network Coding Relay Node
2.      Sink node receive the Pencoding and Ci random coefficient
3.      Applying Gaussian elimination algorithm        % Decoding produce
4.      PNative = product Ci. Pencoding                % Retrieve the no. of native packets
5.      Save PNative in the sink memory
6.  Else
7.      Sink node receive packet from R
8.      Save P in the sink memory
9.  Endif
```

Figure 4.4: The algorithm for the decoding the packets in the sink node

4.4 Wireless Body Sensor Network Performance

In this scenario the WBSN topology is used as depicted in Figure 4.5 because it represents a general case. The WBSN scenario includes 13 biosensor nodes which are placed on the human body, for instance electroencephalogram (K sensor) and electrocardiogram (D sensor). With respect to this scenario, there are some biosensor nodes which sense and measure vital signs of the human body such as Pulse rate, Temperature, Motion sensor, and Blood pressure. The definition of the bottleneck zone is an area within radius (0.6 m) from the sink node, where the radius represents the transmission range of the sensor nodes. The distance between the biosensor nodes and sink node for the single-hop technique, and between biosensor nodes and closest node in the multi-hop technique is shown in Table 4.2 [88]. The WBSN is shown on the left hand side of Figure 4.5 and the topology explains the bottleneck zone which is shown on the right-hand side of the figure. With respect to the network coding approach, there are simple relay nodes and network coding relay nodes added in the bottleneck to reduce the energy consumption for the biosensor nodes as shown in Figure 4.6. Node B and node C are connected directly to the sink node given the short distance between them at 0.3m and 0.2m, respectively. The information in Table 3.3 for Nordic nRF2401 is used to calculate energy consumption for all approaches.

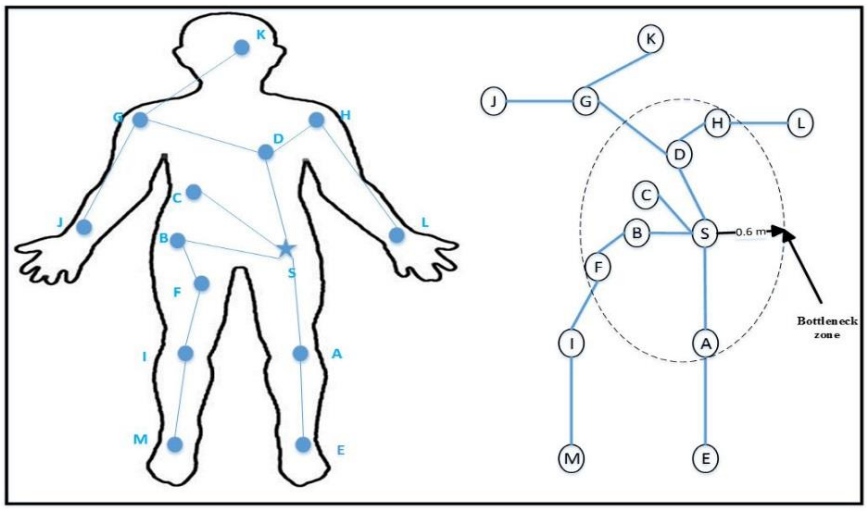

Figure 4.5: WBSN topology with 13 biosensor node and explain the area of the bottleneck zone

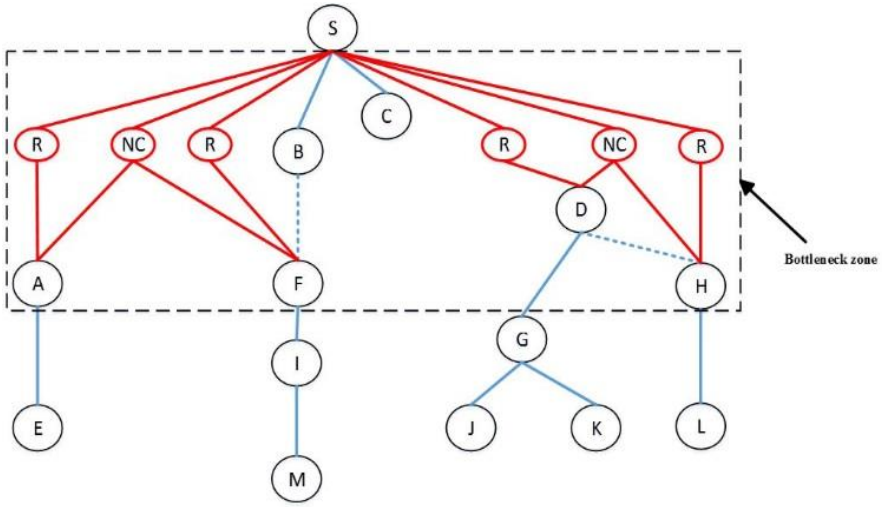

Figure 4.6: The bottleneck zone and tree topology for WBSN with simple relay nodes(R) and network coding relay nodes (NC) added in the bottleneck zone

Table 4.2: The distance (meters) between biosensor node and sink node for the single hop, and between the biosensor and the nearest node for the multi-hop

Sensor	A	B	C	D	E	F	G	H	I	J	K	L	M
Single - Hop	0.6	0.3	0.2	0.5	1.2	0.6	0.7	0.6	0.8	1.0	0.8	0.8	1.5
Multi - Hop	0.6	0.3	0.2	0.5	0.6	0.3	0.2	0.1	0.3	0.6	0.4	0.6	0.6

4.4.1 The LOS and NLOS Performance

Section 3.5 explains the path loss model for the body. The energy consumption is affected by propagation path loss in WBSNs. The single hop approach utilises the line of sight (LOS)

propagation model in all transmissions, and uses the path loss coefficient (n) of LOS, which equals 3.38. However, in the multi hop approach, the NLOS value is utilised for the transmission in WBSN. In addition, the path loss coefficient (n) of NLOS is equal to 5.9. The path loss coefficient along LOS channel is lower than along NLOS channel, which affects the energy usage in WBSN. On the other hand, all transmissions in the relay network approach use the path loss coefficient (n) of NLOS, which is equal to 5.9, except for the nodes that are placed next to sink node, those utilise the path loss coefficient (n) of LOS, which equals 3.38. Similarly, in the network coding approach, for instance, the biosensor nodes B and C are directly connected to the sink node, which use the LOS. However, the biosensor nodes such as A, F, D, and H connect with the sink node through the simple relay node and the NC relay node, which uses the NLOS where the path loss coefficient of the LOS and NLOS are equal to 3.38 and 5.9, respectively. In all approaches, the energy usage for the transmit amplifier in equation (3-5) (in section 3.4) equals to 1.97e-9 J/bit for n=3.38 and 7.99e-6 J/bit for n=5.9.

Each biosensor node consumes energy based on the propagation model and the distance between the sensor node and the sink node. For example, EMG (A) and the ECG (node D) consume more energy that sensor B as they send biomedical packets toward the sink node through a simple relay node and a NC relay node, whereas the body temperature sensor (B) is transmitted directly from the biomedical packets to the sink node.

4.4.2 Energy Consumption Results

The energy consumption for the WBSN bottleneck zone is computed based on the network coding approach comparing single hop [89], multi- hop[89], and relay network approaches.

In the single-hop approach, the biosensor nodes in the bottleneck zone consume more energy based on the distance when compared with other approaches; the biosensor nodes A, F, and H show greater energy consumption, as shown in Figure 4.7. However, in the multi-hop approach, the biosensor nodes relay the packets via the intermediate node towards the sink node. The nodes A, and D have higher energy consumption in the multi-hop but the node C has the same value of energy in most approaches because it is connected only with the sink node, as illustrated in Figure 4.7.

With respect to the relay network approach, adding to the number of relay nodes which forward the packets to the sink node improves the energy efficiency and decreases the energy

usage of biosensor nodes in the bottleneck zone. Moreover, there is at least one possible relay node in line of sight. The energy consumption for all biosensor nodes is lower compared with single-hop and multi-hop approach.

In the network coding approach, simple relay nodes and NC relay nodes are added to the bottleneck zone to reduce the energy consumption for the biosensor nodes in this area. It can be observed that energy usage for the nodes B and D is lower when compared with other approaches except that the values of energy consumption for A, F and H are slightly higher than in the relay network approach because energy consumption of these nodes are calculated based on non-line of sight as illustrated in Figure 4.7. Detailed results are shown in Table 4.3[125].

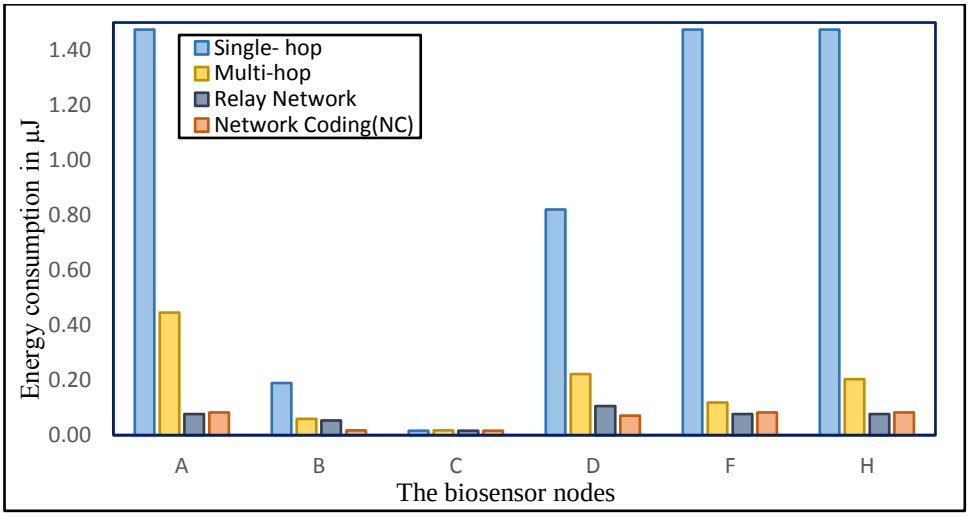

Figure 4.7: Comparison of energy consumption for biosensor nodes in the bottleneck zone based on the single hop, multi-hop, relay network and Network coding

Table 4.3: The energy consumption for the nodes in the all approaches

Node	Energy usage in Single Hop (µJ/bit)	Energy usage in Multi Hop (µJ/bit)	Energy usage in Relay network (µJ/bit)	Energy usage in Network Coding (µJ/bit)
A	1.47414	0.44512	0.07610	0.08263
B	0.18933	0.05937	0.05283	0.01671
C	0.01671	0.01730	0.01671	0.01671
D	0.82028	0.22270	0.10623	0.08264
F	1.47414	0.11874	0.07610	0.08264
H	1.47414	0.20331	0.07610	0.08264

Moreover, each biosensor node sends duplicated packets, one through simple relay node and the second through NC relay node. In the transmission range of 0.3 cm, the NC relay

node receives packets from different nodes and encoded packets are then sent to the sink node. The sink node decodes the received packets and retrieves native packets even if there is a failure in one of the transmission links.

With respect to the tree topology for the body area networks as presented in Figure 4.8 in the first case, the biosensor node A (EMG sensor) sends biomedical packets through two paths, first through the simple relay node, which forwards biomedical packets to the sink node, and second through the network coding relay node, which creates the encoded packets and then transmits them with coefficients to the sink node. If a failure occurs in one of the links (one path) through the transmission, as shown in Figure 4.8 (tree topology), where the dashed red line represents the failed link for node A, successful transmission of the medical packets is achieved through an alternative link. In this case, it can be seen that the energy consumption for node A based on the NC with one link failure saves energy and achieves the delivery of data, as illustrated in Figure 4.9.

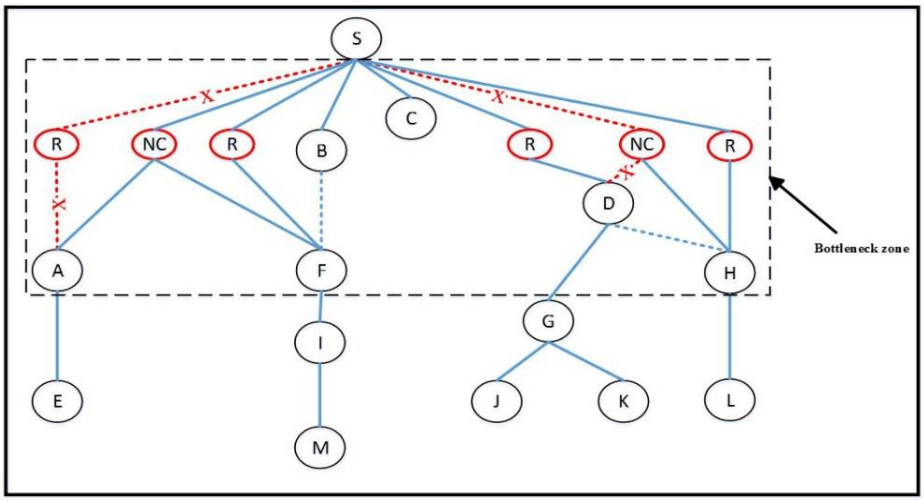

Figure 4.8: Tree topology for WBSN with a failure link for the node A and D

The bar chart shown in Figure 4.10 compares the energy consumption for node A, calculated based on the single hop (1.4741 µJ/bit), multi- hop (0.4451 µJ/bit), relay network (0.0761 µJ/bit), NC (0.0826 µJ/bit,) and NC with one link failure (0.0593 µJ/bit). The significant differences in the energy consumption value for node A in the single hop and the NC with one link failure can be seen in Figure 4.10. The energy usage for node A is higher in the single hop. Moreover, the energy consumption for node A in the relay network scheme is slightly higher than the NC with one link failure. On the other hand, the amount of energy is lower in the later scheme[125].

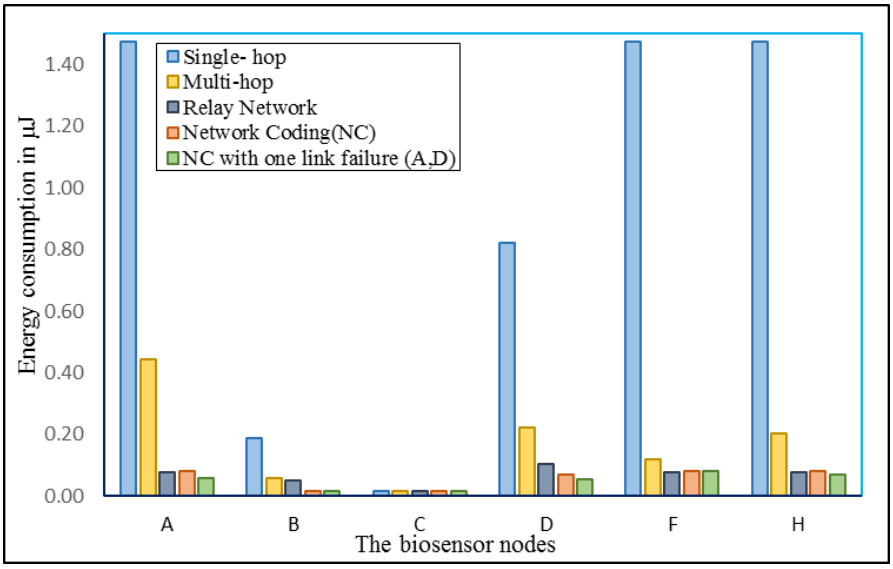

Figure 4.9: Comparison of energy consumption for biosensor nodes for all approaches and NC with a failure link in A and D nodes

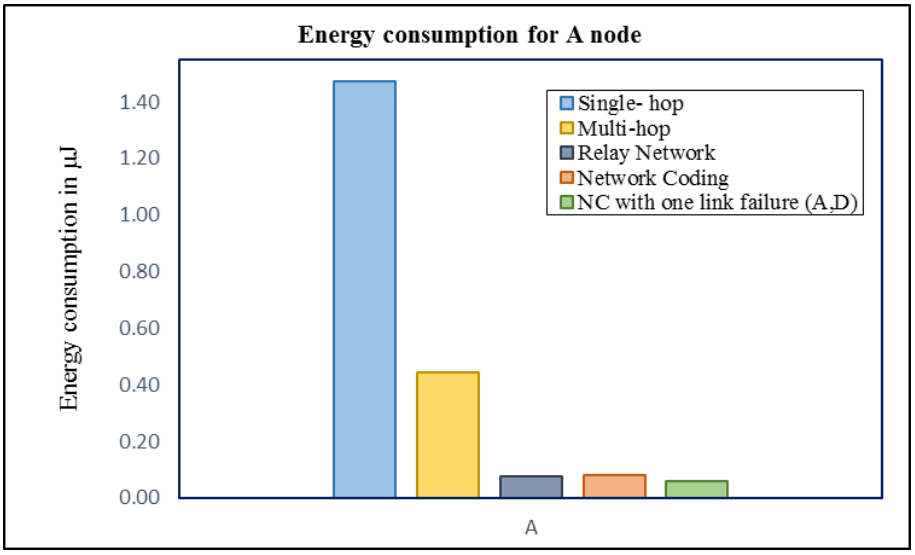

Figure 4.10: Comparison energy consumption for node A in all approaches

According to the bar chart graph shown in Figure 4.11, which compares the energy usage for node D for all approaches, the energy consumption for node D based on the single hop, multi- hop, relay network, NC, and NC with one link failure, are equal to 0.8202µJ/bit, 0.2227µJ/bit, 0.1062µJ/bit, 0.0707 µJ/bit and 0.0534µJ/bit, respectively, which is low in the NC with one link failure.

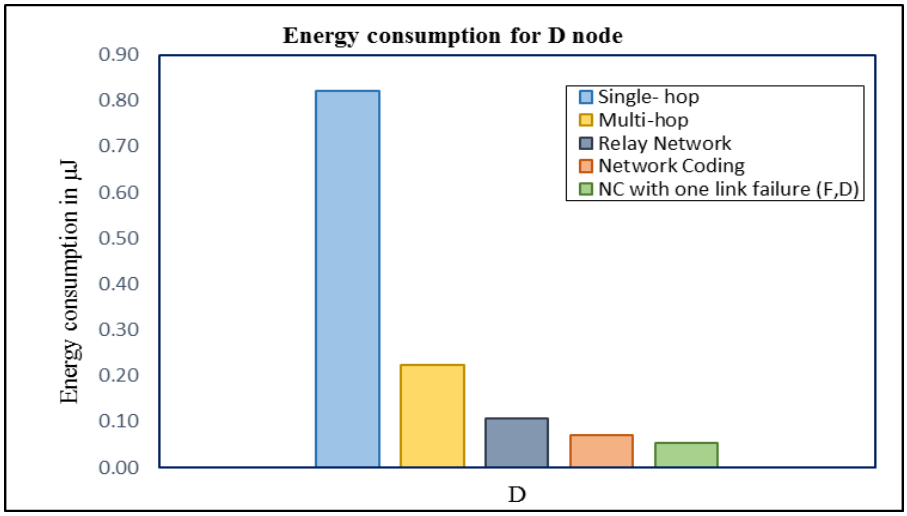

Figure 4.11: Comparison energy consumption for node D in all approaches

In the second case, if there is a failure of links for nodes F and H, as shown in Figure 4.12, the energy consumption is calculated for biosensor nodes in the bottleneck zone based on the single hop, multi-hop, relay network, network coding, and NC with a link failure in F and H nodes, which are compared in Figure 4.13. The energy usage for node F is calculated depending on the single hop, multi- hop, relay network, NC, and NC with one link failure, which are equal to 1.4741µJ/bit, 0.1187µJ/bit, 0.0761µJ/bit, 0.0826 µJ/bit and 0.0593 µJ/bit, respectively. Moreover, the energy consumption for node H based on the single hop, multi-hop, relay network, NC, and NC with one link failure are equal to 1.4741µJ/bit, 0.2033µJ/bit, 0.0761µJ/bit, 0.0826µJ/bit and 0.05281µJ/bit, respectively. The results in this case show more detail in Figure 4.13 concerning the comparison of the energy usage for nodes F and H in all schemes, which are shown in Figure 4.14 and Figure 4.15, respectively. Figure 4.14 and Figure 4.15 also show that, the energy consumption for nodes F and H using NC with a link failure are lower than for other approaches[125].

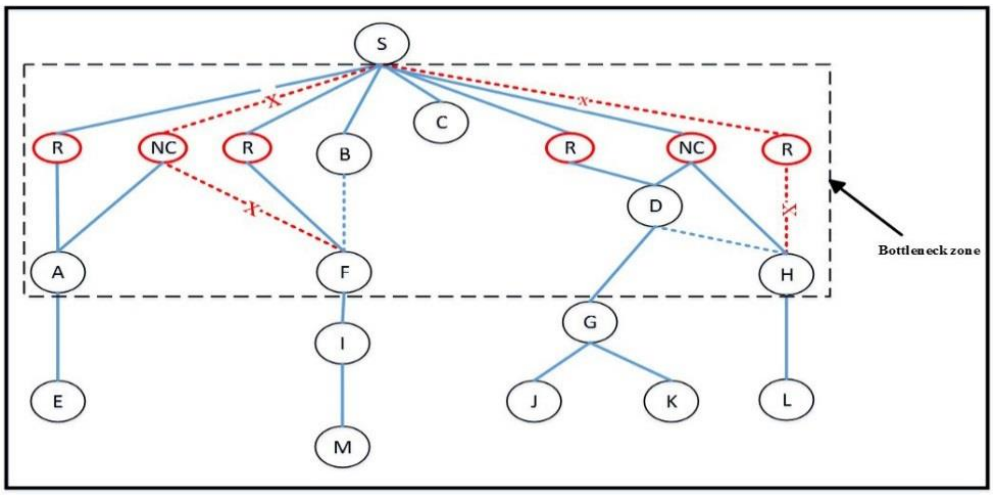

Figure 4.12: Tree topology for WBSN with a failure link for the node H and F

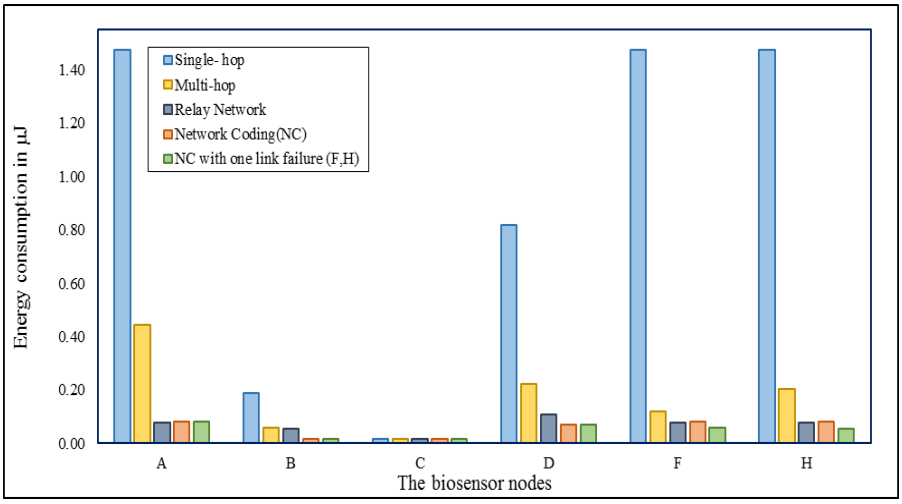

Figure 4.13: Comparison of energy consumption for biosensor nodes for all approaches and NC with a failure link in F and H nodes

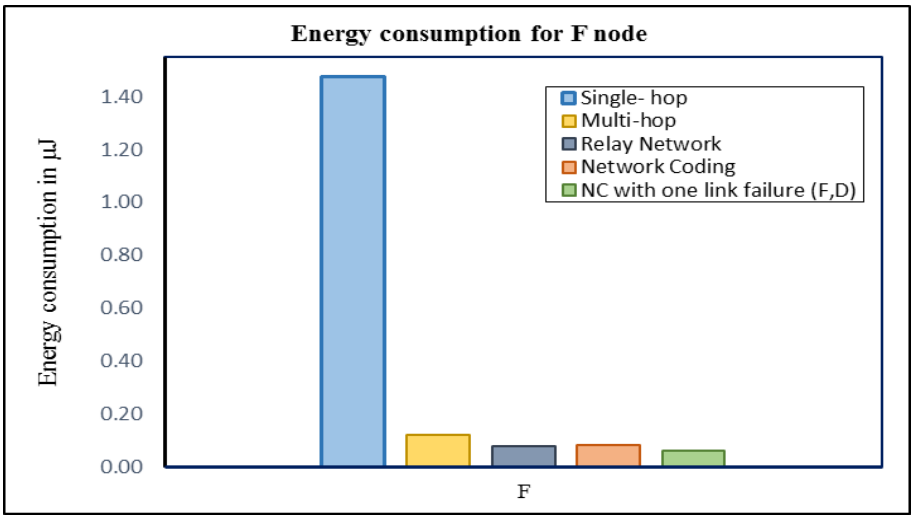

Figure 4.14: Comparison energy consumption for node F in all approaches

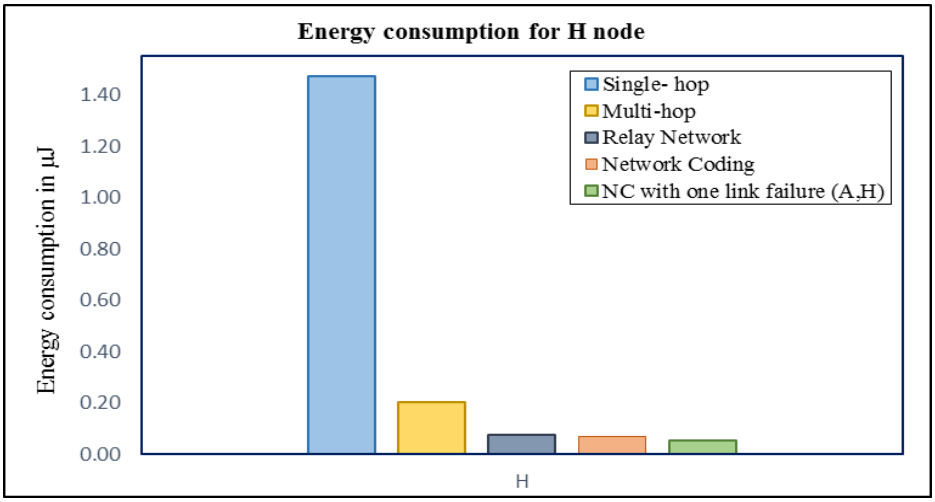

Figure 4.15: Comparison energy consumption for node H in all approaches

Also, in the other cases, the comparisons of the energy consumption for biosensor nodes in the bottleneck zone are shown in Figure 4.16 and Figure 4.17 for all approaches and NC with link failure in the nodes A and H, and nodes F and D, respectively. The energy usage for nodes A and H are equal to 0.0593 µJ/bit and 0.0528 µJ/bit, respectively in NC with link failure in nodes A and H. In addition, nodes F and D energy consumption equals to 0.05939 µJ/bit and 0.0534 µJ/bit respectively based on NC with link failure in nodes F and D.

The energy saved is calculated based on the difference between the proposed approach and other approaches, as shown in Figure 4.18. With regard to NC, the results of the total energy saved are 5.131 µJ/bit, 0.714 µJ/bit, and 0.052 µJ/bit for single-hop, multi-hop, and relay network respectively, as shown in Figure 4.18[125].

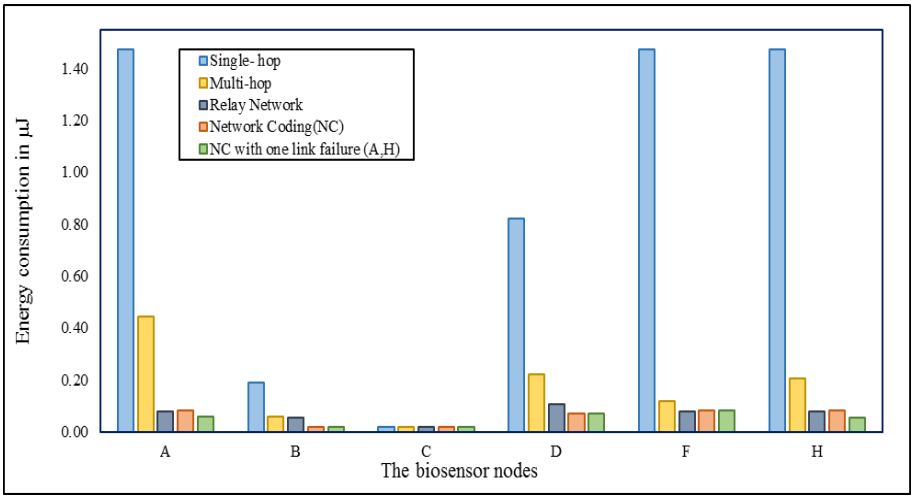

Figure 4.16: Comparison of energy consumption for biosensor nodes for all approaches and NC with a failure link in A and H nodes

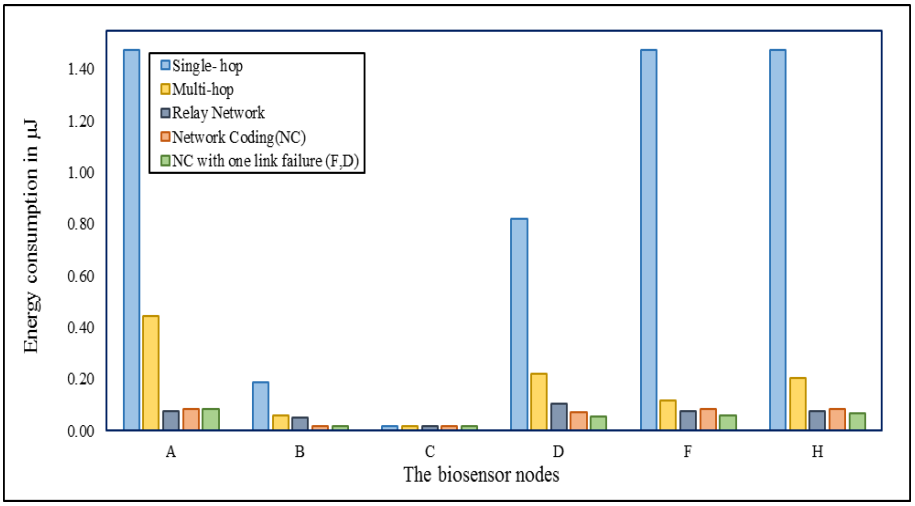

Figure 4.17: Comparison of energy consumption for biosensor nodes for all approaches and NC with a failure link in F and D nodes

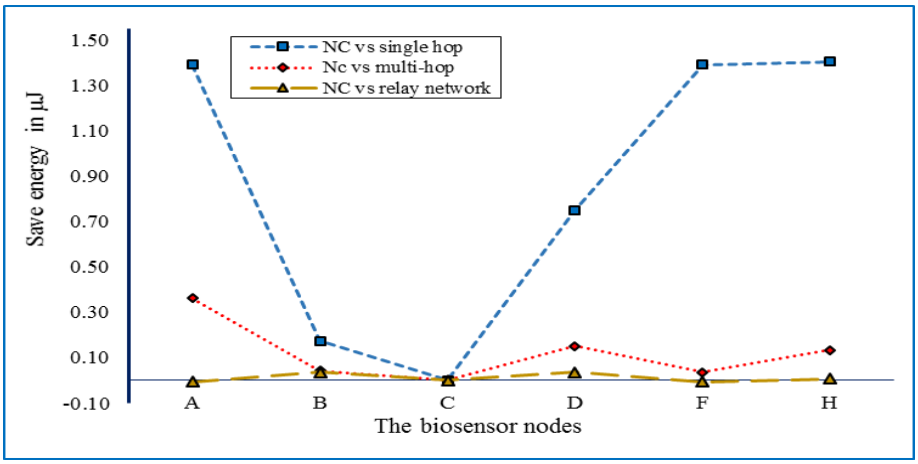

Figure 4.18: Energy saving for biosensor nodes based on the difference between network coding and single hop, multi-hop and relay network

4.5 Chapter Summary

This chapter considered the problem of high energy usage of biosensor nodes which is caused by the bottleneck zone in WBSNs. The design of a novel mathematical model is proposed for body area network topology based on the graph theory, the connection and relationship between the biosensor nodes, simple relay nodes, network coding relay nodes and the sink node are explained in this model. The results show that the proposed RLNC model improves the energy usage for biosensor nodes in the bottleneck zone and guarantees data delivery in the case of link failure. The mathematical model is therefore developed for the enhancement of wireless body networks. Moreover, energy saving for biosensor nodes in the bottleneck zone is achieved through applying the RLNC scheme. The next chapter

will propose Coordinated Duty cycle Algorithm(CDCA) which is applied on nodes in WBSN the duty cycle technique on the proposed approache.

Chapter 5:

Coordinated Duty Cycle Algorithm (CDCA)

5.1 Introduction

In general the energy consumption is a critical issue in a Wireless Body Sensor Network (WBSN), specifically the nodes that are placed next to the sink node consume more energy which limits the network lifetime because all biomedical packets are aggregated through these nodes forming a bottleneck zone. Therefore, a technique is proposed to minimise energy usage for biosensor nodes in the bottleneck zone for WBSNs. By applying the proposed technique which is Coordinated Duty Cycle Algorithm (CDCA) to all nodes in the bottleneck zone, superframe order (SO) selection in CDCA is based on the real traffic and the priority of the nodes in WBSN. Furthermore, a special case of network coding is used, called Random Linear Network coding (RLNC), to encode the biomedical packets to improve the reliability. In this chapter, the combination of the CDCA approach with the RLNC approach for the improvement of energy usage. A mathematical model for WBSN was designed, and it was apparent that energy consumption is reduced with the proposed mechanism; this chapter details the results. Furthermore, the content of this chapter has appeared at 13th international conference (IWCMC)[83].

The chapter is organised as follows: section 5.2 describes the proposal design for coordinated duty cycle algorithm (CDCA), section 5.3 presents wireless body sensor network performance, section 5.4 discusses energy consumption analysis, and finally, chapter summary is drawn in section 5.5.

5.2 The Proposed Design for CDCA Approach

The selection of the superframe order (SO), which represents the summation for the number of Guaranteed Time Slots (GTS) slots and the number of Contention Access Period (CAP) slots, plays the main role in the energy consumption and successful delivery of the biomedical data in WBSN, which has an impact on the performance of the WBSN, for instance, if the value of SO is high and the traffic is low or there is no traffic. The setting of

SO for a long period is not necessary, and it causes an increase in the energy consumption and a delay. In addition, when the value of SO is small, and traffic is high, the network will not be able to process all biomedical packets, which causes the loss of a number of packets. In this situation, the biosensor nodes will save energy but most biomedical packets will be dropped. Hence, the correct selection of the SO based on information about the real traffic and the priority of the nodes in WBSN results in energy saving and delivery of the biomedical packets to the sink node.

With respect to [85],[131],[132], there are different kinds of data, for instance, critical data (CD), normal data (ND), delay sensitive data (DSD) and reliability sensitive data (RSD), which generate from the nature of WBSNs. In this work, the biosensor node generated data is classified into two types: normal data and critical data.

5.2.1 The Calculation for the Initial Slots in WBSN

In WBSN, the data rate is heterogeneous for the biosensor nodes, for example, Electrocardiography(ECG), Electroencephalography(EEG), Electromyography(EMG), blood pressure, and the body temperature sensor, which have 192 Kbps, 86.4 Kbps, 1536 Kbps, 1.92 Kbps, and 1 Kbps, respectively. The number of slots for nodes in WBSN is calculated depending on the data rate and the slots represent the initial values, which are used by the sink node in the proposed approach. Figure 5.1 shows the procedure for the calculation of the slots in WBSN.

According to the procedure as illustrated in Figure 5.1, all biosensor nodes operate on 2.5 GHz. It can be assumed that the length of the symbol is sixteen, then the number of symbols for each biosensor node is calculated by dividing the data rate on the length of the symbol (16 bits is symbol size). For example, the data rate of the ECG nodes is 192 Kbps and nodes would require 12 ksymbols/sec. Moreover, the selection of the sampling frequency is 50 frames/second, which is used to compute the number of symbols per each frame required by the biosensor node to transfer data, for instance, an ECG sensor would need 240 symbols to transfer biomedical data. After that, each node in WBSN requires the number of the slot, and each slot has a limited number of symbols. In this algorithm, each slot has 60 symbols, and the calculation of the number of the slot for the node is computed by dividing the number of the symbol for the node by the number of the symbol per slot, for instance, the ECG sensor needs four slots. Table 5.1 shows the results obtained from the calculation of the slots for nodes in WBSN.

The results are kept in the sink node as an array, which represents the initial value in the proposed algorithm. If the medical staff need to measure the vital signs of the patient in hospital, for example, they select the ECG, EEG, and blood pressure. The sink node has initial slots for each of them such as four slots for ECG, two slots for EEG, and one slot for the blood pressure for the transmission of the biomedical data. Moreover, the medical staff could identify the priority for the nodes in WBSN based on the patient case. Then, the sink node allocates the slots to the node as a GTS slot if the node has high priority, however, it allocates the slots as the CAP slots if the node has a low priority. More details about this point will be discussed in the next sections.

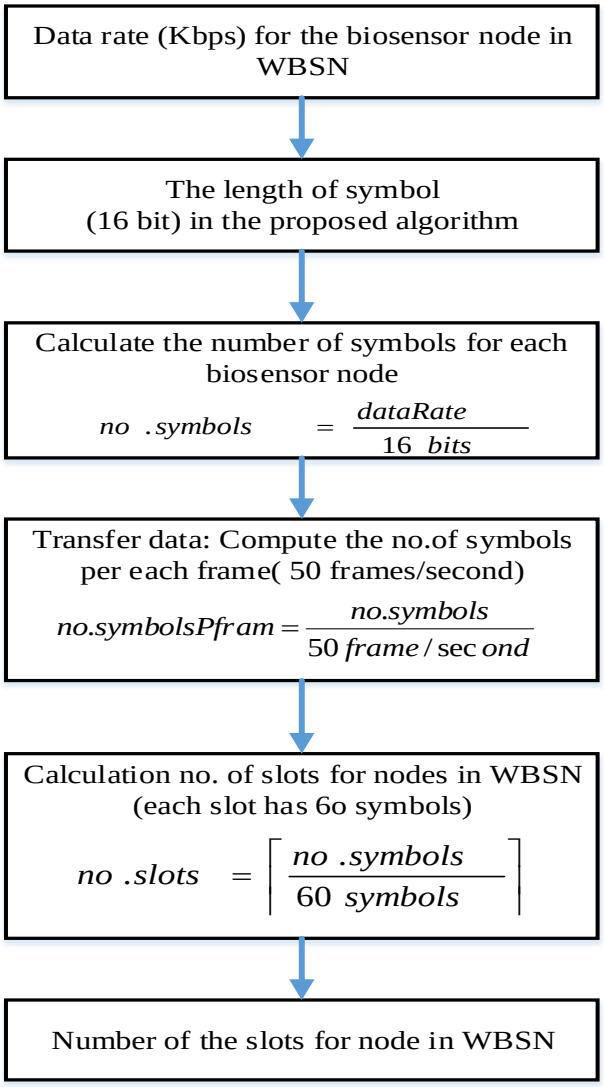

Figure 5.1: The procedure for the calculation of the slots in WBSN, which represent the initial value for the nodes

Table 5.1: The results of the procedure for the calculation of the number of slots for the biosensor nodes in WBSN.

Biosensor node	Data rate	Symbol size	No. of symbol per second	No. symbol per frame	No. slots
ECG	192Kbps	16 bit	12 Ksymbols/sec	240 symbols	4 slots
EEG	86.4 Kbps	16 bit	5.4 Ksymbols/sec	108 symbols	2 slots
EMG	1536 Kbps	16 bit	96 Ksymbols/sec	1920 symbols	32 slots
Blood pressure	1.92 Kbps	16 bit	0.12 Ksymbols/sec	2.4 symbols	1 slots
Body temperature	1 Kbps	16 bit	0.0625 Ksymbols/sec	1.25 symbols	1 slots
Pulse rate	2.4 Kbps	16 bit	0.15 Ksymbols/sec	3 symbols	1 slots
Motion sensor	35 Kbps	16 bit	2.1875 Ksymbols/sec	43.75 symbols	1 slots
Blood saturation	16 Kbps	16 bit	1 Ksymbols/sec	20 symbols	1 slots

5.2.2 The Development in the Reserved Field

Essentially, in the proposed algorithm, the sink node has an array, which includes all information about the biosensor nodes in WBSN such as data rate, the position of the node, and the queue state. The sink node calculates the SO for each biosensor node based on the data rate, which represents the initial values, and saves and updates the value of the SO for each node in the array. Therefore, the configuration of the SO by the sink node indicates the default setting and represents a start point in the proposed algorithm. Then, the SO is adjusted proportionally based on the real behaviour of traffic over time for biomedical data, which is generated through sensing or measuring the vital signs of the human body.

With respect to the standard IEEE 802.15.4, the reserved field in the standard MAC header contains three bits (7-9 bits in the frame control field), as shown in Figure 5.2. Moreover, the bits of the reserved field are set to zero on the transmission and are ignored on the reception. However, in the proposed algorithm, three bits of the reserved field are used as follows: One bit is used to present the level of priority and two bits are used to present the queue state for each node in WBSN. Furthermore, the queue state is equal to zero when the node has no pending packet, and in another case there are three levels for the queue state, as shown in Table 5.2. In addition, the sink node updates the array for all biosensor nodes in WBSN.

Firstly, one bit is allocated to the priority level. The medical staff might identify the priority of the biosensor nodes depending on the case of the patient. The sink node allocates

Guaranteed Time Slots (GTS) in the Contention Free Period (CFP) to the biosensor nodes, which have high priority. The priority of the biosensor node is represented by one bit, and the high priority is equal to one, which presents the critical data, whereas the low priority is equal to zero, which presents normal data, as shown in Figure 5.3 for low priority, the sink node allocates Contention Access Period (CAP) slots for the biosensor nodes in WBSN.

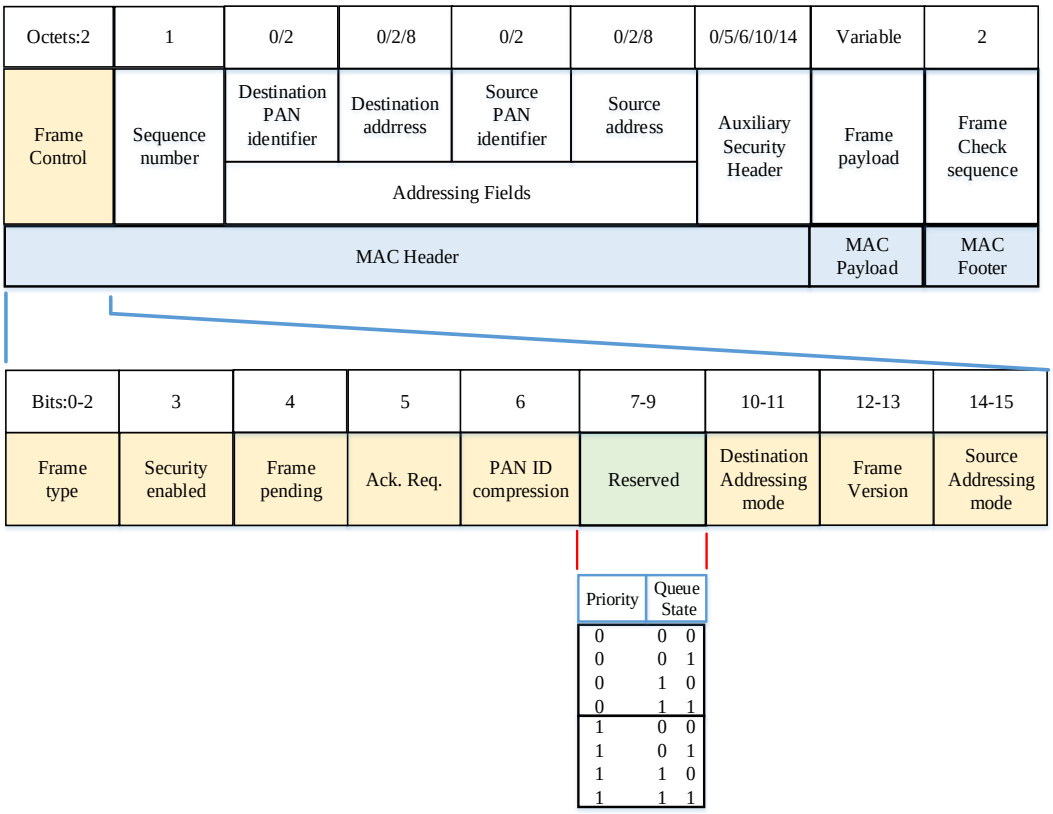

Figure 5.2: General MAC frame format, frame control field and explanation of the values of the reserved field

Table 5.2: The level of the queue state with the priority.

The priority	The levels of the queue state		Kind of data
0	0	0	Normal Data (ND)
0	0	1	ND
0	1	0	ND
0	1	1	ND
1	0	0	Critical Data (CD)
1	0	1	CD
1	1	0	CD
1	1	1	CD

Secondly, the next two bits are used to show the queue state for the biosensor node in WBSN, as illustrated in Figure 5.3. The sink node receives information from the biosensor

node about the queue state, which helps to estimate the network traffic. The queue state can be calculated as shown in equations (5-1) and (5-2). Where NumQueuePkt is the number of biomedical packets inside the queue and QueueSize represents the maximum number of biomedical packets, which can be kept in the queue of the node.

$$queueState = \left\lceil \frac{NumQueuePkt}{a} \right\rceil \quad (5\text{-}1)$$

$$where \qquad a = \left\lceil \frac{QueueSize}{3} \right\rceil \quad (5\text{-}2)$$

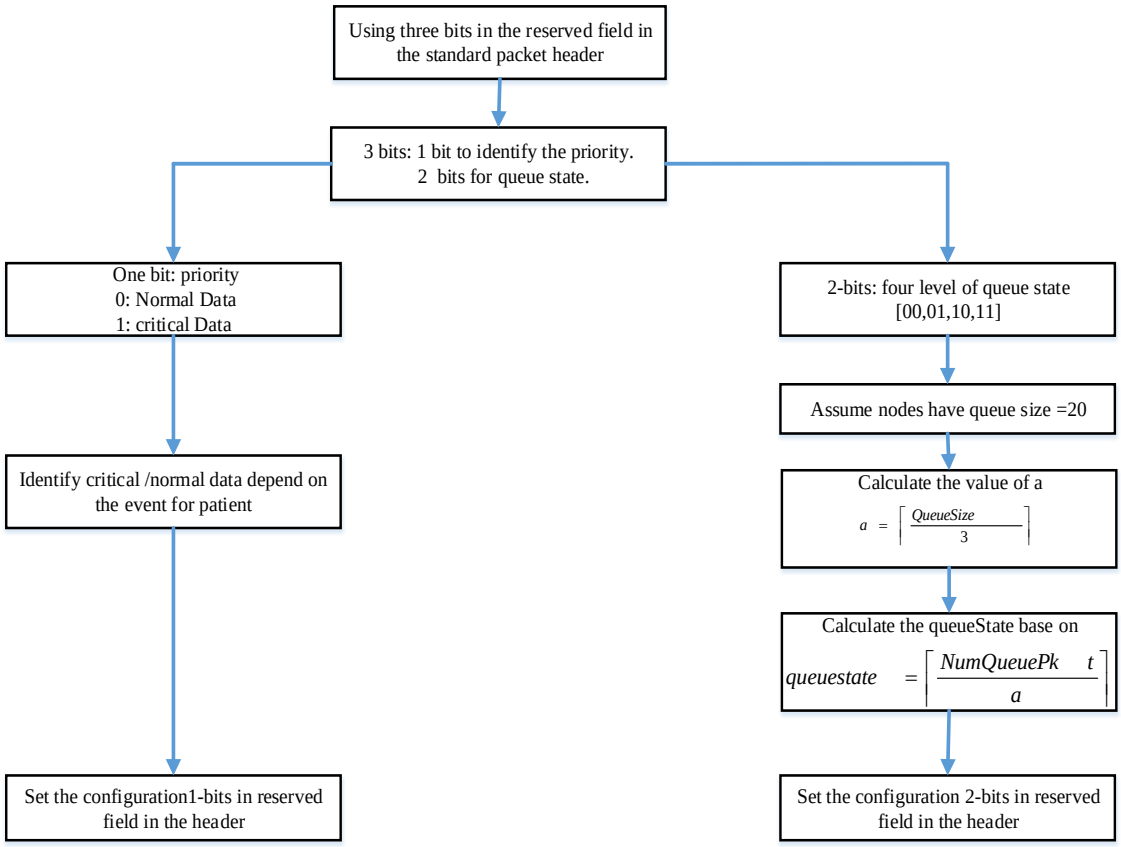

Figure 5.3: The three bits of the reserved field

5.2.3 Coordinated Duty Cycle Algorithm (CDCA)

As far as the priority is concerned, when the patient is at risk and it is a critical case, medical staff should choose the biosensor nodes such as heart rate or electrocardiograms, and they give the priority to the nodes depending on the patient case. Therefore, the generation of the biomedical packets from nodes represent critical data (CD) for the patient. The critical data has high priority in the algorithm of the priority, as shown in Figure 5.4, and needs a certain amount of time for transmission and the highest reliability in WBSN. Furthermore, the sink node allocates the slots, which are termed Guaranteed Time Slots

(GTS) in the Contention Free Period (CFP) depending on the algorithm of SO as presented in Figure 5.5. Then, the sink node updates the format of GTS fields for the node in the MAC header, as illustrated in Figure 5.6. The sink node checks the current GTS slots with the maximum value of the BO in the system. Moreover, it accurately allocates the GTS slots for biomedical nodes in order to save energy consumption and ensures successful delivery of biomedical packets.

The sink node allocates the GTS for the nodes which have a high priority and allocates the remaining slots to the nodes with low priority, as presented in Figure 5.4, and the slot is termed the Contention Access Period (CAP). In addition, the summation of the number of GTS slots and CAP slots represent the SO. For instance, the sink node gives high priority for the ECG sensor and EEG sensor as both nodes generate critical biomedical data. The sink node allocates GTS slots, which include six slots for the ECG and EEG nodes according to Table 5.1. On the other hand, if the sink node has a low priority for the nodes such as the blood pressure and EMG, it allocates CAP slots for the transmission, which are thirty-three. The sink node gives the remaining slots in the active period to the nodes to achieve the transmission and then wait for the next cycle for the completed transmission.

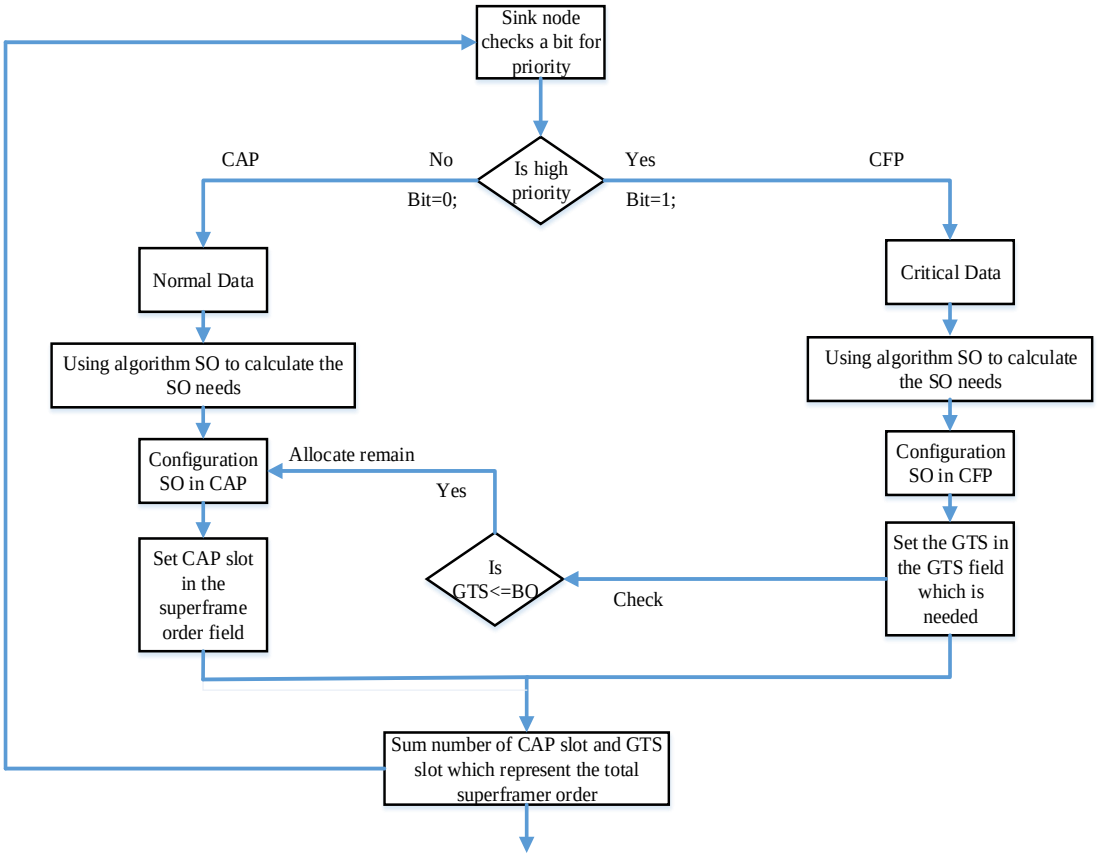

Figure 5.4: The algorithms for the priority of the biosensor node in WBSN

The CDCA algorithm calculates the number of slots for each biosensor node according to the ratio between the remained numbers of pending packets at the queue for the biosensor node to the received number of packets at the sink node. The initial value of slots was calculated for the biosensor nodes in WBSN, as previously reported by the proposed algorithm. Moreover, the value of beacon order (BO) should define the CDCA algorithm. Therefore, the total value of the SO should not exceed the maximum of the BO, as shown in Figure 5.4. The proposed algorithm computes the value of the SO for the nodes depending on the real behaviour of the traffic in the WBSN. In CDCA, the sink node compares between the remaining number of pending packets in the queue for the node and the received packets at the sink node. It determines the next value of the SO for the nodes in WBSN, as presented in Figure 5.5. The CDCA has been explained in the three cases, as below:

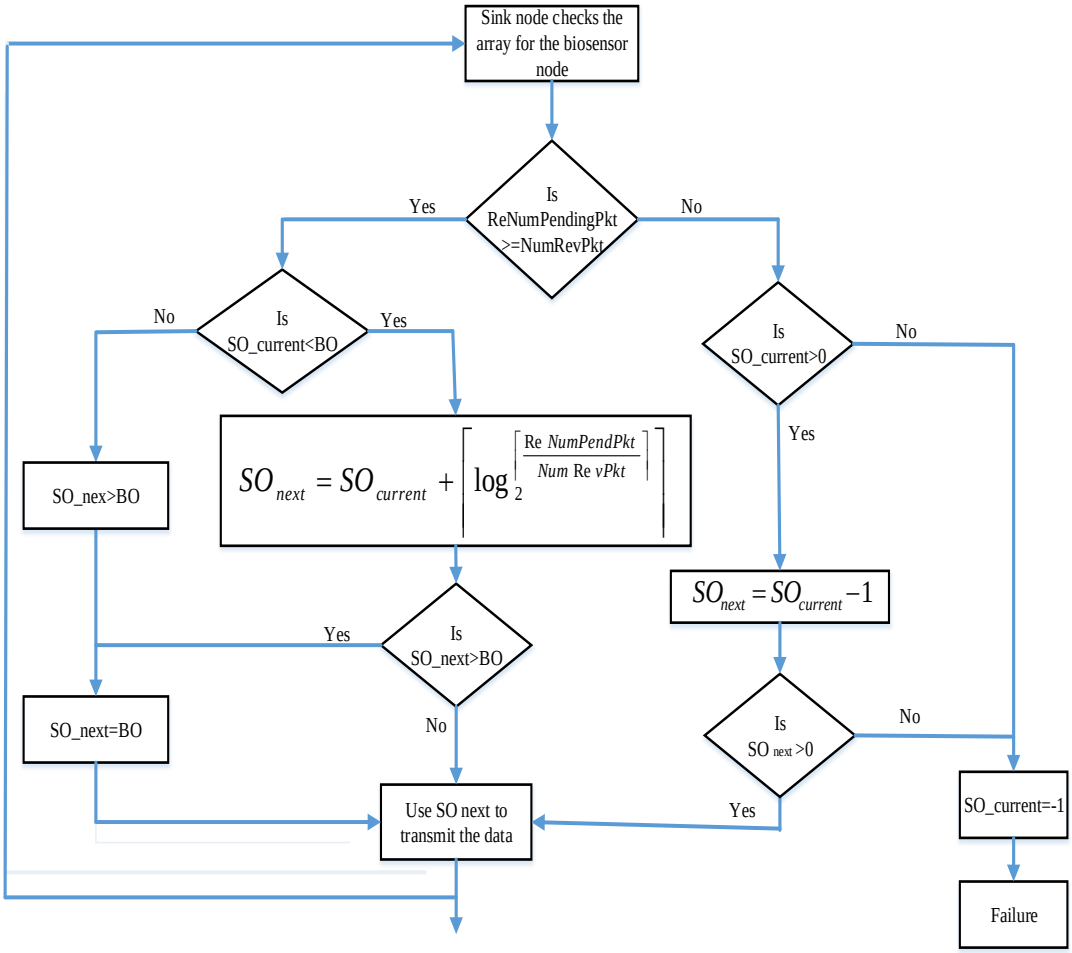

Figure 5.5: The Coordinated Duty Cycle Algorithm (CDCA)

In the first case, if remaining pending packets in the queue are greater than the received packets at the sink node this means the traffic is high, and the active period is not enough to transmit the high traffic. The sink node should increase the value of the SO, as shown in

Figure 5.5. Therefore, increasing the SO duration will make more time available for the data transmission in order to deliver the biomedical packets. In addition, the increment of the value in the new SO increases CAP slots or GTS slots based on the priority. If the degree of the priority is high, the number of GTS slots is increased; otherwise, the CAP slots are increased. The coordinated duty cycle (SO/BO) should be adjusted by increasing the value of the next SO. The coordinated duty cycle (CDC) can affect the energy consumption for the nodes in WBSNs.

$$\begin{aligned} & NumPendingPkt > Num\,\mathrm{Re}ceivePkt \quad \text{and} \quad SO < BO \\ & \rightarrow SO_{next} = SO_{current} + \left\lceil \log 2 \left\lceil \frac{NumPendingPkt}{Num\,\mathrm{Re}ceivePkt} \right\rceil \right\rceil \end{aligned} \tag{5-3}$$

$$coordinated\ duty\ cycle(CDC)_{new} = \frac{SO_{next}}{BO} \tag{5-4}$$

With respect to the constraints, the calculation of the next SO uses the formula in (5-3), where $NumpendingPkt$ and $Num\,\mathrm{Re}ceivePkt$ are the remaining number of pending packets in the queue and the received number of packets at the sink node, respectively. The result of the next SO is used to calculate the new coordinated duty cycle (CDC), as shown in equation (5-4). Then, the new CDC applies the general formula, which is used to compute the energy consumption for the biosensor node in WBSN.

In the second case, the remaining number of pending packets in the queue is lower than the received packets at the sink node. The constraints are emphasised as shown in (5-5), and the sink node reduces the active period through decreasing the value of the SO in order to save energy for the biosensor node in WBSN, as illustrated in Figure 5.5. It determines the next SO and decreases by one, as illustrated in (5-5). As was mentioned in the previous first case, the next SO is used to calculate the coordinated duty cycle (CDC), as presented in (5-4). The new CDC will be able to reduce the energy consumption for the biosensor node in WBSN. This approach saves energy and leads to the successful delivery of biomedical packets for nodes in WBSN.

$$\begin{aligned} & NumPendingPkt < Num\,\mathrm{Re}ceivePkt \quad \text{and} \quad SO > 0 \\ & \rightarrow SO_{next} = SO_{current} - 1 \end{aligned} \tag{5-5}$$

In the third case, if the remaining number of pending packets in the queue is equal to the received packets at the sink node, the sink node maintains the same current value of the SO

for the node in WBSN, as presented in (5-6). Then, the value of CDC is similar to that previous value of CDC.

$$NumPendingPkt = Num\,\mathrm{Re}\,ceivePkt \rightarrow SO_{next} = SO_{current} \quad (5\text{-}6)$$

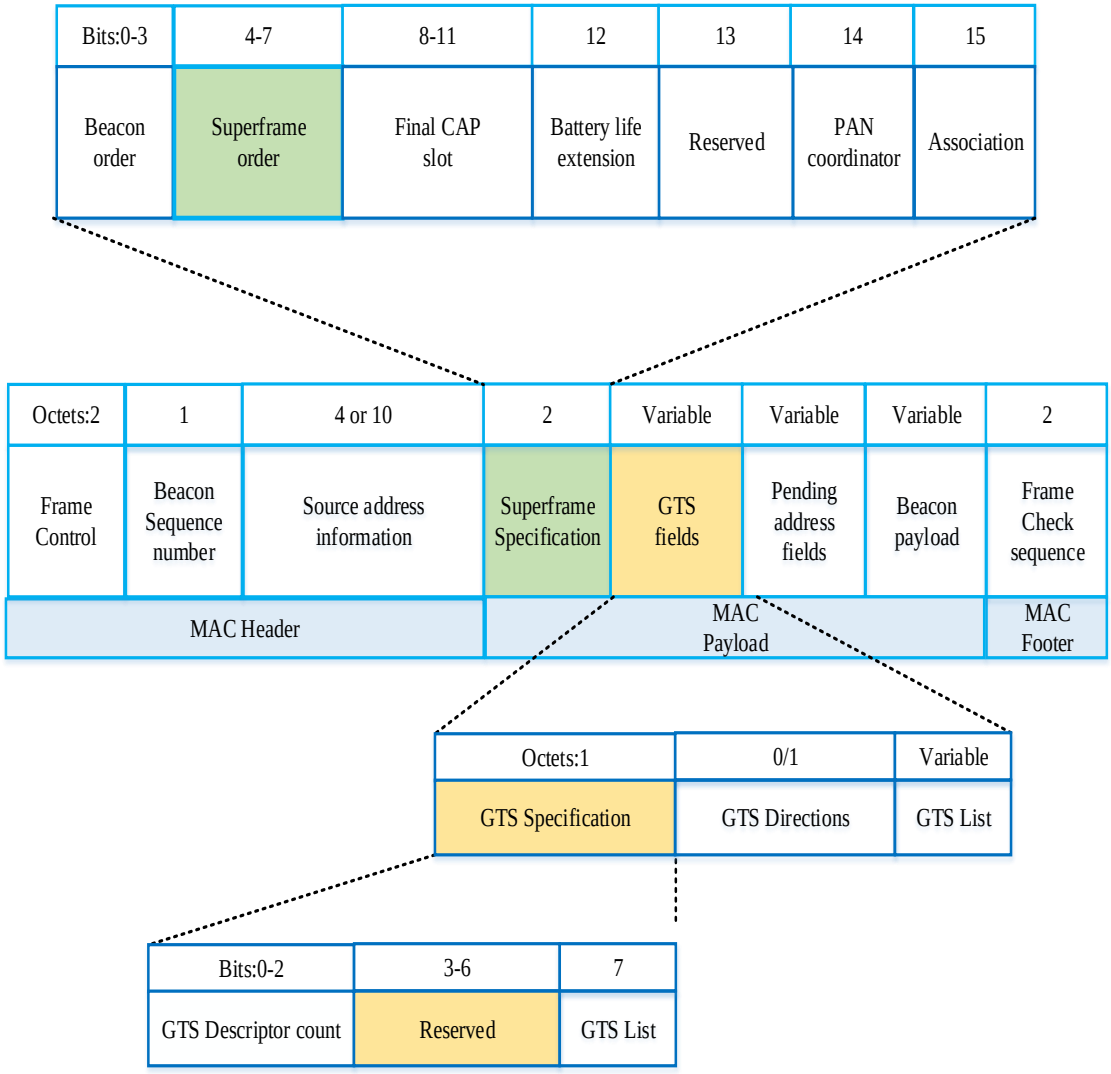

Figure 5.6: The formats for a beacon frame, GTS information, GTS specification, and SO specification

5.2.4 The Implementation CDCA on the Proposed Design Model

With respect to CDCA, the coordinated duty cycle (CDC) is calculated depending on SO and BO values which are affected on the energy consumption for the nodes in WBSNs. The duty cycle achieves energy savings through switching between active and sleep states in the WSN. Let duty cycle is (β), the total energy usage in a time t (period is [0,t]) is given in (5-7) based on the energy consumption formula in Section 3.4.

$$E_T = t[\beta.E_{txr} + (1-\beta)E_{sleep}] \quad (5\text{-}7)$$

Where E_{txr} represents the total energy consumption of transmitting and receiving for the node, β is the duty cycle, and E_{sleep} is the energy consumption per second of the sleep state for a sensor node. The sensor nodes remain in active and sleep states with probability β, (1-β) respectively until time t. All nodes are active when the duty cycle (β)=1, indicating that there is no any energy for sleep[7]. The Nordic nRF2401 has low power consumption, it operates in the 2.4-2.45 GHz range, and is commonly used in WSNs[84].Table 3.3 shows the values of the specific parameters for Nordic nRF2401[84]. The range of duty cycle (β) is shown in (5-8), which is applied on the calculation energy formula.

$$0 \le \beta \le 1 \quad (5\text{-}8)$$

With respect to equation (4-35) that is presented in section 4.2 as shown in (5-9), is used to calculate the energy consumption of WBSN.

$$E^{total}_{whole\_network} = t[(E^t_{TXbr} + E^t_{RXbr} + E^t_{TXrl} + E^t_{TXrs} + E^t_{TXbnc} + E^t_{RXbnc} + E^t_{TXrnc} + E^t_{TXncs})] \quad (5\text{-}9)$$

Substituting (5-9) into equation (5-7), this is obtained:

$$E_T = t[\beta(E^t_{TXbr} + E^t_{RXbr} + E^t_{TXrl} + E^t_{TXrs} + E^t_{TXbnc} + E^t_{RXbnc} + E^t_{TXrnc} + E^t_{TXncs}) + (1-\beta)E_{sleep}] \quad (5\text{-}10)$$

As sleeping energy term has amounted smaller value, so equation (5-11) represents the total energy usage in a time t for nodes in the bottleneck zone WBSN as follows:

$$E_T = t[\beta(E^t_{TXbr} + E^t_{RXbr} + E^t_{TXrl} + E^t_{TXrs} + E^t_{TXbnc} + E^t_{RXbnc} + E^t_{TXrnc} + E^t_{TXncs})] \quad (5\text{-}11)$$

Replacing the terms used in (5-11) by E_{txr} which represents total energy consumption of transmitting and receiving as given in (5-12) for all nodes in the bottleneck zone WBSN.

$$E_T = t[\beta.E_{txr\_nodes\_bottleneck}] \quad (5\text{-}12)$$

The biosensor nodes sense the data and transmit it to neighbouring nodes (or intermediate nodes) which relay the sensed data in the direction of the sink node through the bottleneck zone. In the bottleneck zone, the nodes are classified into two groups: simple relay nodes (R) and network coding relay nodes (Rnc). The former directly communicates to the sink node within a 1-hop or 2-hop range, counting the number of hops from the sink node. On the other hand, the latter encodes the packets before transmission towards the sink node. These nodes are in direct communication with the sink node in the 1-hop range. Furthermore, more details about encoding and decoding algorithms are presented in section 4.3 . The proposed design model is shown in Figure 5.7[83].

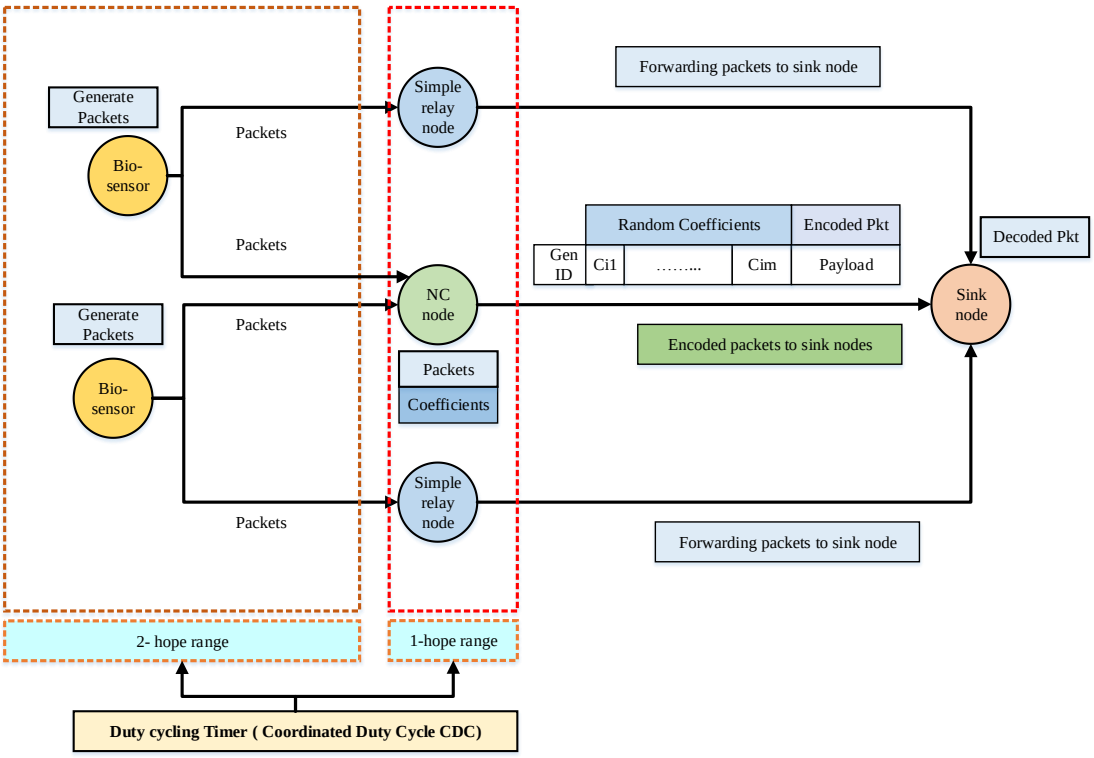

Figure 5.7: The proposed design model of WBSN which employs duty cycle

5.3 WBSNs Performance Evaluation

In this section, the energy consumption is evaluated for the different approaches by using MATLAB R2016b. The energy consumption is calculated based on the different approaches in two scenarios. The first scenario, the binary tree topology is used to distribute the nodes uniformly among the levels. In addition, the same assumptions for all approaches are used for the body area network. The second scenario, WBAN topology is used which includes 13 biosensor nodes on the human body.

5.3.1 Scenario 1: Binary Tree Topology

In this scenario, the binary tree topology is used as depicted in Figure 5.8 because it represents a general case. Each node in this topology has two nodes and all nodes have the same data rate. There are L levels in this topology, the nodes closest to the sink node are at the level L but the nodes furthest away from the sink node are at level 1.

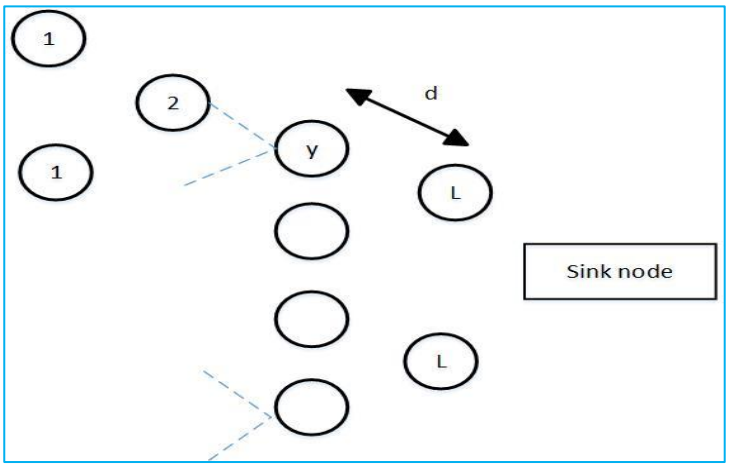

Figure 5.8: The binary tree topology: fixed distance between nodes and number of levels = L

The distance is fixed between. The distance between nodes in the same level is uniform in order to facilitate a more general analysis. The information in Table 3.3 for the Nordic nRF2401 is presented in section 3.4, which is used to calculate energy consumption. The energy usage is calculated for the binary tree based on different approaches such as single-hop, multi-hop, relaying, cooperation, relay network, network coding (NC), and NC with coordinated duty cycle (CDC). Firstly the energy consumption is computed based on NC without CDC. This is compared with a single-hop and multi-hop approach as shown in Figure 5.9, with a distance of 20 cm between nodes[83].

In the single-hop approach, the nodes are situated far away from the sink node, which consumes more energy when compared with any other node, as shown in Figure 5.9. Therefore, they will expire first. However, in the multi-hop approach, the nodes that are far away from the sink node have relayed the packets via the intermediate node towards the sink node. The nodes closest to the sink node have higher energy consumption in the multi-hop analysis. They become hotspots because these nodes are relaying many packets from the nodes on other levels. In NC without CDC, it can be observed that energy usage for the levels 2 and 3 is better when compared with the single-hop and multi-hop as shown in

Figure 5.9. Moreover, the energy of levels 1 and 5 is a balance between two approaches. However, level 4 consumes more energy because the NC approach is applied by adding the relay nodes, and these directly connect to the sink node. Secondly, the energy consumption is measured in the proposed approach with the single-hop and multi-hop techniques, hence it is clear that the energy usage based on the NC with CDC is reduced compared with the single and multi-hop techniques as illustrated in Figure 5.10. Furthermore, there a change in the energy use on levels 4 and 5 when applying duty cycle[83].

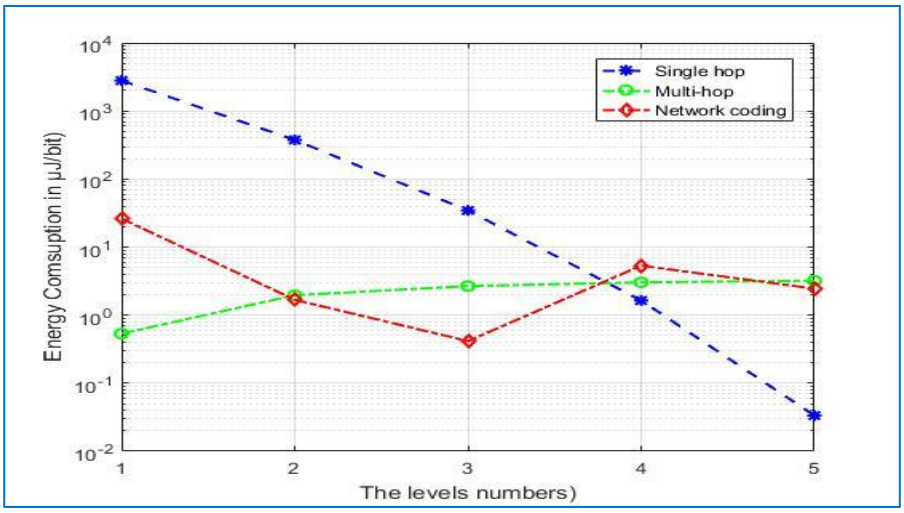

Figure 5.9: The comparison of Energy consumption between single hop, multi-hop and Network coding (L=1/2/3/4/5, n=3.38/5.9, d=0.2)

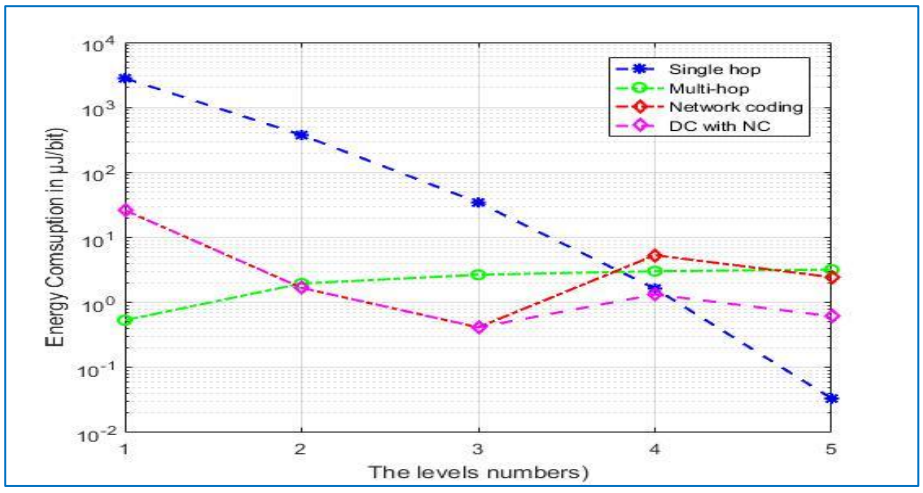

Figure 5.10: Comparison of Energy consumption between single hop, multi-hop, Network coding, and NC with CDC (L=1/2/3/4/5, n=3.38/5.9, d=0.2)

The distance has an impact on the energy communication in WBSNs: the nodes have more energy consumption when the distance is increased between them. Figure 5.11 shows the

outcomes for energy with a 30 cm distance between the nodes. It is clear that the proposed model is affected by increasing the distance between the nodes[83].

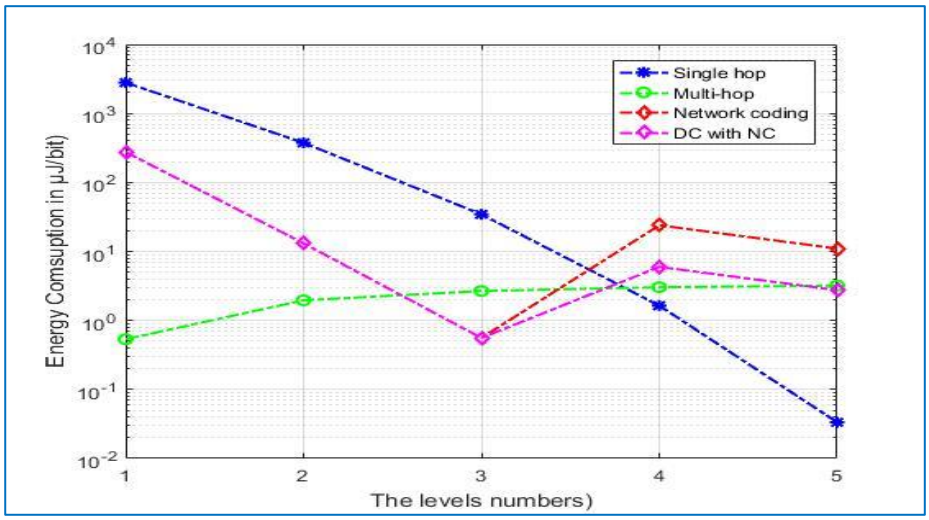

Figure 5.11: Comparison of Energy consumption between single hop, multi-hop, Network coding, and NC with CDC (L=1/2/3/4/5, n=3.38/5.9, d=0.3)

The outcome obtained by applying NC with CDC is reduced energy consumption. The duty cycle β of the WBSN has been varied from 0.1 to 1. As the DC increases from 0.1 to 1, the number of communications within the WBSN increases. Therefore, the energy usage in the WBSN is increased because the number of active nodes is increased in the network. This is clear from Figure 5.12, where the values of the duty cycle are applied on levels 4 and 5, which in turn have an impact on the total energy consumption. On the other hand, the results are compared to the existing techniques such as the relaying, the cooperation and the relay network approaches. The energy consumption is calculated for the different approaches and comparison is undertaken between them. The total energy consumption of all approaches is illustrated in Figure 5.13. Details of the results are shown in Table 5.3 for the full binary tree network[83].

It is clear that the energy usage of the single-hop technique is much higher than that of the other approaches. The total energy consumption and average energy for each sensor node are equal to 294.266 µJ/bit and 4.746 µJ/bit respectively. The nodes situated far away from the sink node consume more power and expire first, such as nodes in level 5. With respect to the multi-hop approach, the total energy usage and the energy for each node are equal to 11.386 µJ/bit and 0.184 µJ/bit, respectively. The nodes placed next to the sink node has more power consumption, such as nodes in level L. These nodes die first, causing failure in the whole WBSN[83].

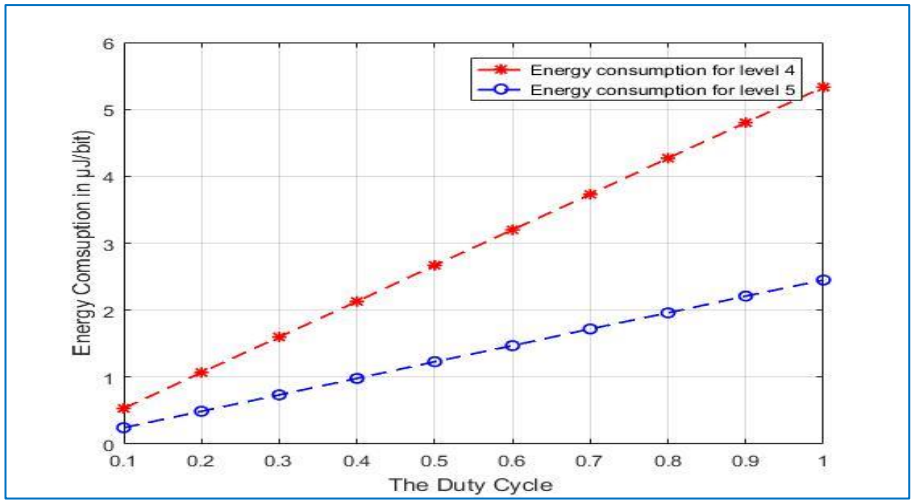

Figure 5.12: Energy consumption for levels 4 and 5 with the values of DC

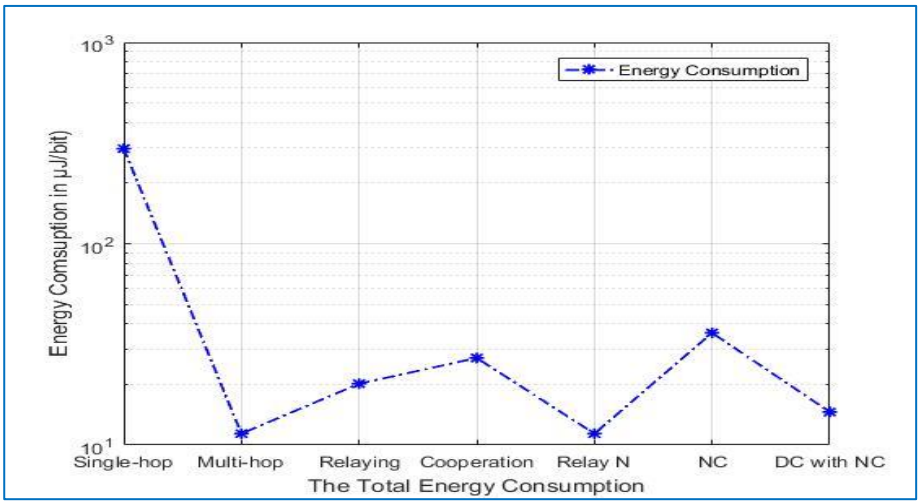

Figure 5.13: Total energy consumptions for different approaches

With regard to the relaying approach, the number of relay nodes is computed which add to the network on level 4, which forward the biomedical packets from nodes far away (these nodes are placed in levels 1 and 2) to the sink node. The total energy usage, the energy for each node and the energy for each relay node are equal to 20.153 µJ/bit, 0.221 µJ/bit and 0.088 µJ/bit, respectively. However, increasing the number of relay nodes on the body causes discomfort for the patient[83].

In the cooperation approach, the number of the relay nodes is computed depending on the limitations imposed by energy usage in the level. Levels 1 and 2 relay the packets to levels 4 and 5 which in turn forward the data to the sink node. The total energy consumption, the energy for each node and the energy for each relay node are equal to 27.058 µJ/bit, 0.436 µJ/bit and 0.076 µJ/bit, respectively. Therefore, reducing the number of relay nodes from that

used in the previous approach causes an increase in energy consumption of the sensor node. In the relay network, the number of relay nodes is much higher (196 relay node) than the other approaches for the full binary tree. This point represents the main drawback of this technique. The total energy usage, the energy for each sensor and energy for each relay node are equal to 11.386 μJ/bit, 0.0173 μJ/bit and 0.0526 μJ/bit, respectively[83].

Table 5.3: Total energy consumption for the binary tree network, the energy for each sensor, for each relay node and the number of a relay node in the case (L=1/2/3/4/5, n=3.38/5.9, d=0.2)

Model	Total energy for network (μJ/bit)	Energy for each sensor (μJ/bit)	Energy for each relay (μJ/bit)	Number of relay node
Single -Hop	296.468	4.781	-	-
Multi -Hop	11.386	0.183	-	-
Relaying	20.153	0.201	0.088	48
Cooperation	27.058	0.436	0.076	18
Relay network	11.386	0.0173	0.0526	196
DC with NC	14.587	N/A	0.151	18

Note: N/A, not applicable (DC applied on some nodes. Therefore, some nodes are active (awake) and others are inactive (sleep); energy consumption for each sensor node cannot be calculated in the whole topology which represent average of energy usage).

The proposed approach is better than the relaying and cooperation methods because the energy consumption is lower. However, the relay network is lower in this respect than other approaches, but there is the drawback of the number of relay nodes, in that 196 nodes are used which would be uncomfortable for the human body. The results in terms of energy consumption are compared for levels 4 and 5 between the proposed approach and existing approaches as shown in Figure 5.14. In summary, one key advantage is minimising the energy consumption based on the duty cycle, which is applied to the nodes closest to the sink node[83].

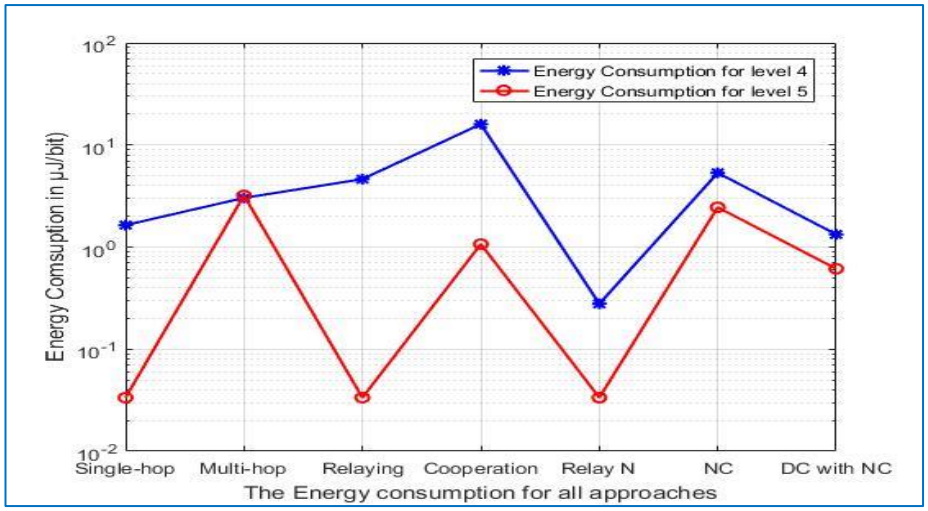

Figure 5.14: Comparison of energy consumption between levels 4 and 5 for all approaches. (Level 4=series1 /Level 5=seies2, n=3.38/5.9, d=0.2)

5.3.2 Scenario 2: WBAN Tree Topology

This scenario uses the same example of the WBAN topology as used in Section 4.4. The same data as shown in Table 4.2 is also used for this scenario.

In the single-hop approach, the biosensor nodes in the bottleneck zone consume more energy based on the distance such as nodes A, F, and H when compared with other approaches as illustrated in Figure 5.15. However, in the multi-hop approach, the biosensor nodes relay the packets via the intermediate node towards the sink node. The nodes A, and D have greater energy consumption in the multi-hop but the node C has the same value of energy in most approaches because it is directly connected to the sink node, as shown in Figure 5.15. The energy consumption for all biosensor nodes in the relay network approach is lower compared with single-hop and multi-hop approach. Detailed results of the energy usage for biosensor nodes in the bottleneck zone and network coding approach are explained in section 4.4.

Looking at Figure 5.15, it can be seen that the energy consumption for biosensor nodes in the bottleneck zone based on the proposed CDCA tend to be smaller than the energy consumption for nodes in all approaches except node A. The duty cycle for node A is equal to one as it requires all time slots and hence no energy saving. In addition, the calculations of energy in all approaches have been considered: the line of sight (LOS) propagation, the non-line of sight (NLOS) propagation, and the distance between biosensor nodes and sink node. Also, the proposed CDCA approach considers the data rate which is heterogeneous

for the biosensor nodes in WBSN, it achieves the energy saving for most biosensor nodes, as required.

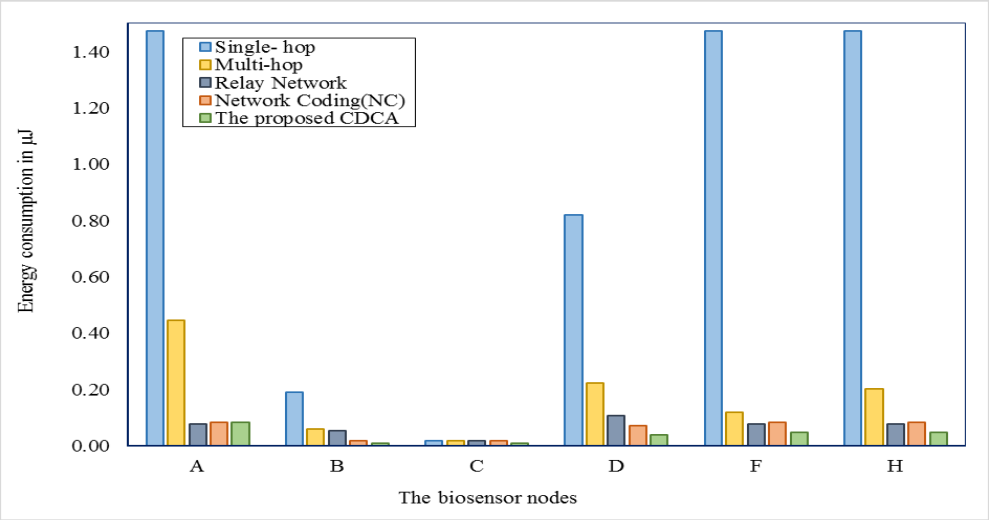

Figure 5.15: Comparison of energy consumption for biosensor nodes in the bottleneck zone based on the single hop, multi-hop, relay network and Network coding, and the proposed CDCA

5.4 Energy Consumption Analysis

With respect to example of WBSN topology, there are some biosensor nodes which sense and measure vital signs of the human body such as electroencephalogram (K sensor) and ECG (D sensor), EMG (A and I sensor nodes), and blood pressure (G sensor). In addition, sequential numbers (1, 2, 3,… 13) are used which represent the sequential alphabet for the sensor nodes (A, B, C,…, M), respectively to ease the use of explanatory nodes on WBAN topology.

To analyse the basic performance of the proposed WBSN which consider the theoretical calculation based on the mathematical model as was explained in section 4.2 and compared without applying the proposed mathematical model. The results obtained from the preliminary analysis of the energy consumption for the biosensor nodes can be compared in Figure 5.16. It can be seen that the energy consumption for biosensor nodes in the proposed WBSN tend to have smaller than the energy consumption for nodes without using the proposed mathematical model. Although, in both calculations of energy have considered the line of sight (LOS) propagation, the non-line of sight (NLOS) propagation, and the distance between biosensor nodes and sink node.

As shown in Figure 5.16, the energy usage for nodes without using the proposed WBSN such as EMG (node 1) and motion sensor (nodes 5 and 13), and node10 increase significantly more than the other nodes because the distance between these nodes and the sink node is approximated at 0.6m. It is clear that more energy saving is achieved by using the proposed mathematical model for WBSN, which use the simple relay node and the network coding relay node to forwarding biomedical packets and encoding biomedical packets toward the sink node, respectively. The simple relay node and NC relay node play an important role in the reduction of the energy usage for biosensor nodes in BAN. However, in the model, the glucose monitor (node 6) and blood pressure monitor (node 8) have more power consumption because the distance has an impact on the calculation of the energy used for nodes in WBSN.

On the other hand, when coordinated duty cycle algorithm (CDCA) employs in the proposed model for WBSNs. The sink node, which has information about all biosensor nodes in the body area network, calculates the number of slots which represent the active period for each node depend on the data rate. Although, the data rate is heterogeneous for the biosensor nodes in WBSN. For example, the data rate for ECG (node 4) has a much greater than the data rate of the body temperature sensor (node 2) which are 196 kbps and 1 kbps, respectively. The sink node computes the number of slots for each node, it calculates and allocates the coordinated duty cycle (CDC) for each node in WBSN. The results demonstrate that the energy consumption for biosensor nodes in the model which employs the coordinated duty cycle has better performance when compare to not using a coordinated duty cycle (CDC) in the same model as shown in Figure 5.16. However, the energy consumption for EMG sensor nodes (which represent nodes 1 and 9) are equal in both calculations as shown in Figure 5.16 because the nodes have a high data rate which is 1536 kbps and they need the whole duty cycle which means that the number of slots (SO) is equal to the beacon order (BO). Details of the results are shown in Table 5.4 for the nodes in WBSN topology.

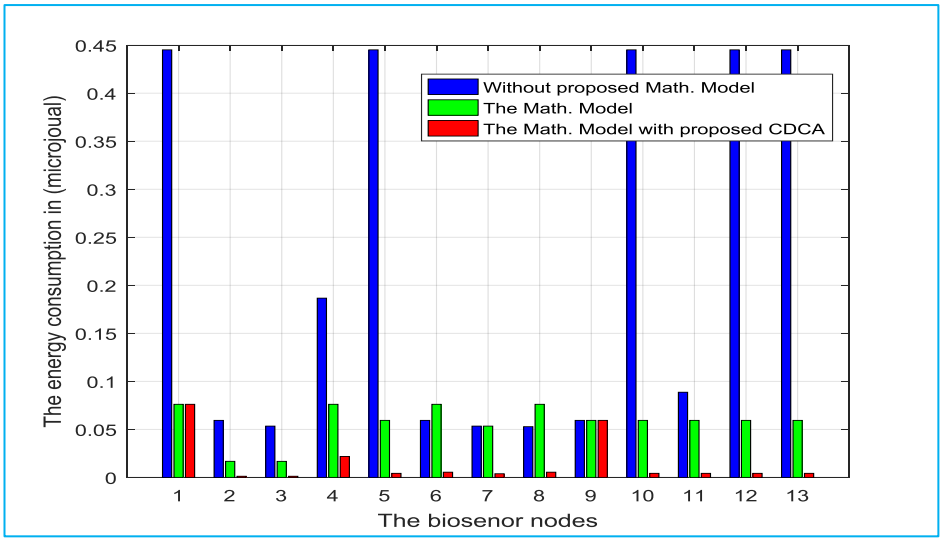

Figure 5.16: The comparison of energy consumption for biosensor nodes without the proposed mathematical model, with the proposed mathematical model for WBSN, and the proposed mathematical model with CDCA

Table 5.4: Comparison of energy consumption for biosensor nodes in WBSN topology base on: without the proposed mathematical model, with the proposed mathematical model for WBSN, and the proposed mathematical model with CDCA

Node	Node number	Energy usage without proposed Math. Model (μJ/bit)	Energy usage with the Math. Model (μJ/bit)	Energy usage with the Math. Model and proposed CDCA (μJ/bit)
A	1	0.44511	0.07610	0.07610
B	2	0.05936	0.01673	0.001195
C	3	0.05340	0.01670	0.001193
D	4	0.18660	0.07610	0.02174
E	5	0.44511	0.05936	0.00424
F	6	0.05936	0.07610	0.00543
G	7	0.05340	0.05340	0.00381
H	8	0.05281	0.07610	0.00543
I	9	0.05936	0.05936	0.05936
J	10	0.44511	0.05936	0.00424
K	11	0.08866	0.05936	0.00424
L	12	0.44511	0.05936	0.00424
M	13	0.44511	0.05936	0.00424

5.5 Chapter Summary

In this chapter, the problem of high energy usage in the bottleneck zone in WBSNs have been considered. The Coordinated Duty Cycle Algorithm (CDCA) design is proposed for WBSNs based on the real behaviour of traffic and the priority of the sensor nodes in WBSNs. In addition, a mathematical model (as proposed in Chapter Four) has been developed for the

enhancement of the design and energy consumption of wireless body area networks through applying the proposed CDCA approach. The combination of the CDCA approach and RLNC type is applied to enhance the energy usage in the bottleneck zone. Moreover, two studied scenarios are considered in this chapter, the results have been analysed numerically. Therefore, the results of our approach show reduction in energy usage in comparison to existing techniques.

The next chapter presents novel statistical model for the reliability in WBSNs and discusses the improvement of the probability for successful reception at the sink node in WBSN will be described.

Chapter 6:

A Reliability Model for the WBSN

6.1 Introduction

In the healthcare and medical applications, the biomedical sensor nodes such as ECG, blood glucose level, heart rate, etc. are generated as various kinds of biomedical packets, which should be transmitted with the highest reliability (guaranteed delivery of data). Therefore, each biomedical sensor node should provide accurate biomedical data because all patient information is paramount in WBSNs like ECG. One of the crucial issues in the design of WBSN is network reliability because it is related to the life of patients. The proposed novel mathematical mode for the reliability in WBSNs is based on the forwarding technique, encoding technique, and a combination of both to calculate the probability of successful reception at the sink node. This work has highlighted RLNC, which employs the relay node to achieve the required level of reliability in WBSN and to guarantee that the biomedical data should be delivered correctly by the sink node. Moreover, the biosensor node sends biomedical packets through the simple relay node (R) and network coding relay node (NC), and the former node forwards packets toward the sink node while the latter node encodes packets based on RLNC. This uses coefficient polynomial from Galois Field (GF) to create the encoding packets and then transmit towards the sink node. The aggregation of biomedical packets in the network coding relay node and use of the RLNC greatly improve the reliability in WBSNs. The RLNC has been presented and results have shown that the RLNC scheme can be very useful in improving reliability for WBSN.

In addition, it is important to compare and discuss between RLNC technique and XOR NC technique, Notice that the encoding technique (which is employed RLNC) offers a better performance than XOR NC technique in terms of reliability and probability for successful reception at the sink node, which is related with lower power.

The chapter is organised as follows. Section 6.2 presents the model of wireless body sensor network. Section 6.3 shows the reliability of Body Area Network (BAN) model design. Section 6.4 describes the studied scenario. Section 6.5 presents the measurement

methods. Section 6.6 discusses performance of proposal technique with existing technique. Section 6.7 presents the validation of the reliability in the bottleneck zone WBSN. The conclusions are drawn in section 6.8.

6.2 The Model of Wireless Body Sensor Network

WBANs are concerned with life-critical biomedical packets such as heart rate or electrocardiograms, which have to be delivered reliably. Therefore, a lost biomedical packet may cause the life of the patient to be at risk or may be the cause of misinterpretation because the total packets would be incomplete. Although there are previous studies in the reliability procedures to address this issue, the reliable data transmission is still a challenge for WBSN and medical monitoring systems, such as in the event of an emergency, and this needs to be considered and developed [4,5]. Reliability is most important for body area network, which represents a key requirement in WBSN application, especially in healthcare. In this chapter, a novel mathematical model for the calculation of the probability for successful reception at the sink node is proposed, which employs the random linear network coding (RLNC). The RLNC technique is resilient for biomedical data to improve the network reliability in WBSN [4].

With regard to the system model in Figure 4.2, the researchers propose a novel mathematical model for body area network (BAN) topology to explain the deployment and connection between biosensor nodes, simple relay nodes, NC relay nodes and the sink node. Moreover, the proposed technique uses RLNC to improve the energy efficiency for the nodes in the bottleneck zone [126]. In this thesis, a general case WBSN topology is illustrated in Figure 4.5, including 13 biosensor nodes, which are placed on the human body. The biosensors comprise EMG sensor (nodes A and I), body temperature sensor (node B), pulse rate sensor (node C), ECG sensor (node D), glucose monitor sensor (node F), and blood pressure monitor (node H).In addition, there are some biosensor nodes which sense and measure vital signs from the human body such as Pulse rate, Temperature, Motion sensor, and Blood pressure.

With respect to the WBSN model, simple relay nodes and NC relay nodes are added to the WBSN topology, as shown in Figure 6.1.The extended WBSN topology is illustrated on the right-hand side and a sample topology is shown on the left hand side, which includes a biomedical sensor node (A), a simple relay node (R), a NC relay node (NC), and the sink node (S).

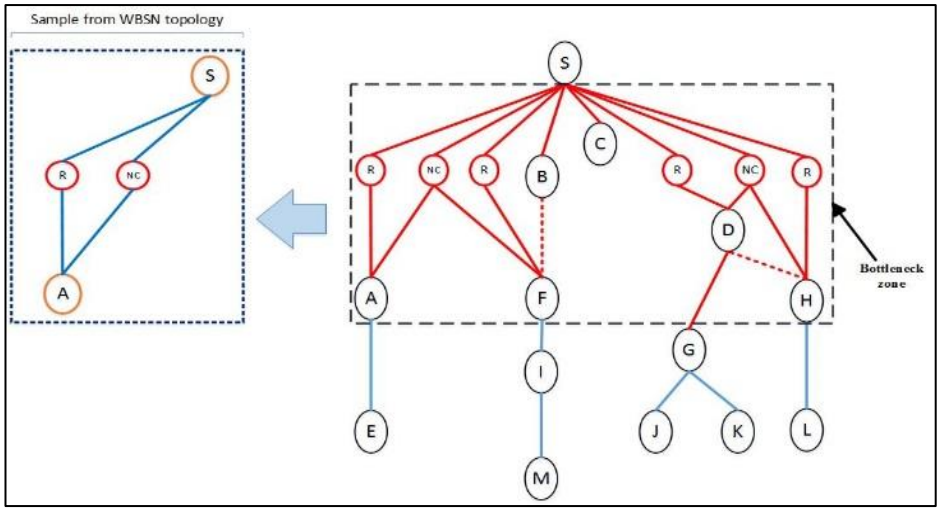

Figure 6.1: Tree topology for WBSN with one sample from WBSN topology

6.3 The Reliability of Body Area Network (BAN) Model Design

A model of a BAN is represented in Figure 4.5 (Chapter four), which includes one element for each wireless device (biosensor node, simple relay node, network coding relay node or sink node) of the network and the number of links (arcs) between them. In order to investigate the transmission reliability of the proposed approach [126] in Figure 4.5, with respect to the sample topology of WBSN as shown in Figure 6.1, this sample topology to theoretically derive the probability for successful reception (PSR) at the sink node is considered, for three techniques such as forwarding, encoding, and combining the forwarding and encoding techniques. Therefore, the successful delivery of biomedical packets at the sink node is studied and the transmission reliability of the WBSN based on the proposed approach is described [126]. Successful delivery, indicates the probability of successful reception (PSR) at the sink node of the biomedical packets transmitted by the biomedical sensor node.

$$p(\textit{successful delivery}) \approx \frac{\text{no. of packets received correctly by sink node}}{\text{total no. packets sent by biosensor node}} \qquad (6\text{-}1)$$

In general, the average bit error probability (p) is calculated based on equations (6-2) or (6-3)[133].The probability of failure (average bit error probability of the link) = p, and the probability of successful = (1- p). In most cases, the values $(p_{AR}),(p_{RS}),(p_{AC}),and\ (p_{CS})$ are assumed to be the same for all links in the network. All terms will be defined in the next sections.

$$p_{b_{M-PSK}} \cong \frac{2}{\max(\log_2 M, 2)} \sum_{i=1}^{\max(\frac{M}{4},1)} Q\left(\sqrt{\frac{2E_b \log_2 M}{N_0}} \quad \sin\frac{(2i-1)\pi}{M}\right) \tag{6-2}$$

$$p_{b_{M-QAM}} \cong 4\left(\frac{\sqrt{M}-1}{\sqrt{M}\log_2 M}\right) \sum_{i=1}^{\sqrt{M/2}} Q\left((2i-1)\sqrt{\frac{3E_b \log_2 M}{N_0(M-1)}}\right) \tag{6-3}$$

Where P_b, PSK, M, E_b/N_0, and QAM are probability of bit-error, phase shift keying, number of symbols in the modulation (the modulation order), energy per bit to noise power spectral density ratio, and quadrature amplitude modulation, respectively.

6.3.1 Reliability of the Forwarding Technique

The biosensor node (A) directly transmits the biomedical packets to the sink node (S) through the simple relay node (R) as shown in Figure 6.2, which represents a sample topology of WBSN using the forwarding technique. The terms, which are used to define the PSR equation at the sink node using the forwarding technique, can be defined as: (p_{AR}) is the average bit error probability of the link from A node to R node; (p_{RS}) is the average bit error probability of the link from R node to S node; $(1-p_{AR})$ is the probability of successful transmission for link A to R, and $(1-p_{RS})$ is the probability of successful transmission for link R to S.

With respect to the probability theory, there are two standard rules, which are the addition law and multiplication law [134] as given in Appendix A and are used in this model to compute the probability of successful reception (PSR) at the sink node. In the forwarding technique, the biosensor node (A) sends biomedical packets towards the sink node through the simple relay node. In this case, there are two assumptions depending on how many packets were correctly received at the sink node (S). In the former case, the probability of successful packets being received at the sink node (t=1, 2….m) is between one packet to m packets, and the equation is shown in (6-4). However, in the latter case, based on the assumption that all biomedical packets (m) are correctly received at the sink node (S), when t is equal to m in (6-4), then the probability of success for all biomedical packets (m) at the sink node (S) is calculated using equation (6-5).

$$(1-p_{AS})_m = \binom{m}{t}\left[(1-p_{AR})(1-P_{RS})\right]^t\left[1-(1-p_{AR})(1-p_{RS})\right]^{m-t} \quad (6\text{-}4)$$

$$(1-p_{AS})_m = \left[(1-p_{AR})(1-P_{RS})\right]^m \quad (6\text{-}5)$$

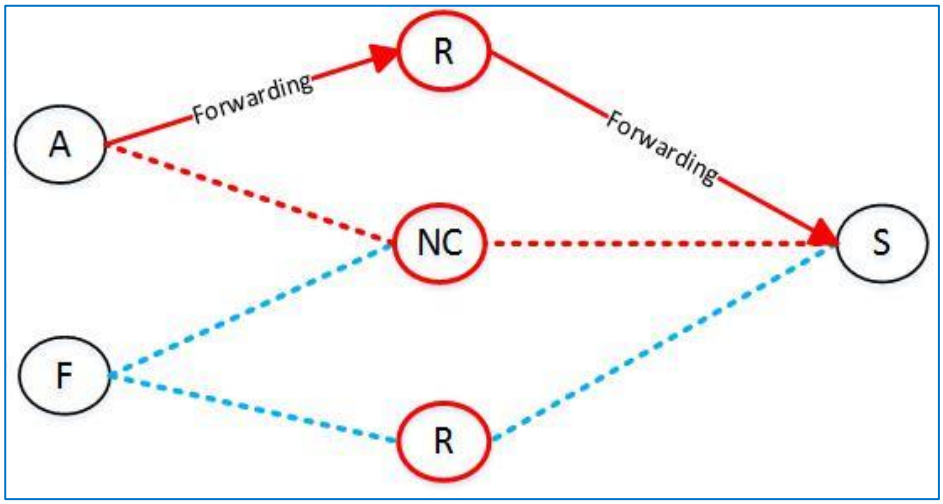

Figure 6.2: Transmission biomedical packets from biosensor node to sink node by using forwarding technique in WBSN

6.3.2 Reliability of the Encoding Technique

The biomedical packets are transmitted from the biosensor node (A) to the network coding relay node (NC), and then the NC relay node encodes the biomedical packets to create the encoding packets based on the Galois field technique. These are then transmitted to the sink node (S) as shown in Figure 6.3, which represents a sample topology for WBSN based on the encoding technique. The terms, which are used to define the PSR at the sink based on the encoding technique, can be defined as: (p_{AC}) is the average bit error probability of the link from A node to NC node. The (p_{CS}) is the average bit error probability of the link from NC node to S node; the $(1-p_{AC})$ is the probability of successful transmission for link A to NC, and the $(1-p_{CS})$ is the probability of successful transmission for link NC to S.

As far as the encoding technique is concerned, there are two transmission parts in the encoding technique. Firstly, there is the forwarding transmission, which transmits biomedical packets (m) from the biosensor node (A) towards the NC node. Secondly, there is the encoding transmission, which encodes the biomedical packets (m') and transmits them

towards the sink node (S). With the encoding transmission, the PSR at the NC node for biomedical packets can be given in (6-6), assuming that the probability of the links are independent. It is assumed that all received packets (m) at the NC relay node are correct. The PSR is represented in (6-7) at the NC node. In this case, the number of transmission packets is equal to the number of received packets.

$$(1-p_{AC})_{i\ from\mathrm{m}} = \binom{m}{i}(1-p_{AC})^{i}\, p_{AC}^{m-i} \tag{6-6}$$

$$(1-p_{AC})_{i\ from\mathrm{m}} = (1-p_{AC})^{m} \qquad if\ i=m \tag{6-7}$$

The probability of successful reception for encoding biomedical packets at the sink node (S) is given in (6-8). Furthermore, the sink node (S) needs to receive at least m coded packets from the NC relay node (C) to be able to recover the original information. The sink node (S) should receive biomedical packets greater than or equal to m packets, which are transmitted from the biosensor node (A). This means that the number of encoded packets should be greater than or equal to the number of native packets that help to recover the original packets in the sink node (S). The relationship between the encoded packet and the native packets is given in (6-8). The PSR for the biomedical packets, which are correctly received at the sink node, are represented in (6-9).

$$(1-p_{CS})_{\mathrm{en}} = \sum_{i=m}^{m'}\binom{m'}{i}(1-p_{CS})^{i}\, p_{CS}^{m'-i} \qquad m' \geq m \tag{6-8}$$

$$(1-p_{AC})(1-p_{CS})_{fen} = (1-p_{AC})^{m}\sum_{i=m}^{m'}\left(\frac{m'}{i}\right)(1-p_{CS})^{i}\, p_{CS}^{m'-1} \tag{6-9}$$

In the formula above the forwarding part (from biosensor node to the NC relay node) is represented as well as the encoding part (from the NC relay node to the sink node). Here, m represents native packets (original packets) from the biosensor node (S) to the NC relay node (C) and m' represents encoding packets, which are transmitted from NC relay node (C) to the sink node (S).

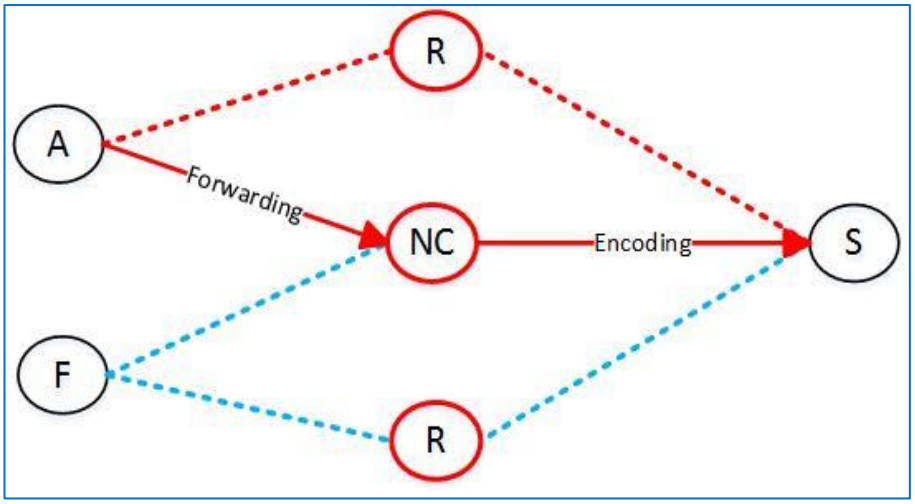

Figure 6.3: Transmission of biomedical packets from the biosensor node to the sink node using encoding technique in WBSN

6.3.3 Reliability of the Combined Technique

The combined technique is a term used to combine the forwarding technique and encoding technique as shown in Figure 6.4, which represents a sample topology for WBSN depending on the combined technique. The biosensor node (A) sends the duplicated biomedical packets to the simple relay node (R) and the NC relay node (C) and then towards the sink node (S). With regard to the serial and parallel reliability rules [134] in Appendix A these rules of reliability are applied in Figure 6.4 to totally calculate the probability for successful reception at the sink node based on the combined technique, which includes the forwarding technique and encoding techniques respectively, as given in (6-10) and (6-11). The probability for successful reception at the sink node (S) can be seen in (6-13) based on the combined technique. Also, the rules of the reliability in Appendix A are applied to compute the total probability for successful reception (PSR) at the sink node as shown in (6-12) based on the combined technique. Finally, (6-12) is used to calculate the total probability for successful reception at the sink node based on (6-4) and (6-9) which is represented in (6-13).

$$p(\,fo\_successful\,) = p(AR \cap RS) \tag{6-10}$$

$$p(en\_successful\,) = p(AC \cap CS) \tag{6-11}$$

$$
\begin{aligned}
p(co\_successful) &= p[(AR \cap RS) \cup (AC \cap CR)] \\
&= p(AR).p(RS) + p(AC).p(CS) \\
&= p(AR).p(RS) + p(AC).p(CS) - [p(AR).p(RS).p(AC).p(CS)] \\
&= p_{AR}.p_{RS} + p_{AC}.p_{CS} - [p_{AR}.p_{RS}.p_{AC}.p_{CS}]
\end{aligned}
\tag{6-12}
$$

$$
\begin{aligned}
&(1-p)_{ARS} \cup (1-p)_{ACS} = \binom{m}{t}\left[(1-p_{AR})(1-P_{RS})\right]^{t}\left[1-(1-p_{AR})(1-p_{RS})\right]^{m-t} + \\
&(1-p_{AC})^{m}\sum_{i=m}^{m'}\binom{m'}{i}(1-p_{CS})^{i}\,p_{CS}^{m'-1} - \\
&\left[\binom{m}{t}\left[(1-p_{AR})(1-P_{RS})\right]^{t}\left[1-(1-p_{AR})(1-p_{RS})\right]^{m-t}.(1-p_{AC})^{m}\sum_{i=m}^{m'}\binom{m'}{i}(1-p_{CS})^{i}\,p_{CS}^{m'-1}\right]
\end{aligned}
\tag{6-13}
$$

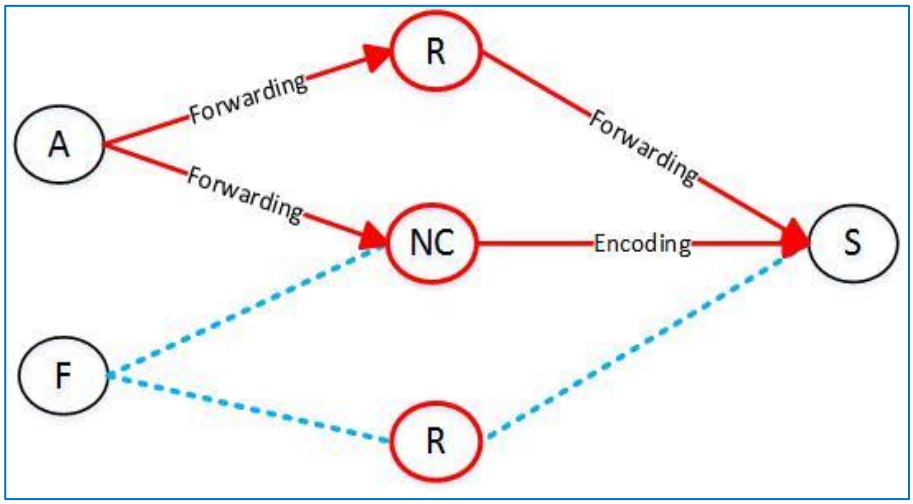

Figure 6.4: Transmission of biomedical packets from biosensor node to sink node using Combined technique

6.4 Studied Scenario: Sample Topology of WBSN

In this section, firstly, the number of relay nodes added between the biomedical sensor node and the sink node in WBSN affects transmission reliability. In multi-hop, the biomedical sensor nodes forward the packets to the sink node through one or more relay nodes. The performance of probability for successful reception (PSR) is affected by the number of relay nodes as illustrated in Figure 6.5.

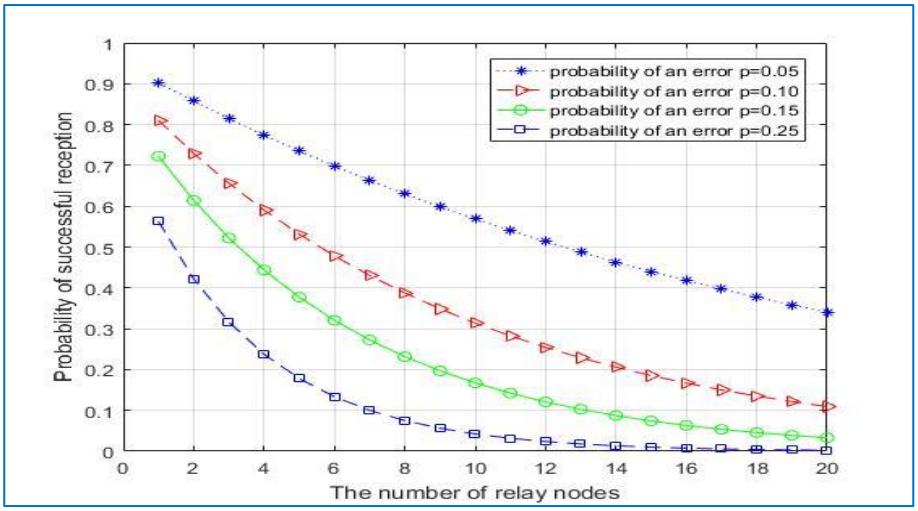

Figure 6.5: Probability of successful reception of a biomedical packet vs. the number of relay nodes

In addition, the probability of successful reception (PSR) at the sink node tends to decrease when the number of relay nodes increases. As influenced by average bit error probability of the link, the increased number of relay nodes may cause a greater number of biomedical packets to drop. Therefore, as few relay nodes as possible are added to ensure more reliable transmission in WBSN. On the other hand, the probability of successful reception (PSR) at the sink node tends to decrease when the probability of an error link decreases, as illustrated in Figure 6.6. Secondly, the reliability of the sample topology for WBSN in the three techniques will be investigated against the energy noise ratio (E_b/N_0), which is the energy per bit to noise power spectral density ratio. With respect to the forwarding technique, the probability of successful reception (PSR) at the sink node is represented as a function of the (E_b/N_0) for biomedical packets in the forwarding technique.

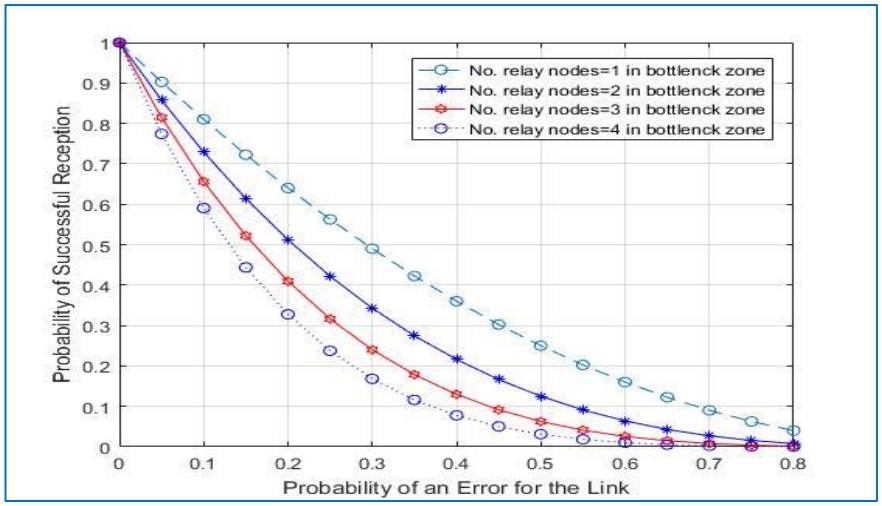

Figure 6.6: Probability of successful reception of a biomedical packet vs. the probability of an error link

The effect of increasing biomedical packets on the probability of success at the sink node have been analysed and this can be seen in Figure 6.7. Additionally, the probability of successful reception at the sink node with different numbers of biomedical packets have been compared. The probability of successful reception for few biomedical packets is generally higher than the probability of successful reception for many biomedical packets. On the other hand, the probability of success at the sink node is a function of the number of received biomedical packets which are received by the relay node. The expected number of correctly received biomedical packets is computed as the product of the biomedical packets and the probability of success at the sink node is shown in Figure 6.8.

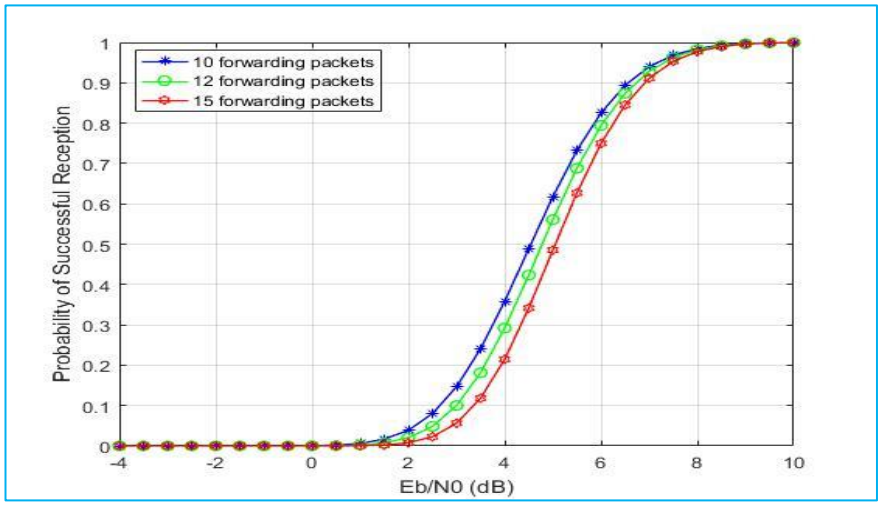

Figure 6.7: Probability of success for a biomedical packet Vs SNR

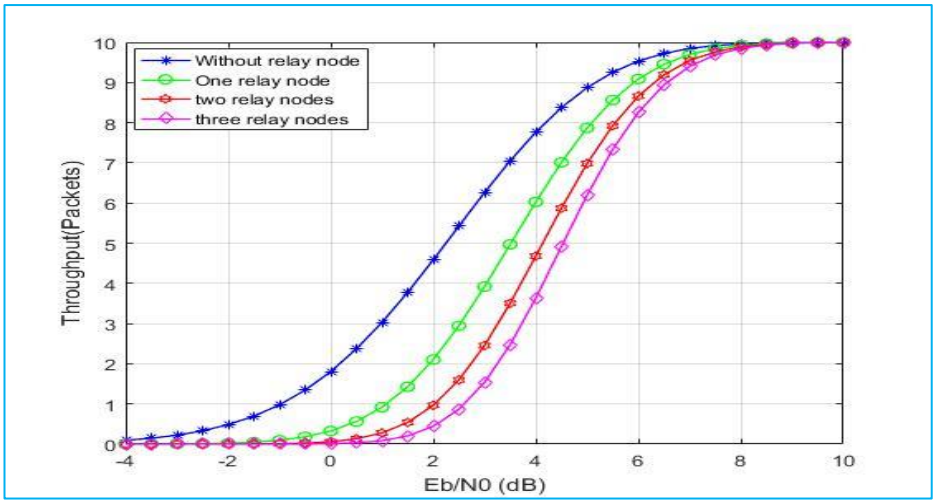

Figure 6.8: Throughput as a function of energy (E_b/N_0) for WBSN in using relay nodes between biosensor node and sink node: without relay node, one, two, and three relay nodes

As far as the encoding technique is concerned, the effect of the number of coded biomedical packets on the PSR at the sink node was analysed. It is essential that the sink node receives at least m coded biomedical packets from the NC relay node to be able to recover the original biomedical packets because the decoding of the biomedical packets depends on the operations, which are performed at the network coding relay node. The probability of successful reception (PSR) at the sink node as a function of the (E_b/N_0) for varied numbers of coded biomedical packets (such as 10, 11, & 15) is shown in Figure 6.9. The results of this study indicate that an increase of coded biomedical packets will lead to an increase in the probability of successful reception at the sink node, as shown in Figure 6.9. With respect to RLNC, which is employed in this technique, increasing the number of the encoded biomedical packets achieves better performance in terms of PSR and (E_b/N_0) and improves network reliability, it is noticed that the PSR for 15 coded biomedical packets is better than 10 packets, as shown in Figure 6.9.

The reliability of WBSN for the three techniques as shown in Figure 6.10 is investigated against the energy to noise ratio (E_b/N_0) , which is the energy per bit to noise power spectral density ratio. Figure 6.10 shows the probability of successful reception (PSR) at the sink node as a function of the energy per bit to noise power spectral density ratio (E_b/N_0) for biomedical packets in the forwarding, encoding, and combined technique. Notice that the encoding technique offers a better performance than the forwarding technique in terms of PSR at the sink node; the encoding technique requires lower energy per bit than the forwarding technique. Figure 6.10, also shows that the combined approach (forwarding and

encoding) can achieve better reliability performance than other approaches. Also, it should be noted that the combined technique based on RLNC offers a better performance than other approaches in the probability of achieving successful reception at the sink node. The combined technique also has the best performance with lower energy consumption per bit than the other techniques. For example, the combined technique requires about 6.1 dB less than the encoding and forwarding technique to achieve better performance of PSR ($PSR \approx 1$) as shown in Figure 6.10.

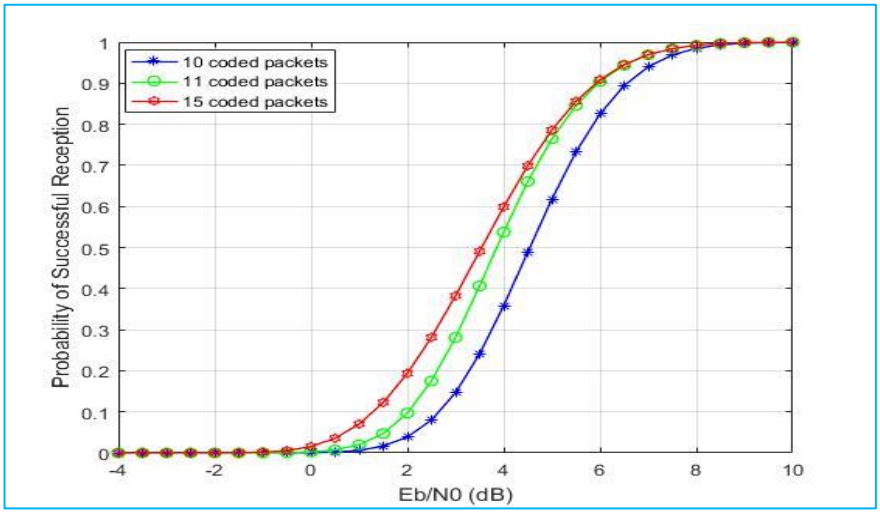

Figure 6.9: Probability of successful Vs SNR

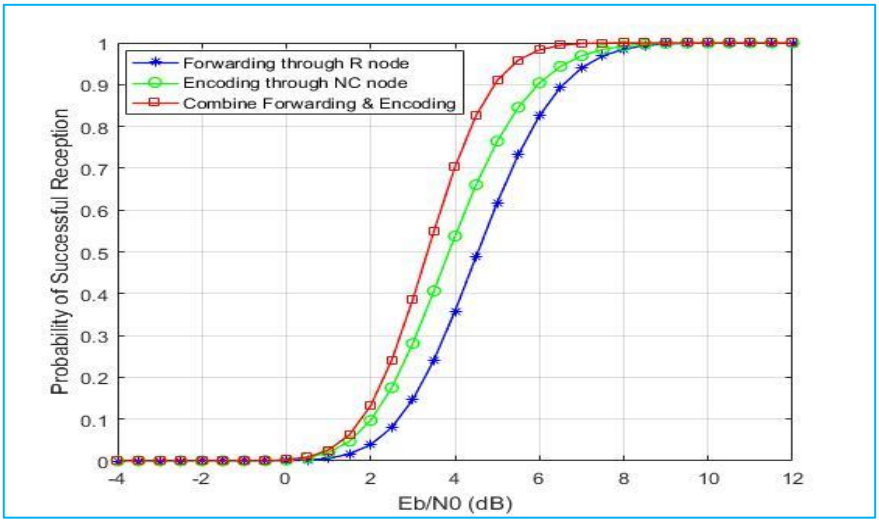

Figure 6.10: Comparison the probability for successful reception at sink node in the three techniques: the forwarding, encoding, and combined technique

6.5 Measurement Methods

In order to calculate the accuracy for the improvement between the three techniques, Kolmogorov-Smirnov test (K-S test) and trapezium rule are used.

6.5.1 Measurement of the Improvement Based on K-S Test

The Kolmogorov-Smirnov test (K-S test) attempts to determine if two data sets differ significantly. It has the advantage of making no assumptions about the distribution of data [135]. With regards to the K- S test, it is used to measure the accuracy of the improvement for the PSR at the sink node in the three techniques, which compares two samples, and is used to find the different distributions in the samples. In Figure 6.11, the K-S test is applied to the results of Figure 6.10. Figure 6.11 shows the graph area is divided into three areas, where the first and third area represent the censoring data, which is the difference between two samples approximately equal to zero. The data set in the second area between them is considered, and use the K-S test to determine the bigger difference between two samples distribution. Moreover, it can be seen from the Figure 6.11, the combined technique is consistently better than the other techniques.

According to K-S test, the accuracy of the improvement in the PSR at the sink node for the comparison of encoding technique with the forwarding technique are shown in Figure 6.12 along with the comparison of the combined technique with the forwarding technique, and the comparison of combined technique with encoding technique are 0.1792, 0.3449, and 0.1658, respectively.

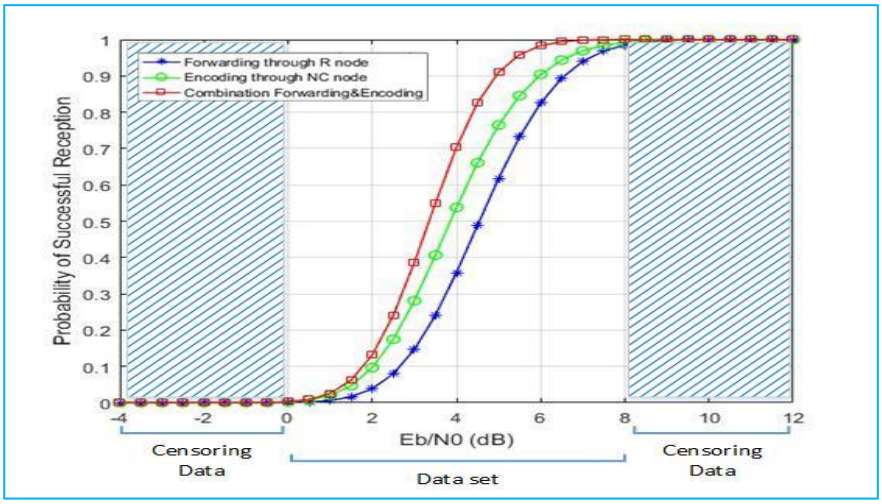

Figure 6.11: The data set which uses Kolmogorov-Smirnov test (K-S test to measure the accuracy of improvement for the PSR in three techniques)

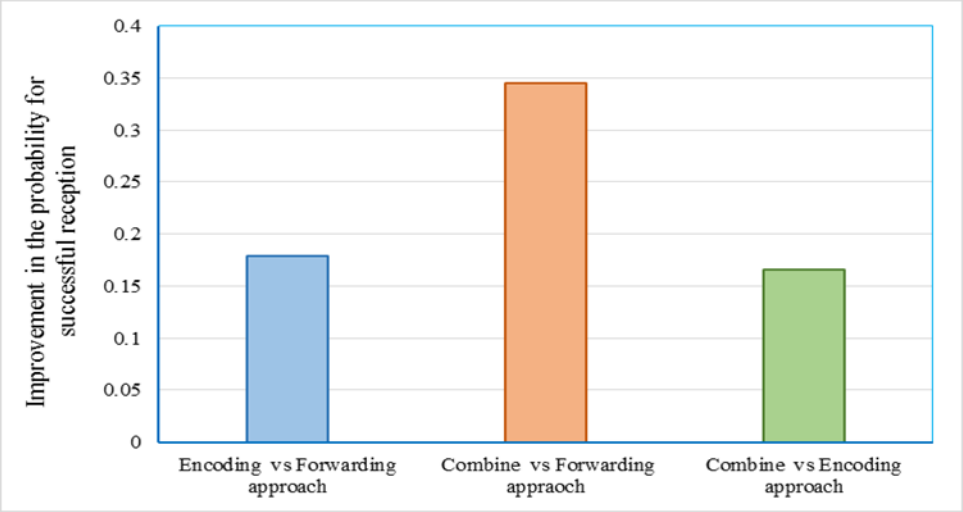

Figure 6.12: The accuracy of the improvement for the PSR at sink

6.5.2 Measurement of the Improvement Based on Trapezium Rule

There is another method to measure the improvement percentage points (points change) of the PSR at the sink node. The trapezium rule [136] is a way of estimating the area under or above the curve, and it gives a method of estimating the numerical integration quadrature. In Figure 6.13, the trapezium rule is applied to the results in Figure 6.10 .The ideal fit is 100% and the worst possible fit is 0%, so the combined technique is better than the encoding technique, which is better than the forwarding technique. Moreover, there is not a curve cross in the experimental range (-4, 12). As can be seen from the Figure 6.13, the combined technique is consistently better than the encoding technique and the encoding technique is consistently better than the forwarding technique.

The trapezium rule is used to calculate the area under the curve based on the formula (6-14), which uses two value points, as shown in Figure 6.13. Then, the equation (6-15) is applied to compute the percentage of the improvement for the probability. With respect to trapezium rule, the areas and the percentages are calculated for the three techniques, as shown in Table 6.1. On the other hand, (6-16) is also used to compute the areas above the curves, and more details about the areas and the percentages are shown in Table 6.2. The percentages of the improvement in the probability for success at the sink node are matched for the above and below calculations.

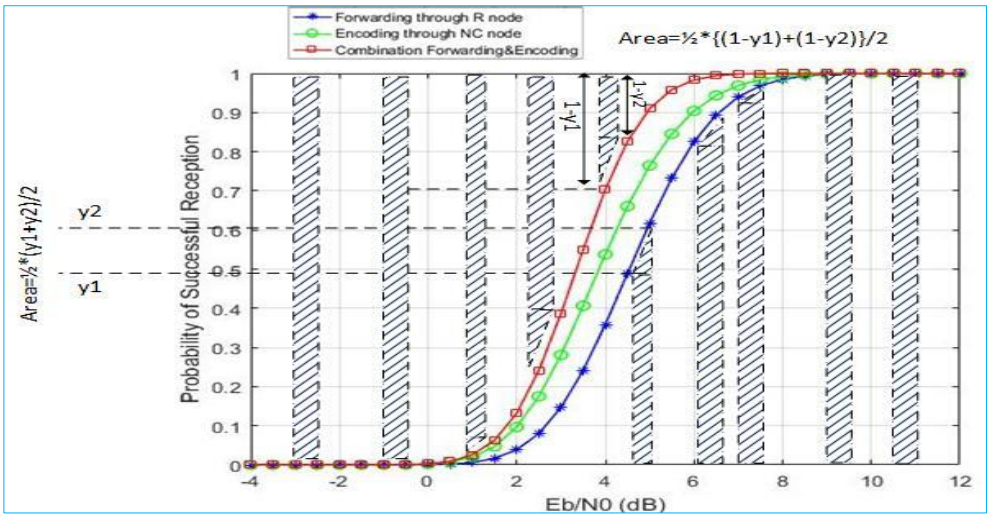

Figure 6.13: The trapezium technique used to calculate the areas

$$area = \frac{1}{2}\left(\frac{y_1 + y_2}{2}\right) \tag{6-14}$$

$$percentage(\%) = \left(\frac{area}{16}\right) * 100 \tag{6-15}$$

$$area = \frac{1}{2}\left\{\frac{(1-y_1)+(1-y_2)}{2}\right\} \tag{6-16}$$

The bar chart illustrates the improvement percentage change for the PSR at sink node for all techniques as shown in Figure 6.14. It can be seen that the improvement percentage of the combined technique to the forwarding technique is 7.66%, and this is a significant improvement. However, the improvement percentage of the combined technique to the encoding technique is 3.59%, and improvement percentage of the encoding technique to the forwarding technique is 4.07%.

Table 6.1: The areas and percentages for the three techniques based on the under curve formula

	Area for the forwarding technique	Area for the encoding technique	Area for the combine technique
Area	7.41512476	8.06614823	8.64146872
Percentage (%)	46.3445297	50.4134264	54.0091795

Table 6.2: The areas and the percentages for the three techniques based on above curve formula

	Area for the forwarding technique	Area for the encoding technique	Area for the combine technique
Area	8.58487523	7.93385176	7.35853127
Percentage (%)	53.6554702	49.5865735	45.9908204
Fit=100- Percentage %	46.3445297	50.4134264	54.0091795

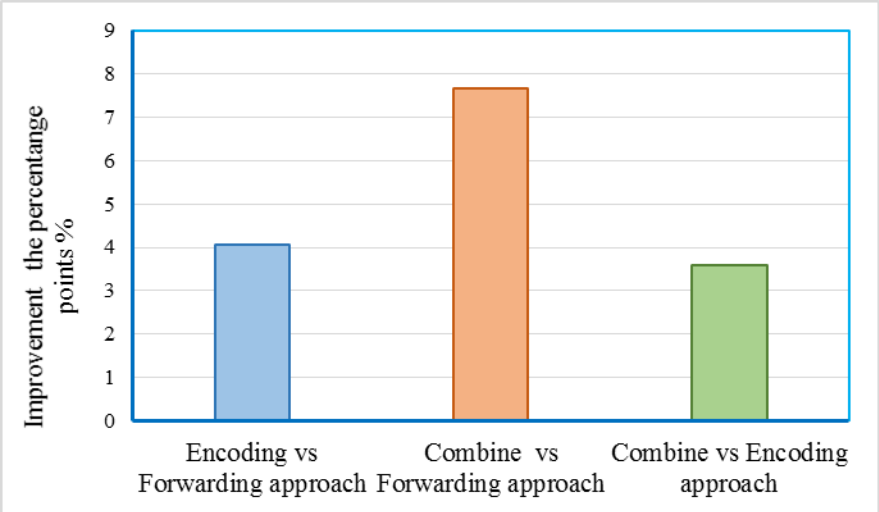

Figure 6.14: The comparison of the improvement percentage for three techniques

6.6 Comparison of the Performance of the Proposed Technique with an Existing Technique

The encoding technique proposes and presents a WBSN based on RLNC, which improves the PSR at the sink node. Figure 6.15 shows the PSR at the sink node as a function of the energy per bit to noise power spectral density ratio (E_b/N_0) for the RLNC scheme and the XOR NC scheme. The value of PSR at the sink node using RLNC scheme and the XOR NC scheme increase with the energy per bit to noise power spectral density ratio (E_b/N_0).Moreover, the performance of the encoding technique is discussed, which employs RLNC and existing technique, which uses the XOR NC scheme in terms of PSR at the sink node, reliability, and average energy per bit.

Figure 6.15 shows an overview of the PSR at the sink node for RLNC technique (proposed scheme) and the XOR NC technique. Notice that the proposed RLNC encoding technique offers better performance and better reliability than the XOR NC technique.

Moreover, the encoding technique provides a higher PSR at the sink node than the XOR NC technique. For example, when the value of (E_b/N_0) is 5.5 dB, the value of the PSR at the sink node is 0.715 and 0.845 for the XOR NC scheme and RLNC scheme, respectively, as shown in Figure 6.15. In [8],the authors showed that the XOR NC technique reduces the packet delivery ratio. However, the RLNC technique enhances the reliability of data delivery. In summary, the results show that the proposed scheme outperforms the XOR NC scheme in terms of reliability and PSR at the sink node, which is related to lower power consumption.

On the other hand, the analysis results are approximately matched with the simulation results for the encoding technique and XOR NC technique, as shown in Figure 6.16.

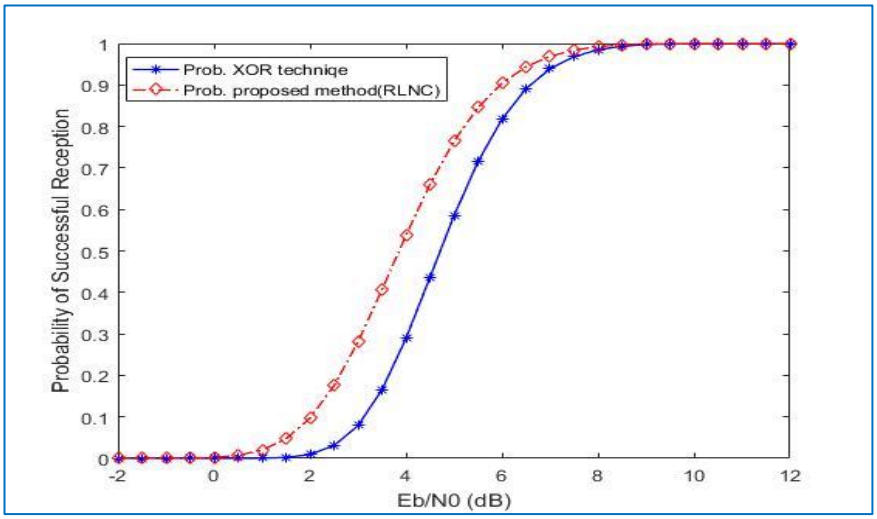

Figure 6.15: Comparison of the probability for successful reception (PSR) at the sink node based on the encoding technique (RLNC) and XOR NC technique

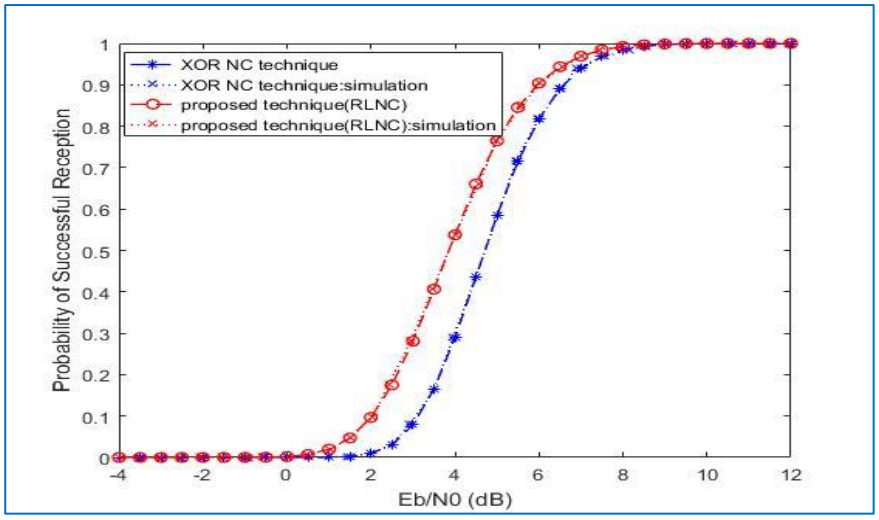

Figure 6.16: Comparison of the analysis and simulation results for the PSR at the sink node based on the encoding technique and XOR NC technique

6.7 The Validation of the Reliability in the Bottleneck Zone WBSN: Mathematical Model vs Simulation Results

In this section, the probability for successful reception at the sink node is theoretically derived (mathematically derived) based on the forwarding, encoding, and combine technique for the biosensor nodes in the bottleneck zone WBSN. The assumptions are described for all links of nodes, which represent the average bit error probability and successful probability, as illustrated in Appendix B Furthermore, the probability for successful reception for the biomedical packets is calculated, which are correctly received at the sink node, and the analysis of the forwarding, encoding, and combine technique are explained in Appendix C , Appendix D , and Appendix E , respectively to reduce the length of this section.

The performance of a WBAN is analytically studied that uses RLNC to explain a high reliability network, which provides a high PSR at the sink node. Moreover, the proposed technique (encoding technique) have been compared to other techniques, such as forwarding technique that do not use any type of network coding family and combined technique mixes two techniques; the first technique does not use network coding and the second technique employs network coding. Each technique has a special strategy for the calculation of the probability, which is described in section 6.3.

The simulation results were obtained through the simulation by using MATLAB software, where the number of biosensor nodes is fixed, as well as the number of relay nodes. It is assumed that each sensor node has ten packets in the first case and one hundred packets in the second case. In addition, all links have the same energy per bit to noise power spectral density ration, and they add the Additive White Gaussian Noise (AWGN) on the channel. The Galois field $GF(2^8)$ is used for the network coding operations and random coefficients to create the encoding packets. Furthermore, the different parameters are used to show the effect on the results such as the number of biomedical packets, the number of coded biomedical packets, and average energy per bit.

The PSR at the sink node is represented as a function of the (E_b/N_0) for biomedical packets in all techniques, which transmit the original packets (m) and encoded packets (m') . The encoding technique should always transmit at least $m+1$ coded packets to have a better performance than the forwarding technique, as shown in Figure 6.17. It should be noted that, the encoding technique employs RLNC, which requires lower energy per bit than the forwarding technique. In addition, the encoding technique has a better performance than the forwarding technique in terms of the PSR at the sink node, and PSR increases dramatically until it reaches to one in the encoding technique (proposed technique). Also, the reliability of the proposed technique is higher than the reliability of the forwarding technique. Moreover, overall, the combined technique has a higher performance than the forwarding and encoding techniques.

The comparisons of the mathematical analysis and simulation of the PSR at the sink node are based on the forwarding, encoding, and combined technique for the nodes in the bottleneck zone WBSN, as shown in Figure 6.17 and Figure 6.18. The analysis results are approximately matched with the simulation results for these techniques. The influence of a number of biomedical packets is simulated, which are employed to calculate the PSR at the sink node on those techniques such as forwarding, encoding (proposed technique), and combining them. The number of biomedical packets seems to have a significant effect on the performance of the techniques, which represents the PSR at the sink node. The effect of the increase of the biomedical packets on the WBSN is simulated, as shown in Figure 6.17 and Figure 6.18.

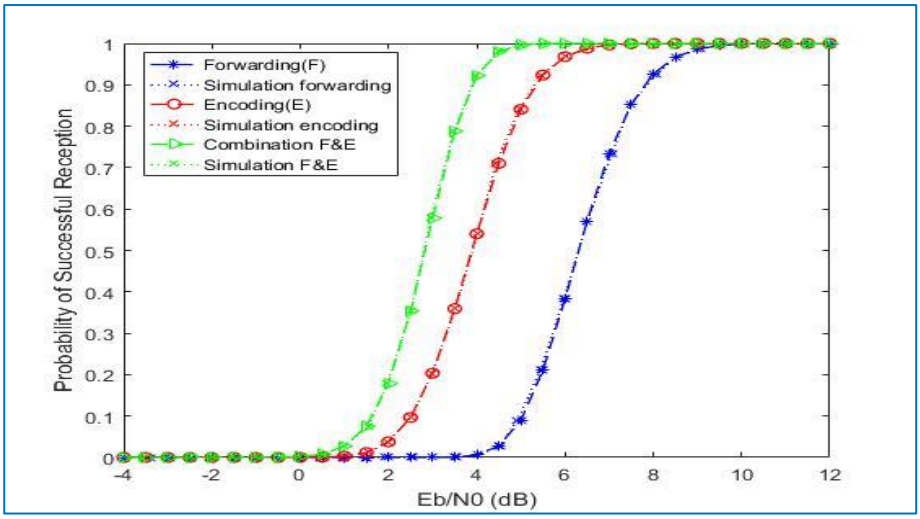

Figure 6.17: Comparison of the analysis and simulation results of the PSR at the sink node based on all the techniques for the nodes in the bottleneck zone WBSN, which use 10 packets

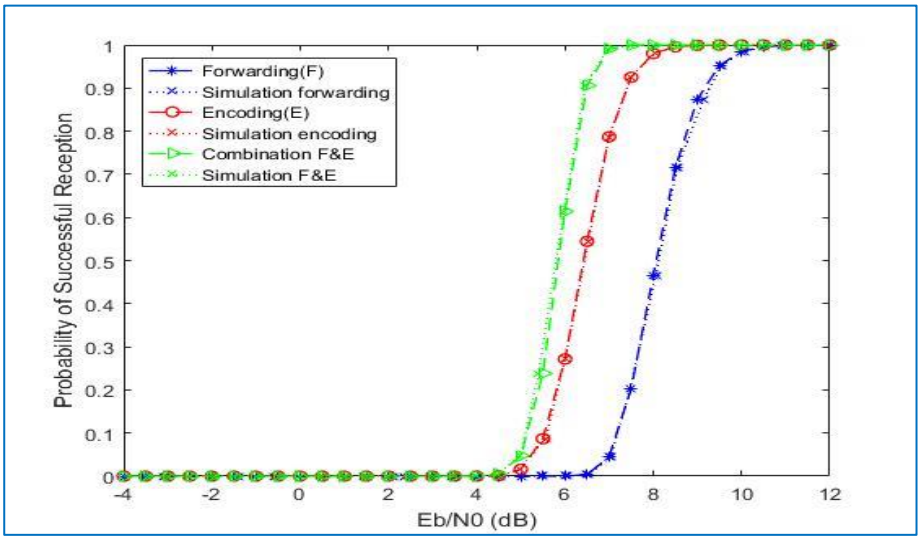

Figure 6.18: Comparison of the analysis and simulation results of the PSR at the sink node based on all the techniques for the nodes in the bottleneck zone WBSN, which use 100 packets and 110 encoded packets

6.8 Chapter Summary

This Chapter considered the transmission reliability for WBSN data based on RLNC employing a relay node to create the coding vector, which is randomly generated based on Galois Field. This is used to create encoded biomedical packets in order to greatly improve the transmission reliability of WBSN for the proposed technique [125].Three techniques, namely forwarding technique, encoding technique, and combined technique were considered. Expressions are derived for the three techniques of the probability for successful reception at the sink node and utilised them to show the relationship between the probability for successful

reception at the sink node and some network parameters, for instance the number of biomedical packets, encoded biomedical packets, and the number of relay nodes depending on theoretical analysis. It was found that network coding significantly improves the reliability of WBSN in the combined technique; however, the forwarding technique is less able to achieve the same results when compared with network coding. Furthermore, comparison between the three techniques, and the experiment of the probability for successful reception (PSR) at the sink node both show that the combined technique is better than other techniques, and encoding technique is better than that of the forwarding technique. The novel mathematical model is therefore developed in order to increase the probability of successful reception (PSR) at the sink node in the WBSN.

On the other hand, the comparison the encoding technique which is employed RLNC and XOR NC technique in terms of probability of successful reception at the sink node and reliability. The results in this Chapter indicate that the RLNC provides a higher probability of successful reception (PSR) at the sink node than XOR NC technique. The next Chapter, therefore, moves on to examine and simulate the proposed CDCA based on the WBSN model in different scenarios.

Chapter 7:

WBSN Performance Validation

7.1 Introduction

According to the proposed CDCA approach with RLNC, as defined in Chapter Four and Chapter Five, the proposed approach is examined in the context of different experiments. The real behaviour of biomedical traffic was considered which includes the remaining number of pending packets in the queue at a biosensor node and the received number of packets at the sink node, along with the priority of the biosensor nodes. Moreover, the proposed CDCA approach has a number of parameters which are used to produce simulation results. The energy consumption performance for nodes in both the mathematical model and the simulation will be compared based on the CDCA approach, which uses the proposed WBSN model. Also, the comparison between CAP slots and GTS slots is offered which represent SO for nodes in different scenarios.

The chapter proceeds as follows: section 7.2 presents the simulation setting, section 7.3 presents validation of the proposed CDCA with RLNC which include the determining SO and validation of energy consumption for all biosensor nodes in a WBSN. Section 7.4 validates the behaviour of CDCA with numerical results in different simulation experiments (different scenarios) which explain the energy consumption for all biosensor nodes and the number of time slots at the bottleneck zone. The chapter is concluded in section 7.5.

7.2 Simulation Setting

The simulation is implemented to validate the proposed WBSN approach which deploys the 13 biosensor node on the human body with a sink node which is placed on the body. In addition, relay nodes are deployed on the body; they assist the sensor nodes through transmissions and receptions, in addition to which some of them apply NC technique. The body area network (BAN) is adopted with the IEEE 802.15.4 protocol, which operates at the 2.4 GHz frequency with data rate of 250 Kbps. With respect to the MAC configuration in this protocol, the standard values for SO and BO are used which represent the initial values

which are then changed depending on the real behaviour of traffic in the WBSN. More details regarding parameters are given in Table 7.1 for the design scenarios by using Matlab. The sink node has an array which contains all information about all biosensor nodes in the topology. In Figure 7.1, one record represents one node in a WBSN, which includes unique ID number, position, data rate, initial number of the superframe order, etc.

Table 7.1: The setting for the simulation

Notation	Description
Area	90 x 240
Biosensor nodes	
No. of nodes	13
Types	EMG, body temperature, pulse rate, ECG, the glucose monitor, blood pressure monitor (examples)
Data rate	Different based on the application
Position	Depends on the function for biosensor node
Sink node	1
Simple relay node	Operates on 2.5 GHz and data rate is 250 Kbps
The length of the symbol	16 bit
The symbol duration	16us@2.4GHz
The sampling frequency	50 frame/second
Each slot	60 symbols
MAC type	IEEE 802.15.4 protocol
MAC configuration	
MAC Header	22 byte (but the range is 7-23 B)
MAC Footer	2 byte
MPDU (MAC Protocol Data Unit)	MAC Header + MAC Payload + MAC Footer
MacBeaconOrder (BO)	14
Nordic nRF2401	in 2.4-2.45 GHz
$\mathbf{E_{TXelec}}$	16.7 nJ/bit
$\mathbf{E_{RXelec}}$	36.1 nJ/bit
$\mathbf{E_{amp(3.38)}}$	1.97e-9 J/bit
$\mathbf{E_{amp(5.9)}}$	7.99e-6 J/bit
Path loss coefficient (n)	LOS=3.38, NLOS=5.9

ID	Dist1	Dist 2	Data rate	X	Y	Connt Relay	Connt NC	Connt Sink	Connt Bio	Gen	Etx	Erx	Prio	Num Slots	Num CAP	Num GTS	Num Pend	Num Rec	SO	New SO	…….	DC
																					……	

Figure 7.1: One record of the array which is inside the sink node

7.3 The CDCA WBSN Validation: Mathematical Model vs Simulation Results

In this section, the CDCA approach and RLNC are validated, which are applied on the mathematical model of WBSN through simulation experiments and comparison without applying CDCA. The scenarios consider the SO number, which has an affect on CDCA and energy consumption for nodes in WBSN.

7.3.1 Determining SO for CDCA WBSN

In order to validate the proposed CDCA WBSN in the real behaviour of traffic over time for biomedical data which is generated through the biomedical sensor nodes, which sense or measure the vital signs from the human body. Each node queue includes a number of biomedical packets; it can keep a maximum number of biomedical packets in its queue that represent the size of the queue. Under the modification of traffic for WBSNs, which represents the ratio between the remaining number of pending packets in the queue at the biosensor node to the received number of packets at the sink node. Moreover, estimating the traffic allows the selection to be corrected for the superframe order (SO) for the biosensor node; this should less than or equal to the beacon order (BO). Basically, the superframe order (SO) is calculated for each biosensor node in the WBSN based on the data rate. In this way, the real behaviour of the traffic in the WBSN is validated and observed by the simulation analysis, which represent a flexible method. Figure 7.2, Figure 7.3 and Figure 7.4 show the experimental data in the number of SO which is selected by the sink node depending on the behaviour of traffic in the proposed WBSN model during simulation. The proposed WBSN model has been implemented on four scenarios which can happened below: in three scenarios, it is assumed that the remaining number of pending packets in the queue is the same for all nodes, and also the received number of packets at the sink node is the same for all nodes in the WBSN, whereas, in the four scenario, each node in the WBSN has generated randomly the number of pending packets in the queue and received packets at the sink node.

In first scenario one, the remaining number of pending packets in the queue for the nodes, for instance, ECG, EEG, blood pressure, and blood oxygen level, is greater than the number of packets received at the sink node. The sink node determines the new superframe order (SO), which represents the next superframe order for the biosensor node. The next SO depends on the ratio of the remaining numbers of pending packets in the queue for the node

to the received number of packets at the sink node. Therefore, the sink node increases the current SO in order to reduce the delay and avoid the dropout of the medical packets. From the chart, as shown in Figure 7.2, it can be seen that the larger SO belongs to the biosensor node, which has a higher data rate. In addition, the node queue has more pending packets than received packets at the sink node. Therefore, the quantitative evaluations of the superframe order for most biosensor nodes are increased in the simulation. This means that the active period for sending biomedical packets toward the sink node is increased by increasing the network traffic. Conversely, the smaller SO belongs to the biosensor node, which has a lower data rate.

For example, the number of slots for the ECG sensor (node 4) and the body temperature sensor (node 2) in the mathematical model without CDCA are four slots and one slot, respectively, as shown in Figure 7.2 (a) depending on the data rate. However, in the simulation, the new SO for the ECG (node 4) has five slots and six slots; if the number of pending packets in the queue is greater than the number of received packets at the sink node by a factor of two or three, respectively, as shown in Figure 7.2 (a and b). Also, the number of the new SO for the body temperature sensor are two slots and three slots with the same values of increase. With respect to the EMG sensor (which represents nodes 1 and 9), this has a higher SO based on the calculation in the mathematical model without CDCA; the value of SO should equal or be less than the BO; the SO for EMG is equal to the BO in the simulation; this happens in all scenarios. Interestingly, the new SO was observed to increase in order to achieve the delivery of biomedical packets at the sink node.

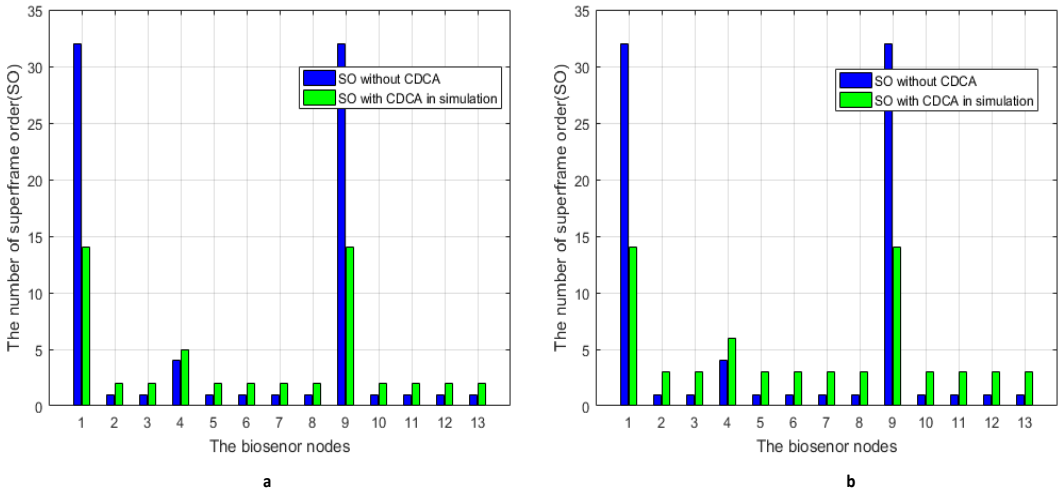

a: The number of pending packets is greater than the number of receive packets by the double.

b: The number of pending packets is greater than the number of receive packets by the triple.

Figure 7.2: Comparison for SO in the mathematical model without CDCA and simulation with CDCA for 13 biosensor nodes when the number of pending packets is greater than the number of received packets

In the second scenario, the remaining number of pending packets at a biosensor node is equal to the received number of packets at the sink node. Therefore, the sink node selects the current SO as the superframe order for the next SO of the biomedical node because the behaviour of traffic is balanced in this situation, as shown in Figure 7.3(a). For example, in both cases, the numbers of slots for the ECG sensor (node 4) and the body temperature sensor (node 2) are four slots and one slot, respectively, in both cases as shown in Figure 7.3(a).

In the third scenario, the remaining number of pending packets at a biosensor node is less than the received number of packets at the sink node. Therefore, the sink node, which depends on the value of the ratio between the remaining number of pending packets in the queue and the received number of packets at sink node, decreases the current superframe order as shown in Figure 7.3 (b), in order to achieve savings in energy consumption and to reduce the delay in the transmission. For instance, the numbers of slots for the ECG sensor (node 4) and the body temperature sensor (node 2) are four slots and one slot in the mathematical model without CDCA, respectively, as presented in Figure 7.3 (b). It can be seen that the new SO is three slots for the ECG sensor (node 4) and one slot for the body temperature sensor (node 2) as shown in Figure 7.3 (b). However, the body temperature

sensor (node 2) has the same value of SO, without change, because the new SO should be set greater than or equal to one slot and so avoid to make new SO equal to zero.

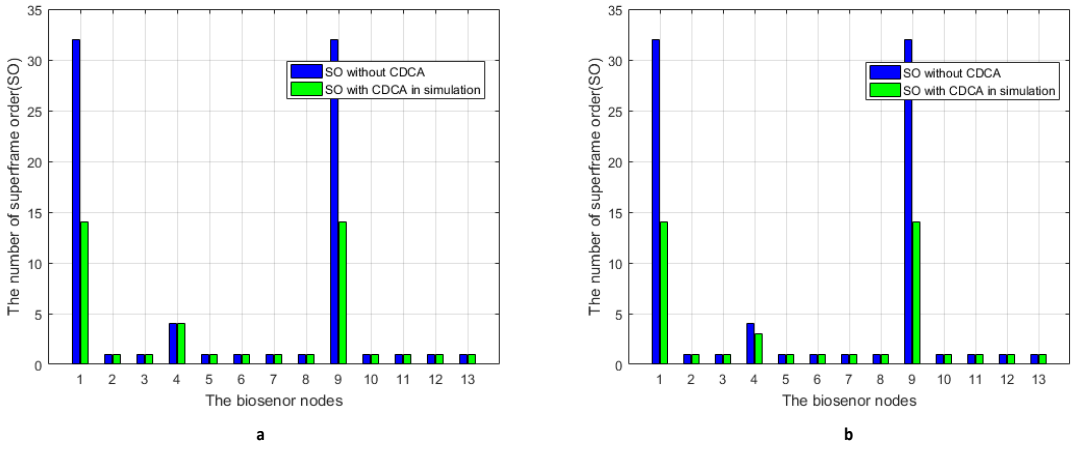

a: The number of pending packets is equal the number of receive packets

b: The number of pending packets is less than the number of receive packets.

Figure 7.3: Comparison for SO in the mathematical model without CDCA and simulation with CDCA for 13 bio-sensor nodes when the number of pending packets is equal to the number of received packets, and less than the number of received packets

In the fourth scenario, each biosensor node in the WBSN has a different value of the number of pending packets; the numbers of pending packets in the queue are randomly generated by the biosensor node. In addition, it is seen that the random generation of the received number of packets at the sink node which are correctly transmitted by each node in the WBSN. In Figure 7.4, the results of the study indicate that the changes in a new SO depend on the traffic, which is randomly generated by the biosensor nodes in the network. The new SO has increased depending on the real traffic, for example, the glucose monitor (node 6) and the blood pressure monitor (node 8) are increased by two slots and one slot, respectively, as shown in Figure 7.4. However, the EMG sensor (node 1 and node 9) decreases to become equal to the BO, and also, the ECG (node 4) is reduced by one slot. Moreover, the body temperature sensor (node 2), the pulse rate (node 3), and the motion sensor (node 5) have the same number slots as illustrated in Figure 7.4. More samples of the results with the same setting for this experiment as shown in Figure 7.5.

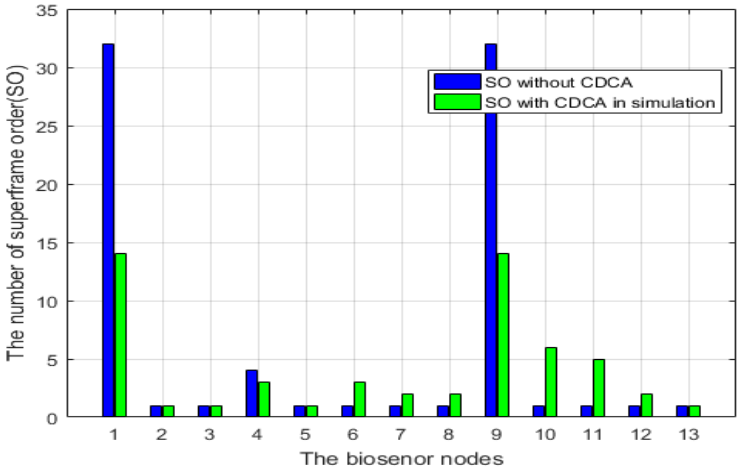

Figure 7.4: Comparison for SO in the mathematical model without CDCA and simulation with CDCA for 13 biosensor nodes in the random generation of packets

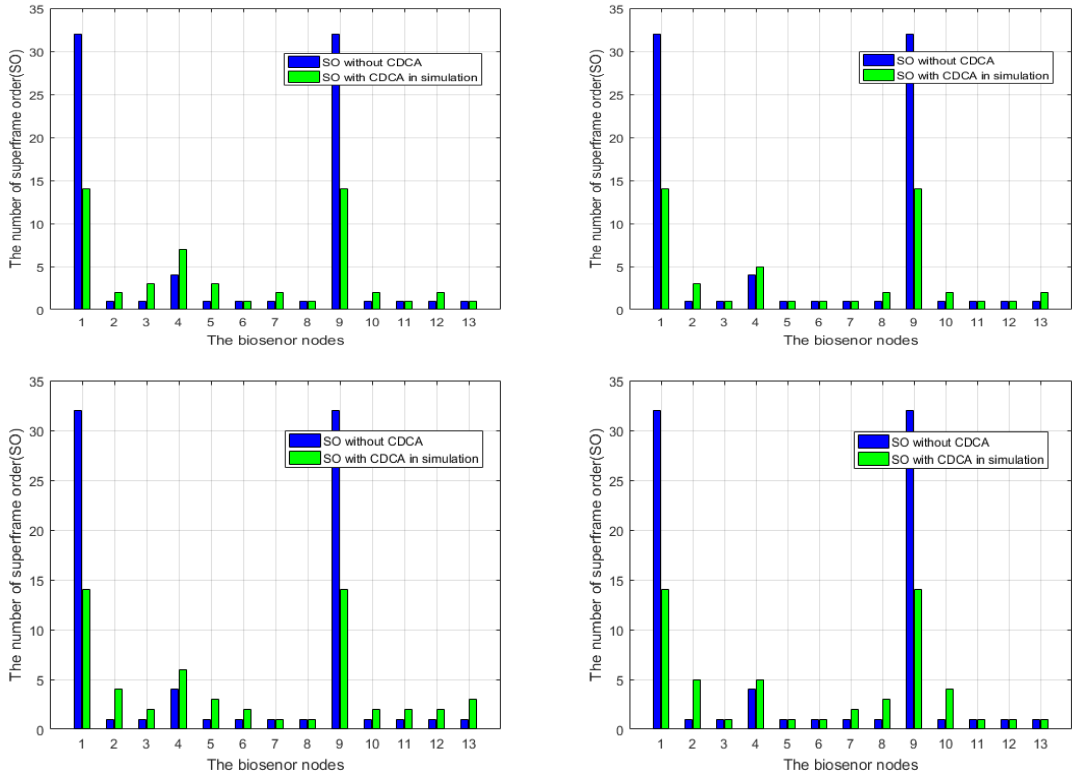

Figure 7.5: Samples of results for the comparison of SO in the mathematical model without CDCA and simulation with CDCA of 13 biosensor nodes in the random generation of packets

7.3.2 Energy Consumption Comparison of CDCA

The simulations are performed to validate the proposed method to consider real traffic for the biomedical packets, which are generated from the biosensor nodes toward the sink

node, and the MAC header. Both might affect the energy usage for nodes in a WBSN. Moreover, each biosensor node consumes the energy depending on the application of the node. For example, the energy consumption of an EMG (node 1) is higher in both calculations – mathematical model and simulation - whereas the energy consumption of the body temperature sensor (node 2) is lower in both calculations, as shown in Figure 7.6. The proposed WBSN has been implemented on four scenarios can be happened as below:

In the first scenario, it can be seen that the energy usage for most nodes in the simulation is higher than the energy consumption for nodes in the mathematical model calculations, as shown in Figure 7.6 (a) because the number of pending packets in the queue is greater than the received packets at the sink node. For instance, the energy usage for the ECG sensor (node 4) in the simulation is higher than the energy in the mathematical model measurement. Overall, the proposed CDCA for WBSN provides savings in energy consumption for nodes in a mathematical model WBSN.

In the second scenario, the energy consumption for nodes in the WBSN is equal in the mathematical model and the simulation, as illustrated in Figure 7.6 (b), because the pending packets are equal in number to the received packets.

In the third scenario, the number of pending packets in the queue is less than the number of received packets at the sink node. Comparing the two results of energy for the ECG (node 4) in Figure 7.6 (c), it can be seen that the energy consumption for the node in the simulation is less than the energy consumption in the mathematical model calculation. Moreover, the energy usage of the body temperature sensor (node 2) in the simulation should be decreased in the mathematical model, however, the SO for node 2 is equal to one slot, which represents the minimum the value in the system. Then, the energy for node 2 is equal in both cases, as shown in Figure 7.6 (c).

In the fourth scenario, it is assumed that each node in the WBSN has a different value of the number of pending packets, which are generated randomly by the biosensor node. In addition, the sink node receives the different number of packets from the nodes. With respect to the assumptions, the results of the scenario are shown in Figure 7.7, which represent the energy consumption for the nodes of a WBSN in the different scenarios (samples).

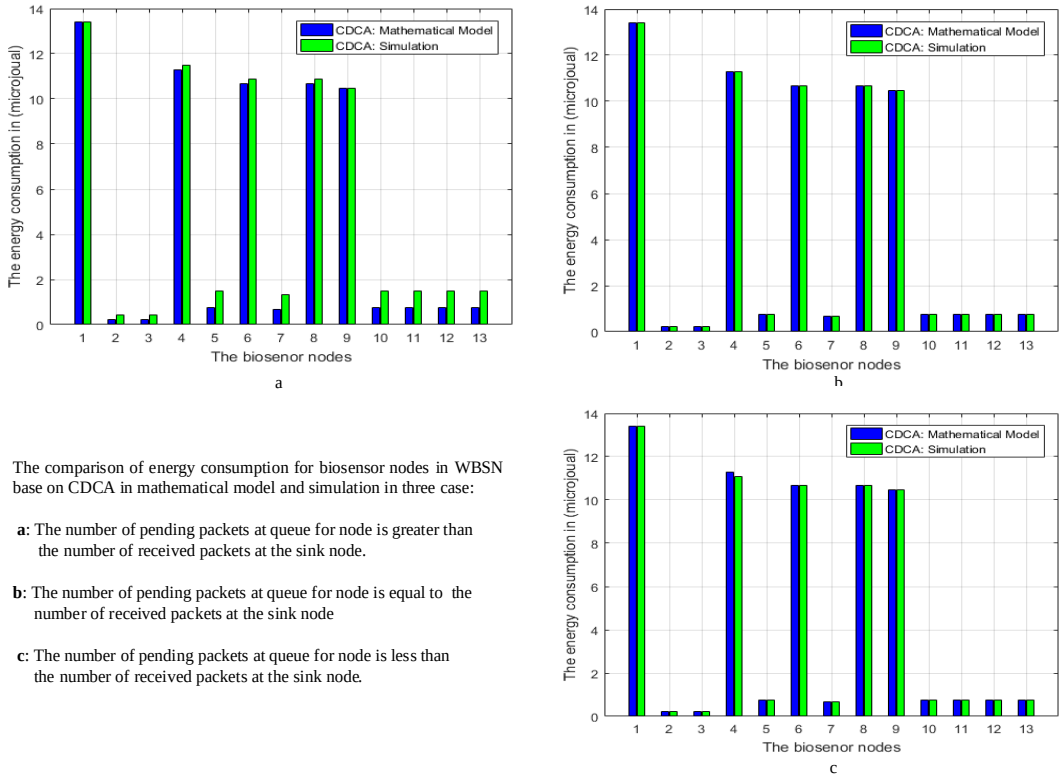

The comparison of energy consumption for biosensor nodes in WBSN base on CDCA in mathematical model and simulation in three case:

a: The number of pending packets at queue for node is greater than the number of received packets at the sink node.

b: The number of pending packets at queue for node is equal to the number of received packets at the sink node

c: The number of pending packets at queue for node is less than the number of received packets at the sink node.

Figure 7.6: Comparison of the energy consumption for the proposed CDCA WBSN based on the mathematical model and the simulation for 13 biosensor nodes

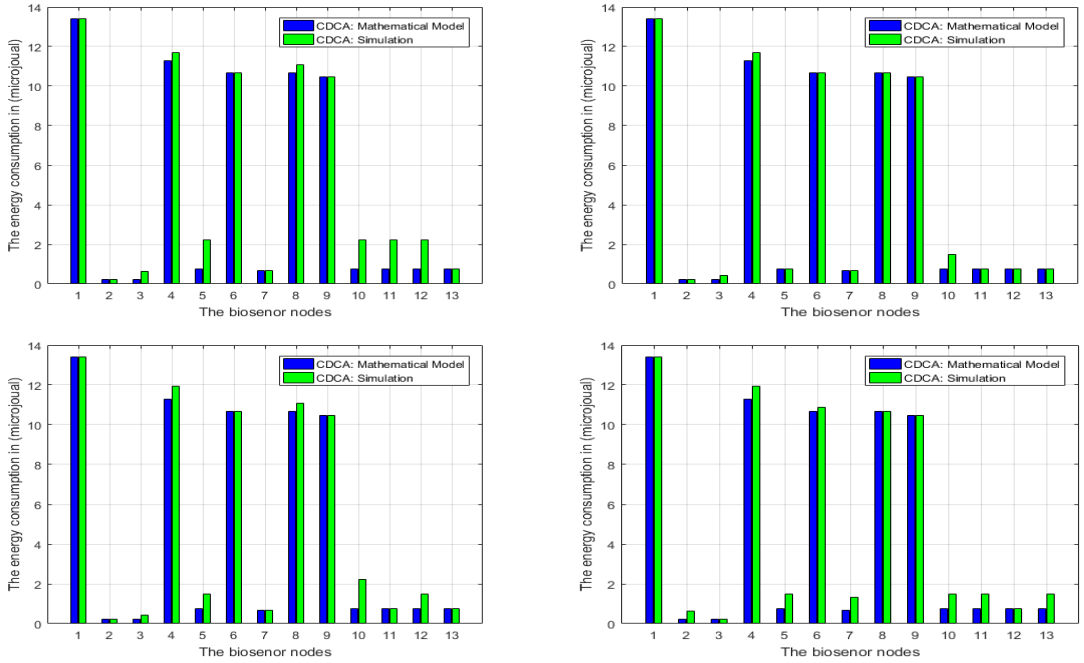

Figure 7.7: Samples of the results for the comparison of the energy consumption for the proposed WBSN: CDCA in the mathematical model and the simulation for 13 biosensor nodes in the random generation of the packets

7.4 The CDCA Bottleneck Zone WBSN Validation: Mathematical Model vs Simulation Results

For the medical monitoring of the patient in an emergency case or critical case, the doctor or nurse chooses the biosensor nodes, which are related to life-critical parameters for the patient such as heart rate, electrocardiograms, oxygen saturation, or blood pressure. Moreover, they should identify the priority of the biosensor nodes which are needed to monitor the patient. The sink node allocates the GTS slots to the biosensor nodes, which provide accurate biomedical data about the patient. The priority of the biosensor node represents by one bit, if high priority it is one and if low priority it is zero, in our system.

In this section, the biosensor nodes in the bottleneck zone are considered, which include the EMG sensor (node 1), the body temperature sensor (node 2), the pulse rate sensor (node 3), the ECG sensor (node 4), the glucose monitor sensor (node 6), and the blood pressure monitor (node 8). The proposed CDCA WBSN has been implemented in the scenarios which can happen, as below:

7.4.1 The First Case

The priority and active status for the nodes in the WBSN are randomly selected as shown in Table 7.2, where the proposed CDCA with proposed model for WBSN has been implemented in the four scenarios which can happen, as below:

Table 7.2: Information of priority and active status for the node in the bottleneck zone WBSN

	EMG	**Body temperature**	**Pulse rate**	**ECG**	**Glucose monitor**	**Blood pressure**
Node no.	1	2	3	4	6	8
Priority	0	1	1	0	1	1
Active	0	1	1	1	1	1

In the first scenario, the comparison for the energy in the mathematical model situation and the simulation for nodes in the bottleneck zone based on CDCA is shown. The energy usage for nodes in the experiment is more than in the mathematical model as illustrated in Figure 7.8 (a) because the summation for the number of GTS slots and CAP in the simulation is higher than the slots in the mathematical model, as shown in Figure 7.8 (b). The sink node allocates the number of GTS slots for the biosensor nodes, which need to send biomedical

packets under the priority condition, whereas the sink node allocates the number of CAP slots to other nodes. For example, in the simulation, the number of GTS slots is eight and the CAP slots number is five, while the total slots are thirteen as shown in Figure 7.8 (b). Then, the duty cycle (DC) for the nodes is calculated, which represents the ratio between the total of the slots (SO) and the Beacon Order (BO).

With respect to the generation of biomedical packets and the level of the priority for the node, the sink node allocates the number of slots and identifies the type of slots for each node in the WBSN, which uses the slots to send the biomedical packets toward the sink node. Moreover, in this scenario, the number of pending packets in the queue is greater than the number of received packets at the sink node.

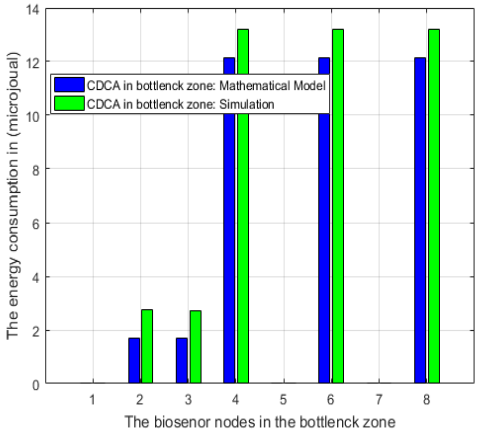

a: The comparison of energy consumption for biosensor nodes in the bottleneck zone in the mathematical model and the simulation based on CDCA when the no. of pending packets is a greater than the no. received packets

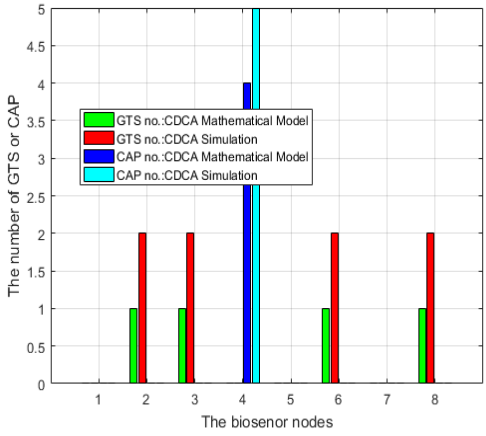

b: The comparison for the number of GTS slots and CAP slots in the mathematical model and the simulation for biosensor nodes in the bottleneck zone based on CDCA, when the no. of pending packets is a greater than the no. of received packets

Figure 7.8: Comparison of the energy consumption, and GTS and CAP slots for nodes in the bottleneck zone in the mathematical model and simulation based on CDCA with no. of pending packets greater than the no. received packets (the first situation)

In the second scenario, the same setting as in the first scenario is used except that the number of pending packets in the queue is equal to the number of received packets at the sink node. It is apparent from Figure 7.9 (a), that the energy for nodes in the bottleneck zone is equal in both calculations. Furthermore, the number of slots is equal in the two cases, as illustrated in Figure 7.9 (b).

In the third scenario, the number of pending packets in the queue is less than the number of received packets at the sink node. From the chart, as shown in Figure 7.10 (a), it can be seen that energy consumption in the simulation is lower than the energy consumption for

nodes in the mathematical model because the value of the duty cycle for nodes in the simulation is less than in the mathematical model. Furthermore, the total number of slots in the simulation is seven whereas the slots in the mathematical model number are eight, as presented in Figure 7.10 (b).

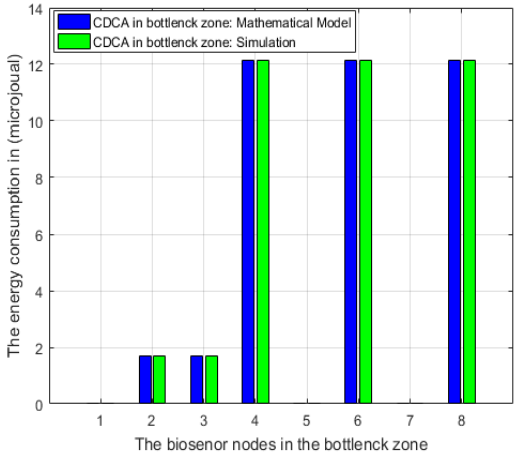

a: The comparison of energy consumption for biosensor nodes in the bottleneck zone in the mathematical and the simulation based on CDCA when the no. of pending packets is an equal to the no. received packets

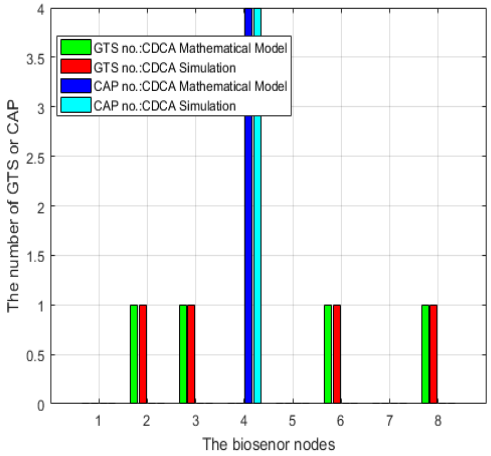

b: The comparison for the number of GTS slots and CAP slots in the mathematical model and the simulation for biosensor nodes in the bottleneck zone based on CDCA, when the no. of pending packets is an equal to the no. of received packets

Figure 7.9: Comparison of the energy consumption, and GTS and CAP slots for nodes in the bottleneck zone in the mathematical model and simulation based on CDCA with no. of pending packets equal to the no. received packets (the first situation)

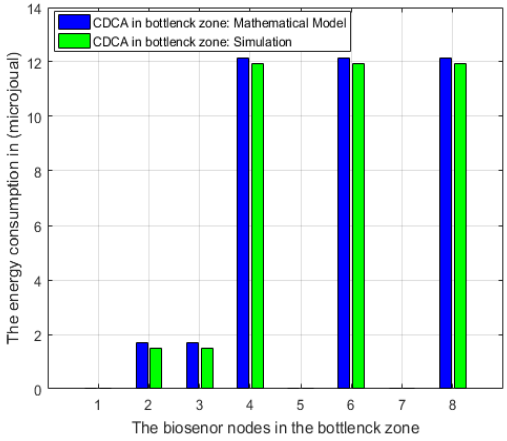

a: The comparison of energy consumption for biosensor nodes in the bottleneck zone in the mathematical model and the simulation based on CDCA when the no. of pending packets is less than to the no. received packets

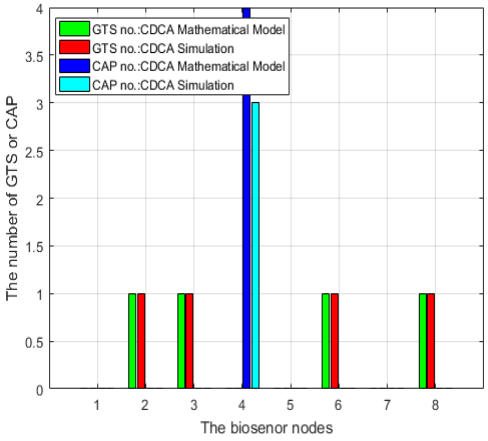

b: The comparison for the number of GTS slots and CAP slots in the mathematical model and the simulation for biosensor nodes in the bottleneck zone based on CDCA, when the no. of pending packets is less than the no. of received packets

Figure 7.10: Comparison of the energy consumption, and GTS and CAP slots for nodes in the bottleneck zone in the mathematical model and simulation based on CDCA with no. of pending packets less than the no. of received packets (the first situation)

In the fourth scenario, it is assumed that, each node in the WBSN has randomly generated the number of pending packets in the queue and received packets at the sink node. The energy consumption for nodes in the simulation is higher than in the mathematical model because the value of duty cycle based on CDCA in the simulation is higher than in the mathematical model calculation, as illustrated in Figure 7.11 (a). Moreover, each node requires the identification of the slot type, which depends on the level of the priority and on determining the number of slots, which depends on the data rate and ratio between the pending packets and received packets. Therefore, the total slots represents the summation of GTS slots and CAP slots. Although the CDCA approach is utilised in both mathematical model and simulation, the number of slots is different in the two cases. For instance, in the simulation, the GTS slots number six whereas the number of CAP slots is three, as shown in Figure 7.11 (b). However, in the mathematical model calculation, the GTS and CAP slots number four for the both, as presented in Figure 7.11 (b).

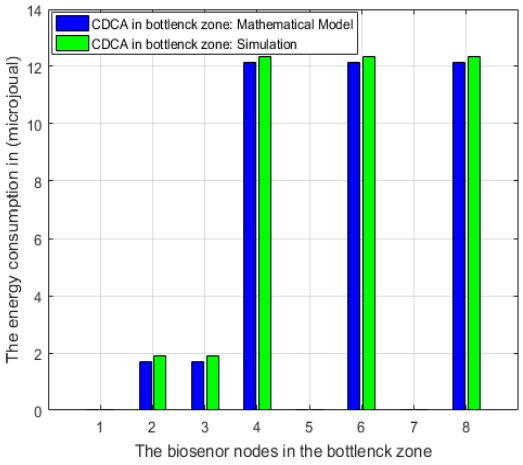

a: The comparison of energy consumption for biosensor nodes in the bottleneck zone in the mathematical model and the simulation based on CDCA when the no. of pending packets is generated randomly, also received packets

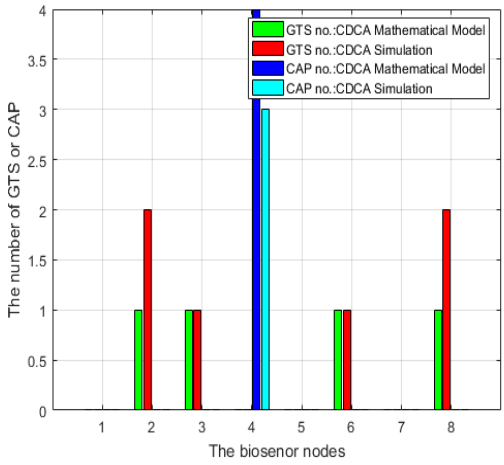

b: The comparison for the number of GTS slots and CAP slots in the mathematical model and the simulation for biosensor nodes in the bottleneck zone based on CDCA, when the no. of pending packets is generated randomly, also received packets

Figure 7.11: Comparison of the energy consumption, and GTS and CAP slots for nodes in the bottleneck zone in the mathematical model and simulation based on CDCA with no. of pending packets generated randomly, likewise the no. of received packets (the first situation)

7.4.2 The Second Case

In this case, the priority and active status of the nodes are randomly selected as shown in Table 7.3, and the, CDCA with WBSN model has been implemented in the four scenarios which can happen, as below. Furthermore, the comparison of the energy in the mathematical model and the simulation for nodes in the bottleneck zone and the number of time slots as

follows: when the number of pending packets in the queue is greater than the number of received packets at the sink node as shown in Figure 7.12 , when the number of pending packets in the queue is equal to the number of received packets at the sink node as illustrated in Figure 7.13, when the number of pending packets in the queue is less than number of received packets at the sink node as shown in Figure 7.14, and when generating randomly the number of pending packets in the queue and received packets at the sink node as shown in Figure 7.15. However, the results that are obtained here show similar behaviour to the results reported in the previous case in the terms of the energy consumption and number of time slots for nodes in a WBSN.

Table 7.3: Information as to priority and active status for the nodes in bottleneck zone of WBSN

	EMG	**Body temperature**	**Pulse rate**	**ECG**	**Glucose monitor**	**Blood pressure**
Node no.	1	2	3	4	6	8
Priority	0	0	1	1	1	0
Active	0	0	1	1	1	1

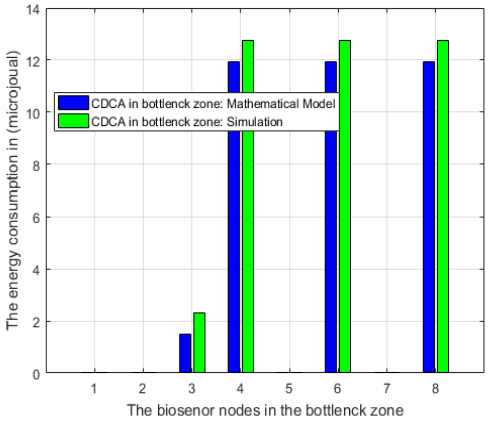

a: The comparison of energy consumption for biosensor nodes in the bottleneck zone in the mathematical model and the simulation based on CDCA when the no. of pending packets is a greater than the no. received packets

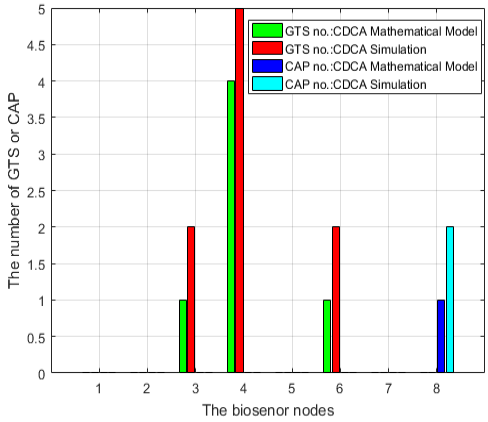

b: The comparison for the number of GTS slots and CAP slots in the mathematical model and the simulation for biosensor nodes in the bottleneck zone based on CDCA, when the no. of pending packets is a greater than the no. of received packets

Figure 7.12: Comparison of the energy consumption, and GTS and CAP slots for nodes in the bottleneck zone in the mathematical model and simulation based on CDCA with no. of pending packets greater than the no. of received packets (the second situation)

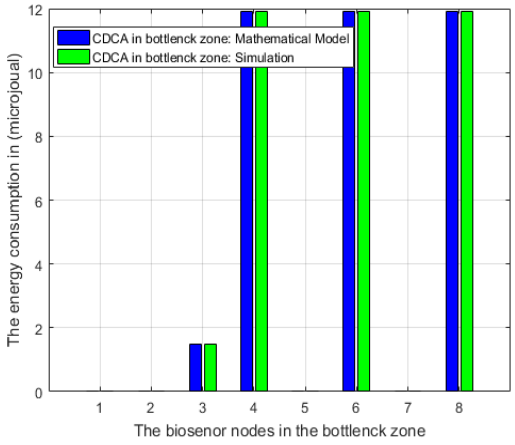

a: The comparison of energy consumption for biosensor nodes in the bottleneck zone in the mathematical and the simulation based on CDCA when the no. of pending packets is an equal to the no. received packets

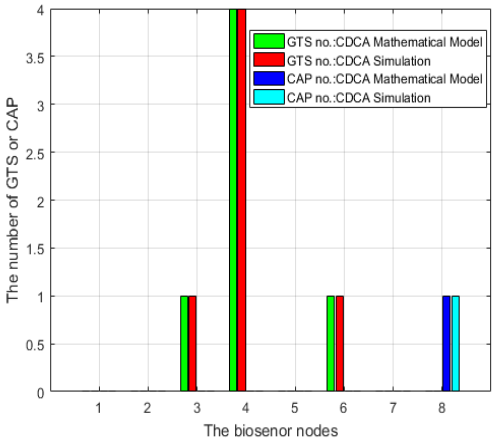

b: The comparison for the number of GTS slots and CAP slots in the mathematical model and the simulation for biosensor nodes in the bottleneck zone based on CDCA, when the no. of pending packets is an equal to the no. of received packets

Figure 7.13: Comparison of the energy consumption, and GTS and CAP slots for nodes in the bottleneck zone in the mathematical model and simulation based on CDCA with no. of pending packets equal to the no. of received packets (the second situation)

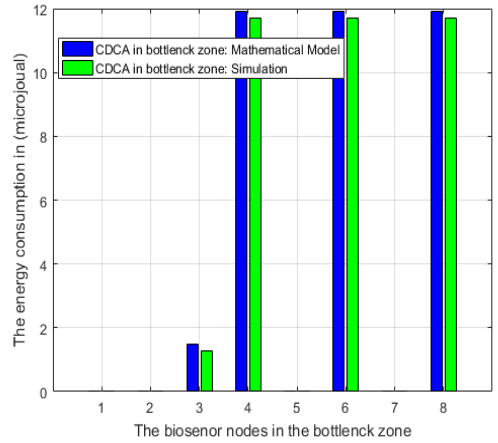

a: The comparison of energy consumption for biosensor nodes in the bottleneck zone in the mathematical model and the simulation based on CDCA when the no. of pending packets is less than to the no. received packets

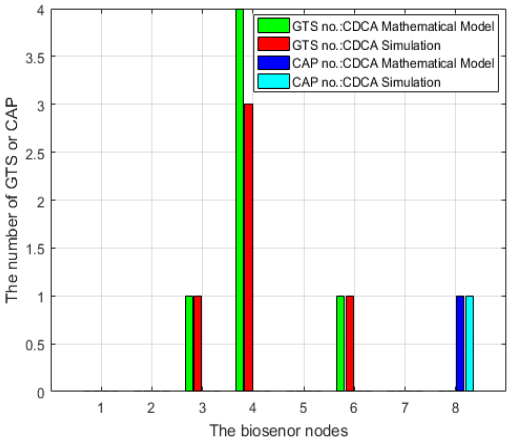

b: The comparison for the number of GTS slots and CAP slots in the mathematical model and the simulation for biosensor nodes in the bottleneck zone based on CDCA, when the no. of pending packets is less than the no. of received packets

Figure 7.14: Comparison of the energy consumption, and GTS and CAP slots for nodes in the bottleneck zone in the mathematical model and simulation based on CDCA with no. of pending packets less than the no. of received packets (the second situation)

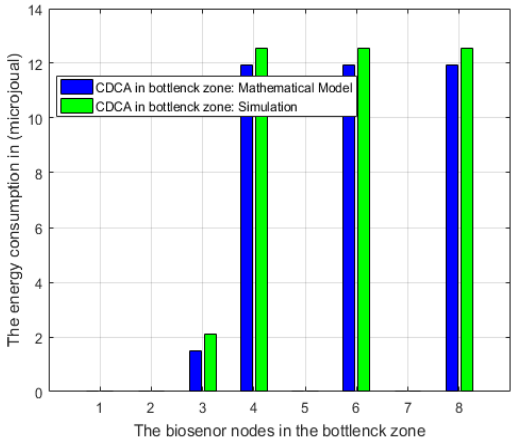

a: The comparison of energy consumption for biosensor nodes in the bottleneck zone in the mathematical model and the simulation based on CDCA when the no. of pending packets is generated randomly, also received packets

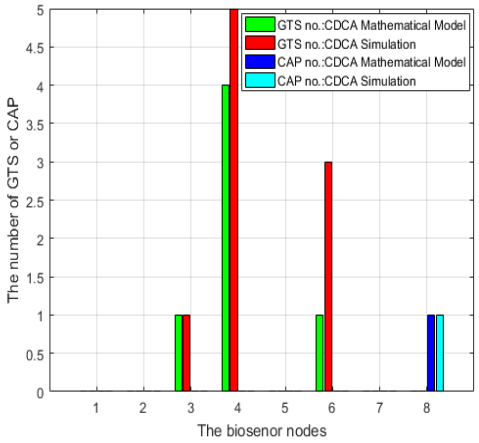

b: The comparison for the number of GTS slots and CAP slots in the mathematical model and the simulation for biosensor nodes in the bottleneck zone based on CDCA, when the no. of pending packets is generated randomly, also received packets

Figure 7.15: Comparison of the energy consumption, and GTS and CAP slots for nodes in the bottleneck zone in the mathematical model and simulation based on CDCA with no. of pending packets generated randomly, likewise the no. of received packets (the second situation)

7.5 Chapter Summary

In this chapter, the CDCA in the proposed WBSN model is experimentally discussed through simulation experiments which consider the real behaviour of traffic for nodes in WBSNs. The number of SO are evaluated, compared, and observed in two cases: without CDCA and with CDCA depending on the data rate for the nodes in the WBSN, the number of pending packets in the queue at the node, and the number of received packets at the sink node. From the scenarios, it can be seen that SO number has an impact on the energy consumed through an effect on CDCA in WBSN. Furthermore, the energy consumption scenarios consider CDCA in the mathematical model which is based on the proposed mathematical model and simulation model.

Depending on the real behaviour of traffic and the priority of the biosensor nodes in the bottleneck zone, the scenarios examine and compare the energy in the mathematical model and the simulation based CDCA; in addition, the experiments test the number of GTS slots and CAP slot for nodes in the bottleneck zone of a WBSN in both analyses where the nodes are active. From the scenarios, it can be seen that GTS slots are allocated to the nodes which have priority.

The improved performance from the CDCA with WBSN model is achieved using the selection of SO for nodes which require guaranteed delivery of biomedical data and

identification of the priority nodes under the real behaviour of the traffic in WBSNs, and also, reduced energy consumed for nodes in the WBSN are achieved. However, the proposal performance is dependent on biomedical sensor function and application.

Chapter 8:

Conclusions and Future Work

8.1 Conclusions

In WBSN application, the measurement of the multiple medical parameters is required to monitor patients in the hospital by using biomedical sensor nodes, which are implanted inside the body of the patient or attached to the patient. Examples include EMG, ECG, temperature, oxygen saturation, heart rate, and blood pressure. Also, the monitored patient requires more attention because emergency or normal medical data is related to the life of the patient. Therefore, the energy usage of each biosensor node and reliable transmission of biomedical data are of extreme significance in wireless body area networks (WBANs) to collect the medical data of the patient.

The current study is concerned with reducing the energy consumption of biomedical sensor nodes and reliably transmission of biomedical data. In addition, the WBSN parameters in this study, such as the distances and locations of the biomedical sensor nodes on the human body relative to the sink node; WBSNs topology, which includes the adding of the relay node; and the propagation model, for instance line of sight (LOS) and non-line of sight (NLOS) propagation, affect energy consumption for WBSNs. Also, a reliable transmission of medical data in WBSNs. The research objectives were proposed and achieved successfully to fulfil the aim of this research.

An overview of the development in the three main terms are provided, as follows: MAC protocol, Duty Cycle (DC), and Network Coding (NC) technique, to explain the research problem. The explanation of most MAC WBSN protocols is based on the energy efficiency; these are considered in the main research problem. The DC is implemented in the IEEE 802.15.4 MAC standard; the key idea is to use duty cycle to reduce the energy consumption of biosensor nodes. The performance of duty cycle is analysed through adjustment in the Beacon Order (BO) and Superframe Order (SO), which affect the value of duty cycle, to mitigate the research problems. Therefore, the fixed BO and dynamic SO approaches can reduce energy usage. However, the increase in the SO required will increase the energy

consumption for the nodes. In this thesis, DC is used to reduce the energy consumption through decreasing the active period (wake up duration) for the biosensor node in a WBSN based on data rate, priority, and traffic changes, especially the nodes in the bottleneck zone of the WBSN.

It has also been shown that NC can provide great transmission reliability and better rates of packet loss through mixing biomedical packets at certain intermediate nodes. One of the NC family is Random Linear Network Coding (RLNC), which is employed at the relay nodes. RLNC is used to improve the reliability of data delivery in medical applications which is addressed by the research problem, and has achieved the research aim.

A novel mathematical model for body area network (BAN) topology was presented to explain the deployment and connection between biosensor nodes, simple relay nodes, network coding relay nodes, and the sink node. The RLNC technique is employed in the simple relay node to improve energy savings and guarantee data delivery in the case of link failure based on BAN topology. In addition, a queue for biomedical packets and selected a sequence coefficient based on the Galois Field $GF(2^8)$ to create encoded packets have been used. The encoding and decoding algorithm have been presented, which are implemented to successfully create encoded packets and recover the decoded packets (that is, recover the native packets) based on RLNC.

Furthermore, the performance of the energy consumption for nodes has been investigated in the different approaches, for instance single hop, multi-hop, relay network, and NC approaches. The path loss coefficient along a LOS (line of sight) channel is lower than along an NLOS (non-line of sight) channel, which affects the energy usage in WBSNs. Therefore, the energy consumption is affected by the propagation path loss, such as the LOS and NLOS in WBSNs; the path loss coefficient of the LOS and NLOS are equal to 3.38 and 5.9, respectively. Also, the distance has an impact on the energy consumption of nodes in the bottleneck zone of a WBSN. The research concludes that energy savings can be achieved by using RLNC in the link failure cases; the results of the total energy saved are 5.131 μJ/bit, 0.714 μJ/bit, and 0.052 μJ/bit for single-hop, multi-hop, and relay network respectively. However, the nodes which use the NLOS have more energy consumption because the path loss coefficient is a higher value; also it places nodes further from the sink node.

Coordinated Duty Cycle Algorithm (CDCA) was presented based on the real behaviour of traffic and the priority of the sensor nodes that enhance the energy savings in the

bottleneck zones of WBSNs through combination with RLNC. The CDCA has considered parameters such as data queue size, queue state, the remaining number of pending packets in the queue for the node, the received packets at the sink node, initial values of SO, and the level of priority, etc. The performance of algorithms have been evaluated which are used to complete the implementation of CDCA. Firstly, a theoretical calculation of slots for nodes was presented in Chapter 5 by using the procedure based on the data rate for biosensor nodes. Secondly, the priority algorithm is used to identify the types of SO slots, which are GTS slots and CAP slots for the biosensor node in the WBSN depending on the selection of biosensor node by medical staff. The sink node allocates the GTS slots to the selected node which has high priority. Thirdly, consideration is given to the real behaviour of the traffic in the WBSN. Finally, the CAP slots and GTS slots are collected to obtain the SO slots; SO with BO are used to calculate the Coordinated Duty Cycle (CDC). The CDC plays the main role in the energy consumption and successful delivery of the biomedical data in the WBSN.

The results demonstrate that energy savings for biosensor nodes in the model which employs CDCA presents a better performance when compared to the model without CDCA in WBANs. Analysis of this case was performed and describe in Chapter 5 which included comparison of the energy consumption of nodes using a mathematical model, without the mathematical model; and a mathematical model with CDCA, according to IEEE 802.15.4 standard. It can be concluded that CDCA achieves energy savings for most biosensor nodes in WBSNs, however it will not achieve energy savings for the nods which have a raised traffic rate. The challenges of the CDCA were explored by increasing the traffic rate for nodes in WBSNs. Another potential challenge is a decrease in the current value of SO by one unit to determine the next SO when the remaining number of pending packets in the queue for the node is less than the received packets at the sink node. However, the current SO should be reduced by more than one unit depending on the ratio between the pending packets in the queue and the received packets at the sink node.

The performance study of RLNC in BANs is considered in Chapter six; a novel mathematical model for reliability in WBSNs was presented in the same chapter and Appendixes C, D, and E for the sample of WBSN and the bottleneck zone of a WBSN, respectively. The model is based on the forwarding technique, encoding technique, and a combination of both to calculate the probability of successful reception (PSR) at the sink node. However, the expressions derived for the reliability do not represent a general case for

all bottleneck zone WBSN topologies because they depend on the mathematical model and WBSN topology. Although the theoretical aspects of reliability are used in this expression.

The effect of the number of relay nodes have been analytically studied, increasing biomedical packets, and the number of coded biomedical packets on the PSR at the sink node. The PSR at the sink node decreases when the number of relay nodes and the number of biomedical packets increase; whereas PSR at the sink node has been increased when there is an increase in the number of coded biomedical packets. Furthermore, the PSR obtained by simulations converges to the mathematical model in the forwarding technique, encoding technique, and a combination of both.

According to K-S test, the accuracy of the improvement in the PSR at the sink node for the comparison encoding technique with the forwarding technique, the comparison combined technique with the forwarding technique, and the comparison combined technique with encoding technique, are 0.1792, 0.3449, and 0.1658, respectively. Also, in the trapezium rule, the improvement percentages of the PSR at the sink node are 7.66%, 3.59%, and 4.07% for the combined technique to the forwarding technique, the combined technique to the encoding technique, and the encoding technique to the forwarding technique, respectively. Two scenarios were examined and described in Chapter six based on the different numbers of packets; RLNC provides improvement in terms of reliability and probability for successful reception at the sink node, which is related to lower power.

The results show that RLNC is useful in medical applications; RLNC showed a significant advantages over XOR NC in terms of reliability and PSR at the sink node, which is related to lower power; it is clear that RLNC can be employed to improve the reliability of WBSNs. The numerical and simulation results indicate that the proposed encoding technique, which employed RLNC, provides a higher PSR at the sink node than the XOR NC technique. Finally, the PSR obtained by simulations converges to the mathematical model in RLNC and XOR NC.

The performance of the SO number is investigated and compared by both simulation and numerical approaches with CDCA and without CDCA based on the real behaviour of the traffic for nodes in WBSNs. The comparison of SO for 13 biosensor nodes depending on the difference in the number of pending packets in the queue and the number of received packets at the sink node. The performance results of SO have illustrated that the simulation results with CDCA considerably vary to the numerical results without CDCA, which

justifies the effect of CDCA on WBSNs. In addition, a range of mathematical model and simulation results have been illustrated in order to characterise the energy consumption for 13 biosensor nodes based on the real traffic for biomedical packets. The results obtained through the mathematical model and the simulation illustrates the efficiency of CDCA.

There are two situations; each has randomly selected priority and active status for nodes; CAP slots, and GTS slots. Simulation results show that CDCA provides savings in energy consumption for nodes in the bottleneck zone of the WBSN when compared against the mathematical model. Also, the CAP slots and GTS slots are correctly chosen to achieve the delivery of data at the sink node. However, CDCA could not save the energy consumption for high traffic rate nodes because if the summation of CAP and GTS slots is equal to BO, then the duty cycle is equal to one. Furthermore, modifications in the data rate, level of priority, traffic rate, active status, and time slots for nodes need to be dealt with. These modifications proved CDCA is more suitable and adaptive to operate with WBSNs because CDCA operates with heterogeneous nodes in WBSNs. Also, the whole proposed model achieves successful reduction in energy consumption and improves reliability.

8.2 Future work

Although the reduction of energy consumption and improvement of the reliability of WBSN have been studied in this thesis, there are still some challenges remaining as future work. It might be possible to improve the work in this thesis by focusing on its challenges and to provide some solutions to the problems that these challenges raise. The recommendations for future work are given below.

In future investigations, the CDCA will attempt to solve the problem with increasing traffic data; the proposed solution for this problem includes many steps such as the identification of the maximum data rate of nodes which can operate with CDCA, reducing the traffic load by using encoding at intermediate nodes, extending the active duration depending on the required slots, and also, extend BO with SO. However, it is still more complicated to implement this algorithm; but the expectation of results is proportionally accepted for energy savings and to guarantee delivery of data at the sink node.

One of the challenges is decreasing the current value of SO by one unit to determine the next SO, in Section 5.2.3 (in the second case), especially when the remaining number of pending packets in the queue for the node is less than the received packets at the sink node.

To develop CDCA is by accurate determining the next SO to achieve more energy savings and guarantee delivery of data. A new expression derived is subtracted from the equation instead of subtracting 1, which achieves the development of CDCA. Another potential challenge is that the expression derived for the reliability for the bottleneck zone in a WBSN does not represent a general case for all WBSN topologies because it depends on the mathematical model and WBSN topology. However, it will facilitate deriving the expressions for any WBSN topology depending on the theoretical rules in Appendix A with the same strategy.

The employment of RLNC, in some of the relay nodes, creates the encoding packets in the NC relay node which is placed in the bottleneck zone of the WBSN; the proposed WBSN model has been performed and evaluated. Future research could apply the RLNC technique over all simple relay nodes in the bottleneck zone of the WBSN to improve the reliability of the transmission. It is expected that the probability of successful reception at the sink node is further improved because all simple relay nodes exploit the benefits of RLNC.

One direction for future research is the analysis and simulation of the probability of successful reception at the sink node computed for the whole WBSNs, and exploring the performance of the RLNC and XOR NC techniques which are used in WBSNs, then comparing between the techniques. The expectation is that the performance of RLNC is better than the performance of XOR NC. Furthermore, part of the work considers the reliability of performance and the probability of successful reception at the sink. One of the important future pieces of work could be the performance of throughput and delay.

Implementation of the proposed WBSN model, which includes CDCA and RLNC using 13 biosensor nodes in a test bed scenario, will be an important stage in its full validation. In addition, implementation of BAN on the human body involves running the CDCA with modifications in terms of matters such as the priority, queue size, and active status; the mobility of the human body will affect the energy consumption. The performance of energy usage and reliability should be investigated in both the above situations. The single hop, multi-hop, relay network, and proposed approach based on MAC IEEE 802.15.4 are considered in this thesis. In the future, the proposed WBSN model may be modified and extended for implementation based on the MAC IEEE 802.15.6 standard. The new model may have various assumptions to adapt to the MAC protocol for IEEE 802.15.6 standard. Then, a new model will be evaluated by both analysis and simulation.

References

[1] K. M. S. Thotahewa, J.-M. Redoute, and M. R. Yuce, *Ultra Wideband Based Wireless Body Area Networks*. New York: Springer Science & Business, 2014.

[2] M. Iftikhar, N. Al Elaiwi, and M. S. Aksoy, "Performance Analysis of Priority Queuing Model for Low Power Wireless Body Area Networks (WBANs)," *Procedia Comput. Sci.*, vol. 34, pp. 518–525, 2014.

[3] T. Rault, A. Bouabdallah, and Y. Challal, "Energy efficiency in wireless sensor networks: A top-down survey," *Comput. Networks*, vol. 67, pp. 104–122, 2014.

[4] A. Darwish and A. E. Hassanien, "Wearable and implantable wireless sensor network solutions for healthcare monitoring," *Sensors*, vol. 11, no. 6, pp. 5561–5595, 2011.

[5] S. Marinkovic and E. Popovici, "Network Coding for Efficient Error Recovery in Wireless Sensor Networks for Medical Applications," in *2009 First International Conference on Emerging Network Intelligence*, 2009, pp. 15–20.

[6] S. L. S. Lee and H. S. Lee, "Analysis of Network Lifetime in Cluster-Based Sensor Networks," *IEEE Commun. Lett.*, vol. 14, no. 10, pp. 900–902, 2010.

[7] R. R. Rout, S. Member, and S. K. Ghosh, "Enhancement of Lifetime using Duty Cycle and Network Coding in Wireless Sensor Networks," *IEEE Trans. Wirel. Commun.*, vol. 12, no. 2, pp. 656–667, 2013.

[8] K.-H. Lee, J.-H. Kim, and S. Cho, "Power saving mechanism with network coding in the bottleneck zone of multimedia sensor networks," *Comput. Networks*, vol. 96, pp. 58–68, 2016.

[9] J. Mingers, "Combining IS Research Methods: Towards a Pluralist Methodology," *Inf. Syst. Res.*, vol. 12, no. 3, pp. 240–259, 2001.

[10] D. Howcroft and B. Light, "A study of user involvement in packaged software selection," in *Proceedings of International Conference on Information Systems (ICIS 2002)*, 2002, p. 7.

[11] B. Braem, "Reliable and Energy Efficient Protocols for Wireless Body Area Networks," Universiteit Antwerpen (Belgium), 2011.

[12] E. Jovanov, A. Milenkovic, C. Otto, and P. C. de Groen, “A wireless body area network of intelligent motion sensors for computer assisted physical rehabilitation,” *J. Neuroeng. Rehabil.*, vol. 2, no. 1, pp. 1–10, 2005.

[13] M. Salayma, A. Al-Dubai, I. Romdhani, and Y. Nasser, “Wireless Body Area Network (WBAN): A Survey on Reliability, Fault Tolerance, and Technologies Coexistence,” *ACM Comput. Surv.*, vol. 50, no. 1, pp. 1–38, 2017.

[14] S. Movassaghi, M. Abolhasan, J. Lipman, D. Smith, and A. Jamalipour, “Wireless Body Area Networks: A Survey,” *IEEE Commun. Surv. Tutorials*, vol. 16, no. 3, pp. 1658–1686, 2014.

[15] L. Atallah, B. Lo, R. King, and G.-Z. Yang, “Sensor Placement for Activity Detection Using Wearable Accelerometers,” in *In 2010 International Conference on Body Sensor Networks (BSN)*, 2010, pp. 24–29.

[16] G. Zhong Yang, *Body Sensor Networks*. London: Springer, 2006.

[17] I. F. Akyildiz, W. Su, Y. Sankarasubramaniam, and E. Cayirci, “A survey on sensor networks,” *IEEE Commun. Mag.*, vol. 40, no. 8, pp. 102–114, 2002.

[18] B. Latré, B. Braem, I. Moerman, C. Blondia, and P. Demeester, “A survey on wireless body area networks,” *Wirel. Networks*, vol. 17, no. 1, pp. 1–18, 2011.

[19] X. Liu, Y. Zheng, M. W. Phyu, B. Zhao, and X. Yuan, “Power & area efficient wavelet-based on-chip ECG processor for WBAN,” in *2010 International Conference on Body Sensor Networks (BSN 2010)*, 2010, pp. 124–130.

[20] M. Chen, S. Gonzalez, A. Vasilakos, H. Cao, and V. C. M. Leung, “Body area networks: A survey,” *Mob. Networks Appl.*, vol. 16, no. 2, pp. 171–193, 2011.

[21] S. Ullah, H. Higgins, B. Braem, B. Latre, C. Blondia, I. Moerman, S. Saleem, Z. Rahman, and K. S. Kwak, “A comprehensive survey of wireless body area networks on PHY, MAC, and network layers solutions,” *J. Med. Syst.*, vol. 36, no. 3, pp. 1065–1094, 2012.

[22] American Heart Association, “What is a pacemaker,” 2017. [Online]. Available: http://www.heart.org/idc/groups/heart-public/@wcm/@hcm/documents/downloadable/ucm_300451.pdf.

[23] R. Schmidt, T. Norgall, J. Mörsdorf, and E. Al., “Body Area Network BAN – a Key Infrastructure Element for Patient-Centered Medical Applications,” *Biomed. Tech. Eng.*, vol. 47, no. 1, pp. 365–368, 2002.

[24] S. Arnon, D. Bhastekar, D. Kedar, and A. Tauber, “A comparative study of wireless communication network configurations for medical applications,” *IEEE Wirel. Commun.*, vol. 10, no. 1, pp. 56–61, 2003.

[25] R. Cavallari, F. Martelli, R. Rosini, C. Buratti, and R. Verdone, “A Survey on Wireless Body Area Networks: Technologies and Design Challenges,” *IEEE Commun. Surv. Tutorials*, vol. 16, no. 3, pp. 1635–1657, 2014.

[26] T. Hayajneh, G. Almashaqbeh, S. Ullah, and A. V. Vasilakos, “A survey of wireless technologies coexistence in WBAN: analysis and open research issues,” *Wirel. Networks*, vol. 20, no. 8, pp. 2165–2199, 2014.

[27] IEEE-SA Standards Board, *IEEE Standard for Local and metropolitan area networks — Part 15 . 4 : Low-Rate Wireless Personal Area Networks (LR-WPANs) Amendment 1 : MAC sublayer*. 2012.

[28] N. F. Timmons and W. G. Scanlon, “Analysis of the performance of IEEE 802.15.4 for medical sensor body area networking,” in *2004 First Annual IEEE Communications Society Conference On Sensor and Ad Hoc Communications and Networks (IEEE SECON 2004).*, 2004, pp. 16–24.

[29] I. Lamprinos, A. Prentza, E. Sakka, and D. Koutsouris, “Energy-efficient MAC Protocol for Patient Personal Area Networks.,” in *27th Annual Conference In Engineering in Medicine and Biology Society. IEEE-EMBS 2005.*, 2005, pp. 3799–3802.

[30] S. Ullah Riazuul Islam, A. Nessa, Y. Zhong, and K. Sup Kwak, “Performance Analysis of Preamble Based TDMA Protocol for Wireless Body Area Network,” *Commun. Softw. Syst.*, vol. 4, no. 3, pp. 222–226, 2008.

[31] O. C. Omeni, A. C. W. Wong, A. J. Burdett, and C. Toumazou, “Energy efficient medium access protocol for wireless medical body area sensor networks.,” *IEEE Trans. Biomed. Circuits Syst.*, vol. 2, no. 4, pp. 251–9, 2008.

[32] C. LI, H.-B. LI, and R. KOHNO1, “reservation based dynamic TDMA protocol for

medical body area networks," *IEICE Trans. Commun.*, vol. 92, no. 2, pp. 387–395, 2009.

[33] B. Otal, C. Verikoukis, and L. Alonso, "Highly Reliable Energy-saving MAC for Wireless Body Sensor Networks in Healthcare Systems," *IEEE J. Sel. Areas Commun.*, vol. 27, no. 4, pp. 553–565, 2009.

[34] G. F. G. Fang and E. Dutkiewicz, "BodyMAC: Energy efficient TDMA-based MAC protocol for Wireless Body Area Networks," in *2009 9th International Symposium on Communications and Information Technology. ISCIT 2009.*, 2009, pp. 1455–1459.

[35] N. F. Timmons and W. G. Scanlon, "An Adaptive Energy Efficient MAC Protocol for the Medical Body Area Network," in *wireless Communication, Vehicular Technology, Information Theory and Aerospace & Electronic Systems Technology, Wireless VITAE 2009. 1st International Conference*, 2009, pp. 587–593.

[36] K. Kyung-Sup, U. Sana, K. Dae-Han, L. Cheol-Hyo, and L. Hyung-Soo, "A Power-Efficient MAC Protocol for WBAN," *Korea Inst. Intell. Transp. Syst.*, vol. 8, no. 6, pp. 131–140, 2009.

[37] S. J. Marinković, E. M. Popovici, C. Spagnol, S. Faul, and W. P. Marnane, "Energy-efficient low duty cycle MAC protocol for wireless body area networks.," *IEEE Trans. Inf. Technol. Biomed.*, vol. 13, no. 6, pp. 915–925, 2009.

[38] H. Su and X. Zhang, "Battery-dynamics driven TDMA MAC protocols for wireless body-area monitoring networks in healthcare applications," *IEEE J. Sel. Areas Commun.*, vol. 27, no. 4, pp. 424–434, 2009.

[39] K. a. Ali, J. H. Sarker, and H. T. Mouftah, "Urgency-Based MAC Protocol for Wireless Sensor Body Area Networks," in *2010 IEEE International Conference on Communications Workshops*, 2010, pp. 1–6.

[40] H. Li and J. Tan, "Heartbeat-driven medium-access control for body sensor networks," *IEEE Trans. Inf. Technol. Biomed.*, vol. 14, no. 1, pp. 44–51, 2010.

[41] Y. Zhang and G. Dolmans, "Priority-guaranteed MAC protocol for emerging wireless body area networks," *Ann. Telecommun. - Ann. Des Télécommunications*, vol. 66, no. 3–4, pp. 229–241, 2010.

[42] J. Yuan, C. Li, and W. Zhu, “Energy-efficient MAC in Wireless Body Area Networks,” in *Proceedings of the 2013 International Conference on Information Science and Technology Applications,(ICISTA-13), China*, 2013, pp. 17–19.

[43] F. Xia, L. Wang, D. Zhang, D. He, and X. Kong, “An adaptive MAC protocol for real-time and reliable communications in medical cyber-physical systems,” *Telecommun. Syst.*, vol. 58, no. 2, pp. 125–138, 2014.

[44] R. H. Kim and J. G. Kim, “Delay Reduced MAC Protocol for Bio Signal Monitoring in the WBSN Environment Bio-MAC Protocol,” *Adv. Sci. Tech. Lett.*, vol. 94, pp. 42–46, 2015.

[45] C. Zhang, Y. Wang, Y. Liang, M. Shu, and C. Chen, “An energy-efficient MAC protocol for medical emergency monitoring body sensor networks,” *Sensors*, vol. 16, no. 3, pp. 1–19, 2016.

[46] C. Zhang, Y. Wang, Y. Liang, M. Shu, J. Zhang, and L. Ni, “Low Duty-Cycling MAC Protocol for Low Data-Rate Medical Wireless Body Area Networks,” *Sensors*, vol. 17, no. 5, p. 1134, 2017.

[47] M. V Funde, M. A. Gaikwad, and P. A. W. Hinganikar, “Review of Lifetime Enhancement of Wireless Sensor Networks,” *IORD J. Sci. &Technology*, vol. 2, no. 2, pp. 35–39, 2015.

[48] G. Anastasi, M. Conti, M. Di Francesco, and A. Passarella, “Energy conservation in wireless sensor networks: A survey,” *Ad Hoc Networks*, vol. 7, no. 3, pp. 537–568, 2009.

[49] X. Ding, X. Sun, C. Huang, and X. Wu, “Cluster-level based link redundancy with network coding in duty cycled relay wireless sensor networks,” *Comput. Networks*, vol. 99, pp. 15–36, 2016.

[50] R. C. Carrano, D. Passos, L. C. S. Magalhaes, and C. V. N. Albuquerque, “Survey and taxonomy of duty cycling mechanisms in wireless sensor networks,” *IEEE Commun. Surv. Tutorials*, vol. 16, no. 1, pp. 181–194, 2014.

[51] A. Shashikala and P. B. Manoj, “Comparative Study of Duty Cycle and Network Coding based Analysis of Lifetime for Wireless Sensor Networks,” *Int. J. Adv. Comput. Eng. Commun. Technol.*, vol. 3, no. 2, pp. 6–11, 2014.

[52] R. C. Carrano, D. Passos, L. C. S. Magalhães, and C. V. N. Albuquerque, “Nested block designs: Flexible and efficient schedule-based asynchronous duty cycling,” *Comput. Networks*, vol. 57, no. 17, pp. 3316–3326, 2013.

[53] W. Ye, J. Heidemann, and D. Estrin, “An energy-efficient MAC protocol for wireless sensor networks,” in *Twenty -First Annual Joint Conference of the IEEE Computer and Communications Societies ,Proceedings. INFOCOM 2002*, pp. 1567–1576.

[54] T. van Dam and K. Langendoen, “An Adaptive energy-efficient MAC protocol for wireless sensor networks,” in *Proceedings of 1st international conference on Embedded networked sensor systems*, 2003, pp. 171–180.

[55] J. Polastre, J. Hill, and D. Culler, “Versatile Low Power Media Access for Wireless Sensor Networks Categories and Subject Descriptors,” in *Proceedings of the 2nd international conference on Embedded networked sensor systems*, 2004, pp. 95–107.

[56] L. Cheng, C. Chen, J. Ma, and L. Shu, “Contention-based geographic forwarding in asynchronous duty-cycled wireless sensor networks,” *Int. J. Commun. Syst.*, vol. 25, pp. 1585–1602, 2012.

[57] M. Buettner, G. V. Yee, E. Anderson, and R. Han, “X-MAC: a short preamble MAC protocol for duty-cycled wireless sensor networks,” in *Proceedings of the 4th international conference on Embedded networked sensor systems (SenSys 2006)*, 2006, pp. 307–320.

[58] A. EI-Hoiydi, J. D. Decotignie, C. Enz, and E. Le Roux, “WiseMAC, an Ultra Low Power MAC Protocol for the WiseNET Wireless Sensor Network,” in *1st international conference on Embedded networked sensors systems*, 2003, pp. 302–303.

[59] I. Ramachanran, A. K. Das, and S. Roy, “Analysis of the Contention Access Period of IEEE 802.15.4 MAC,” *ACM Trans. Sensors Networks*, vol. 3, no. 1, pp. 1–29, 2007.

[60] M. Neugebauer, J. Plönnigs, and K. Kabitzsch, “A new beacon order adaptation algorithm for IEEE 802.15.4 networks,” in *Proceedings of the Second European*

Workshop on Wireless Sensor Networks, EWSN 2005, 2005, pp. 302–311.

[61] A. Barbieri, F. Chiti, and R. Fantacci, "Proposal of an Adaptive MAC Protocol for Ef cient IEEE 802.15.4 Low Power Communications," in *Global Telecommunications Conference (GLOBECOM'06)*, 2006, pp. 1–5.

[62] J. Jeon, W. L. Jong, Y. H. Jae, and H. K. Wook, "DCA: Duty-cycle adaptation algorithm for IEEE 802.15.4 beacon-enabled networks," in *Vehicular Technology Conference. VTC2007-Spring. IEEE 65th.*, 2007, pp. 110–113.

[63] J. Lee, J. Y. Ha, J. Jeon, D. S. Kim, and W. H. Kwon, "ECAP: A bursty traffic adaptation algorithm for IEEE 802.15.4 beacon-enabled networks," in *Vehicular Technology Conference.VTC2007-Spring.2007 IEEE 65th.*, 2007, pp. 203–207.

[64] J. H. Lim and B. T. Jang, "Dynamic duty cycle adaptation to real-time data in IEEE 802.15.4 based WSN," in *Consumer Communications and Networking Conference, CCNC 2008, 5th IEEE*, 2008, pp. 353–357.

[65] B. Gao and C. He, "An individual beacon order adaptation algorithm for IEEE 802.15.4 networks," in *2008 11th IEEE Singapore International Conference on Communication Systems, ICCS 2008*, 2008, pp. 12–16.

[66] C. Suh, Z. H. Mir, and Y. B. Ko, "Design and implementation of enhanced IEEE 802.15.4 for supporting multimedia service in Wireless Sensor Networks," *Comput. Networks*, vol. 52, no. 13, pp. 2568–2581, 2008.

[67] A. Koubâa, A. Cunha, M. Alves, and E. Tovar, "TDBS: A time division beacon scheduling mechanism for ZigBee cluster-tree wireless sensor networks," *Real-Time Syst.*, vol. 40, no. 3, pp. 321–354, 2008.

[68] M. Jianlin, X. Fenghong, and L. Hua, "RL-based superframe order adaptation algorithm for IEEE 802.15.4 networks," in *Control and Decision Conference, CCDC 2009,Chinese*, 2009, pp. 4708–4711.

[69] B. H. Lee and H. K. Wu, "Study on a dynamic superframe adjustment algorithm for IEEE 802.15.4 LR-WPAN," in *Vehicular Technology Conference,VTC 2010-Spring, 2010 IEEE 71st*, pp. 1–5.

[70] M. Valero, A. Bourgeois, and R. Beyah, "DEEP : A Deployable Energy Efficient 802 . 15 . 4 MAC Protocol for Sensor Networks," in *2010 IEEE International*

Conference Communications(ICC), pp. 1–6.

[71] Y. Gadallah and M. Jaafari, “A Reliable Energy-Efficient 802.15.4-Based MAC Protocol for Wireless Sensor Networks,” in *Wireless Communications and Networking Conference (WCNC), 2010 IEEE*, pp. 1–6.

[72] R. De Paz Alberola and D. Pesch, “Duty cycle learning algorithm (DCLA) for IEEE 802.15.4 beacon-enabled wireless sensor networks,” *Ad Hoc Networks*, vol. 10, no. 4, pp. 664–679, 2012.

[73] M. Khanafer, M. Guennoun, and H. T. Mouftah, “Adaptive sleeping periods in IEEE 802.15.4 for efficient energy savings: Markov-based theoretical analysis,” in *IEEE International Conference on Communications (ICC)*.

[74] P. Pelegris and K. Banitsas, “Investigating the efficiency of IEEE 802.15.4 for medical monitoring applications,” in *2011 Annual International Conference of the IEEE Engineering in Medicine and Biology Society, EMBS*, pp. 8215–8218.

[75] X. Li, C. J. Bleakley, and W. Bober, “Enhanced Beacon-Enabled Mode for improved IEEE 802.15.4 low data rate performance,” *Wirel. Networks*, vol. 18, no. 1, pp. 59–74, 2012.

[76] J. Hurtado-lópez and E. Casilari, “An Adaptive Algorithm to Optimize the Dynamics of IEEE 802.15.4 Networks,” in *Mobile Networks and Management*, D. Pesch, A. Timm-Giel, R. Agüero, B.-L. Wenning, and K. Pentikousis, Eds. Cham: Springer International Publishing, 2013, pp. 136–148.

[77] C. H. S. Oliveira, Y. Ghamri-Doudane, and S. Lohier, “A duty cycle self-adaptation algorithm for the 802.15.4 wireless sensor networks,” in *Global Information Infrastructure Symposium, GIIS 2013,*.

[78] M. H. S. Gilani, I. Sarrafi, and M. Abbaspour, “An adaptive CSMA/TDMA hybrid MAC for energy and throughput improvement of wireless sensor networks,” *Ad Hoc Networks*, vol. 11, no. 4, pp. 1297–1304, 2013.

[79] L. Bin, Z. Yan, and C. Wen Chen, “MAC protocol in wireless body area networks for E-health: challenges and a context-aware design,” *IEEE Wirel. Commun.*, vol. 20, no. 4, pp. 64–72, 2013.

[80] H. Rasouli, K. Yousef S., and R. Habib F., “ADCA : Adaptive Duty Cycle

Algorithm for Energy Wireless Sensor Networks," *IEEE Sens. J.*, vol. 14, no. 11, pp. 3893–3902, 2014.

[81] M. Shu, D. Yuan, C. Zhang, Y. Wang, and C. Chen, "A MAC protocol for medical monitoring applications of wireless body area networks.," *Sensors*, vol. 15, no. 6, pp. 12906–31, 2015.

[82] A. Moravejosharieh and J. Lloret, "A Survey of IEEE 802.15.4 Effective System Parameters for Wireless Body Sensor Networks," *Int. J. Commun. Syst.*, vol. 29, no. 7, pp. 1269–1292, 2010.

[83] H. Alshaheen and H. Takruri Rizk, "Improving the Energy Efficiency for a WBSN based on a Coordinate Duty Cycle and and Network Coding," in *2017 13th International Wireless Communications and Mobile Computing Conference (IWCMC)*, pp. 1215–1220.

[84] B. Braem, B. Latré, I. Moerman, C. Blondia, E. Reusens, W. Joseph, L. Martens, and P. Demeester, "The need for cooperation and relaying in short-range high path loss sensor networks," in *Sensor Technologies and Applications, 2007. SensorComm 2007. International Conference on. IEEE*, pp. 566–571.

[85] J. I. Bangash, A. W. Khan, and A. H. Abdullah, "Data-Centric Routing for Intra Wireless Body Sensor Networks," *J. Med. Syst.*, vol. 39, no. 9, p. 91, 2015.

[86] E. Reusens, W. Joseph, G. Vermeeren, and L. Martens, "On-Body Measurements and Characterization of Wireless Communication Channel for Arm and Torso of Human," in *4th International Workshop on Wearable and Implantable Body Sensor Networks*, New York: Springer, 2007, pp. 264–269.

[87] a. Fort, J. Ryckaert, C. Desset, P. De Doncker, P. Wambacq, and L. Van Biesen, "Ultra-wideband channel model for communication around the human body," *IEEE J. Sel. Areas Commun.*, vol. 24, no. 4, pp. 927–933, 2006.

[88] A. Ehyaie, M. Hashemi, and P. Khadivi, "Using relay network to increase life time in wireless body area sensor networks," in *IEEE International Symposium on a World of Wireless, Mobile and Multimedia Networks & Workshops, 2009. WoWMoM 2009.*, pp. 1–6.

[89] E. Reusens, W. Joseph, B. Latre, B. Braem, G. Vermeeren, E. Tanghe, L. Martens,

I. Moerman, and C. Blondia, “Characterization of On-Body Communication Channel and Energy Efficient Topology Design for Wireless Body Area Networks,” *Inf. Technol. Biomed. IEEE Trans.*, vol. 13, no. 6, pp. 933–945, 2009.

[90] J. Elias, “Optimal design of energy-efficient and cost-effective wireless body area networks,” *Ad Hoc Networks*, vol. 13, no. PART B, pp. 560–574, 2014.

[91] F. D’Andreagiovanni and A. Nardin, “Towards the fast and robust optimal design of wireless body area networks,” *Appl. Soft Comput.*, vol. 37, pp. 971–982, 2015.

[92] R. Ahlswede, N. C. N. Cai, S.-Y. R. Li, and R. W. Yeung, “Network information flow,” *IEEE Trans. Inf. Theory*, vol. 46, no. 4, pp. 1204–1216, 2000.

[93] R. Ahlswede, N. Cai, S.-Y. R. Li, and R. W. Yeung, “Network Information Flow,” *IEEE Trans. Inf. Theory*, vol. 46, no. 4, pp. 1204–1216, 2000.

[94] S. Y. R. Li, R. W. Yeung, and N. Cai, “Linear network coding,” *IEEE Trans. Inf. Theory*, vol. 49, no. 2, pp. 371–381, 2003.

[95] A. A. Shahidan, N. Fisal, N. N. Ismail, F. Yunus, and S. H. S. Ariffin, “Data Recovery in Wireless Sensor Networks using Network Coding,” vol. 3, pp. 69–73, 2015.

[96] E. Magli, M. Wang, P. Frossard, and A. Markopoulou, “Network coding meets multimedia: A review,” *IEEE Trans. Multimed.*, vol. 15, no. 5, pp. 1195–1212, 2013.

[97] K. V Rashmi, N. B. Shah, and P. vijay Kumar, “Network Coding,” *Reson. J.*, pp. 604–621, 2010.

[98] A. Nagarajan, M. J. Schulte, and P. Ramanathan, “Galois field hardware architectures for network coding,” in *Architectures for Networking and Communications Systems (ANCS), 2010 ACM/IEEE Symposium on*, pp. 1–9.

[99] C. Fragouli, J.-Y. Le Boudec, and J. Widmer, “Network Coding: An Instant Primer,” *ACM SIGCOMM Comput. Commun. Rev.*, vol. 36, no. 1, p. 63, 2006.

[100] R. Lidl and H. Niederreiter, *Introduction to finite fields and their applications*. Cambridge: Cambridge University Press, 1986.

[101] R. W. Yeung, L. Shuo-yen Robert, N. Cai, and Z. Zhang, *Network Coding Theory*.

Hanover: Now Publishers, 2006.

[102] A. A. Shahidan, N. Fisal, N. N. Ismail, F. Yunus, and S. H. S. Ariffin, "Data Recovery in Wireless Sensor Networks using Network Coding," *J. Teknol.*, vol. 73, no. 3, pp. 69–73, 2015.

[103] A. A. Kadhim, T. A. Sarab, and H. Al-Raweshidy, "Improving Throughput Using Simple Network Coding," in *Developments in E-systems Engineering (DeSE), 2011,IEEE,* pp. 454–459.

[104] H. Alnuweiri, M. R. Rebai, and R. Beraldi, "Network-coding based event diffusion for wireless networks using semi-broadcasting," *Ad Hoc Networks*, vol. 10, no. 6, pp. 871–885, 2012.

[105] H. Alnuweiri, M. R. Rebai, and R. Beraldi, "Network-coding based event diffusion for wireless networks using semi-broadcasting," *Ad Hoc Networks*, vol. 10, no. 6, pp. 871–885, 2012.

[106] T. Ho, R. Koetter, M. Medard, D. R. Karger, and M. Effros, "The benefits of coding over routing in a randomized setting," in *IEEE International Symposium on Information Theory, 2003. Proceedings.*, p. 442.

[107] T. Ho, M. Médard, J. Shi, M. Effros, and D. R. Karger, "On randomized network coding," *Proc. Annu. Allert. Conf. Commun. Control Comput.*, vol. 41, no. 1, pp. 11–20, 2003.

[108] R. Koetter and M. Medard, "An algebraic approach to network coding," *IEEE/ACM Trans. Netw.*, vol. 11, no. 5, pp. 782–795, 2003.

[109] B. Li and D. Niu, "Random network coding in peer-to-peer networks: From theory to practice," *Proc. IEEE*, vol. 99, no. 3, pp. 513–523, 2011.

[110] R. R. Rout, S. K. Ghosh, and S. Chakrabarti, "Co-operative routing for wireless sensor networks using network coding," *IET Wirel. Sens. Syst.*, vol. 2, no. 2, p. 75, 2012.

[111] S. Pfletschinger, M. Navarro, and C. Ibars, "Energy-efficient data collection in WSN with network coding," in *2011 IEEE, GLOBECOM Workshops (GC Wkshps).*, pp. 394–398.

[112] K. S. Deepak and A. V. Babu, “Improving energy efficiency of incremental relay based cooperative communications in wireless body area networks,” *Int. J. Commun. Syst.*, vol. 28, no. 1, pp. 91–111, 2013.

[113] E. Kartsakli, A. Antonopoulos, L. Alonso, and C. Verikoukis, “A cloud-assisted random linear network coding medium access control protocol for healthcare applications.,” *Sensors*, vol. 14, no. 3, pp. 4806–30, 2014.

[114] X. Shi, M. Medard, and D. Lucani, “When Both Transmitting and Receiving Energies Matter: An Application of Network Coding in Wireless Body Area Networks,” in *In International Conference on Research in Networking*, pp. 119–128.

[115] K. Yokota, A. Manada, and H. Morita, “An XOR Encoding for Wireless Body Area Networks,” in *BodyNets 13 Proceedings of the 8th International Conference on Body Area Networks*, pp. 240–243.

[116] M. Razzaque, S. Javadi, Y. Coulibaly, and M. Hira, “QoS-Aware Error Recovery in Wireless Body Sensor Networks Using Adaptive Network Coding,” *Sensors*, vol. 15, no. 1, pp. 440–464, 2014.

[117] Z. J. Haas and T.-C. Chen, “Cluster-based cooperative communication with network coding in wireless networks,” *2010 - Milcom 2010 Mil. Commun. Conf.*, pp. 2082–2089, 2010.

[118] X. Liu, X. Gong, and Y. Zheng, “Reliable Cooperative Communications Based on Random Network Coding in Multi-Hop Relay WSNs,” *IEEE Sens. J.*, vol. 14, no. 8, pp. 2514–2523, 2014.

[119] G. E. Arrobo and R. D. Gitlin, “Improving the Reliability of Wireless Body Area Networks,” in *Engineering in Medicine and Biology Society, EMBC, 2011 Annual International Conference of the IEEE*, pp. 2192–2195.

[120] G. Arrobo and R. Gitlin, “New approaches to reliable wireless body area networks,” in *Microwaves, Communications, Antennas and Electronics Systems (COMCAS),2011 IEEE International Conference on*, pp. 1–6.

[121] S. Movassaghi, M. Shirvanimoghaddam, and M. Abolhasan, “A Cooperative Network Coding Approach to Reliable Wireless Body Area Networks with

Demodulate-and-Forward," in *Wireless Communications and Mobile Computing Conference(IWCMC), 2013 9th International IEEE*, pp. 394–399.

[122] S. Movassaghi, M. Shirvanimoghaddam, M. Abolhasan, and D. Smith, "An energy efficient network coding approach for Wireless Body Area Networks," in *2013 IEEE 38th Conference on Local Computer Networks (LCN)*, pp. 468–475.

[123] Y.-F. Meng, T.-F. Qin, and J. Xing, "Sensor Cooperation Based on Network Coding in Wireless Body Area Networks," in *2014 International Conference on Wireless Communication and Sensor Network (WCSN)*, pp. 358–361.

[124] A. Taparugssanagorn, F. Ono, and R. Kohno, "Network coding for non-invasive Wireless Body Area Networks," in *2010 IEEE 21st International Symposium on Personal, Indoor and Mobile Radio Communications Workshops (PIMRC Workshops)*, pp. 134–138.

[125] H. Alshaheen and H. Takruri Rizk, "Improving the energy efficiency for the WBSN bottleneck zone based on random linear network coding," *IET Wirel. Sens. Syst.*, vol. 8, no. 1, pp. 17–25, 2018.

[126] H. Alshaheen and H. Takruri Rizk, "Improving the Energy Efficiency for Biosensor Nodes in the WBSN Bottleneck Zone Based on a Random Linear Network Coding," in *2017 11th International Symposium on Medical Information and Communication Technology (ISMICT)*, pp. 59–63.

[127] P. Meena Priya Dharshini and M. Tamilarasi, "Adaptive Reliable Cooperative Data Transmission Technique for Wireless Body Area Network," in *2014 International Conference on Information Communication and Embedded Systems (ICCES)*, no. 978, pp. 4–7.

[128] Z. J. Haas and T.-C. Chen, "Cluster-based cooperative communication with network coding in wireless networks," in *Military Communications Conference, 2010 - MILCOM 2010*, pp. 2082–2089.

[129] G. E. Arrobo and R. D. Gitlin, "Minimizing energy consumption for cooperative network and diversity coded sensor networks," in *Wireless Telecommunications Symposium(WTS) , 2014*, pp. 1–7.

[130] J. A. Bondy and U. S. R. Murtty, *Graph theory with applications*. London:

Macmillan, 1976.

[131] A. Razzaque, C. S. Hong, and S. Lee, "Data-centric multiobjective QoS-aware routing protocol for body sensor networks," *Sensors*, vol. 11, no. 1, pp. 917–937, 2011.

[132] M. M. Monowar, M. Mehedi Hassan, F. Bajaber, M. A. Hamid, and A. Alamri, "Thermal-Aware Multiconstrained Intrabody QoS Routing for Wireless Body Area Networks," *Int. J. Distrib. Sens. Networks*, vol. 2014, pp. 1–14, 2014.

[133] M. K. Simon and M.-S. Alouini, *Digital communication over fading channels*. Hoboken, N.J: Wiley-Interscience, 2005.

[134] Y. Suhov and M. Kelbert, *Probability and Statistics by Example: Basic Probability and Statistics*. New York: Cambridge University Press, 2005.

[135] NIST, "NIST/SEMATECH e-Handbook of Statistical Methods," 2012. [Online]. Available: http://www.itl.nist.gov/div898/handbook/eda/section3/eda35g.htm.

[136] Vivax Solutions, "Integration - The Trapezium Rule / Trapezoidal Rule or Trapezoid Rule," 2017. [Online]. Available: http://www.vivaxsolutions.com/maths/altrapzrule.aspx.

[137] G. Grimmett and D. Stirzaker, *Probability and Random Processes*, 3rd ed. Oxford: Oxford University Press, 2001.

[138] W. W. Hines, D. C. Montgomery, D. M. Goldsman, and C. M. Borror, *Probability and Statistics in Engineering*, 4th ed. New York: John Wiley & Sons, 2002.

Appendices

Appendix A
Some Basic Rules of the Probability

Some of basic theories of reliability are explained as the following:

Theorem 1[137]:

In general, when two events A and B are termed to be independent of each other, meaning that the probability of one event occurring does not change the probability that the other event occurs. In [137], the events A and B are independent if

$$P(A \cap B) = P(A)P(B) \tag{A.1}$$

If there are events such as A_1, A_2, A_3,……A_i which are independent, the joint probability of the these sets is the product of their probabilities. Also, the serial system reliability is the product of the independent subsystem reliabilities. In general, a family $\{A_i : i \in I\}$ is called independent if

$$P\left(\bigcap_{i\in J} A_i\right) = \prod_{i\in J} P(A_i) \tag{A.2}$$

For all finite subsets J of I

More explanation about (A.1), when A and B are said to be independent events, if and only if the probability of A and B occurring simultaneously is equal to the product of their probabilities [138].

$$\begin{gathered} P(A \cap B) = P(A)P(B) \\ \text{Definition : If A and B are independent events} \\ P(A|B) = P(A) \quad \text{and} \quad P(B|A) = P(B) \end{gathered} \tag{A.3}$$

This definition is often called multiplication rule [138].

Theorem 2 [138]**:**

In [138], the addition law of probability is described as given in (A.4); the probability of either A or B, or both occurring in the probability of A plus the probability of B, minus the probability that they both occur. If two events are A and B then:

$$P(A \cup B) = P(A) + P(B) - P(A \cap B) \tag{A.4}$$

Where $P(A \cap B)$ is explained in (A.1) and (A.3).

Theorem 3 [138]**: Binomial distribution**

In [138]**,** authors assume that X is represented as a random variable, where n is a positive integer, and where p is a real number between zero and one $0 < p < 1$. The probability of x "success" in n independent trials and $(n - x)$ "failure" is given by relationship in (A.5) which represents the binomial distribution [138].

$$\begin{aligned} p_X(x) &= \binom{n}{x} p^x (1-p)^{n-x} && x = 0,1,\ldots\ldots,n \\ &= 0 && \text{Otherwise} \end{aligned} \tag{A.5}$$

Where p is the probability of an individual "success"; $\binom{n}{x}$ is the binomial coefficient which represents the number of ways in which the x "successes" can occur in the n trials.

$$\binom{n}{x} = \frac{n!}{x!(n-x)!} \tag{A.6}$$

Appendix B

Assumptions of the Links in the Bottleneck Zone WBSN

The biosesnor nodes are connected with other nodes such as biosensor nodes, relay nodes, and NC relay nodes in the network of WBSN. The assumption for all nodes is described, which are an average bit error probability and successful probability. The basic assumption for links in the bottleneck zone WBAN network are:

For node A

The node (A) connects to the sink node (S) through relay node (R). Therefore, let (p_{AR}) be an average bit error probability of the link from A node to R node, and let (p_{RS}) be average bit error probability of the link from R node to S node.

So that,

The $(1-p_{AR})$ is the probability of success for link A to R

The $(1-p_{RS})$ is the probability of success for link R to S

Also, the node (A) has another link to the sink node (S) through network coding relay node (C). Therefore, let (p_{AC}) be the average bit error probability of the link from A node to C node.

Let (p_{CS}) be average bit error probability of the link from C node to S node, so that:

The $(1-p_{AC})$ is the probability of success for link A to C

The $(1-p_{CS})$ is the probability of success for link C to S

For node F

The node (F) connects to the sink node (S) through relay node (R).Therefore, let (p_{FR}) be average bit error probability of the link from F node to R node and let (p_{RS}) be average bit error probability of the link from R node to S node, so that:

The $(1-p_{FR})$ is the probability of success for link F to R

The $(1-p_{RS})$ is the probability of success for link R to S

Also, the node (F) has another link to the sink node (S) through network coding relay node (C).Therefore, let (p_{FC}) be average bit error probability of the link from F node to C node, and let (p_{CS}) be the average bit error probability of the link from C node to S node, so that:

The $(1-p_{FC})$ is the probability of success for link F to C

The $(1-p_{CS})$ is the probability of success for link C to S

For node B and Cbio

Both nodes B and Cbio are directly connected to the sink node, therefore, let (p_{BS}) be the average bit error probability of the link from B node to S node, and let (p_{CbioS}) be average bit error probability of the link from Cbio node to S node, so that:

The $(1-p_{BS})$ is the probability of success for link B to S

The $(1-p_{CbioS})$ is the probability of success for link Cbio to S

For node D

The node (D) connects to the sink node (S) through relay node(R). Therefore, let (p_{DR}) be average bit error probability of the link from D node to R node. Let (p_{RS}) be average bit error probability of the link from R node to S node, so that:

The $(1-p_{DR})$ is the probability of success for link D to R

The $(1-p_{RS})$ is the probability of success for link R to S

Also, the node (D) has another link to the sink node(S) through network coding relay node(C).Therefore, let (p_{DC}) be average bit error probability of the link from D node to C node. Let (p_{CS}) be average bit error probability of the link from C node to S node, so that:

The $(1-p_{DC})$ is the probability successful for link D to C

The $(1-p_{CS})$ is the probability successful for link C to S

For node H

The node (H) connects to the sink node (S) through relay node (R). Therefore, let (p_{HR}) be average bit error probability of the link from H node to R node, and let (p_{RS}) be average bit error probability of the link from R node to S node, so that:

The $(1-p_{HR})$ is the probability successful for link H to R

The $(1-p_{RS})$ is the probability successful for link R to S

Also, the node (H) has another link to the sink node (S) through network coding relay node (C). Therefore, let (p_{HC}) be average bit error probability of the link from H node to C node, and let (p_{CS}) be average bit error probability of the link from C node to S node, so that:

The $(1-p_{HC})$ is the probability of success for link H to C

The $(1-p_{CS})$ is the probability of success for link C to S

As a general rule, the probability of successful of the packets, which are transmmitted toward the sink node through relay node:

Let x is a node

Let (p_{XR}) be average bit error probability of the link from X node to R node

Let (p_{RS}) average bit error probability of the link from R node to S node (B.1)

So that,

Let $(1-p_{XR})$ is the probability of success for link X to R

Let $(1-p_{RS})$ is the probability of success for link R to S

As a general rule, the probability for success for the packets, which are transmmitted toward the sink node through network coding relay node:

Let x is a node

Let (p_{XC}) be average bit error probability of the link from X node to C node

Let (p_{CS}) average bit error probability of the link from C node to S node (B.2)

So that,

Let $(1-p_{XC})$ is the probability of success for link X to C

Let $(1-p_{CS})$ is the probability of success for link C to S

Appendix C

Finding the Total of PSR at Sink Node by Using Forwarding Technique

In this case, the probability for success for the packets is computed based on forwarding the packets toward the sink node though the relay node (R) as shown in Figure C.1. The probability for success of the bottleneck zone is calculated as given in equation (C.1). In addition, m represents the number of packets, which is transmitted from the sensor node (such as node A, node F, node D, and node H) toward the sink node through relay node (R). Let t represent the number of received packets at the sink node (S). The total of the probability for successful reception at sink node is based on the forwarding technique, as shown in equation (C.1).

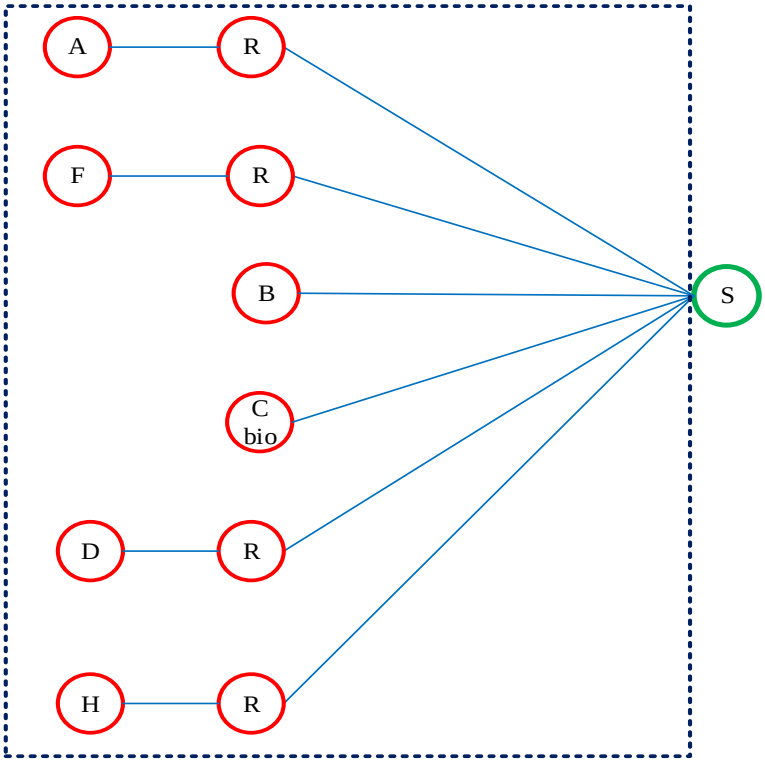

Figure C.1: The topology for the nodes in the bottleneck zone based on the forwarding technique

$$p(Forword\_successful) = 1 - p(forward\_failure)$$
$$p(Forword\_successful) = 1 - [p(failure_{ARS}).p(failure_{FRS}).p(failure_{BS}) \quad \text{(C.1)}$$
$$.p(failure_{Cbio}).p(failure_{DRS}).p(failure_{HRS})]$$

Where

$$p(failure_{ARS}) = p(failure_{AR} \cup failure_{RS}) = p(AR) + p(RS) - [p(AR).(RS)]$$
$$p(failure_{FRS}) = p(failure_{FR} \cup failure_{RS}) = p(FR) + p(RS) - [p(FR).p(RS)]$$
$$p(failure_{BS}) = p(BS)$$
$$p(failure_{CbioS}) = p(CbioS) \quad \text{(C.2)}$$
$$p(failure_{DRS}) = p(failure_{DR} \cup failure_{RS}) = p(DR) + p(RS) - [p(DR).p(RS)]$$
$$p(failure_{HRS}) = p(failure_{HR} \cup failure_{RS}) = p(HR) + p(RS) - [p(HR).p(RS)]$$

The probability of failure for transmision packets from node A to sink node through the relay node R is shown in (C.3), also for node F as shown in (C.4).

$$p(failure_{ARS}) = \binom{m}{t} p(failure_{ARS})^{m-i}.(1 - p(failure_{ARS}))^{t}$$
$$p(failure_{ARS}) = p(AR) + p(RS) - [p(AR).p(RS)] \quad \text{(C.3)}$$
$$p(failure_{ARS}) = \binom{m}{t} [p_{AR} + p_{RS} - (p_{AR}.p_{RS})]^{m-t}.[1 - \{p_{AR} + p_{RS} - (p_{AR}.p_{RS})\}]^{t}$$

$$p(failure_{FRS}) = \binom{m}{t} p(failure_{FRS})^{m-t}.(1 - p(failure_{FRS}))^{t}$$
$$p(failure_{FRS}) = p(FR) + p(RS) - [p(FR).p(RS)] \quad \text{(C.4)}$$
$$p(failure_{FRS}) = \binom{m}{t} [p_{FR} + p_{RS} - (p_{FR}.p_{RS})]^{m-t}.[1 - \{p_{FR} + p_{RS} - (p_{FR}.p_{RS})\}]^{t}$$

The probability of failure for transmision packets from node B and Cbio are directly connected to sink node as shown in (C.5) and (C.6), respectively:

$$p(failure_{BS}) = \binom{m}{t} p(failure_{BS})^{m-t}.(1 - p(failure_{BS}))^{t}$$
$$p(failure_{BS}) = \binom{m}{t} p_{BS}^{m-t}.(1 - p_{BS})^{t} \quad \text{(C.5)}$$

$$p(\mathit{failure}_{CbioS}) = \binom{m}{t} p(\mathit{failure}_{CbioS})^{m-t}.(1 - p(\mathit{failure}_{CbioS}))^{t}$$
$$p(\mathit{failure}_{CbioS}) = \binom{m}{t} p_{CbioS}^{m-t}.(1 - p_{CbioS})^{t} \quad \text{(C.6)}$$

The probability of failure for transmision packets from node D and node H are shown in (C.7) and (C.8), respecively.

$$p(\mathit{failure}_{DRS}) = \binom{m}{t} p(\mathit{failure}_{DRS})^{m-t}.(1 - p(\mathit{failure}_{DRS}))^{t}$$
$$p(\mathit{failure}_{DRS}) = p(DR) + p(RS) - [p(DR).p(RS)] \quad \text{(C.7)}$$
$$p(\mathit{failure}_{DRS}) = \binom{m}{t} [p_{DR} + p_{RS} - (p_{DR}.p_{RS})]^{m-t}.[1 - \{p_{DR} + p_{RS} - (p_{DR}.p_{RS})\}]^{t}$$

$$p(\mathit{failure}_{HRS}) = \binom{m}{t} p(\mathit{failure}_{HRS})^{m-t}.(1 - p(\mathit{failure}_{HRS}))^{t}$$
$$p(\mathit{failure}_{HRS}) = p(HR) + p(RS) - [p(HR).p(RS)] \quad \text{(C.8)}$$
$$p(\mathit{failure}_{HRS}) = \binom{m}{t} [p_{HR} + p_{RS} - (p_{HR}.p_{RS})]^{m-t}.[1 - \{p_{HR} + p_{RS} - (p_{HR}.p_{RS})\}]^{t}$$

Appendix D

Finding the Total of PSR at the Sink Node by Using the Encoding Technique

The total of probability for successful reception at the sink node is computed as given in equation (D.1) based on the encoding technique. Each node transmits packets toward the sink node through the network coding node (D), which generates the encoding packets. The topology WBSN in this technique is shown in Figure D.1. The NC relay node should receive at least m linearly independent packets, let m' representing the encoding packets. The probability for success of the bottleneck zone is calculated as given in equation (D.1).

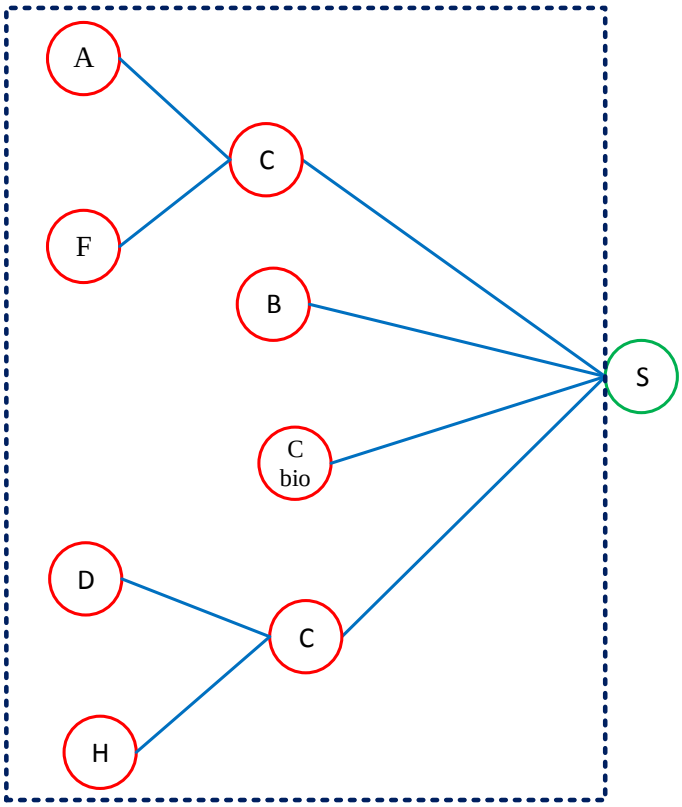

Figure D.1: The topology for the nodes in the bottleneck zone based on the encoding technique

$$p(encode\_successful) = 1 - p(encode\_failure)$$
$$p(encode\_successful) = 1 - [p(failure_{AFCS}).p(failure_{BS}).p(failure_{Cbio}) \quad \text{(D.1)}$$
$$.p(failure_{DHCS})]$$

Where

$$p(\mathit{failure}_{AFCS}) = 1 - p(\mathit{successful}_{AFCS})$$
$$p(\mathit{successful}_{AFCS}) = (1-p_{AC})^{m}.(1-p_{FC})^{m}.\sum_{i=m}^{m'}\binom{m'}{i}(1-p_{CS})^{i}.p_{CS}^{m'-i} \quad \text{(D.2)}$$

where $m' \geq m$

The proability of failure for node B and Cbio are shown in (D.3) and (D.4), respectively.

$$p(\mathit{failure}_{BS}) = \binom{m}{t} p(\mathit{failure}_{BS})^{m-t}.(1-p(\mathit{failure}_{BS}))^{t}$$
$$p(\mathit{failure}_{BS}) = \binom{m}{t} p_{BS}^{m-t}.(1-p_{BS})^{t} \quad \text{(D.3)}$$

$$p(\mathit{failure}_{CbioS}) = \binom{m}{t} p(\mathit{failure}_{CbioS})^{m-t}.(1-p(\mathit{failure}_{CbioS}))^{t}$$
$$p(\mathit{failure}_{CbioS}) = \binom{m}{t} p_{CbioS}^{m-t}.(1-p_{CbioS})^{t} \quad \text{(D.4)}$$

The proability of failure for $p(\mathit{failure}_{DHCS})$ is shown in (D.5).

$$p(\mathit{failure}_{DHCS}) = 1 - p(\mathit{successful}_{DHCS})$$
$$p(\mathit{successful}_{DHCS}) = (1-p_{DC})^{m}.(1-p_{HC})^{m}.\sum_{i=m}^{m'}\binom{m'}{i}(1-p_{CS})^{i}.p_{CS}^{m'-i} \quad \text{(D.5)}$$

where $m' \geq m$

Appendix E

Finding the Total of PSR at the Sink Node by Using the Combined Technique

The total probability for successful reception at the sink node based on the combination method. Each node transmits packets toward the sink node through the relay node and network coding node as shown in Figure E.1, except the node B and Cbio are directly connect to the sink node.

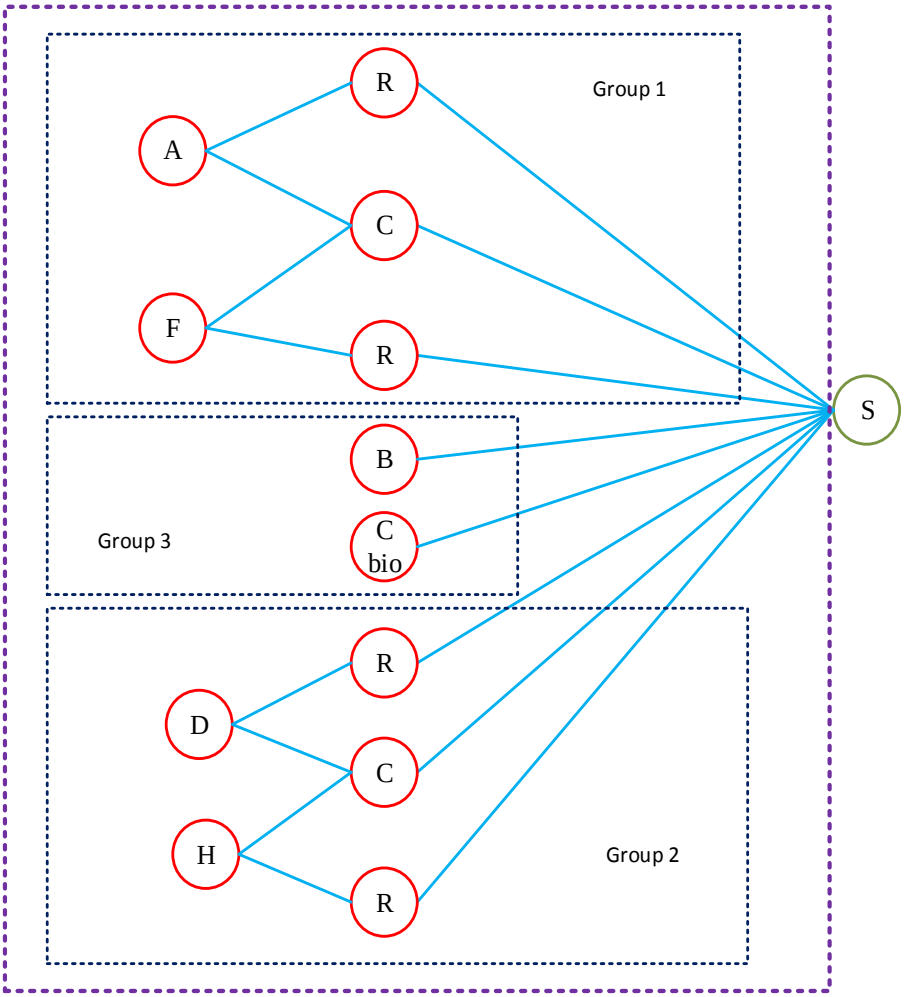

Figure E.1: Nodes connected to the sink node through relay nodes and network coding nodes

$$p(combination\_successful) = 1 - p(combination\_failure)$$
$$p(combination\_successful) = 1 - [p(failure_{group1}).p(failure_{group2}) \quad \text{(E.1)}$$
$$.p(failure_{group3})]$$

The analysis of the probability of the failure for this scheme is shown as follows:

Group1, the $p(failure_{group1})$ is calculated as shown in (E.2).

$$p(failure_{group1}) = p(failure_{ARS}) \cap p(failure_{AFCS}) \cap p(failure_{FRS}) \quad \text{(E.2)}$$

Where

$$p(failure_{ARS}) = \binom{m}{t} p(failure_{ARS})^{m-i}.(1 - p(failure_{ARS}))^{t}$$
$$p(failure_{ARS}) = p(AR) + p(RS) - [p(AR).p(RS)]$$
$$p(failure_{ARS}) = \binom{m}{t} [p_{AR} + p_{RS} - (p_{AR}.p_{RS})]^{m-t} \quad \text{(E.3)}$$
$$.[1 - \{p_{AR} + p_{RS} - (p_{AR}.p_{RS})\}]^{t}$$

$$p(failure_{AFCS}) = 1 - p(successful_{AFCS})$$
$$p(successful_{AFCS}) = (1 - p_{AC})^{m}.(1 - p_{FC})^{m}.\sum_{i=m}^{m'} \binom{m'}{i} (1 - p_{CS})^{i}.p_{CS}^{m'-i} \quad \text{(E.4)}$$

where $m' \geq m$

$$
\begin{aligned}
&p(\,failure_{FRS}\,) = \binom{m}{t} p(\,failure_{FRS}\,)^{m-t}.(1-p(\,failure_{FRS}\,))^{t} \\
&p(\,failure_{FRS}\,) = p(FR) + p(RS) - [p(FR).p(RS)] \\
&p(\,failure_{FRS}\,) = \binom{m}{t} [p_{FR} + p_{RS} - (p_{FR}.p_{RS})]^{m-t} \\
&.[1-\{p_{FR} + p_{RS} - (p_{FR}.p_{RS})\}]^{t}
\end{aligned}
\qquad \text{(E.5)}
$$

Group 2: the $p(\,failure_{group2}\,)$ is computed as shown in (E.6).

$$p(\,failure_{group2}\,) = p(\,failure_{DRS}\,) \cap p(\,failure_{DHCS}\,) \cap p(\,failure_{HRS}\,) \qquad \text{(E.6)}$$

Where

$$
\begin{aligned}
&p(\,failure_{DRS}\,) = \binom{m}{t} p(\,failure_{DRS}\,)^{m-t}.(1-p(\,failure_{DRS}\,))^{t} \\
&p(\,failure_{DRS}\,) = p(DR) + p(RS) - [p(DR).p(RS)] \\
&p(\,failure_{DRS}\,) = \binom{m}{t} [p_{DR} + p_{RS} - (p_{DR}.p_{RS})]^{m-t} \\
&.[1-\{p_{DR} + p_{RS} - (p_{DR}.p_{RS})\}]^{t}
\end{aligned}
\qquad \text{(E.7)}
$$

$$
\begin{aligned}
&p(\,failure_{DHCS}\,) = 1 - p(successful_{DHCS}\,) \\
&p(successful_{DHCS}\,) = (1-p_{DC})^{m}.(1-p_{HC})^{m}.\sum_{i=m}^{m'} \binom{m'}{i} (1-p_{CS})^{i}.p_{CS}^{m'-i}
\end{aligned}
\qquad \text{(E.8)}
$$

where $m' \geq m$

$$
\begin{aligned}
&p(\,failure_{HRS}\,) = \binom{m}{t} p(\,failure_{HRS}\,)^{m-t}.(1-p(\,failure_{HRS}\,))^{t} \\
&p(\,failure_{HRS}\,) = p(HR) + p(RS) - [\,p(HR).p(RS)\,] \\
&p(\,failure_{HRS}\,) = \binom{m}{t} [\,p_{HR} + p_{RS} - (p_{HR}.p_{RS})\,]^{m-t} \\
&.[1-\{p_{HR} + p_{RS} - (p_{HR}.p_{RS})\}]^{t}
\end{aligned}
\tag{E.9}
$$

Group 3: The calculation of $p(\,failure_{group3}\,)$ is given in (E.10).

$$
p(\,failure_{group3}\,) = p(\,failure_{BS}\,) \cap p(\,failure_{CbioS}\,) \tag{E.10}
$$

$$
\begin{aligned}
&p(\,failure_{BS}\,) = \binom{m}{t} p(\,failure_{BS}\,)^{m-t}.(1-p(\,failure_{BS}\,))^{t} \\
&p(\,failure_{BS}\,) = \binom{m}{t} p_{BS}^{m-t}.(1-p_{BS}\,)^{t}
\end{aligned}
\tag{E.11}
$$

$$
\begin{aligned}
&p(\,failure_{CbioS}\,) = \binom{m}{t} p(\,failure_{CbioS}\,)^{m-t}.(1-p(\,failure_{CbioS}\,))^{t} \\
&p(\,failure_{CbioS}\,) = \binom{m}{t} p_{CbioS}^{m-t}.(1-p_{CbioS}\,)^{t}
\end{aligned}
\tag{E.12}
$$